

THÈSE DE DOCTORAT
DE L'UNIVERSITÉ PIERRE ET MARIE CURIE

Spécialité : Neurobiologie

École doctorale ED3C

Présentée par
Jean-Baptiste PASSOT

Pour obtenir le grade de
DOCTEUR
DE L'UNIVERSITÉ PIERRE ET MARIE CURIE

ÉTUDE COMPUTATIONNELLE DU RÔLE DU CERVELET DANS LES
MOUVEMENTS VOLONTAIRES ET LA NAVIGATION SPATIALE

Soutenue le 02 septembre 2011 devant le jury composé de :

Rapporteurs : Jeffrey KRICHMAR - Université de Californie
Eduardo ROS - Université de Grenade
Examineurs : Eric BURGUIÈRE - Institut de Technologie du Massachusetts
Bruno GAS - Université Pierre et Marie Curie
Daniel WOLPERT - Université de Cambridge
Directeur : Angelo ARLEO - Université Pierre et Marie Curie

ROLE OF THE CEREBELLUM IN ADAPTIVE VOLUNTARY MOVEMENTS AND
SPATIAL COGNITION: A NEUROCOMPUTATIONAL STUDY

Résumé

Il a été démontré que le cervelet joue un rôle fondamental dans le contrôle moteur adaptatif. Plus récemment, il a été proposé que le cervelet serait aussi impliqué dans des tâches plus cognitives, et notamment dans la mémoire spatiale. Or, l'organisation anatomo-fonctionnelle uniforme du cortex cérébelleux suggère que ce dernier traite les informations avec un ensemble de principes computationnels identiques pour l'ensemble de ses fonctions. En se basant sur cette hypothèse de travail, ma thèse a pour objectif de mettre en évidence les propriétés computationnelles ainsi que les processus d'adaptation du cervelet communs aux apprentissages moteurs et à la cognition spatiale.

Dans la première partie de la thèse, nous nous intéressons aux mécanismes d'apprentissage procédural sous-tendant l'émergence d'une réponse comportementale adaptée au contexte sensorimoteur. Nous épousons l'hypothèse que le cervelet (et plus particulièrement le microcomplexe cérébelleux) offre un substrat neural approprié pour l'acquisition de modèles internes de l'interaction entre un sujet et son environnement. Si l'existence de tels modèles est aujourd'hui largement acceptée, il existe encore un débat sur le type de modèles encodés par le cervelet. De plus, très peu de travaux ont recherché les bénéfices apportés par un couplage de modèles de type prédictif (dit forward) et correcteurs (dit inverse). Aucune étude n'a souligné le fait que ce couplage pourrait apporter des capacités d'apprentissage permettant une consolidation de mémoires procédurales une fois la tâche réalisée (i.e. offline), comme cela semble être le cas chez les humains pendant des phases de sommeil après avoir réalisé une tâche procédurale. Nous proposons un nouveau schéma de couplage de modèles internes du cervelet tenant compte de ces aspects et nous l'appliquons à une tâche d'adaptation motrice afin de démontrer son efficacité et sa pertinence dans des apprentissages procéduraux. Le microcomplexe cérébelleux est modélisé en

utilisant un réseau de neurones formels impulsionnels reproduisant les éléments fondamentaux de la cytoarchitecture cérébelleuse. Le modèle est testé sur une tâche d'adaptation de rotation, utilisée par Huber et ses collaborateurs afin d'étudier l'apprentissage moteur chez les humains avant et après une phase de sommeil. Les résultats obtenus sur une version simulée de ce paradigme montrent que seul le modèle d'apprentissage couplant prédiction et correction est capable de reproduire les résultats expérimentaux dont la consolidation mnésique post-sommeil.

Dans la seconde partie de ma thèse, nous inscrivons notre modèle de microcomplexe cérébelleux dans une architecture neurale plus étendue afin d'étudier le rôle du cervelet dans la composante procédurale (i.e. la mise en place d'une réponse motrice adaptée au contexte) et déclarative (i.e. la mise en place d'une représentation de l'environnement) de la cognition spatiale. Nous nous basons sur une étude de génétique comportementale qui a montré que des souris transgénique L7-PKCI ayant un déficit d'apprentissage spécifique du cervelet ont des déficits d'apprentissage lors de la résolution de tâches de navigation spatiale. Nos résultats de simulation suggèrent qu'un déficit purement local de la composante procédurale (i.e. l'optimisation de la commande motrice lors de la réalisation d'un mouvement) ne permet pas d'expliquer l'ensemble des résultats expérimentaux. Nous proposons une nouvelle hypothèse selon laquelle le comportement exploratoire de ces souris transgéniques serait sous-optimal en comparaison des souris contrôles. Finalement, nos résultats de simulations montrent que le cervelet serait impliqué dans l'intégration des informations idiothétiques (e.g. proprioceptives), ce qui affecterait indirectement la mise en place d'une représentation stable de l'environnement au niveau des cellules de lieu hippocampiques —et par conséquent l'acquisition de mémoires à caractère déclaratif. Ce travail a donné lieu à plusieurs prédictions testables expérimentalement : d'une part au niveau cellulaire où nous proposons des différences significatives entre les propriétés d'encodage spatial de l'activité des cellules de lieux hippocampiques des souris contrôles et mutantes ; d'autre part au niveau comportemental où nous suggérons une différence significative dans la stratégie d'exploration d'environnement inconnus mise en oeuvre par les souris cérébelleuses en comparaison d'un groupe contrôle. Cette dernière prédiction est en train d'être testée au sein de notre laboratoire.

Abstract

The cerebellum plays a major role in motor control. It is thought to mediate the acquisition of internal models of body-environment interactions (Ito, 1984). More recently, the cerebellum has also been proposed to play a role in non-motor tasks, and experimental findings have begun to unravel its implication in spatial cognition (Petrosini et al., 1998; Burguière et al., 2005). A remarkably uniform synaptic organization of the cerebellar cortex suggests that both the motor-related and cognitive functions of the cerebellum might be implemented using the same computational principles. The main objective of this thesis is to unveil the unified computational rules that could account for the functional roles of the cerebellum in both motor and spatial cognitive processes.

In the first part of the thesis, we address how multiple cerebellar microcomplexes encoding internal predictive and corrective models might collaborate to efficiently participate in the adaptation of motor behaviors. The proposed connectionist architecture takes inspiration from the cerebellar microcomplex circuit (Ito, 2006), using spiking neural populations to process information. Long-term synaptic plasticities are implemented to achieve adaptive motor control. It is shown that the system can acquire representations of closed-loop sensorimotor interactions, suitable to adapt the behavioral response to changing sensory contexts. The coupling model is validated on a rotation adaptation task proposed by Huber et al. (2004). The simulation results of the neural architecture reproduce the experimental findings on the human procedural learning task both during a training phase (online) and after a night of sleep (offline consolidation). The sleep-dependent consolidation observed experimentally is mimicked by an offline learning phase during which a replay of the contextual information elicited during online training takes place.

In the second part of the thesis, we examine the extent to which the framework of cerebellar internal models can be applied to navigation. The

cerebellar functions in both procedural and declarative memories related to spatial cognition are studied by integrating our model in an extended neural architecture. We focus on behavioral genetic data suggesting that L7-PKCI mice (lacking LTD in parallel fiber–Purkinje cell synapses) are impaired in learning the procedural component of spatial navigation (Burguière et al., 2005). In order to validate this hypothesis, the performance between simulated control mice and transgenic simulated L7-PKCI mice is compared in both the Morris water-maze and the Starmaze (Rondi-Reig et al., 2005) tasks. Our findings show that a purely local impairment of the procedural component cannot explain all the experimentally observed differences between the goal-searching behavior of the mutant and control populations (Burguière et al., 2005). We propose a new hypothesis according to which mutants’ spatial learning impairment reflects a deficit in the trade-off between exploration and exploitation strategies. Based on this assumption, we are able to reproduce the entire set of behavioral results (Burguière et al., 2005). Furthermore, we argue that the deficit in the exploration-exploitation balance might be due to suboptimal spatial representations in L7-PKCI mice, which would result in increased exploration in novel environments. We evaluate this assumption by coupling our cerebellar model to an existing model of hippocampal spatial learning (Arleo and Gerstner, 2000; Sheynikhovich et al., 2009). Our simulation results suggest that the cerebellum may play an important role in integrating proprioceptive information to infer future state variables such as body orientation and position (Wolpert et al., 1998). This ability might be impaired in L7-PKCI mutants, thus affecting hippocampal multisensory integration which mediates stable spatial representations learning (Arleo and Rondi-Reig, 2007). This work gives rise to a testable prediction on the difference between the free exploratory behavior of control animals (Fonio et al., 2009) and L7-PKCI mutants.

Acknowledgments

Table of contents

Résumé	i
Abstract	iii
Acknowledgments	iv
Table of contents	vii
1 Introduction	1
1.1 Motivation	1
1.2 Our approach: artificial neural networks	4
1.3 Roadmap of the dissertation	5
I THE CEREBELLUM	9
2 Anatomofunctional and electrophysiological properties	13
2.1 Gross anatomy	13
2.2 Anatomo-functional divisions of the cerebellum	13
2.2.1 Anatomical transversal divisions	14
2.2.2 Functional longitudinal organization	16
2.3 Connectivity	16
2.3.1 The vestibulo-cerebellum	18
2.3.2 The spinocerebellum	18
2.3.3 The cerebro-cerebellum	19
2.4 Microzones and microcomplexes	20
2.4.1 Microzones	20
2.4.2 Microcomplexes	20
2.5 The cerebellar cortex	21
2.5.1 Internal circuitry	24

2.5.2	Cellular Types	24
3	Cerebellar functions	33
3.1	Historical introduction	33
3.2	Sensorimotor role of the cerebellum	34
3.2.1	Cerebellum participates in fine tuning of coordinated movements	35
3.2.2	Cerebellum participates in motor learning	36
3.2.3	Cerebellum participates in timing of movements	41
3.3	Cerebellum and non motor functions	42
3.3.1	Anatomical evidences	43
3.3.2	Neuroimaging	43
3.3.3	Neuropsychological and clinical descriptions	44
4	Cerebellar plasticity	47
4.1	PF-PC LTD	49
4.2	PF-PC LTPs	49
4.3	CF-PC LTD	50
4.4	MF-GR LTD and LTP	50
4.5	PC-DCN LTD and LTP	51
4.6	MF-DCN LTD and LTP	51
4.7	Interneurons' LTD and LTP	52
4.8	Non-synaptic plasticity	52
5	Cerebellar models and theories	53
5.1	Models of motor learning	53
5.1.1	The classical model	53
5.1.2	Modeling VOR	57
5.1.3	Modeling eyeblink conditioning	62
5.2	Models for the passage of time	65
5.2.1	Passage of time in the granular layer	65
5.2.2	Passage of time in the Purkinje cell	68
5.2.3	Passage of time in the olivary system	69
5.3	Models for voluntary movements	71

II THE ROLE OF THE CEREBELLUM IN ADAPTIVE VOL-

UNITARY MOVEMENTS	73
Abstract	75
6 Introduction	77
6.1 The internal model hypothesis	77
6.2 Coupling of internal models	82
6.3 Our approach	84
6.4 Effect of sleep on motor learning	85
7 Material and methods	87
7.1 The Task	87
7.2 Integrated model for adaptive voluntary movements	88
7.2.1 Overall model architecture	88
7.2.2 Cerebellar microcomplex model	90
7.2.3 Neuronal models	93
7.2.4 Encoding MF cerebellar inputs	95
7.2.5 Decoding cerebellar outputs	97
7.2.6 Synaptic efficacy and plasticity rules	101
7.2.7 Encoding of error/teaching signals	103
7.3 Simulated environment	107
7.4 Measures of performance	109
8 Simulations	111
8.1 Fixed angular deviation protocol	111
8.1.1 Results	112
8.2 Evolutive angular deviation protocol	114
8.2.1 The protocol	116
8.2.2 Results	117
8.3 Offline consolidation	120
8.3.1 Consolidation after a subsequent offline consolida- tion process	120
8.3.2 Time course and limit of offline consolidation	122
9 Properties of the internal models	125
9.1 Bistability and performances of the forward model	125
9.1.1 Bistability measures	126
9.1.2 Results	126
9.2 LTD-LTP compensation	127

9.2.1	Protocol	129
9.2.2	Results	129
9.3	Sparsification in the granular layer	130
9.3.1	Global activity	130
9.3.2	Kurtosis	132
10	Discussion	135
10.1	Contributions	135
10.2	Sleep and memory consolidation	136
10.3	Properties of cerebellar circuitry	141
10.4	Limitations and future work	145
III	THE ROLE OF THE CEREBELLUM IN SPATIAL COGNITION	149
	Abstract	151
11	Introduction	155
11.1	Spatial deficits in human	156
11.2	Spatial deficits in rodents' models	158
11.2.1	The cerebellum, procedural and declarative learning	159
11.3	Unresolved questions	160
11.4	Our approach	160
12	Material and methods	165
12.1	Integrated model of procedural and declarative spatial learning	165
12.1.1	Overall model architecture	165
12.1.2	Cerebellar microcomplex model	167
12.1.3	Hippocampal model	169
12.1.4	Spatial behaviour policy	172
12.2	Spatial learning tasks and statistical analyses	173
12.2.1	Morris Water Maze and Starmaze tasks	173
12.2.2	Behavioral analysis	174
12.2.3	Statistical analyses of unitary and population neural activities	174

13 Results	177
13.1 Adaptation in forward and inverse cerebellar models	177
13.2 Cerebellar role in local <i>vs.</i> global procedural spatial learning	181
13.3 Cerebellar role in declarative spatial learning	183
14 Discussion	197
14.1 Contributions	197
14.2 Testable predictions emerging from the model	200
14.3 The cerebellum and path integration	201
14.4 Unifying multiple experimental observations	204
14.5 Limitations and future works	207
15 Supplementary Methods	211
15.1 Cerebellar microcomplex model	211
15.1.1 Neuronal models	212
15.1.2 Encoding MF cerebellar inputs	213
15.1.3 Decoding cerebellar outputs	215
15.1.4 Synaptic efficacy and plasticity rules	217
15.1.5 Encoding of error/teaching signals	219
15.2 Statistical analyses of neural activities	221
16 Supplementary Results	225
16.1 Cerebellar role in <i>local</i> procedural spatial learning	225
Conclusion	231
17 General discussion and conclusion	231
17.1 Main results and contributions	232
17.1.1 Cerebellum and adaptive motor behavior	232
17.1.2 Cerebellum and spatial cognition	233
17.2 Limitations and perspectives	235
17.2.1 Studying inter-structure interactions in the genera- tion of movements	235
17.2.2 Consolidation of learning during sleep	237
17.2.3 Validating the hypotheses/predictions derived by the model	238
17.3 Toward a unified principle for motor and non motor tasks .	239

17.3.1	Are timing and internal model's theories mutually exclusive?	239
17.3.2	Neural code of cerebellar cell assemblies	240
17.3.3	The internal mental models hypothesis	241
Annexes		247
A	Neurocomputation of voluntary movement	247
A.1	Computational properties of movement	248
A.1.1	The curse of dimensionality	248
A.1.2	The state and the context	248
A.1.3	The notion of hierarchy	249
A.1.4	The sensorimotor loop	250
A.2	Optimal control theories	253
A.2.1	Open-loop motor control	254
A.2.2	Close-loop motor control	255
A.2.3	Predictive control models	256
A.2.4	Limitations	258
A.3	Structures involved in voluntary movement	259
B	Spatial cognition: a short introduction	263
B.1	Multisensory integration	263
B.1.1	Type of information	264
B.2	Interaction between multiple spatial strategies	266
B.3	Memory used in spatial cognition	268
B.4	Paradigms and protocols	269
B.4.1	The Morris watermaze	270
B.4.2	The starmaze	271
B.5	Structures involved in spatial cognition	272
B.5.1	The hippocampus	273
B.6	Cellular bases of spatial cognition	275
B.6.1	Hippocampal place cells	275
B.6.2	Grid and head direction cells.	278
C	Sleep consolidation in procedural tasks	279
C.1	Simulated finger tapping task	279
C.1.1	Protocol	279
C.1.2	Results	280

C.2	A new task to elucidate the role of sleep in procedural learning	281
C.2.1	Protocol	281
C.2.2	Expected results	282
Bibliography		285

Chapter 1

Introduction

1.1 Motivation

The cerebellum is a region of the brain which plays an essential role in motor control, most notably through the fine tuning and coordination of movements (Holmes, 1939; Thach et al., 1992; Miall et al., 2001). This structure has also been shown to be fundamental for several types of motor learning, mediating sensorimotor adaptation (Ito, 1974; Thach et al., 1992; Attwell et al., 2002) and permitting instrumental conditioning (McCormick and Thompson, 1984; Koekkoek et al., 2003).

In addition to its role in motor tasks, the cerebellum is also thought to be involved in cognitive processes; however, this is still only partially understood and therefore remains controversial (Thach, 1998; Glickstein and Doron, 2008).

Recent anatomical studies have established that cerebellar outputs target non-motor cortical areas, providing the substrate to influence cognitive tasks (see Strick et al., 2009 for a recent review). The class of functions supposedly associated with cerebellar activity has become very diverse and includes language, attention, and emotion related processes (Glickstein, 2007; Timmann and Daum, 2007; Glickstein and Doron, 2008). Recent experimental findings have also begun to unravel the implication of the cerebellum in spatial cognition (Mandolesi et al., 2001; Petrosini et al., 1998; Rondi-Reig et al., 2005; Burguière et al., 2005); a function which requires multiple parallel structures and memory substrates (Eichenbaum et al., 1999; Burgess et al., 2002; McNaughton et al., 2006; Moser et al., 2008).

Yet, anatomically, the cerebellum presents a striking feature: the synaptic organization of the cerebellar cortex is remarkably uniform. This suggests that it processes information using unified computational principles. Based on this working hypothesis, the main objective of my thesis is to unveil the computational rules implemented in the cerebellar circuitry which could explain its function in both motor and cognitive processes. More precisely, we focus our research on the role of the cerebellum (*i*) in the adaptation of voluntary movements, and (*ii*) in navigation tasks.

Cerebellum and voluntary movement. Since biological sensory feedback is conveyed at a low speed and sensory information can be noisy, fast and coordinated movements cannot be executed using only feedback information (Wolpert and Ghahramani, 2000; Shadmehr et al., 2010). To resolve these issues, the internal model hypothesis has emerged, proposing that the brain — and more specifically the cerebellum — acquires internal models of the body and the world (Ito, 1970, 1984; Kawato et al., 1987). An internal model is a representation of a dynamical system that approximates its input-output relationship with the environment. In practice, there is strong evidence coming from behavioral, fMRI and physiological studies that some internal models can be created and stored within the cerebellum (Wolpert et al., 1998; Kawato et al., 2003; Ito, 2005). In motor control theory, internal models are divided into two groups identified as forward and inverse models.

Forward models predict the state of a body part and the sensory outcome of an action. These models are thought to be used in motor learning and control (Ito, 1984; Miall et al., 1993; Wolpert and Miall, 1996; Jordan and Rumelhart, 1992), in state and sensory estimation (Goodwin, 1984; Miall et al., 1993), as well as in context prediction (Wolpert and Kawato, 1998). Evidence of the existence of such models has been reinforced by experimentation (Bell et al., 1997; Eskandar and Assad, 1999; Mulliken et al., 2008).

Inverse models work in the opposite direction, providing the motor command which will cause a desired change in the state of a system. In other words, an inverse model maps a desired target location to a set of motor commands (Kawato, 1999) and are therefore adapted to achieve some desired state transition (e.g., Contreras-Vidal et al., 1997; Schweighofer et al., 1998).

While some authors suggested that a forward model could be first

formed in the cerebellar cortex and then converted to an inverse model (Darlot et al., 1996; Ito, 2006), most of the existing studies only consider one system or the other. The type of model implemented in the cerebellum is still being debated in the literature (e.g., Pasalar et al., 2006; Dean et al., 2010). Very few works investigate the advantages of coupling both types of internal models (e.g., Jordan and Rumelhart, 1992; Wolpert and Kawato, 1998), and none underline the fact that this scheme would bring offline learning capabilities. This is quite surprising, since sleep — a major type of offline processing state — contributes to the consolidation and enhancement of procedural tasks in which the cerebellum is undoubtedly implied (e.g., Thach et al., 1992).

In the first part of my thesis, we consider the procedural learning mechanisms of the cerebellar circuitry in the context of adaptive voluntary movements. Using a neurocomputational approach, we investigate how cerebellar microcomplexes can implement both predictive and corrective internal models with the same neural architecture and how these models could work cooperatively to promote efficient motor learning online, as well as enhancement during simulated sleeping phases.

Cerebellum and spatial cognition. Spatial cognition is defined as the ability of an animal to acquire spatial knowledge, organize it, and employ it to adapt its motor response to a specific context (Arleo and Rondi-Reig, 2007). Like other high-level brain functions, spatial cognition calls upon parallel information processing mediated by multiple neural substrates that interact to promote appropriate spatial behavior (Arleo and Rondi-Reig, 2007).

Spatial cognition requires both declarative and procedural learning in order to elaborate multimodal representations supporting spatial behavior (Arleo and Rondi-Reig, 2007). Declarative learning allows spatiotemporal relations between multiple cues or events to be encoded (O'Keefe and Conway, 1978; Eichenbaum, 2001). Procedural learning mediates the acquisition of an ensemble of procedures to solve a navigation task (Whishaw, 1985; Whishaw and Mittleman, 1986; Whishaw, 1991). The declarative and procedural components of spatial cognition are widely interrelated and involve multiple brain areas (McDonald and White, 1993, 1994; White and McDonald, 2002; Arleo and Rondi-Reig, 2007). Completing the large body of experimental works which has provided evidence for a role of the hippocampal formation in declarative spatial learning

(O'Keefe and Conway, 1978; Morris et al., 1982; Eichenbaum et al., 1990; Cain and Saucier, 1996; Burgess et al., 2002), some studies have begun to elucidate the contribution of the cerebellum to this component of spatial navigation (Lalonde and Botez, 1986; Petrosini et al., 1998; Mandolesi et al., 2001; Burguière et al., 2005).

However, a comprehensive interpretation of all experimental findings is still lacking. For instance, the following issues remain open: could a purely local motor control deficit explain all the observed impairments in cerebellar subjects? Is the cerebellum also implied in the formation of more global (high-level) procedural memories? Does cerebellar learning contribute to the declarative component of spatial cognition? A quantitative theoretical framework could shed light on the cerebellar role in the multiple information processing stages of spatial learning and goal-directed navigation.

To the best of our knowledge, no computational study has addressed these issues so far. We therefore examine in which measures the framework of cerebellar internal models we used in the study of voluntary movements can be applied to spatial cognition, and provide a better understanding of the cerebellar roles during a navigation behavior. The rationale is to complete the existing behavioral observations with quantitative accounts testing specific hypotheses on the link between synaptic plasticity mechanisms, cell discharge properties, interstructure coupling, and behavioral responses.

1.2 Our approach: artificial neural networks

The models presented in this manuscript rely on the artificial neural network paradigm (Haykin, 1999). A neural network is a massively parallel distributed system suitable for the storage and processing of complex information.

The elementary constituents of a biological neural network are simple computing units referred to as neurons. Each neuron receives a large number of input connections termed dendrites, and transmits its response through the axon output connection. The computational power of a neural network derives from the massive interconnections between its neurons. Synapses are the elementary components that mediate the interaction between neurons.

An artificial neural network is a machinery designed to model the adaptive way in which the brain processes information to perform a given task. In particular, a neural network resembles the brain in two aspects (Haykin, 1999): (i) It acquires the necessary knowledge to solve a problem through a non-symbolic learning process; (ii) Storing this knowledge occurs through the modification of the weights of the inter-connections between neurons (i.e., synaptic plasticity).

Therefore, artificial neural networks offer a suitable tool for designing a model of the cerebellar circuitry with learning capabilities, and allow us to model the functional properties as well as the anatomical interconnections between the different brain regions involved in adaptive voluntary movements and spatial learning.

1.3 Roadmap of the dissertation

This thesis consists of three main parts. The first part (Chapters 2 to 5) reviews the anatomofunctional properties of the cerebellum, the functions and the main theoretical works related to the structure. The second part (Chapters 6 to 10) constitutes the first set of contributions of this thesis. It addresses the procedural learning mechanisms of the cerebellar circuitry in the context of adaptive voluntary movements. The third part (Chapters 11 to 16) presents a neurocomputational study of the role of the cerebellum in spatial cognition. We conclude this thesis by discussing the results of both studies and we propose future developments.

Topics treated in each chapter are:

Part 1 - The cerebellum

Chapter 2 (p. 13) reviews anatomical and electrophysiological properties of the cerebellum.

Chapter 3 (p. 33) addresses the functions of the cerebellum in motor and non-motor tasks.

Chapter 4 (p. 47) describes the plasticity sites of the cerebellar circuitry.

Chapter 5 (p. 53) resumes the main theoretical and computational studies in relation with the cerebellar functions.

Part 2 - Cerebellum and adaptive voluntary movement

Chapter 6 (p. 77) examines the role of the cerebellum in adaptive voluntary movement, briefly reviews the role of sleeping in procedural learning, and proposes a new coupling scheme to account for both online and offline adaptation.

Chapter 7 (p. 87) describes the overall model architecture, and includes a detailed description of the cerebellar microcomplex model.

Chapter 8 (p. 111) presents our simulation results in a rotation adaptation task.

Chapter 9 (p. 125) analyses the properties of the internal models mediating the acquisition of the adapted behavior.

Chapter 10 (p. 135) discusses our simulation results and summarizes the contributions and limitations of this first study.

Part 3 - Cerebellum and spatial cognition

Chapter 11 (p. 155) reviews the speculated roles of the cerebellum in navigation tasks and defines the question being investigated.

Chapter 12 (p. 165) describes the methods used to answer the question. We detail the overall model architecture, the cerebellar and hippocampal models and the spatial learning tasks.

Chapter 13 (p. 177) presents our main simulation results. We assess the learning capabilities of the simulated internal models and we present the behavioral results. Also, we derive possible behavioral correlates of cerebellar synaptic plasticity deficits in navigation tasks.

Chapter 14 (p. 197) discusses our simulation results and addresses how our study could unify multiple experimental observations.

Chapter 15 (p. 211) presents supplementary methods, including a detailed description of the implemented models and the mathematical definitions of the measures used in this study.

Chapter 16 (p. 225) details supplementary results.

The main text of this dissertation terminates with Chapter 17 (p. 231) in which the achievements and the limitations of this thesis are discussed, and where possible future directions of research are described.

Supplementary chapters have been added at the end of the thesis (Chapters A to C). Chapter A (p. 247) reviews approaches and theories related to the neurocomputation of movements. Chapter B (p. 263) gives a short introduction to spatial cognition, reviewing the memories, strategies and structures used when solving a navigation task. Finally, chapter Chapter C (p. 279) presents additional results for the coupling of internal models, and also proposes a new protocol to address the role of the cerebellum in sleep consolidation processes.

Part I

THE CEREBELLUM

The cerebellum is a structure of the central neural system (CNS) present in all classes of vertebrates; a similar structure can be observed in most primitive organisms (Larsell and Jansen, 1970). As shown in figure 1.1, there are considerable variations in the size and shape of the cerebellum of different species.

In this document, we focus on the cerebellum of mammals. Although it has notable differences in the size of its subparts, its gross anatomy is similar across species. In mammals, the cerebellum gathers more than 50 percent of all neurons of the CNS despite a relatively small size (10 to 15 per cent of the size of the brain), giving it a massive computational power. It also presents a striking feature: its synaptic organization is remarkably uniform. This highly regular arrangement suggests that the cerebellum process information with a single and characteristic computation principle.

The knowledge we have of the cerebellar's function mainly comes from symptoms following lesions and pathologies targeting this structure, and from the connectivity it has with the rest of the brain. Functionally, the cerebellum has long been known to play a major role in sensory-motor control — coordinating the movement and making them accurate — and more generally in motor learning. More recently, it has also become clear that the cerebellar function is not limited to movement, and that cerebellar processing might play a role in cognitive functions such as language, attention learning, pain, emotion, addiction, and spatial cognition.

The role of the cerebellum has also been better described thanks to neurocomputational approaches which have intended to define the computational rules driving the cerebellar circuitry. This field of research uses a very large database of anatomical, physiological and functional data accumulated through decades. This interdisciplinary approach has mainly been made possible with the pioneer work of Eccles, Ito and Szentagothai who gave in 1967 a clear description of the synaptic organization of the cerebellum.

In this part of the document, we review the anatomy, the functions and the theories related to the mammal's cerebellar formation.

In the first chapter, we consider its anatomy. We present its functional organization, the transversal and lateral subdivisions, and its connectivity with the rest of the CNS; we also give a clear account of its synaptic organization, considered to be one of the most regular of the CNS.

In a second chapter, we address the main functions of the cerebellum:

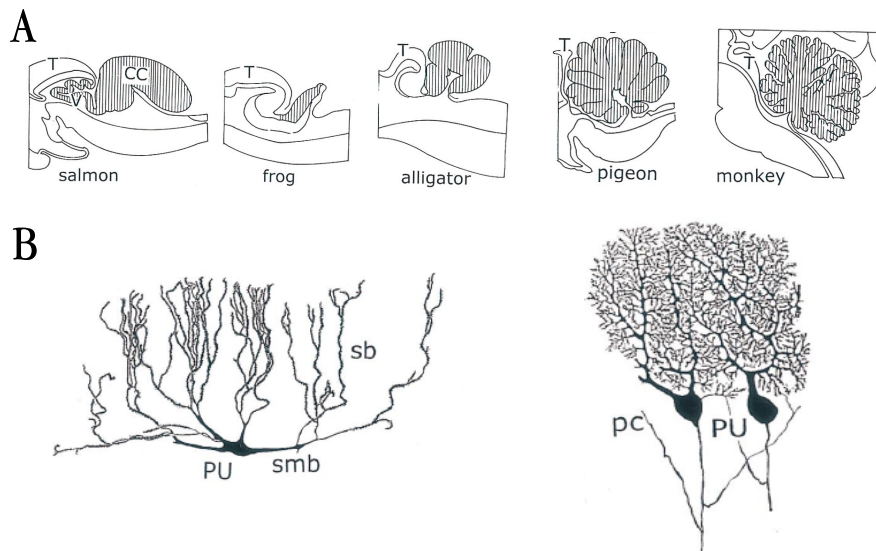


Figure 1.1: Differences across species (taken from Voogd and Glickstein, 1998) **A.** Sagittal sections representing the variation in the external form of the cerebellum of different vertebrate species **B. and C.** Drawing of Purkinje cells of cartilaginous fish (**B.**) and mammals (**C.**).

we describe its general contribution to sensorimotor processing, we explain the main disturbances resulting from lesions and pathologies, and we give a short review on why the cerebellum is thought to be implicated in non-motor functions.

In a third chapter, we give a brief account of the main plasticity sites that have been observed, and we describe their functional roles.

In the last chapter of this part, we concentrate on theoretical and computational studies that have attempted to determine a general framework to explain the functions at the level of information processing.

Chapter 2

Anatomofunctional and electrophysiological properties

2.1 Gross anatomy

The mammalian cerebellum is a medial structure located at the back of the head (see figure 2.1); it is connected to the brain stem by three symmetrical pairs of tracts, namely the inferior, middle and superior cerebellar peduncles.

Externally, the cerebellum is constituted of two hemispheres joined medially and delimited by the vermis (latin for *worm*), a fine midline zone. The surface of the cerebellum — the cerebellar cortex — is a thin layer of neural tissue which is folded, forming many transverse fissures, and concealing the convolution of the white matter. Four pairs of nuclei, known as the deep cerebellar nuclei, are embedded in the white matter, and constitute the only output of the cerebellum (see figure 2.1).

2.2 Anatomico-functional divisions of the cerebellum

Phylogenetic studies have revealed a transversal and a longitudinal organization of the cerebellum in mammals.

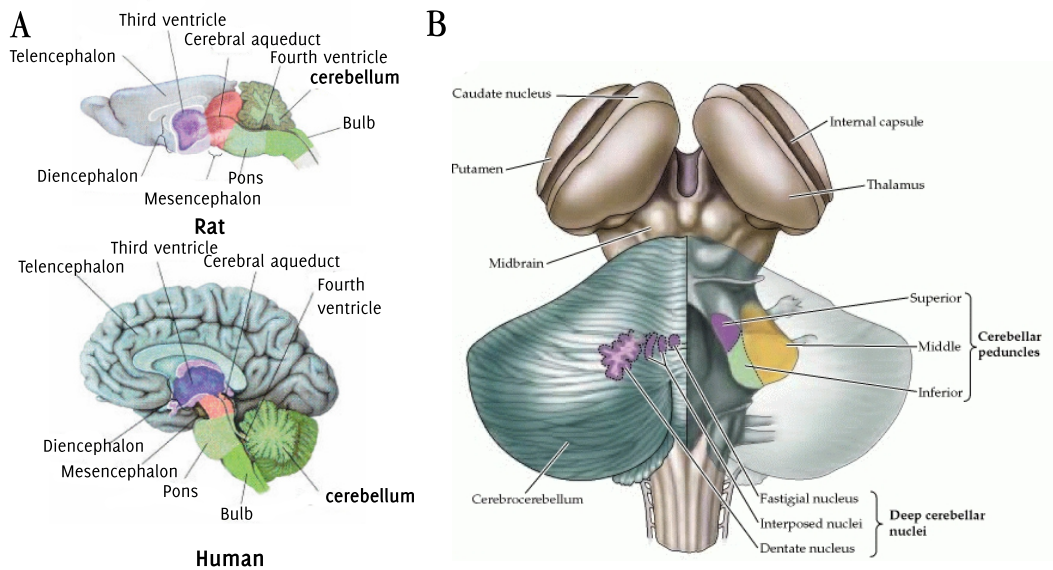


Figure 2.1: Position and anatomy of the cerebellum **A.** Location of the cerebellum in sagittal cut of the rat brain (top) and human brain (bottom) (taken from Nixon, 2003). **B.** Dorsal view of the cerebellum. Deep cerebellar nuclei and cerebellar peduncles are indicated (from Purves, 2002).

2.2.1 Anatomical transversal divisions

The cerebellum is divided into three anatomically distinct lobes by two deep transverse fissures. Figure 2.2A presents a schematic view of these major anatomical subdivisions. The primary fissure separates the anterior lobe (red in figure 2.2A) and the posterior lobe (white in figure 2.2A), both lobes constituting the body of the cerebellum. The flocculonodular lobe (orange in figure 2.2A) is separated from the rest of the structure by the posterolateral fissure. The flocculonodular lobe, also known as archeocerebellum or vestibulocerebellum, is the oldest cerebellar part in evolution, and has appeared with the first vertebrates (see Voogd and Glickstein, 1998 for review).

To a smaller extent, the anterior and posterior lobes of mammals are divided into nine lobules - also called *folia* - by smaller folds. The anterior lobe comprises lobules I to V and the posterior lobe, lobules VI to IX. The flocculonodular lobe is considered by anatomists as the tenth lobule (Larsell, 1952). Lobules are also shown in figure 2.2A.

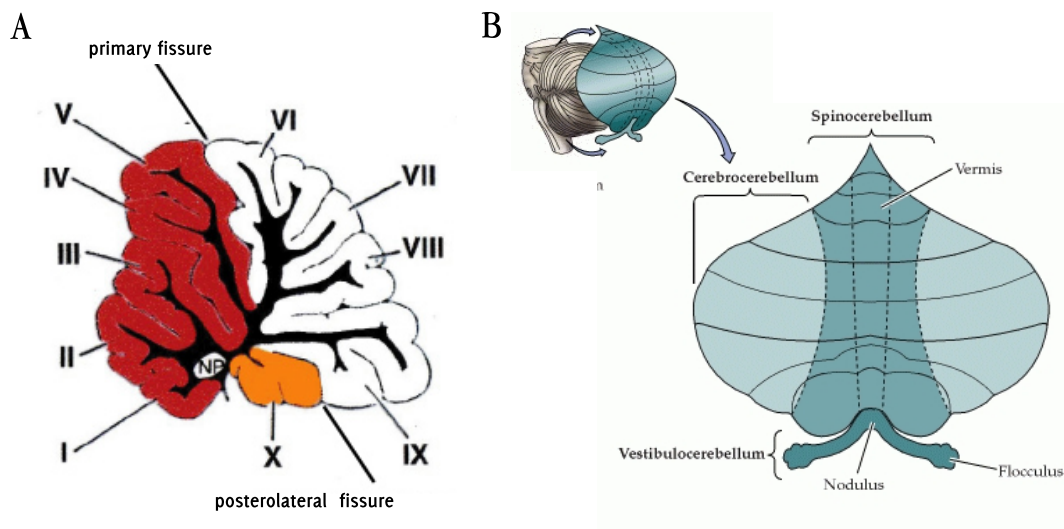


Figure 2.2: Anatomical and functional divisions of the cerebellum **A.** Transversal organization of the cerebellum; composed of ten lobules (numbered I to X). The cerebellar cortex is composed of the anterior lobe (red) and posterior lobe (white), separated by the primary fissure, and the flocculonodular lobe (orange - taken from Burguière et al., 2005). White substance is painted in black. **B.** Unfolded cerebellar cortex shows the main longitudinal organization of the cerebellum. Intermediate and lateral parts of the hemisphere are located on both side of the vermis. Nodulus and flocculus lobe constitute the vestibulo cerebellum. The cerebrocerebellum is identified as the lateral part of the cerebral hemispheres, and the vermis and intermediate part of the hemisphere are defined as the spinocerebellum.

2.2.2 Functional longitudinal organization

The flocculonodular, anterior and posterior lobes have long been considered as three functionally distinct regions of the cerebellum. However, it has been shown in the end of the 1970s that this transversal subdivision poorly reflected the functional regions of the cerebellum, which appear to be better described by a longitudinal organization (Voogd and Glickstein, 1998).

The cerebellum is divided into two parts by the vermis - a narrow mid-line zone. On both sides of the vermis lie the intermediate and lateral parts of the hemispheres. The medial zone of the anterior and posterior lobes, also referenced as intermediate part of the hemisphere, constitutes the spinocerebellum (because it is the only area which receives somatosensory information from the spinal cord); and the lateral zone defines the cerebrocerebellum (see figure 2.2B).

These main sections have been further subdivided into seven major parallel longitudinal zones (A,B,C, C1, C2, C3, D1 and D2) on each side of the vermis. Each subdivision is reciprocally connected either to a subset of deep cerebellar nuclei located in the white substance or to a vestibular nucleus situated in the bulb. Each subdivision also receives a set of climbing fibers from a discrete area of the inferior olive.

2.3 Connectivity

Cerebellar peduncles carry afferent and efferent information to and from the cerebellum. Most of the efferent connections are conveyed by the superior peduncle, whereas afferent connections travel mainly through the middle and inferior peduncles. The inferior peduncle's fibers connect the cerebellum to the bulb and gather afferent connection from the vestibular nuclei and the spinal cord. Main afferent and efferent connections are summarized in figure 2.3.

The flocculonodular lobe and the three mediolateral regions of the body of the cerebellum (the vermis, the intermediate and the lateral parts of the hemispheres) respectively receive different afferent inputs, project to different parts of the nervous system, and represent distinct functional divisions, as described below (note that a few indications on the functional characteristics are given here and will be detailed in chapter 3, page 33)

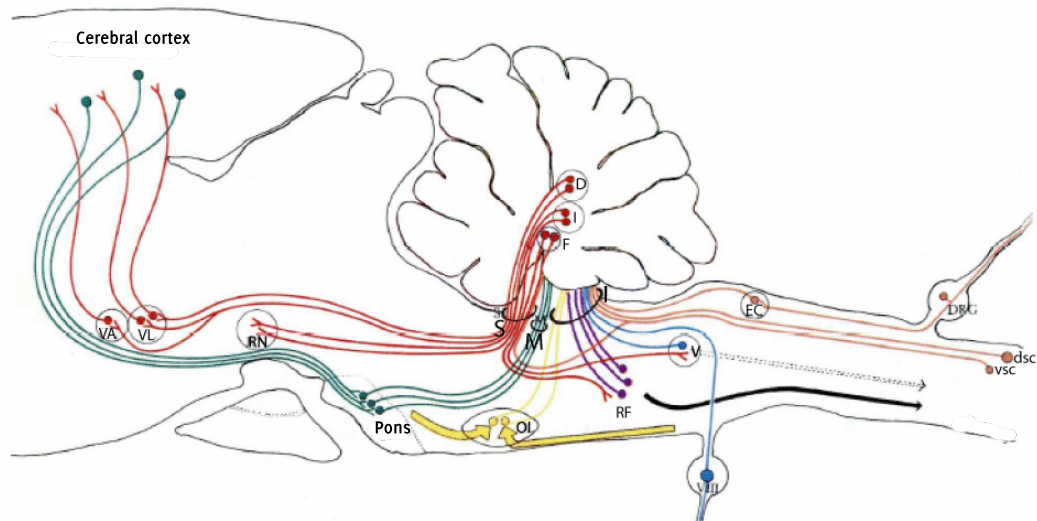


Figure 2.3: Main afferent and efferent connections of the cerebellum Afferents from the spinal cord (orange) arise from the ventral and dorsal spinocerebellar tracts and drive through the inferior and superior cerebellar peduncles. Afferents from vestibular nucleus (V) and primary vestibular fibers (VIII) project to the fastigial nucleus (F) and the flocculonodular lobe. Afferents from the reticular formation (RF, pink) target the cerebellar cortex of the vermis. Inferior olivary fibers (IO) drive through the inferior peduncle and project to all the cerebellar cortex. Afferents from the pons arise from the cerebral cortex and project to the entire cerebellar cortex via the middle peduncle (M). The majority of efferent connections (red) go through superior peduncle (S). The dentate nucleus (D) projects to the thalamus — the ventrolateral and ventroanterior nucleus (VL and VA) — and target the cerebral cortex. Efferents from the interposed nucleus target the red nucleus (RN) and fastigial nucleus, which in turn project to the reticulate formation and vestibular nuclei.

2.3.1 The vestibulo-cerebellum

The flocculonodular lobe receives input from the primary vestibular afferents — through mossy fibers — and projects to the lateral vestibular nuclei. It also receives visual inputs from the superior colliculus and from the pontine nuclei. Purkinje cells of the vestibulocerebellum target neurons in the medial and lateral vestibular nuclei. Functionally, the vestibulocerebellum is thought to regulate balance and eye movements (Yamada and Noda, 1987; Andersson and Oscarsson, 1978). The medial vestibular nuclei control eye movements and coordination of the eye with the head (Yamada and Noda, 1987). The lateral vestibular nuclei modulate the lateral and medial vestibulospinal tract, which control axial muscles and limb extensors, and by extension balance during stance and gait (Andersson and Oscarsson, 1978).

2.3.2 The spinocerebellum

Somatosensory information arises from the spinal cord and is forwarded exclusively to the spinocerebellum (the vermis and the intermediate cortex). Direct and indirect mossy fibers pathways (e.g., the ventral and dorsal spinocerebellar tracts) provide the cerebellum with somatic sensory information and descending motor commands. The ventral tract carries self-generated information and the dorsal tract conveys sensory feedback during movement.

The vermis receives visual, auditory, and vestibular inputs, as well as somatic sensory input from the head and proximal parts of the body. It projects to the fastigial nucleus, which sends fibers to cortical and brain stem regions. In turn, these regions send descending motor orders, to control proximal muscles of the body and limbs, and influence posture, locomotion and gaze direction.

Adjacent intermediate parts of the hemispheres receive somatosensory inputs from the limbs and project via the interposed nucleus to lateral corticospinal and rubrospinal systems. These systems control the more distal muscles of the limbs.

The spinocerebellum contains two sensory (somatotopic) maps of the body. In both maps, the head and trunk are located in the vermis. The limb representations are located on either side of the midline, in the intermediate part of the cerebellar hemispheres (Edgar Adrian and Ray Snider,

1940).

Purkinje Cells from the spinocerebellum target somatotopically different deep nuclei that modulate the descending motor pathways. First, neurons in the vermis target the fastigial nucleus which in turn projects to the brain stem's reticular formation and to the lateral vestibular nuclei. Both regions project to the spinal cord and to the fastigial nucleus neurons and control proximal muscles via the thalamus. The latter neurons affect the head, neck and proximal part of limbs. Then, neurons in the intermediate part of the cerebellar hemisphere project to the interposed nucleus, which indirectly targets the spinal cord and the limbs, by controlling areas of the primary motor cortex.

Functionally, the spinocerebellum is thought to regulate body and limb movement.

2.3.3 The cerebro-cerebellum

The lateral hemispheres (the cerebrocerebellum, zone D) receive inputs exclusively from the cerebral cortex. Mossy fibers travel through the middle cerebellar peduncle to the contralateral dentate nucleus. Purkinje neurons in the lateral cerebellar cortex project to the dentate nucleus neurons, which mainly send axons through the superior cerebellar peduncle (Voogd and Glickstein, 1998). The superior peduncle targets the thalamus, which in turn projects to premotor and primary motor areas of the cerebrum, prefrontal cortex, superior parietal cortex and basal ganglia (Na et al., 1997; Kelly and Strick, 2003; Clower et al., 2005; Kelly and Strick, 2003; Middleton and Strick, 2001). Also, neurons from the dentate nucleus target the contralateral parvocellular red nucleus, which sends axons to the inferior olivary nucleus, and hence connects back to the contralateral cerebellum via the climbing fibers (feedback loop) (Padel, 1993). Parvocellular neurons also receive input from the lateral premotor area. A recent discovery highlights direct and bidirectional connections between the cerebellum and the basal ganglia (Bostan et al., 2010).

The role of the cerebrocerebellum is still controversial. It is quite clear, from clinical observations, that it plays an important role in planning movements and integrating sensory information (see Ghez and Thach, 2000 for a simple review). It also seems to engrave more cognitive functions, as recent studies suggest (see section 3.3, page 42).

2.4 Microzones and microcomplexes

2.4.1 Microzones

Previously, we showed that the functional units of the cerebellar cortex have been identified as longitudinal zones. These zones can be divided into smaller microzones (Oscarsson, 1976). A single microzone contains about 1000 Purkinje cells which are arranged longitudinally in a long (up to 200 μm) narrow strip. Anatomico-functionally, a microzone is defined as a group of Purkinje cells presenting the same somatotopic receptive field. They have been identified electrophysiologically by recording areas of the cerebellar cortex that were activated by distinct stimulations of olivary neuron afferents (Andersson and Oscarsson, 1978; Thomson et al., 1989). Hence, each microzone of the cerebellar cortex receives climbing fibers from a different group of olivary neurons (Ekerot and Larson, 1982). This organization is thought to be formed via a developmental mechanism in combination with a cellular segregation operation: the mono-innervation of Purkinje cells by climbing fiber (Fuhrman et al., 1994). Furthermore, olivary neurons are electrically coupled through gap-junctions (Llinas et al., 1974) thus allowing the emergence of functional groups of olivary neurons where activity is synchronized (Sugihara et al., 1993).

2.4.2 Microcomplexes

As we previously mentioned, each longitudinal zone of the cerebellar cortex targets a specific cerebellar nucleus. Consequently, each microzone also combines with a small group of neurons in a cerebellar or vestibular nucleus. The combination of a microzone with a set of subcortical structures (cerebellar or vestibular nucleus, the inferior olive and the red nucleus) constitutes a corticonuclear microcomplex, or cerebellar microcomplex, and is hypothesized to be the operational unit of the cerebellum (Ito, 1984). Anatomical details are given by Ito (2001). The human cerebellum is thought to contain thousands of microcomplexes (in the order of 5000, see Ito, 2006), each one playing a role by interacting with a functional system in the spinal cord, the brainstem, the subcortical structures and the cerebral cortex. Notably a microcomplex associated with ocular reflexes has been thoughtfully described in the vestibulo-cerebellum and interconnected vestibular nuclei (Tan et al., 1995b,a; Nagao et al., 1985) and was

also identified in the C3 zone of the cat, a para-vermis area. Jörntell et al. (1996) showed that a microzone of the C3 zone sends signals to a specific sensory motor area through two pathways (interposed nucleus and red nucleus) and receives input signals from the same area through climbing fibers (See also Ekerot and Jörntell, 2001; Apps and Garwicz, 2005 for review).

In the next section, the cytoarchitecture of the cerebellar cortex and the detailed path of information in a olivo-cortico-nuclear microcomplex will be presented.

2.5 The cerebellar cortex

The detailed investigation of the cerebellar cortex started with the work of Golgi, followed by the extensive contribution of Ramon y Cajal who described the fine structure of the CNS and provided a detailed view of the cerebellar cortical network.

It has been shown that the cerebellar cortex is divided into three layers - namely molecular, Purkinje cell, and granular layer. It is composed of seven types of neurons connected in a very specific and uniform way (see figure 2.4A-B).

The molecular layer is located at the surface of the cerebellar cortex, it contains the stellate and basket cells (two types of interneurons), the parallel fibers and the Purkinje cell's dendritic tree. Below the molecular layer, the Purkinje cell layer gathers the somas of the Purkinje cells. Finally, the granular layer — the deepest of the cerebellar cortex — contains the somas of granular cells, an ascending section of granular cell's axons, the Golgi cells, the Lugaro cells, the unipolar brush cells, and the glomeruli, an intricate formation that receives contacts from mossy fibers and inhibitory cells from the same layer.

Furthermore, the cerebellum contains a large quantity of glial cells which are located in the gray and white matter. In the following section, we will give an overview on the cytoarchitecture of the cerebellar cortex and describe the internal circuitry and cellular components of the cerebellar microcomplex.

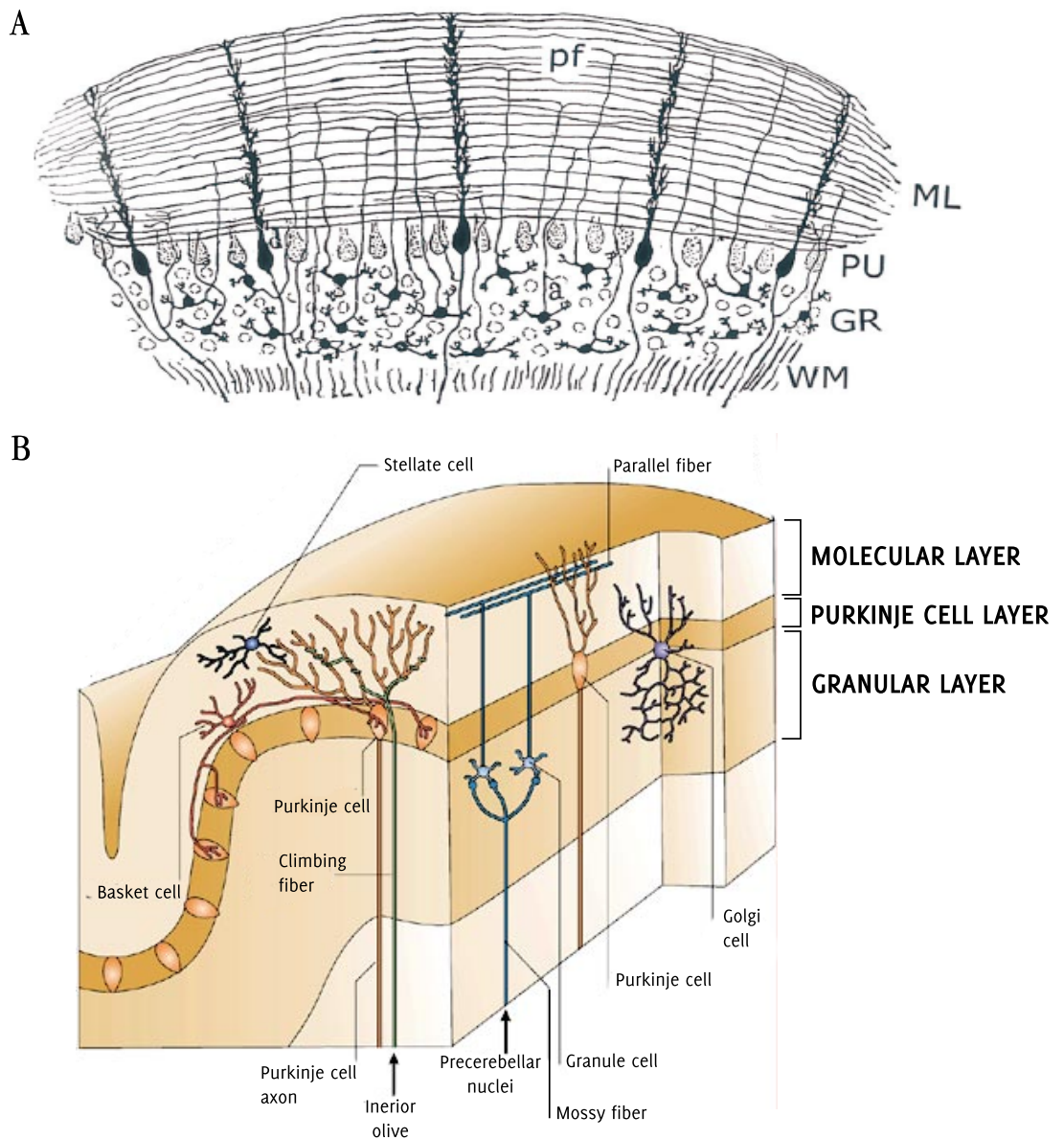


Figure 2.4: The cerebellar cortex **A.** Drawing from Ramon-y-Cajal of the cerebellar cortex (from Voogd and Glickstein, 1998) pf: Parallel fibers, ML: Molecular layer, PU: Purkinje cell layer, GR: Granular layer, WM: White matter. **B.** Simplified scheme of the surface of the cerebellar cortex showing the different layers (granular, Purkinje cell and molecular) of cells, and most of cerebellar cell types in their respective layer (from Apps and Hawkes, 2009).

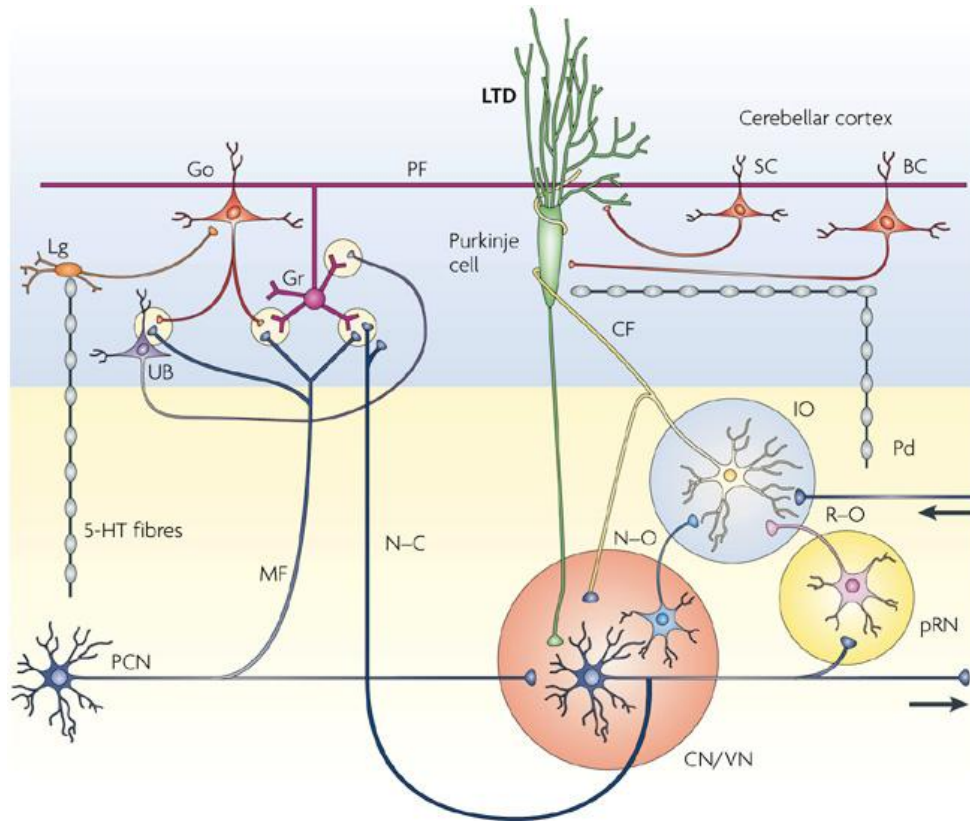


Figure 2.5: Neural circuit and path of information in a cerebellar microcomplex (from Ito, 2008). Mossy fiber (MF) projections arise from the precerebellar nuclei (PCN) and reach both the neurons of the deep cerebellar nuclei (CN) (or vestibular nuclei, VN), and the Purkinje cells through activation of granule cells and inhibitory interneurons. Golgi cells are excited by both mossy fibers and granule cells and retro propagate an inhibitory signal toward granular cells. Signals conveyed by the climbing fiber originate in the inferior olive nucleus. BC, basket cell; CN/VN, cerebellar nuclei/ vestibular nuclei; Go, Golgi cell; Gr, granule cell; IO, inferior olive; CF, Climbing fiber; Lg, Lugaro cell; MF, mossy fibre; N-C, nucleo-cortical projection; N-O, nucleo-olivary projection; PCN, precerebellar nucleus; PF, parallel fiber; Pd, peptidergic fibre; pRN, parvocellular red nucleus; R-O, rubro-olivary projection; SC, stellate cell; UB, unipolar brush cell

2.5.1 Internal circuitry

The path of information is described in figure 2.5. Mossy fibers reach the cerebellum and target both the deep cerebellar nuclei (DCN) and neurons from the granular layer, mostly granule cells and to a lesser extent, Golgi cells. The outflow of information from the cerebellum is conveyed by the axons of the DCN and vestibular nuclei, which project to different areas of the central nervous system. The sole output of the cerebellar cortex is the axons of the inhibitory Purkinje cells. Purkinje cells receive two major excitatory inputs, fundamentally different in the way they are organized. Each Purkinje cell receives the excitatory input of a single climbing fiber, which create numerous synapses with the dendritic tree of the PC. Climbing fibers also create collaterals that innervate the DCN with a few synapses and might also project sparsely to most types of neurons in the cerebellar cortex. In contrast, a single PC receives hundred thousands of synapses from parallel fibers. Parallel fibers also drive inhibitory basket and stellate cells, which in turn project to PC. Closing the loop, granule cells receive excitatory signals from the same mossy fibers that innervate DCN. Granule cells and mossy fibers also send projection to Golgi cells, which in turn inhibit the granular cells (mutual inhibition).

2.5.2 Cellular Types

Purkinje Cells (PCs)

Purkinje cells have first been described by the physiologist Johannes Purkinje in 1837 and are considered as the central element of the cerebellar circuit. Purkinje cells are inhibitory (GABAergic) neurons, and ones of the most voluminous neurons of the central nervous system: the ovoid soma of the mouse Purkinje cell measures on average 20 μm (Caddy and Herup, 1990). From the soma rises a very peculiar dendritic tree, highly organized, and entirely located in the molecular layer of the cerebellar cortex. The dendritic arborization can extend up to 400 μm in the sagittal plane, but is contained in a very narrow branch of 15 to 20 μm in the transversal plane. The large number of parallel fibers having synaptic contacts with the dendritic arborization of a PC allows an important convergence of information. It has been shown that, in humans, a single Purkinje cell can integrate information of up to 200,000 parallel fibers (Fox and Barnard, 1957), and 80,000 (Palay, 1974) or 175,000 (Napper and Harvey, 1988) in

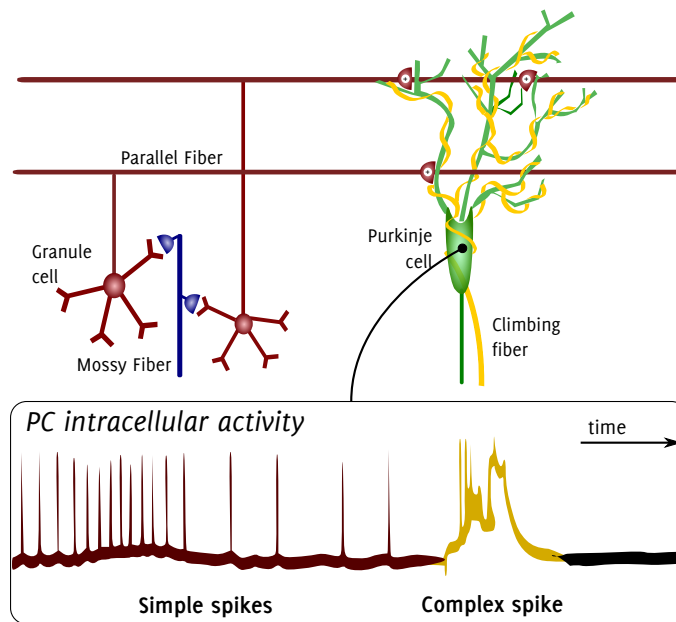


Figure 2.6: Simple and complex Purkinje cell spikes. Intracellular recording of a single Purkinje cell showing simple spikes (red) due to PF stimulation and a complex spike (yellow) caused by a climbing fiber discharge.

the rat.

A purkinje cell sends its axon into a vestibular or cerebellar nucleus (Ito and Yoshida, 1964). It constitutes the only efferent pathway of the cerebellar cortex and represents almost three quarters of the total synaptic contacts of a Purkinje cell. Also, the axon of the Purkinje cell can create bifurcation and send recurrent collaterals to neighboring Purkinje cells (Mugnaini, 1970; Hawkes and Leclerc, 1989; O'Donoghue and Bishop, 1990). These collaterals cause reciprocal inhibition among Purkinje cells within 300 μm of the parent axon. Additionally, collaterals target basket cells, which, in turn, inhibit Purkinje cells. Therefore, Purkinje cells are thought to be involved in a mixed reciprocally inhibitory network containing Purkinje cells and basket cells.

Electrophysiological properties. The spiking activity of cerebellar Purkinje cells relies on the synaptic stimulation of its afferent connections. Two types of spikes, namely simple-spikes and complex-spikes, can be observed from the recording of a single Purkinje cell activity (see figure 2.6). Simple-spikes are standard action potentials similar to those observed in

other areas of the central nervous system. PCs fire simple-spikes spontaneously at a frequency of 40 Hz on average (Apps and Hawkes, 2009). The irregular discharge of the cell is modulated by both the excitatory PFs contact with the PC dendritic tree and the inhibitory interneurons (stellate and basket cells).

By contrast, the complex-spike is unique to Purkinje cells and is characterized by multiple after-discharge action potential (a typical example of the complex membrane potential shape is shown in figure 2.6). Complex-spikes occur at very low frequency of about 1 Hz, they are caused by the activation of the whole PC's dendritic tree from a unique and very powerful discharge of the climbing fiber.

Granule cells

Granule cells are — with unipolar brush cells in the vestibulo-cerebellum — the only excitatory glutamatergic neurons of the cerebellar cortex. Granule cells are thought to be the smallest (soma is 5 μm in diameter) and most numerous neurons in the entire mammalian brain (10^{10} to 10^{11}) (Braintenberg and Atwood, 1958; Zagon et al., 1977). These latter properties give a granular aspect to this layer. Each granule cell receives input from mossy fiber terminals via only four to five excitatory synapses (Eccles et al., 1967; Chadderton et al., 2004). Functionally, this small convergence in the mossy fiber-granule cell pathway is quite intriguing and, consequently, different roles have been proposed for it. The principal theory states that the granular layer re-encodes and disambiguates the information, and therefore facilitates the integration of the information at the Purkinje cell level. This would be achieved by a sparse recoding (each granule cell represents an integration of a small number of mossy fibers). Additionally, this would minimize interferences between tasks being learned, thereby increasing information storage capacity (Philippona and Coenen, 2004; Brunel et al., 2004). See sec. 5.1.1 (page 53) for a detailed explanation.

Granule cell axons ascend vertically from the granular layer to the molecular layer and then bifurcate into two parallel fibers that run along the folia of the cerebellar surface for 2 to 3 *mm* on each side (Harvey and Napper, 1988; Mugnaini, 1983; Pichitpornchai et al., 1994; Coutinho et al., 2004; Arata and Ito, 2004). A large divergence characterizes the parallel fiber-Purkinje cell connection. One single parallel fiber passes through the

dendritic arborization of more than 450 Purkinje cells and forms synaptic contacts with approximately 50% of Purkinje cells they pass (Eccles et al., 1967). Each Purkinje Cell is innervated only once (up to twice) by the same parallel fiber (Harvey and Napper, 1988) on the intermediate or large diameter regions of spiny branchlets. Fifty simultaneously active granule cells are sufficient to excite a single Purkinje cell.

Ascending segments. The ascending segment of a granule cell axon also constitutes an important synaptic input of the Purkinje cell: about 20% of the granule cell-Purkinje cell synapses comes from this ascending segment (Ito, 2006). The ascending segment contacts exclusively the distal regions of Purkinje cell dendrites (Gundappa-Sulur et al., 1999). Since the location of connections of parallel fibers is different and ascending segment synapses are resistant to LTD-inducing protocols, it has been suggested that they play a very specific still unknown role, in Purkinje cell function.

Silent synapses. An interesting finding shows that up to 80% of parallel fiber-Purkinje cell synapses are silent or have a very low transmission efficacy (Wang et al., 2000; Isope and Barbour, 2002). Ekerot and Jörntell (2001) suggested that silent synapses are produced functionally by LTD, and that learning can reversely convert silent synapses to active synapses by the induction of long term potentiation.

Unipolar brush cells

Unipolar brush cells are located in the granular layer of the vestibulocerebellum. These cells receive excitatory synapses on their dendritic brush from a single mossy fiber terminal (Diño et al., 1999) and send axons that make contacts with both granular cells and unipolar brush cells (Diño et al., 2001). Functionally, these cells are thought to amplify the mossy fiber inputs in the vestibulocerebellum (Kalinichenko and Okhotin, 2005).

Basket and stellate cells

Basket and stellate cells are inhibitory neurons of the molecular layer, that convey feedforward inhibition to Purkinje cells. Basket cells create inhibitory synapses with the bottom part of a Purkinje cell's soma (Tigyi et al., 1990), and stellate cells do the same with Purkinje cell dendrites.

Basket and stellate cells are often collectively called inhibitory interneurons in the molecular layer. They receive excitatory inputs from parallel fibers. Basket cells receive collaterals from climbing fibers and from Purkinje cell axons (Palay, 1974; Jaeger et al., 1988). These inhibitory interneurons are also mutually and reciprocally inhibited (Kondo and Marty, 1998) and coupled with each other via electrical synapses (Mann-Metzer and Yarom, 1999). These interconnections might create an oscillation at high frequency rates (100 Hz to 250 Hz) as it was suggested by a neurocomputational study (Maex and De Schutter, 2005) and recorded at the cerebellar cortical surface in 1935 (Adrian, 1935). Activations of basket and stellate cells induce powerful inhibitory postsynaptic potentials in Purkinje cells (Eccles et al., 1967) and provoke a highly irregular rate in the discharge of the same Purkinje Cell (Eccles et al., 1967). This irregular rate has been shown to be mainly caused by inhibitory interneurons rather than excitatory synaptic influence (Häusser and Clark, 1997; De Schutter and Bower, 1994; Jaeger and Bower, 1999; De Schutter, 1999). The functional role of this irregular discharge is not fully understood but it was suggested from a modeling study that it could help Purkinje cells to optimally respond to external inputs (Van Vreeswijk and Sompolinsky, 1996). Wehr and Zador (2003) proposed that the feedforward inhibition might increase the temporal precision of the cerebellar computations. Indeed, feedforward inhibition would reduce randomness as only coincident granule cell inputs would be summed effectively enough to excite a PC.

Golgi cells

Golgi cells are the main inhibitory interneurons of the granular layer. They receive up to 5,000 inputs from parallel fibers and a bit more than 200 from mossy fibers terminals (Pellionisz and Szentágothai, 1973; Ekerot and Jörntell, 2001). They also receive inhibitory synapses from Lugaro cells. A Golgi cell, in turn, extends a broadly branching axon to up to 5700 granule cells in the cat (Palkovits et al., 1977). Golgi cells discharge tonically at about 5 Hz to decrease the firing rate of granule cells via GABA synapses (Chadderton et al., 2004). The main hypothesis about their function is that it should help stabilize the parallel fiber discharge regardless of large changes in mossy fiber firing (Albus, 1971). They can also decrease noise (Philipona and Coenen, 2004). It has also been shown that Golgi cell's inhibition might induce oscillation in the spike discharge of

the granular cells (Maex and De Schutter, 2005), which would account for the oscillations recorded in the granular layer of freely moving rats (Hartmann and Bower, 1998) and monkeys (Pellerin and Lamarre, 1997; Courtemanche et al., 2002; Courtemanche and Lamarre, 2005; Middleton et al., 2008; Courtemanche et al., 2010; Hartmann et al., 2010)

Lugaro cells

Lugaro cells are inhibitory interneurons located at the frontier of granular and Purkinje cell layer (Aoki et al., 1986; Sahin and Hockfield, 1990). Lugaro cells are activated by serotonergic fibers and, in turn, inhibit Golgi cells. A single Lugaro cell projects onto 150 Golgi cells (Dieudonne and Dumoulin, 2000) and one Golgi cell is thought to be the target for more than 10 Lugaro cells. If the role of this cellular substrate is still not well understood, an interesting possibility is that Lugaro cells play a role in synchronizing activity among Golgi cells located along the parallel fiber beam, as observed in anesthetized rats (Vos et al., 1999). Therefore, Lugaro cells may switch the operation of Golgi cells from an asynchronous to synchronous population-wise.

Afferents

The cerebellar cortex of mammals possesses two major entry pathways: the mossy fibers and the climbing fibers. Other sources, the monoaminergic and cholinergic fibers, arise in a diffuse way in all layers of the cerebellar cortex.

Mossy fibers. Mossy fibers are glutamatergic fibers that have been discovered by Ramon y Cajal in 1888. They arise from numerous sources in peripheral nerves, the spinal cord, and the brain stem and target a characteristic and specific structures of the granular layer of the cerebellar cortex called the glomerulus. Within this structure, granule cell dendrites are excited by mossy fiber terminals and inhibited by Golgi cells. The descending dendrites of some Golgi cells also receive excitatory synapses directly from a mossy fiber terminal. A mossy fiber supplies excitatory synapses to 400-600 granule cells: this large divergence has the effect of spreading the input signal to a large number of granule cells. The efficacy of synaptic transmission is thought to be affected by the activity-dependent induction

of LTP (D'Angelo et al., 1999, 2005), the enhancement of intrinsic excitability (Armano et al., 2000), and Golgi cell inhibition (Chadderton et al., 2004). The mossy fibers also produce many collaterals in the white substance that target the deep cerebellar nuclei.

Climbing fibers. The climbing fiber is the axon of a neuron of the inferior olive. This is a very specific structure of the cerebellum with no counterpart elsewhere in the central nervous system. Climbing fibers divide in the molecular layer of the cerebellum and travel through the granular layer of the cerebellar cortex. They mainly innervate Purkinje cell neurons, but connections can also be found with the majority of cerebellar cell types (Scheibel and Scheibel, 1954; Palay, 1974). Interestingly, each Purkinje cell is innervated by one climbing fiber (Crepel et al., 1976; Mariani and Changeux, 1981; Hashimoto and Kano, 2003; Scelfo and Strata, 2005), creating a tremendous number of synaptic contacts with the proximal dendrites of a Purkinje cell. Nieto-Bona et al. (1997) showed that in the rat, a single climbing fiber can form up to 26,000 contacts. It makes contact with only a few Purkinje cells (7 in average in the rat). Inferior olive neurons discharge at very low rate (1 to 2 Hz *in vivo*), and up to 10 Hz when activated with drugs. In slices, inferior olive neurons discharge with a highly regular rhythm, it was therefore proposed that one of the functions of the climbing fiber is to provide a periodic clock for coordinating movements or motor timing (Kazantsev et al., 2004; Llinás, 2009). However, it seems that in awake behaving animals, the signal occurs randomly (e.g., (Keating and Thach, 1995)). A coherent account of the interplay between rhythmicity, randomness, and synchrony in climbing fiber activity has been proposed recently, with a particular focus on chaos theory (Schweighofer et al., 2004; Kitazawa and Wolpert, 2005). The most influential theory has been proposed by Eccles, Marr, Albus and Ito, suggesting that the climbing fibers convey a learning signal that drives adaptation of the cerebellar system via plasticity mechanisms. This hypothesis has been reinforced by two fundamental findings: first, climbing fiber signals induce long term plasticity in co-activated parallel fiber-Purkinje cell synapses and second, climbing fibers convey information regarding errors in the operation of neural control systems.

Monoaminergic and cholinergic fibers. Monoaminergic fibers (noradrenergic and serotonergic) travel through cerebellar peduncles. Noradrenergic fibers arise from the locus coeruleus and distribute their chemical signals to the white matter, the granular layer, and the molecular layer. Serotonergic fibers come from the raphe median and principally target the deep cerebellar nuclei. Monoaminergic fibers are mainly thought to regulate synaptic transmission between cortical interneurons and Purkinje Cells (Oertel, 1993). Cholinergic fibers arise from the vestibular nucleus, and project to the flocculonodular lobe (Altman and Bayer, 1977). They might participate in modulating the activity of Purkinje cell in this nucleus.

Chapter 3

Cerebellar functions

In this chapter, we review the hypothesized functions of the cerebellum. Each section and subsection highlights a specific cerebellar role. A short historical introduction is given at first.

3.1 Historical introduction

"...we ought to think that the cerebellum too, which must be the source of the nerves for the whole body, contains a very large quantity of this pneuma [air, natural spirit], and that the intervening regions that connect the parts of it are the pathways for pneuma. Erasistratus [300-260 B.C.E] was right when he declared that the epencranis (for this is what he calls the cerebellum) has a more intricate structure than the encephalon. On the other hand, when he says that the epencranis itself and along with it the encephalon are more complex in man than in other animals because man's intelligence is greater than theirs, it seems to me that his understanding is no longer so correct; for even donkeys have an exceedingly complex encephalon, whereas judging by their stupidity it ought to be perfectly simple and uncomplicated." (Galen, 131-200 AD)

The cerebellum has been first mentioned in scientific literature in the fourth century B.C. in the biological writing of Erasistratus (335–280 BC). At this time, early anatomists described the cerebellum as a distinct division of the brain; and Galen, one of the first to give a clear description of the structure, named it *parencephalon* (Latin for "same as brain"), in opposition to the *encephalon* ("brain"). He also noted that cerebellar tissues were more solid than the rest of the brain, and concluded that its role might be to

strengthen the motor nerves. Afterwards, and during an extended period of time, people thought the cerebellum to be the seat of memory. There was a popular belief that the prominence of the *occiput* - the bone overlying the cerebellum - was a measure of the power of intellect, and that memory was located in the fourth ventricle or in the cerebellum. Later, in the 17th century, cerebellar function was ascribed to the control of involuntary movement related to cardiac and respiratory functions (Clarke and O'Malley, 1996). This idea of the cerebellum as the seat of vital function was mainly promoted by Thomas Willis and supported by clinical observation. Another theory was advanced at the beginning of the 19th century, by Gall and Spurzheim, who claimed that the cerebellum controlled sexual activity. This theory was (in part) considered valid till the beginning of the 20th century (an historical review can be found in Clarke and O'Malley, 1996).

3.2 Sensorimotor role of the cerebellum

The first clear hypothesis of a sensory-motor role of the cerebellum has been proposed at the beginning of the 19th century by Luigi Rolando. In 1809, he observed that damages to the cerebellum resulted in motor disturbances (see Ito, 2002 for review). Some 15 years later, Flourens (1824) revealed that animals with cerebellar lesions presented a loss of coordination, and observed that cerebellar ablation did not forbid initiation of movements, and did not consequently produce paralysis. While Flourens argued that cerebellar lesions impaired directly the coordination and the integration of movements, an alternative view was drawn by Luciani (1892) who suggested that cerebellar lesions caused deficits in single muscle control rather than mis-coordination. He identified three related fundamental deficits that he called *atonia* (loss of muscle tone), *asthenia* (weakness of muscle) and *astacias* (deficit in the regularity and stability of muscles contraction). At the end of the 19th century, it was widely accepted that the primary function of the cerebellum was related to sensory-motor control but there were divergent interpretations on its causes due to Flourens and Luciani differential views.

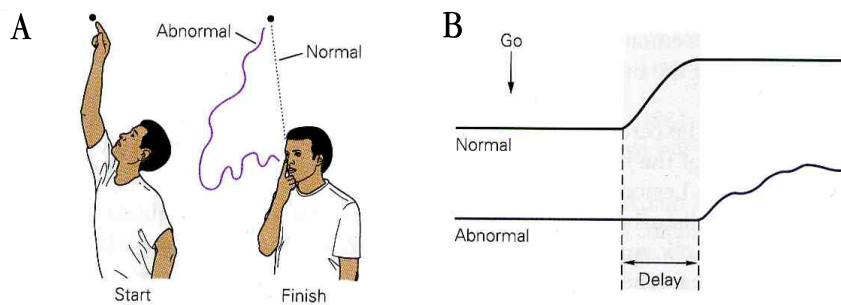


Figure 3.1: Examples of human defects observed after cerebellar lesions (taken from Ghez and Thach, 2000) **A.** In a finger to nose task, starting from a raised arm position, a cerebellar patient moves its shoulder first and elbow second, showing decomposition problems, and presents inaccuracy in both range and direction. When getting closer to the nose, tremor also increases. **B.** In a task where the a cerebellar patient with a lesion to the right cerebellar hemisphere is told to clench both hands at the same time after the presentation of a signal, initiation of left hand movement is delayed.

3.2.1 Cerebellum participates in fine tuning of coordinated movements

The first half of the 20th century has produced numerous detailed descriptions of clinical symptoms associated with cerebellar diseases or lesions in humans.

Disorders of the human cerebellum were described originally by Babinski in 1899 and by Holmes (Babinski, 1899; Holmes, 1939). Holmes conducted clinical researches on the consequences of gunshot destructive lesions in the cerebellum during the first and second World War. He demonstrated that cerebellar lesions classically produced *ataxia* (gait disturbance), *hypotonia* (lack of muscular tone), *dysmetria* (lack of movement coordination) and *nystagmus* (impairment of ocular reflexes). He suggested that most of the symptoms could be explained by Luciani's theory, but remarked that more complex cerebellar ataxia could not be simply justified in terms of single elementary deficits (Holmes, 1939). He also confirmed that paralysis or sensory deficits was not the consequence of cerebellar damages or ablation in humans.

More recent experiments have reinforced the idea of a direct involvement of the cerebellum in the complex coordination of movements rather

than a simple single joint control (see Thach et al., 1992 for review). For example, Thach and coworkers studied the effect of deep cerebellar nuclear inactivation in monkeys and showed that each nuclear inactivation produced an incapacitating impairment of complex movements which was independent from the others impairments (Thach et al., 1992).

Also, in a functional magnetic resonance imaging (fMRI) , Miall et al. (2001) demonstrated that areas in the lateral cerebellar hemispheres and in the vermis were activated with the independent control of hands and eyes in a tasks where subjects had to follow a moving target with a cursor controlled by a joystick (Miall et al., 2001).

Other examples of impaired coordination and cerebellar deficits in humans are presented in figure 3.1.

3.2.2 Cerebellum participates in motor learning

While it is clear that the cerebellum is used in the control of smooth and accurate movements, its contribution has also been investigated in motor learning. Evidences of such capabilities largely come from analysis of eyelid conditioning and eye movements reflexes; but it has also been demonstrated in a large set of more complex tasks.

Eyeblink conditioning

Definition. Eyeblink conditioning (EBC) is a classical form of pavlovian conditioning where the cerebellum is known to be largely implicated (e.g., McCormick and Thompson, 1984).

EBC is based on the innate reflex of many mammals which close the eyelid when the cornea is exposed to an aversive stimulus, for example a puff of air. This puff of air could be identified as an unconditioned stimulus (US) that causes the closing of the eyelid, namely the unconditioned response (UR). Grant and colleagues developed a paradigm where the eyelid closing could be conditioned by another stimulus, generally a sound presented before the puff of air (Grant et al., 1960). In this paradigm, the tone would eventually become the conditional stimulus (CS) permitting to anticipate the puff of air (US). Before conditioning, no response is elicited by the presentation of the CS. After conditioning, the UR is anticipated by the simple presentation of the CS (see figure 3.2a). This anticipated response constitutes the conditioned response (CR).

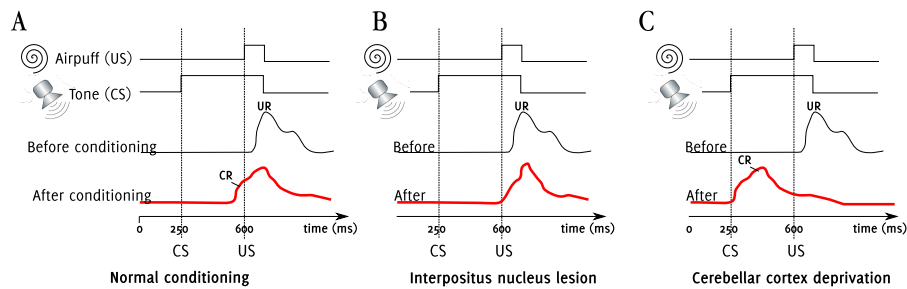


Figure 3.2: Eyeblink conditioning A puff of air (US) and a tone (CS) are conjointly presented to a naive animal. **A.** In a control animal, before conditioning, the response is observed only after presentation of the US. After conditioning, the expression of the response is conditioned by the presentation of the CS and occurs just before the US. **B.** In an animal with a lesion in the interpositus nucleus, after the same conditioning paradigm, the expression of EBC is not conditioned by the presentation of the CS. Hence, the CR is not observed. **C.** After a cerebellar inactivation; the CR is still observed, but timing is disrupted and eventually occurs right after the presentation of the CS, and is not timed to the US.

Role of the interpositus nucleus and the cerebellar cortex. Results from lesions, inactivations, and neural recording studies seem to demonstrate that the dorsolateral portion of the anterior interpositus nucleus of the cerebellum is an essential site for CR acquisition and expression in EBC (see figure 3.2b; Lincoln et al., 1982; Lavond et al., 1985, 1993). Conversely, the importance of cerebellar cortex in EBC is still a matter of debate in the scientific community. The most admitted conclusion is that the cerebellar cortex (and more precisely HVI lobule) is not essential for learning the eyeblink CR, but plays a significant contribution in expressing a normal conditioning, notably in finely timing the conditioned response (Attwell et al., 2001). This contribution is supported by two lines of evidence. First, when animals are deprived of cerebellar cortical output, responses are preserved but their timing is disrupted (see figure 3.2c; Garcia and Mauk, 1998); second, in L7-PKCI mice, lacking LTD between parallel fiber and Purkinje cell, the conditioned response is still present, but the accurate timing is lost (Koekkoek et al., 2003). The long term depression at PF-PC synapses is hence hypothesized to have an important functional role for learning the timed behavioral CR in EBC (for review, see Ito, 2006).

Ocular reflexes

The vestibulo-ocular reflex (VOR) is a reflex movement of the eye that stabilizes images on the retina during head movements. It produces an eye movement in the opposite direction to the movement of the head, and preserves the image on the center of the visual field. VOR is a typical feedforward control system with no feedback loop, and has both rotational and translational aspects (Paige and Seidman, 1999). Gonshor and Melvill-Jones (1976) reported that dove prism goggles that reverse the right-left axis of the visual field gradually depressed and reversed the VOR in human subjects (Gonshor and Jones, 1976). The neuronal circuitry implied in the adaptation of the VOR is well identified and described, and is known to implicate the cerebellum. A typical protocol of VOR adaptation is presented in figure. 3.3.

It has been demonstrated that ablation of the flocculus prevents learning of VOR adaptation (Ito, 1974; Nagao and Ito, 1991; Nagao, 2003) and that lesions of the inferior olive abolished adaptive gain changes in the VOR (Ito and Myashita, 1975). Eventually, it has been shown that a temporary inactivation of the cerebellar cortex prevents the expression of a rapid adaptation of the VOR (Attwell et al., 2002).

Cerebellum has also been proved to be determinant in the adaptation of other ocular reflexes, such as the the optokinetic eye movement response and ocular following response, two reflexive movements of the eyes expressed after a displacement of the visual field (for review, see Ito, 2006).

Voluntary movement

The two paradigms we just detailed demonstrated that cerebellum is actively participating in motor learning in some simple and reflexive adaptation and classical conditioning tasks. As mentioned earlier, the cerebellum has also been shown to participate in the adaptation of more complex voluntary movements. The role of the cerebellum in such paradigms has been studied in many tasks such as throwing of objects while looking through prism (Martin et al., 1996a,b), adapting finger grip-force (Kawato et al., 2003), reaching (Kitazawa and Yin, 2002; Norris et al., 2004; Miall et al., 2007), manipulating new objects (Imamizu et al., 2000), and smooth pursuit eye movements (Kahlon and Lisberger, 2000).

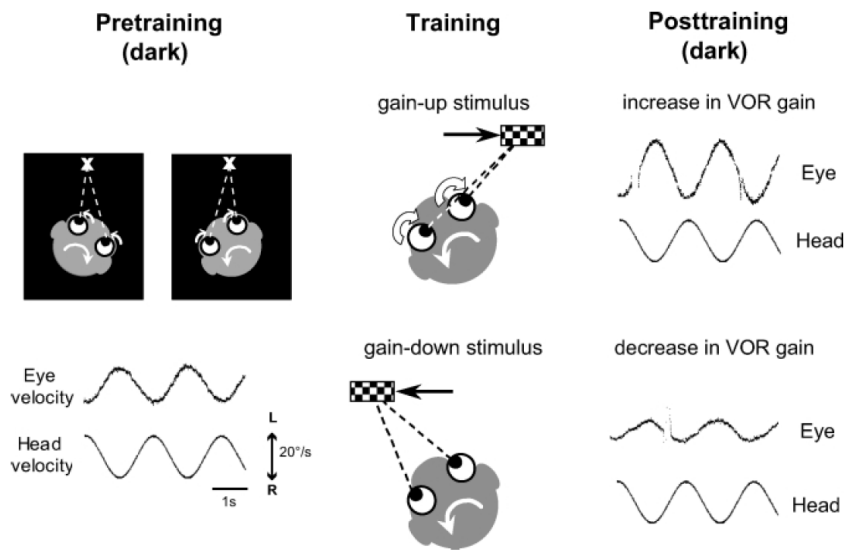


Figure 3.3: Motor learning in the VOR. (Boyden et al., 2004) “Before learning (left), eyes move with the same speed, but in the opposite direction of the head, keeping the eyes stationary in world coordinates. An increase in VOR gain is produced by training (middle) with image motion in the direction opposite that of the head (gain-up stimulus). A decrease in VOR gain is produced by training with image motion in the same direction as the head (gain-down stimulus). After each training session, the VOR is remeasured in the dark (right) with the same head movement stimulus used in the pretraining measurements.” (Boyden et al., 2004)

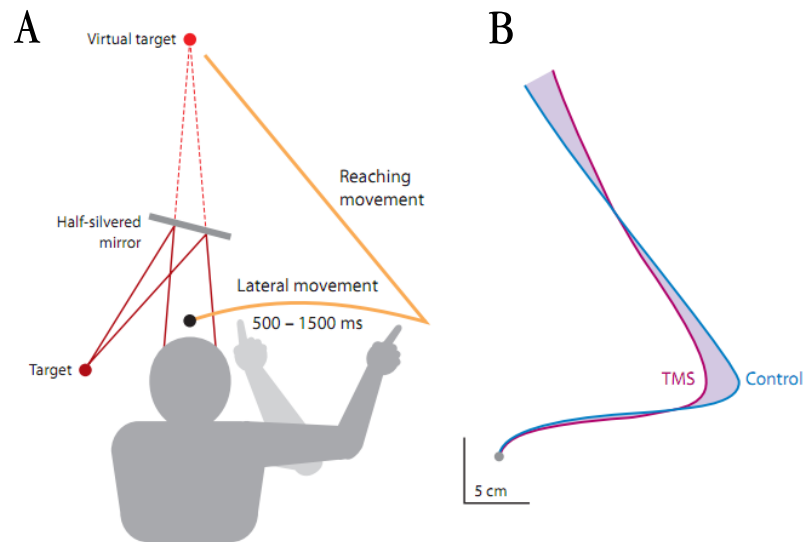


Figure 3.4: Example of cerebellar involvement in a reaching task (taken from Miall et al., 2007) **A.** Volunteers were asked to move their hand laterally until they heard a tone, at which point they would reach toward a target. The cerebellum was disrupted via a TMS pulse soon after the tone. **B.** Reach trajectories from a trial in which TMS was applied to the cerebellum, and a trial in which no TMS was applied. Application of TMS produces a movement in which the estimate of the state of the arm appears to be delayed with respect to its actual state, resulting in missing the target to the right.

For example, the cerebellum has been shown to play a role in a reaching task where subjects had to interrupt a slow voluntary lateral movement to rapidly reach towards a visually defined target (Miall et al., 2007). The authors showed that by disrupting the function of the cerebellum using a transcranial magnetic stimulation (TMS), it was possible to deviate the reaching movement and induce errors in the initial direction and in the final position of finger. The range of reported errors suggested that the cerebellum was responsible for estimating the hand position over the reaching period (see figure 3.4 and Miall et al., 2007).

In another study, Imamizu and colleagues (2000) demonstrated that the cerebellum was highly activated when manipulating new tools (Imamizu et al., 2000). Authors trained subjects to manipulate three different types of computer mice: (i) a rotated mouse whose cursor appeared at a rotated position, (ii) a velocity mouse whose cursor velocity was proportional to

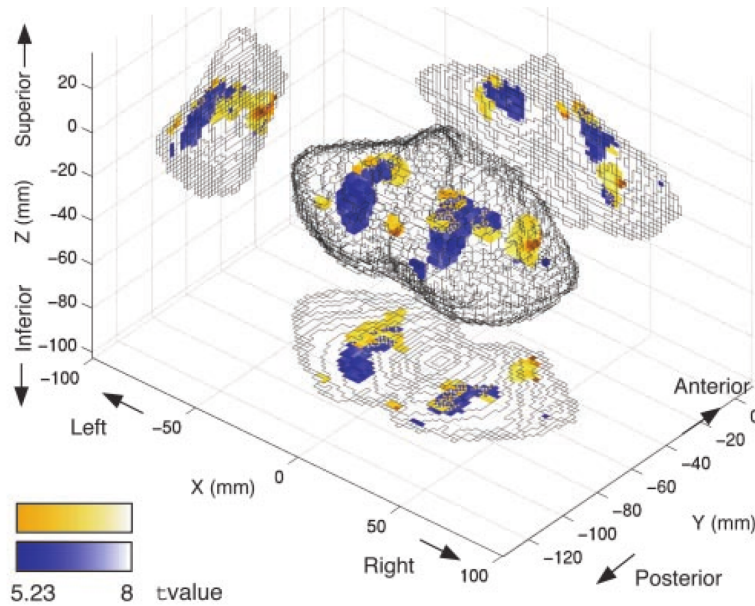


Figure 3.5: Manipulation of new tools (pointing devices), taken from Imamizu et al., 2003 Cerebellar regions related to manipulation of a new tool as revealed by multiple regression analysis. Regions are shown in superior-posterior-lateral view (Center), lateral view from right side (Left), superior view (Bottom), and posterior (Right) view. Orange and blue colors indicate regions where the activation was correlated with the manipulation of rotated and velocity mouse, respectively. (Kawato et al., 2003)

the mouse position, and (iii), a normal mouse. An fMRI study showed that subjects could easily switch between mice and that the lateral and posterior cerebellar activities for two different tools were spatially segregated, thus indicating a spatial and functional modularity in the neural organization of cerebellar processes (see figure 3.5).

3.2.3 Cerebellum participates in timing of movements

While there have been overgrowing evidence of a role of the cerebellum in motor coordination and learning, other authors proposed that the cerebellum might have a more general purpose and would provide an internal clock (e.g., Lamarre and Mercier, 1971; Llinás and Yarom, 1986; Ivry et al., 1988; Keele and Ivry, 1990). This timing idea was first advocated by Braintenberg and Atwood (1958), soon before Eccles, Ito and Szentágothai reviewed the cerebellar circuitry (Eccles et al., 1967). Since, there has been

a continuous debate as to whether the role of the cerebellum in motor coordination and learning could be directly derived from a cerebellar timing function.

The main evidence comes from neuro-psychological studies, showing that cerebellar patients are impaired in discriminating between two different interval durations and in maintaining a simple rhythm. They produce, in comparison with control subjects, variable temporal intervals and their temporal judgment are less accurate. Authors suggested that medial cerebellar damage impairs motor execution, while lateral cerebellar damage impairs the internal timing of responses (Ivry et al., 1988; Ivry and Keele, 1989). In another study, Manto et al. (1996, 1995) also identified critical motor timing component of the cerebellar processing in a fast single-joint movements by using electromyographic recordings (Manto et al., 1996, 1995).

However, it seems unlikely that the cerebellum only act has a pure timing operator. Indeed, there does not seem to appear a clock-like timing signal, neither in the discharge pattern of the Purkinje cells, nor in the deep cerebellar nuclei (Keating and Thach, 1995, 1997). Instead, it has been proposed that the inferior olive could help to organize movement in time: hence, coordination, motor learning and timing might not be exclusive as suggested by Mauk and co-authors (2000). The cerebellum might contribute to the synchronization of movements via motor learning, and with specific temporal information (Mauk et al., 2000). This idea is well illustrated with the analysis of the previously presented eyelid-conditioning. When the task has been learned, the response is elicited just before the appearance of the unconditioned stimulus, letting suppose that there is an internal mechanism inside the cerebellum that is capable of encoding both the motor command that lead to a blink and the temporal properties of the response. Hence, it is possible that motor coordination, learning and timing are mechanisms encoded in the cerebellum.

3.3 Cerebellum and non motor functions

The debate of a non-motor role of the cerebellum arose at the beginning of the 1990s, when Leiner showed that the expansion of lateral lobes of the cerebellum and the size of the dentate nucleus had occurred jointly with the expansion of the frontal lobe of the cerebral cortex during evolution

(Leiner et al., 1991). Since it correlated with the progressive increase of cognitive capabilities in animal, the authors proposed that the cerebellum might be implied in cognitive functions. Since, the cerebellum is believed to participate in a wide range of non-motor functions, although its precise role is still highly controversial (e.g., Glickstein, 2007; Glickstein and Doron, 2008 for recent review).

Recent anatomical studies demonstrated that cerebellar outputs target non motor areas, thus giving cerebellum the anatomical substrate to influence cognitive tasks (see Strick et al., 2009 for a recent review). Furthermore, neuroimaging and neurophysiological studies emphasized nonmotor aspects of the cerebellar function. In this section, we give a short review of these lines of investigation.

3.3.1 Anatomical evidences

The cerebellum receives information from frontal, parietal, temporal and occipital lobes (Glickstein et al., 1985; Schmahmann, 1996) and sends projection to the ventrolateral nucleus of the thalamus (VTN) (Allen and Courchesne, 2003; Brooks and Thach, 1981). Although it has long been thought that the VTN was only projecting to the primary motor cortex, it has been demonstrated that it also sends efferents to a wide number of cortical areas, including, frontal, prefrontal and parietal cortex (for a review, see Strick et al., 2009), in separated close loop circuits. Thus, a lesion in a subregion of the cerebellar cortex can lead to limited deficit, either motor or not, depending on the site of the lesioned circuit (e.g. Allen and Tsukahara, 1974; Fiez et al., 1992; Gottwald et al., 2004; Schmahmann and Sherman, 1998). Furthermore, if the closed-loop circuit is a general rule of the cerebellar architecture, it is suspected that the full extent of cerebellar influence over non-motor areas could be much larger than we already know (e.g. Brodal, 1978; Schmahmann and Pandya, 1991). These anatomical evidences are also completed by neuroimaging studies and neuropsychological and clinical descriptions.

3.3.2 Neuroimaging

Functional imaging reveals the activation of cerebellar zones during the execution of non-motor experimental tasks. A wide number of cognitive procedures have been tested and have reported activity in different areas

of the cerebellar cortex. For example, an imagery study showed that during reading, the cerebellum was activated differently depending on the task being performed: a phonological task where the subjects have to decide if a pair of words is rhyming would mainly activate the lateral region of the cerebellar cortex, whereas a semantic task would cause a higher activation of the deep cerebellar nuclei (Fulbright et al., 1999). Also, during an associative linguistic task, Peterson (1989) demonstrated that the right hemisphere of the cerebellum showed greater blood flow when subjects had to substitute the verb being shown by the corresponding noun or synonym as compared with a task where subjects simply had to read or repeat nouns (Petersen et al., 1989). Other studies focusing on memory showed that memory encoding involves the cerebellum, and more particularly the posterior-superior part (Fliessbach et al., 2007).

3.3.3 Neuropsychological and clinical descriptions

Human lesion studies shed light on the functional relevance of the cerebellar activation observed in neuroimaging studies. The range of tasks associated with cerebellar lesions or related disease is also very diverse. (e.g. language, attention, learning, pain, emotion or addiction (Glickstein, 2007; Glickstein and Doron, 2008; Timmann et al., 2009 for review), it has been observed that children with a history of posterior fossa tumors are at risk for a variety of intellectual, emotional, and educational impairments (Cantelmi et al. (2008))

Emotional and attentional disorders

Schmahmann et Sherman (1998) observed that patients with cerebellar lesions exhibited a large set of symptoms in a variety of tasks ranging from motor execution, verbal and spatial cognition, language, attention and emotion (Schmahmann and Sherman, 1998). This set of symptoms was termed the cerebellar cognitive affective syndrome. Subsequent studies further documented the effects of cerebellar damages, collectively providing evidences for impairments on standardized and experimental measures of attention and executive control, procedural memory, working memory, language and visual-spatial processing (Timmann and Daum, 2007). Also, in autism, it has been proposed that the cerebellum could be one of the structure responsible for some of the observed symptoms (e.g.,

Amaral et al., 2008). In such mental troubles, cerebellar impairment might cause deficits in attention, social interaction, verbal or non verbal communication, stereotyped movements and obsessions. Parvizi (2001) proposed that the cerebellum might regulate emotion according to the context and that the absence of control could lead to inappropriate responses and mood disorders (apathy, lack of empathy, disinhibition, impulsive acts, irritability, inappropriate jokes and regressive behaviors (Parvizi et al., 2001).

Eventually, some psychotic symptoms such as schizophrenia, depression and anxiety might sometimes be related to cerebellar damages (Andreasen and Pierson, 2008).

Language disorders

Riva and Giorgi (2000) observed language deficits in children after resection of cerebellar tumor. In the main, it was remarked verbal hypospontaneity, with brief and delayed answers, suggesting that cerebellum may act in planning speech production (Riva and Giorgi, 2000). Altered speech perception has also been reported and appears to affect the temporal component used to judge the duration of a syllable or sound (Ackermann et al., 2007). Recently, it has also been proposed a role of the cerebellum in dyslexia (Nicolson and Fawcett, 2005).

Visuospatial and time perception disorders

Visuospatial disorders have been reported in some cerebellar patients, and cerebellar role in the judgment in orientation has also been suggested (Molinari and Leggio, 2007). Visual memory also seem to be altered (Schmahmann and Sherman, 1998). Furthermore, time perception appears to be disturbed in patient presenting cerebellar atrophy or unilateral damage (Ivry et al., 1988; Harrington et al., 2004).

Cerebellum and spatial cognition

More recently, the cerebellum has been shown to be implicated in spatial cognition. Orientation problem and goal directed behavior deficit have been reported after cerebellar lesions in animals (e.g., Petrosini et al., 1996). The precise role of the cerebellum in spatial cognition will be detailed in chapter 11, page 155.

Chapter 4

Cerebellar plasticity

As mentioned in the previous chapter, learning in the cerebellum has been revealed by simple associative tasks such as eyelid conditioning and other adaptation processes like ocular reflexes. It has long been proposed that a long term depression at parallel fibers and Purkinje cell's synapses (PF-PC LTD) would constitute a suitable mechanism to adapt the dynamics of the microcomplex and to retain the motor memory (Marr, 1969; Albus, 1971). Or, in recent years, it has become clear that this form of plasticity, referred as 'cerebellar LTD' (Hansel et al., 2001), might not account on its own for all form of learnings (see Hansel et al., 2001 for a review, and Schonewille et al., 2011). Indeed, many behavioral studies reveal that many plasticity sites might participate to the setup of memories in the cerebellum. Evidence comes from, in part, Pavlovian eyelid conditioning, where disconnecting the cerebellar cortex abolishes one component of learning — the response timing — but preserves the expression of abnormally timed responses. Depending on the type of plasticity and its location in the neuronal circuit, their roles could be either complementary or independent of the PF-PC LTD (Boyden et al., 2004; De Zeeuw and Yeo, 2005), and play distinct but fundamental functions, such as regulating the dynamics of the movements, storing memory for different time scales or providing direction changes in the amplitude of movements (Boyden et al., 2004; De Zeeuw and Yeo, 2005). A good understanding of cerebellar plasticity mechanism is of fundamental importance since each one must act in combination with a specific encoding of the neuronal signal. In this chapter, we review the plasticities of the cerebellar formation, and we give insights on their postulated functions. The plasticity sites reviewed in this chapter are summarized in figure 4.1.

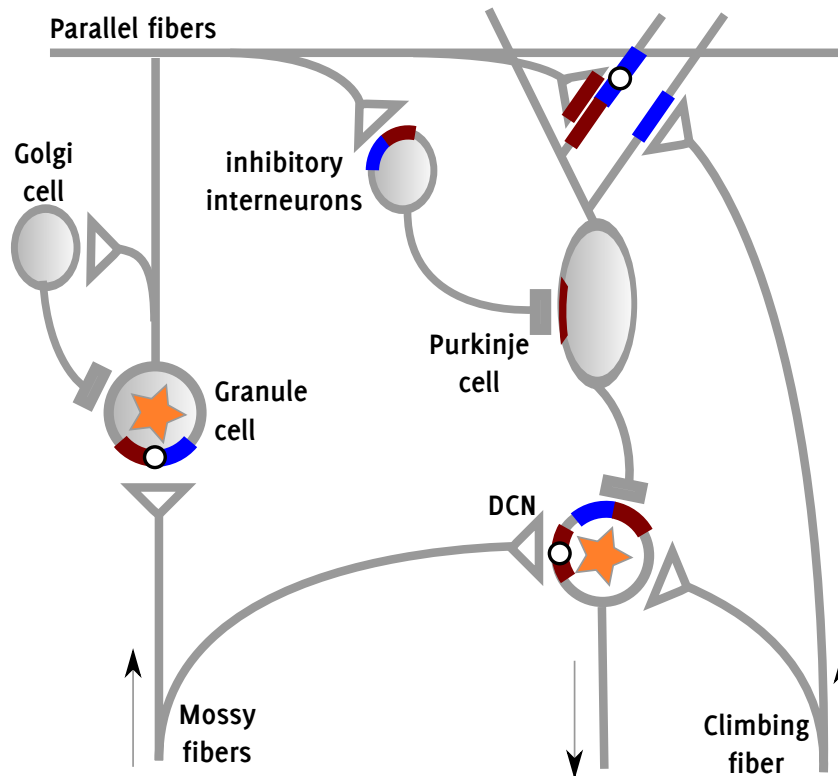


Figure 4.1: Plasticity sites (adapted and completed from Hansel et al., 2001) The main plasticity sites are shown in the neuronal cerebellar circuit (adapted from Hansel et al., 2001). Color bars at the level of synapses indicate referenced LTD (blue) and LTP (red). The localization of the color bar (pre or post synaptic) indicates the site of expression of each plasticity. An orange star in the soma of neurons indicates an intrinsic plasticity. The heterosynaptic plasticities are indicated by a small white circle in the color bar.

4.1 PF-PC LTD

PF-PC LTD has first been observed by Ito in 1982 (Ito and Kano, 1982) and since, it has been considered as the main mechanism responsible for cerebellar learning. PF-PC LTD is heterosynaptic, it needs the conjoint stimulation of the climbing fiber (CF) and the parallel fibers (PF) to occur. Also, PF-PC LTD is expressed post synaptically (Wang and Linden, 2000; Xia et al., 2000). A repeated induction of PF-PC LTD leads to a saturation of the response, with a maximum decrease of about 50 % (Hansel et al., 2001). A complete description of the cellular mechanisms involved is behind the scope of this document, but can be found in Evans (2007). Safo and Regehr (2008) examined the timing dependence of LTD by using an induction protocol consisting of a single CF activation paired with a PF burst, and with the relative timing of CF and PF activation systematically varied (Safo and Regehr, 2008). LTD was most prominent when PF activation occurred before CF activation. LTD peaked for PF activity approximately 80 *ms* before CF activation. Also, half of this maximum amplitude is observed if CF spikes 300 *ms* after the PF burst, thus suggesting that timing is fundamental. Heterosynaptic LTD has been the first to be discovered in the cerebellum and its function is mainly thought to contribute to motor learning (see chapter 5 for more information). However, a recent reevaluation suggests that this synaptic plasticity would not be essential for motor learning (Schonewille et al., 2011).

4.2 PF-PC LTPs

Homosynaptic presynaptic potentiation at PF-PC synapses can be induced after a low frequency stimulation (2 to 8 *Hz*) without a stimulation of the climbing fiber (Sakurai, 1987). Bear (2003) suggests that this plasticity could participate in the integration of parallel fibers signals. A form of LTP that is expressed postsynaptically in the Purkinje cells has been characterized less than 10 years ago by Lev-Ram and colleagues (Lev-Ram et al., 2002; Coesmans et al., 2004). This PF-PC LTP is homosynaptic, and it has been suggested that it could reverse PF-PC LTD (Boyden et al., 2004), and therefore may participate to motor learning. Also, very recent studies using cerebellar mice for which the expression of post synaptic LTP at the PF-PC synapses was blocked suggest that this plasticity might be as

important as PF-PC LTD (Schonewille et al., 2010a).

4.3 CF-PC LTD

Hansel and Linden (2000) showed that an homosynaptic LTD between CF-PC synapses could be induced after a tetanization of the climbing fibers (Hansel and Linden, 2000). This LTD does not propagate to PF-PCs synapses, and is thought to be postsynaptic (Hansel et al., 2001). Functionally, it has been proposed that CF-PC LTD could play a role during the development of the neuronal system and might cause the elimination of surplus climbing fibers (Hansel et al., 2001). Because of a limited amplitude of the attenuation ($\approx 20\%$ of EPSC) and a very slow firing rate of inferior olive *in vivo* ($\approx 1 - 2$ Hz), it is likely that CF-PC LTD is of no relevance for cerebellar function, but this is still to be determined (see Hansel et al., 2001).

4.4 MF-GR LTD and LTP

LTP at MF-GR's synapses can be induced by using a theta burst pattern or a single tetanus paired with a postsynaptic depolarization of mossy fiber EPSC (D'Angelo et al., 1999; Armano et al., 2000). Furthermore, low-frequency stimulation causes a LTD at MF-GR's synapses (Armano et al., 2000). These plasticities are expressed postsynaptically; also, the Golgi cell projections to the glomeruli seem to be a necessary condition for the plasticity to occur (Armano et al., 2000). The role of MF-GR LTP and LTD is not completely understood. It might enhance coincidence detection in the granular layer, and re-encode the information to convey optimal signals to Purkinje cell layer (Schweighofer et al., 2001). Albus (1971) suggested that LTD could permit sparse coding of the information. As remarked by Hansel (2001), a regulation of synaptic strength at this synapse, together with changes in intrinsic excitability and in the strength of Golgi cell-granule cell connections, may have a critical influence on the selection of mossy fiber patterns to be relayed to the cerebellar cortex (Hansel et al., 2001).

4.5 PC-DCN LTD and LTP

LTP and LTD have been observed at the level of Purkinje cell-deep cerebellar nuclei's synapses. These plasticities can occur following repeated stimulations of Purkinje cells and with conjoint activations of mossy fibers (Morishita and Sastry, 1996; Aizenman et al., 1998; Ouardouz and Sastry, 2000). This synaptic plasticity could reflect an hypothetical long-term memory storage outside the cerebellar microcomplex, in the cerebellar and vestibular nuclei. For example, anatomical studies have shown that, following a simple paradigm of eyeblink conditioning, there was an increased number of excitatory synapses in the pontine deep cerebellar nuclei, which could reflect a memory site at this level.

4.6 MF-DCN LTD and LTP

The first plasticity mechanisms that have been observed between mossy fibers and deep cerebellar nuclei are an homosynaptic LTP and LTD. Both could be induced by stimulations at very high frequency of the mossy fibers (Racine et al., 1986), which is unlikely to occur in standard condition *in vivo*. More recently, Zhang and Linden observed a postsynaptic LTD after a burst of stimulations of mossy fibers (Zhang and Linden, 2006). The same year, Pugh and Raman suggested that a LTP may also occur at the MF-DCN's synapses, but that it would not follow a simple Hebbian's rule (Pugh and Raman, 2006). They observed that standard tetanization protocols fail to potentiate the nuclear cells and showed that a significant activation of mossy fibers paired with an hyperpolarization of deep cerebellar nuclei would induce a potentiation of MF-DCN's synapses. They observed two necessary conditions: (i) High frequency stimulation of the afferent mossy fibers, and (ii) a post-inhibitory rebound of the cerebellar nuclei. A repeated induction of PF-PC LTD leads to a saturation of of the response, with a maximum increase of about 60 % (Pugh and Raman, 2006). The authors suggested that the Purkinje cell inhibition may guide the strengthening of excitatory synapses in the cerebellar nuclei; in this condition, MF-DCN LTP would be heterosynaptic. Functionally, such a plasticity site is thought to be required for associative learnings and might participate in many motor and non motor adaptive tasks (Boyden et al., 2004).

4.7 Interneurons' LTD and LTP

The parallel fiber–stellate cell synapse has been shown to have several forms of plasticity. Rancillac and Crepel (2004) described an LTP and an LTD (Rancillac and Crépel, 2004) ; and Soler-Llavina and Sabatini (2006) have identified a form of post-synaptic LTD (Soler-Llavina and Sabatini, 2006). At the stellate cell–Purkinje cell synapse, there is a post-synaptic form of plasticity termed rebound potentiation (RP) (Kano et al., 1992). Modification of the interneuron–Purkinje cell synaptic strengths are likely to have a major influence on Purkinje cells output. For example, it has been demonstrated that a single action potential evoked by an inhibitory interneuron can generate delays in the Purkinje cell firing and that a tonic inhibitory input can drastically modulate the spike firing pattern in Purkinje cells (Häusser and Clark, 1997). Furthermore, a modeling study has suggested that these inhibitory synapses might be a site for long term storage of memory encoded by PF-PC plasticities (Kenyon, 1997).

4.8 Non-synaptic plasticity

While the synaptic plasticities are considered as the main cause of the memory storage in the cerebellum, another type of plasticity, non-synaptic, may be of high functional importance in the way the cerebellum processes and stores information. One hypothesis is that information processing and memory may involve the intrinsic excitability plasticity of the cerebellar neurons. This type of plasticity has been shown to occur in deep cerebellar nuclei (Aizenman and Linden, 2000) and in granular cells (Hansel et al., 2001). In these two cellular types, it has been observed an increased number of spikes without change in the relative size of EPSP following an induction protocol.

Chapter 5

Cerebellar models and theories

In 1967, Eccles, Ito and Szentágothai depicted the cerebellar circuitry in the manuscript “The Cerebellum as a Neuronal machine” (Eccles et al., 1967). This book stimulated discussions on the operational mechanisms of the neural structure, and, a few years later, David Marr (1969) and James Albus (1971) independently published theoretical models of the cerebellar circuitry which intended to explain its machinelike function with some unified principles. These neurocomputational works have helped to better understand its precise role in classical conditioning, motor learning and voluntary movements (see Ito, 2006 for a review). Furthermore, many predictions made from these studies have later been verified experimentally, re-enforcing the importance of a computational approach (e.g., Medina et al., 2000, 2001).

In this chapter, I review the most influential theoretical works and modeling studies describing the computational rules driving cerebellar functions.

5.1 Models of motor learning

5.1.1 The classical model

Most of the existing models are based on the presumed adaptive role of the cerebellum (Eccles et al., 1967) and derived from the conceptualization work made in parallel by David Marr and James Albus, published respectively in 1969 and 1971. Ten years later, Ito and Kano discovered a heterosynaptic long-term depression at parallel fibers-Purkinje cell’s (PF-PC)

synapses (Ito and Kano, 1982), validating experimentally the existence of a plasticity predicted by both Albus and Marr's models¹. Consequently, the resulting theoretical system is often referred as the Marr-Albus-Ito model.

The theory, in its simple form, can be summarized in four fundamental points:

1. Mossy fibers signals convey contextual sensorimotor information. They drive the firing of granule cells, which optimally recode the input signal, and in turn excite Purkinje cells.
2. Neurons of the inferior olive encode an error signal and target the Purkinje cell through the climbing fiber.
3. The convergence of both the contextual signal and the error signal to a Purkinje cell leads to a diminution of the efficacy of PF-PC synapses.
4. A diminution of the strength of PF-PC synapses leads to an augmentation of the activity of the cerebellar nuclei targeted by the Purkinje cells, and to the emergence of a response adapted to the contextual information.

The granular layer optimally encodes the input signal. According to the theory, the granular layer re-encodes optimally the sensorimotor signals arising from mossy fibers (Marr, 1969; Philipona and Coenen, 2004). This optimal encoding is supposed to minimize destructing interferences between learning tasks, and optimize neuronal resources by evicting redundancies. Such a recoding is supposed to convey a contextual representation to the Purkinje cells that simplifies the integration of information, hence facilitating learning. It has been proposed that a sparse coding (Willmore and Tolhurst, 2001; Assisi et al., 2007) — i.e. a code where each information is encoded by only a few neuronal units — at the level of parallel fibers would provide such properties (Philipona and Coenen, 2004): a sparse coding increases the amount of information conveyed by a single spike; conversely reduces the amount of energy needed to transmit a signal (Olshausen and Field, 2004), and therefore maximizes the efficacy of the information transfer. Some experimental data (Miyashita, 1988;

¹The most basic difference between the Marr and Albus theories is that Marr assumed that climbing fiber activity would cause parallel fiber synapses to be strengthened, whereas Albus proposed that they would be weakened.

Olshausen and Field, 2004) and theoretical arguments support a sparse coding at the level of parallel fibers². First, the huge amount of granular cells ($10^{10} - 10^{11}$) provides the neuronal resources to sparsely encode many contexts; then, LTD and LTP at mossy fiber-granule cell synapses and backward inhibition of Golgi favors such an encoding (Földiák, 1990; Schweighofer et al., 2001). Golgi cells are supposed to play an important role in the formation of a sparse code in the granular layer by inhibiting a large field of granular cells. This retroactive loop would functionally regulate the activity of the granular cells, and also limit noise (Philipona and Coenen, 2004). Third, most of PF-PC synapses are silent (Brunel et al., 2004). Finally, a Purkinje cell only needs a few conjointly active parallel fibers to be activated.

Purkinje cells integrate the information. In the Marr-Albus-Ito theory, the Purkinje cell is considered as the central element of the cerebellar microcomplex. Each Purkinje cell can integrate a huge amount of information. According to Brunel et al. (2004), by considering only two computational states (active and inactive), a Purkinje cell could classify in two sets as much as 5 *ko* of information. This massive processing power is due to the particular architecture of the cell (a very large dendritic tree) and the high number of parallel fibers that project onto it ($\approx 200,000$ in humans). In this sense, a Purkinje cell is often considered as a perceptron: a simple and abstract neuronal network capable of linear associations (Rosenblatt, 1958; Albus, 1971).

The climbing fiber conveys a teaching signal. The theory postulates that the strength of each PF-PC connection is plastic and that the climbing fiber drives the adaptation process by sending a teaching signal. Evidence of this supervised learning has been discovered experimentally by Ito (1982), thus giving credit to the theory. Also, in order to reverse learning and protect synapses from saturation, the theory postulates an homosynaptic LTP at PF-PC synapses. This was also validated experimentally by Lev-Ram et al. (2002). These plasticity sites are described in chapter 4.

²Also, other areas of the brain commonly use this type of code (e.g., the primary visual area Vinje and Gallant, 2000)

Applications and open questions. The Marr-Albus-Ito model has been applied to a wide range of tasks in motor learning, ranging from ocular reflexes (VOR, OKR and OFR), classical conditioning, voluntary movements.

In the VOR adaptation and the eyeblink conditioning, the conditioned stimulus reaches the granular layer via the mossy fibers and targets the Purkinje cells by means of the parallel fibers, whereas the information from the unconditioned stimulus reaches the cerebellum through the climbing fibers. In the two paradigms, the arrangement of the neuronal circuitry fits well the modifiable path scheme described by the theory (see section 5.1.2 and 5.1.3 for VOR and eyeblink conditioning models, respectively).

In voluntary movements, the Marr-Albus-Ito model has been used to explain coordination and the fine tuning of movements (see section 5.3). It has also been proposed that the cerebellum may replace reflex control with predictive control (during a navigation task) using such an adaptation scheme (McKinstry et al., 2006, 2008).

Furthermore, the standard scheme accounts for a possible role of the cerebellum in higher level functions and the formation of internal models for mental actions (Ito, 2008). The theory also gains credits with experimental data and thanks to many theoretical supports (see Ito, 2006 for review).

However, the standard model can not account for all experimental observations, and other models based on a different set of hypothesis have accurately described unexplained phenomena.

First, the role of the climbing fiber remains controversial (see Simpson et al., 1996; Kitazawa and Wolpert, 2005; Bengtsson and Hesslow, 2006; McKay et al., 2007 for recent reviews). Although the predominant view given by the Marr-Albus-Ito theory proposes that the axon of the inferior olive acts as a teacher and drives synaptic plasticity, another view, inherited from the work of Llinas et al. (1974), suggests that the inferior olive might provide a timing signal to the targeted Purkinje cells. The main line of evidence of this theory relies on the synchronization that has been observed in vitro in olivary neurons (Llinas et al., 1974; Llinás and Yarom, 1981; Lampl and Yarom, 1997, and see section 5.2.3).

Second, the classical theory does not take into consideration most plasticity sites that have been reported so far (see chapter 4). While some of these plasticities integrate well with the standard theory (e.g., MF-GR plas-

ticity could provide an optimal sparse encoding of the input signal) other plasticity sites still need a consistent explanation on their possible functions.

Third, the postulated adaptive role of PF-PC LTD is still debated. Very recent findings suggest that PF-PC LTD is not essential for cerebellar motor learning: Schonewille et al. (2011) showed that there is no motor learning impairment in mutant mice lacking PF-PC LTD.

Fourth, anatomical and neurophysiological properties of the cellular substrates are still not fully understood. For example, the bistability of the Purkinje cell caused by the climbing fiber's discharge is not reported by the classical model. Furthermore, the functional role of some neural substrates (e.g., the differentiation of inhibitory interneurons), and the computational properties of some connections (e.g., PC's axon collateral, IO-DCN connections, ascending segment of the granule cell's axon) are still a matter of debate (Ito, 2006).

Finally, although the Marr-Albus-Ito model can explain simple motor learnings, other models also inspired from the biological properties of the cerebellar microcircuitry have successfully explained such adaptation processes and finely reproduced neurophysiological properties of the cerebellar substrates. These discrepancies are highlighted in the next subsection, in which the neurocomputational works related to the study of VOR adaptation and eyeblink conditioning are presented.

5.1.2 Modeling VOR

VOR provides a simple model for the study of cerebellar adaptation (see section 3.2.2) for which the path of information has been studied thoroughly.

Path of information. The VOR adaptation in a stationary visual environment is represented by a gradual change of the vestibular nuclei signal. This change is mediated by a trineuronal arc from the vestibular afferents to the oculomotor neurons. Vestibular nuclei receive information about head rotation and transmit these informations to the oculomotor nuclei which activate motoneurons responsible for the eye rotation. In parallel, primary and secondary vestibular afferents send projections to the cerebellar flocculus through mossy fibers. The latter fibers excite the population of granular cells which in turn project to Purkinje cells. Purkinje cells

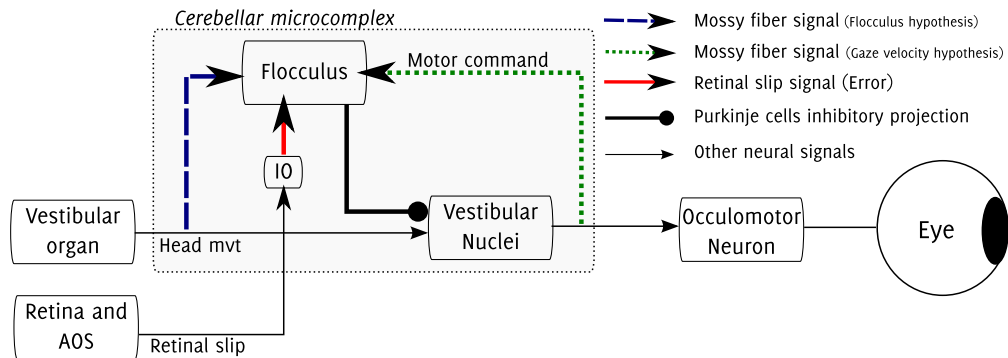


Figure 5.1: VOR system. The VOR system is divided into four parts, namely the vestibular nuclei, the flocculus, the oculomotor system and the retina and accessory optic system. The set of vestibular nuclei is the controller of the VOR and forms with a microzone of the floccular lobe a cerebellar microcomplex acting as an adaptive controller. The manipulated object — i.e. the oculomotor system together with the eyeball — is controlled by the vestibular nuclei. The retinal slip signals are eventually sent to the flocculus by climbing fibers as error signals (for review, see Ito, 1998; Broussard and Kassardjian, 2004). The error signals are sensed and mediated at the level of the retina and the accessory optic system.

also receive the retinal slip from the climbing fiber signal (Maekawa and Simpson, 1973; Ito et al., 1977). Purkinje cells then modulate the activity of the vestibular nuclei and the whole parallel pathway is known to be responsible for VOR adaptation (Ito, 1974).

The VOR system is presented in the block diagram of figure 5.1. Although the VOR provides a well studied model of cerebellar adaptation system, the neuronal mechanisms responsible for the adaptation are still under debate. Several models propose how adaptation could be obtained: they are mainly divided into two groups, known as the flocculus models (Ito, 1970, 1998) and the gaze velocity models (Raymond and Lisberger, 1998; Lisberger, 2009).

Flocculus and gaze velocity models. The flocculus hypothesis postulates that VOR adaptation is induced by a synaptic plasticity in the flocculus guided by error signals conveyed by climbing fiber inputs. It follows the description of the Marr-Albus-Ito model and proposes that the mossy fibers send head related movement signals to the flocculus (figure 5.1, dashed blue line) and that the climbing fiber signal (figure 5.1, red line) induces the long term depression of PF-PCs synapses (Ito, 1998).

This model is mainly supported by the experimental proof of PF-PC LTD and LTP, and by other theoretical works (e.g., Fujita, 1982).

However, it is unlikely that VOR adaptation can be accounted by only a synaptic plasticity in the cerebellar cortex. Indeed, the flocculus hypothesis can't finely reproduce neurophysiological data, and generalization to other tasks such as smooth-pursuit³ and VOR cancellation⁴ is not described by the model. However, Tabata et al. (2002) proposed an extension of the flocculus model where a single learning site at the level of the cerebellar cortex could finely reproduce the pattern of action potentials and extend to other paradigm such as VOR cancellation and smooth pursuit.

Another set of models — the gaze velocity models — has been proposed to account for the role of the cerebellum in VOR adaptation. The gaze velocity hypothesis (Miles and Lisberger, 1981; Lisberger, 1994) assumes that the flocculus receives motor commands via the mossy fibers (figure 5.1, dotted red line) and adapts its internal dynamics through learning that occurs in both the cerebellar cortex and the vestibular nuclei (Miles and Lisberger, 1981; Lisberger, 1994; Raymond and Lisberger, 1998; Lisberger, 2009). According to the model, the adaptation of the spiking pattern of a Purkinje cell could be due to a synaptic plasticity at the MF-DCN synapses. In this theory, the climbing fiber does not convey a teaching signal at the floccular level. Lisberger's model was designed based on detailed physiological data (Lisberger, 1994) involving not only in VOR but also in VOR cancellation and in smooth pursuit tasks. The main advantage of such a model is the physiological support: it can accurately reproduce the spiking patterns of the different neuronal units of the cerebellar microcomplex.

Other computational studies of VOR adaptation suggest that two or more long-term plasticity sites could have an important functional role. For example, it has been suggested that it could account for specificity and generalization of procedural learning, and describe mechanisms of memory transfer.

Specificity and generalization. Generalization is defined as the ability to express a behavioral response in a different context from which it has been

³ Primates use smooth-pursuit eye movements to accurately track a slow moving target.

⁴VOR cancellation is caused by tracking a moving target paired with equivalent head turns.

initially learned. A learning must be generalized to other situations; otherwise, the unique features of each context would always prevent its behavioral expression. Conversely, too much generalization is not adapted: a response should not be expressed in an inappropriate context. The process that prevents mis-adapted learning is called specification. A simple example of two abstract neural networks for specificity and generalization is presented in figure 5.2.

The study of the VOR demonstrated that the cerebellum is able to extract the important features of a context and to express learning in new situations (generalization), and also isolate input signals that need context-dependent responses (specificity).

Specificity has been observed in VOR learning across the head rotation and tilt frequency dimensions (see Boyden et al., 2004 for review). For example, when a VOR gain has been learned with the head twisted 90° to the right, learning is not expressed when the head is twisted 90° to the left (Yakushin et al., 2000). Since the two latter signals come in two separate pathways, the stimulus must activate highly separated population of neurons at the sites of plasticity, suggesting a sparse encoding of the two types of afferents.

Contrariwise, some generalization of learning has also been observed across the dimension of frequency in tilt and in head rotation in VOR learning. For example, in the frequency dimension, VOR learning gain is expressed with a frequency of 0.5 Hz when training is previously done with 5 Hz stimuli, but not the other way around (see Raymond and Lisberger, 1996). One possible mechanism would be that active neurons during a low frequency would be a subset of those active at high frequency. Another possibility relies on the existence of a less-sparse sub-network in the cerebellar microcomplex.

It has been proposed that the distinction between generalization and specification might be the reflection of different plasticity mechanisms that could operate on separate representations. An hypothesis is that the cerebellar cortex — and more specifically the granular layer — could contain the sparse representation of the input signal and that the deep cerebellar nuclei could engrave a less-sparse representation scheme (see Thach et al., 1992; Boyden et al., 2004 for reviews).

Memory transfer. The study of memory transfer intends to determine the precise location of motor memory in the cerebellum. Motor memory

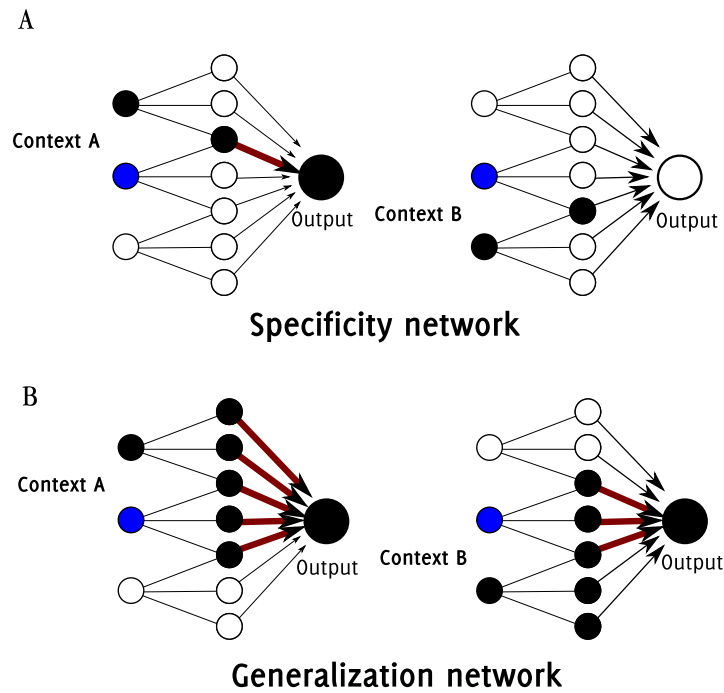


Figure 5.2: Specificity versus generalization Networks (adapter from Boyden et al., 2004)

Two abstract neural networks for specificity (A) and generalization (B) after learning. The circuit is divided into three layers: an input layer, an association layer, and an output layer. **A:** A sparse coding enables to link particular inputs to particular outputs. Context A causes a learned motor output to be elicited when a combination of two inputs is present (black and blue dots). The common stimulus (blue dot) does not elicit the motor output in the presence of Context B. **B:** A less-sparse representation easily activates the association layer due to stronger input connections, and the common stimulus can elicit the learned motor output in contexts which are different from those used during training. Open circles and filled circles indicate inactive and active neurons, respectively. Red connections have been learned and reinforced by synaptic plasticity rules.

is either argue to be stored in the cerebellar cortex, or the cerebellar nuclei, or both.

According to Masuda (2006), memory may be acquired in the cerebellar cortex and then be transferred to the cerebellar nuclei (Masuda, 2006; Obayashi, 2004). To account for this phenomenon, the authors presented a model for such a memory transfer in the cerebellum. The model was used to investigate the roles of different sites of long-term plasticity in VOR learning. They proposed that mossy fiber to cerebellar nucleus synapses, as well as Purkinje cell to cerebellar nucleus synapses undertake long-term plasticity on a longer time scale compared to PF-PC plasticity. The authors also proposed that the cerebellar cortex might in fact serve as a transient memory, and that a synaptic plasticity between mossy fibers and cerebellar nucleus occurs after an inhibition of the same nucleus by the Purkinje cell. Since the mossy fibers can create fewer connections with cerebellar nuclei compared to the high PF-PCs convergence, the authors suggested that this memory transfer should only be partial (Masuda, 2006).

5.1.3 Modeling eyeblink conditioning

As for the VOR adaptation, the circuitry of eyeblink conditioning (EBC) has been well identified, and EBC is a common protocol to study the adaptive role of the cerebellum (see section 3.2.2).

The blink reflex is engendered by the accessory abducens and abducens motor nuclei which control the eye muscles and produce the unconditioned blink response to a corneal stimulation. The unconditioned stimulus (US) is transmitted to these nuclei through the trigeminal nucleus, which also sends projections to the dorsal accessory olive, nucleus of the inferior olive (Christian and Thompson, 2003). Climbing fibers rise from this region and project to the cerebellum (Christian and Thompson, 2003), sending information of the US to Purkinje cells and deep cerebellar nuclei. When the conditional stimulus (CS) is an auditory tone, it is conveyed via the cochlear nuclei to the pontine nuclei (Gould et al., 1993) which in turn gives rise to mossy fiber axons projecting to the cerebellum via the middle cerebellar peduncle (Steinmetz et al., 1986; Lavond et al., 1987). Therefore, the CS and the US converge in the cerebellum at the level of the deep cerebellar nuclei and the Purkinje cells, which control the activity of the facial and abducens nuclei, supplying the motor output of the reflexive eyeblink. Consequently, the cerebellum has been identified

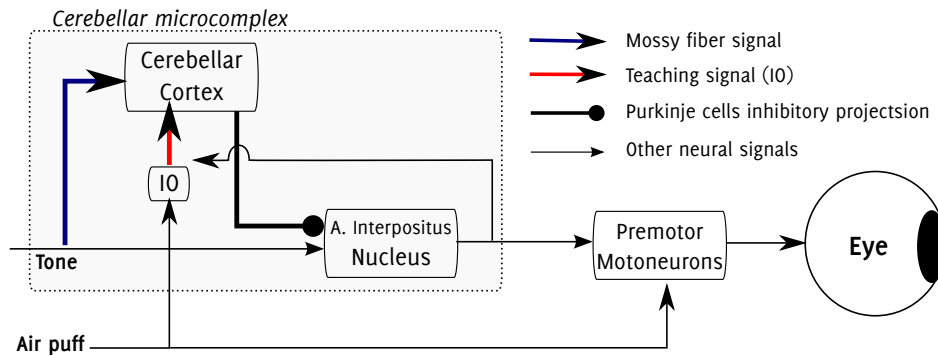


Figure 5.3: Eyeblink conditioning control scheme (adapted from Ito, 2006).

as one of the essential structures for learning EBC.

Modeling eyeblink conditioning. The arrangement of the neuronal circuitry for the eyeblink conditioning fits well the modifiable path scheme as described in the diagram 5.3, and the classical adaptive model proposed by Marr-Albus-Ito can partly explain how eye blink conditioning is learned.

By inhibiting the deep cerebellar nuclei, Purkinje cell's activity prevents the CR execution. If LTD decreases the PC activity at the appropriate time after several presentations of paired stimuli (CS-US), then it releases the interpositus nucleus from a tonic inhibition and allows for execution of the CR. According to this scheme, deep cerebellar nuclei contain the gain of the conditioned response while the cerebellar cortex contains information about the time of release of the response (Perrett et al., 1993). As a result, interpositus nucleus cells discharge prior to the CR execution and in a pattern of increased frequency of response that predicts the temporal form of the behavioral CR (McCormick and Thompson, 1984).

Furthermore, the study of saving in eyeblink conditioning and its neurocomputational properties suggest new plasticity sites located outside the cerebellar cortex.

Saving. Saving is defined as the residual learning of a task after an extinction training has been performed. During reacquisition training, saving is apparent because re-learning occurs faster than the original one

(Napier et al., 1992)⁵.

By using a large-scale computer model of the cerebellum in a simulated eyeblink conditioning protocol, Medina et al. (2001) made predictions on the location of long-term memory sites in the cerebellum. First, they suggested that the initial learning of eyeblink conditioning could also induce a plasticity in the cerebellar nucleus encoding the short-latency response. Then, they inferred that extinction should not affect strongly the nucleus plasticity. Eventually, they predicted that relearning might occur faster than the initial learning because of the residual plasticity in the nucleus (Medina et al., 2001).

The authors tested and validated these predictions in a EBC protocol performed on rabbits. If the site of learning of the short-latency response is still uncertain, many evidences suggest that it might be mediated by a plasticity site located in the interpositus nucleus (Garcia and Mauk, 1998; Halverson et al., 2010). Note that other models of saving have been proposed but are not presented in this thesis (see for example Napier et al. 1992; Kehoe 1988).

The question of timing. The classical Marr-Albus-Ito theory can account for a gain adaptation in the VOR and the expression of a short-latency response — the closure of the eyelid — in a classical conditioning task. However, it does not take into consideration the crucial role of cerebellar processing in timing. The Marr-Albus-Ito theory proposes that the granular cells act as a spatial pattern discriminator, and any direct implementation of the theory can only generate a response that varies through time if the input signal also varies. In the eyeblink conditioning paradigm, the cerebellar cortex tunes the firing of Purkinje cells so that deep cerebellar nuclei are uninhibited just before the release of the air puff (Perrett et al., 1993). Yet, this occurs without any temporal information at the input stage of the cerebellum. This finding suggests that cerebellar circuitry might process time internally (Yamazaki and Tanaka, 2009). This is the object of the next section.

⁵The existence of saving is one of the evidences supporting the notion that extinction does not erase completely the memory of the task (Houten, 1972)

5.2 Models for the passage of time

Different models have been put forth to account for the passage of time in the cerebellum. They can be classified into three categories which postulate different locations of timing information. The first category assumes a representation of time in the granular layer; the second category states that Purkinje cells encode the timing; the third class of models defends that timing intervals might be generated by neurons of the inferior olive. In this section, I review the three types of models.

5.2.1 Passage of time in the granular layer

These models are generally considered as an extension of the classical Marr-Albus-Ito theory, since they do not reinterpret the function of the climbing fiber. The models of time representation in the cerebellar granular layer are further divided into four types, namely delay lines, spectral timing, oscillator, and random projections models.

Delay lines. The first hypothesis of a cerebellar function in timing has been advanced 10 years before Marr and Albus' conceptualization works on the cerebellar circuitry. In 1958, Braintenberg and Atwood proposed that the climbing fiber could control the timing of excitation of a Purkinje cell by modulating the conduction velocity of parallel fibers. Parallel fibers would hence serve as delay line (Braintenberg and Atwood, 1958). The hypothesis was based on the morphological features of the cerebellar cortex, but experimental results failed to validate the theory. Indeed, the conduction velocity was found to be 0.25 m.s^{-1} and the length of parallel fiber to be inferior to 5 mm (Eccles et al., 1967). Therefore, the maximum imposed delay would be inferior to 25 ms and could not account for observed delays in motor learning and conditioning. Years later, by deriving Braintenberg's idea, the tapped-delay-line hypothesis has been proposed by Moore et al. (1989). In this model, the time varying activity is generated by arranging neurons in a sequential chain (see figure 5.4A), the last neuron in the chain receiving the signal with a time delay due to conduction velocity and synapses processing time. The authors argued that this sequential linkage might be constructed in the precerebellar nuclei, the input stage of the granular layer. Consequently, the granule cells would become active sequentially in the same delay line pattern. However, no

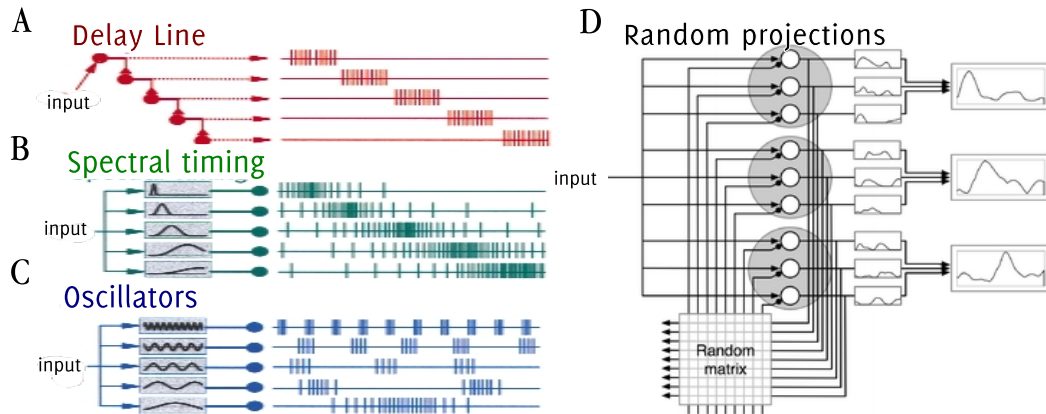


Figure 5.4: Schematics of the four main models for the passage of time in granular layer. (A,B and C taken from Medina et al., 2000, D taken from Yamazaki and Tanaka, 2009)

A. Delay line model: The simple delay-line generates time-varying activity by arranging neurons in a chain so that each synapse (red triangles) adds a discrete delay to the signal originated by a single input. Hypothetical raster plots for five mossy fibers are arranged top to bottom according to their position in the chain. **B.** Spectrum model: Spectrum models assume that neurons can respond to an input signal with a broad range of time constants. **C.** Oscillation model: A pool of pacemaker neurons oscillating at different frequencies can also be used to encode time. Different times during presentation of an input signal can be distinguished from each other because the combination of neurons active at any point is unique to a particular time. **D.** Random projection model: Granule cells activities are fed back via a random matrix which represents the recurrent connections from granule to Golgi cells and Golgi to granule cells. The feedback inhibition produces randomly repetitive transitions of active and inactive states of the cells (small solid boxes). Large shaded circles represent populations of granule cells that are commonly active at a certain time. For each population, the total activity of the cells exhibits a peak at the time characteristic of the population (large solid boxes). Therefore, these populations of granule cells become active sequentially in response to a CS.

such anatomical organization has been reported so far, and it is therefore unlikely that such a synaptic organization occurs in precerebellar nuclei.

Spectral timing models. Spectral timing models have been proposed by Bullock et al. (1994), and make the assumption that different granule cells respond to a same stimulus with a wide distribution of membrane time constants (see figure 5.4B). This hypothesis hence suggests various delays in the activation of granule cells. Once a granule cell becomes active, it induces an inhibition of a connected Golgi cell, preventing the granule cell to be activated more than once when a single context is presented. This type of model, however, seems biologically unlikely, since it would need the membrane time constants of different granule cells to vary from tenth to millisecond up to the second. In addition, the backward connectivity of a Golgi cell to the granular layer is supposed to inhibit a large field of neurons, thus invalidating the 1:1 Golgi cell to granule cell connection ratio, suggested by the model.

Oscillators models. The oscillator model has been proposed by Fujita to account for the passage of time in the granular layer (Fujita, 1982). The main idea behind the oscillator model is that one contextual signal is represented by the sequential activation of a population of granule cells (see figure 5.4C) instead of an individual cell (as it was the case in delay lines and spectral timing models) . In an oscillator model, granule cells are supposed to oscillate with different phases and frequencies in response to a single contextual signal. Consequently, individual granule cells become active repeatedly during the presentation of the same signal. By looking at the activity of different granule cells, it is possible to find for each time step a population activity which is different from the same population at any other time step. In oscillator models, the lowest firing rate among granule cells determines the longest representable time interval. Garenne and Chauvet (2004) suggested that MF-GR synapses enable GR to fire from 1 Hz to 100 Hz, admitting a passage of time up to the second. As reported by Yamazaki and Tanaka (2009), to generate this large variety of time lags, their model assumed a wide distribution of mossy fiber-granule cell synaptic efficacies. However, if the synaptic efficacy changed, different sequences of active granule-cell populations could be generated for the same input signal, which in turn lead to an unstable time representa-

tion. Recent experimental studies showed that MF-granule cell synapses are likely to be plastic (see chapter 4), thus, the robustness of the model is debated.

Random projection model. Random projection models (see figure 5.4D) have first been proposed by Mauk and Buonomano (2004), and have been analyzed in more details by Yamazaki and Tanaka (2005, 2007, 2009). In a random projection model, the cerebellum is reinterpreted to be a liquid state machine (Maass et al., 2002). A constant signal at the input stage of the cerebellar cortex generates apparently random transitions and repeated activations of granule cells. Because of the dynamics of the granular layer network, with random recurrent connections to and from Golgi cells, the same population of active granule cells appears only once during the presentation of a signal. This therefore allows a population of active granule cells to encode a unique and precisely timely tuned response to a specific stimulus. According to the random projection model, the passage of time is caused by the feedback inhibitory signals from the Golgi cells. Yamazaki and Tanaka (2007) built a realistic network respecting the known convergence of neurons in the granular layer of the cerebellum. They determined that two conditions were necessary in order to observe an usable passage of time information in the granular layer. First, a granule cell must integrate inputs with a long membrane time constant; and second, the connectivity between the granular cells and the Golgi cells must be random. Although this type of models is a promising framework to resolve timing issue in the cerebellum, further studies still need to clarify how the resulting network is resistant to noise and to what extent the change in the mossy fiber-granule cell connection strengths affects the representation.

5.2.2 Passage of time in the Purkinje cell

Other authors have proposed a possible mechanism for the passage of time in the electrophysiological properties of Purkinje cells, thus locating the passage of time outside the granular layer. Fiala et al. (1996) proposed that this might be represented by the slow process of intracellular signal transduction mediated by the metabotropic glutamate receptor (mGluR) inside the Purkinje cell. The variation in the number of mGluRs expressed on the dendrites for different Purkinje cells would result in different latencies in the elevation of intracellular Ca^{2+} concentration for those cells, pro-

ducing a spectrum of intracellular Ca^{2+} transients across different Purkinje cells. In their model, the authors also assumed that the concentration of mGluR is constant. Hence, they need a population of Purkinje cells with a large spectrum of predetermined response latencies to account for all possible time delays.

Steuber et al. (2006) developed an extended version of the model, where the time delay between parallel fibers input and mGluR is adaptive. In the model, a single Purkinje cell can learn to recognize a precise temporal onset by adapting the latencies of its calcium responses after the activation of the mGluR.

5.2.3 Passage of time in the olivary system

In models reviewed in the last subsections, the role of the climbing fiber was to induce a modification of the strength of the PF-PC synapses. This classical view is challenged by two findings. First, the neurons from the olivary nucleus tend to have an oscillatory activity (Llinás and Yarom, 1981; Llinas et al., 1974; Lampl and Yarom, 1997); and second, following the discharge of the olivary neurons, the climbing fiber induces a strong modulation of the Purkinje cell activity. Some authors argue that the olivary discharge might in fact convey another source of information to Purkinje cell and propose that the climbing fibers regulate the output of these latter cells with a timing signal (Welsh et al., 1995; Yarom and Cohen, 2002).

Llinas et al. (1974) observed that the olivary neurons are electrically coupled by gap-junctions. They suggested that this coupling might synchronized the activity across neurons of the same olivary region (Sugihara et al., 1995; Lang, 2001; Blenkinsop and Lang, 2006), and proposed that it might regulate the output of targeted Purkinje cells with a timing signal adapted to the task being performed (Llinas et al., 1974; Llinás and Yarom, 1986; Lampl and Yarom, 1997). The authors mainly based their assumption on electrophysiological data of neurons of the inferior olive recorded *in vitro*, showing that these neurons present an intrinsic oscillatory activity. This rhythmic activity might explain how olivary neurons could generate spatiotemporal pattern (Yarom and Cohen, 2002). The main problem of this theory is that very few studies have demonstrated *in vivo* a rhythmicity of the olivary neuron discharge (Sugihara 1995; Lang 1999). Furthermore, when rhythmicity was demonstrated, it was shown to induce

behavioral deficits. Chorev et al. (2007) suggested that two modes of oscillation of the olivary neurons and some transient oscillatory rhythms might explain why a periodic IO discharge can't be observed experimentally in vivo when recorded on long time period. Authors showed that olivary neurons present a slow and a fast rhythmic processes. The slow rhythmic process ($0.2 - 2$ Hz) makes the cell transit from quiescent periods to subthreshold oscillations with a fast rhythmic (6 to 12 Hz). Consequently, spikes are more likely to occur during the depolarized phase of these fast oscillations. Models of the oscillatory activity have been developed to explain how this activity could be obtained (e.g., Manor et al., 1997; Schweighofer et al., 1999; Loewenstein et al., 2005). Oscillations are mainly thought to be generated by network dynamics and coupling between olivary cells (Placantonakis et al., 2006).

Two main functions can be envisaged for such rhythmic processes: first, it could constitute a timing for the error message conveyed to Purkinje cell, thus extending the classical model proposed by Marr-Albus-Ito. Otherwise, it could have a more global timing function, thus predicting that the IO nucleus would enclose a timing system capable of generating a quasi infinite subset of time intervals ranging from 10ms to the second (see also Ivry and Spencer, 2004). Each cycle could served independently as a timing device, and, in such a case, IO neurons could play a role in modulating motor components at very short time scales.

A recent study intended to show that inferior olive neurons might regulate synaptic plasticity and timing in the cerebellar cortex at the same time, and hence help to integrate the learning and timing theories. Authors demonstrated that a single spike in the soma of olivary neurons are translated into a burst of axonal spike in the climbing fiber. Importantly, the number of spikes in the burst has been shown to be dependent of the phase of the subthreshold oscillations, and therefore conveys the state of the olivary network to the targeted Purkinje cells. The shape of the burst have dramatic impact on the activity of the cell. Depending on the number of spikes in the burst, the complex spikes is modulated and long-term potentiation and depression at parallel fiber-Purkinje cell synapses is hence dependent to the phase of discharge of olivary neurons (Mathy et al., 2009).

If these recent results clearly challenge the view that the climbing fiber conveys an all-or-none signal to the cerebellar cortex, it still needs to be determined how timing pattern could be learned, stored and used. Fur-

thermore, it is fundamental to determine if this timing signal is then used to drive learning between parallel fiber to Purkinje cell synapses at precise onset, or if the latter plasticity is in fact a factor that causes the oscillations and timing function of olivary neurons through the inhibitory projections from the deep cerebellar nuclei to the olivary nuclei.

5.3 Models for voluntary movements

Early models and theories try to describe how the cerebellum could coordinate and finely tuned the movements. The Tonic Reinforcer Model was based on Luciani's principles and proposed that the cerebellum tuned vestibular and cerebellar nuclei, reticular formation and cerebral motor cortex so that they responded optimally to non-cerebellar inputs. This model was based on the work of Granit et al. (1955) and Gilman (1969). Also, the Command-Feedback Comparator Model proposed that the cerebellum integrated information as a linear system (see Allen and Tsukahara, 1974; Brooks and Thach, 1981; Evarts and Thach 1974). According to the model, the lateral cerebellum helped to initiate the movement, whereas the intermediate cerebellum corrected errors during its execution. Also, the Combiner-Coordinator Model proposed that the cerebellum coordinates movements by translating them from one reference frame (e.g. the body musculature) into another reference frame (e.g. the movement in space) — see Thach et al. (1992) for a review. Despite their relative simplicity, these models neither account for motor learning nor timing, and lack experimental evidences. Progressively, they have been replaced by a global framework of voluntary movements, known as the internal model hypothesis.

In most biological system, a fast and coordinated movement cannot be executed only by using the sensory feedback from the limbs. Indeed, biological sensory feedback is conveyed at low speed and the sensory information can be noisy and incomplete (see Shadmehr et al., 2010 for review). To resolve this issue, the internal model hypothesis suggests that the cerebellum could acquire internal models of the body and the world (Ito, 1970, 1984; Kawato et al., 1987). These internal models would act as estimators of the state and sensory feedback of a body part, or directly control the limb by sending motor commands or corrective signals.

The internal model theory explains how the cerebellar circuitry can

build up and store predictive or corrective models (Wolpert and Miall, 1996; Wolpert and Ghahramani, 2000). This theory is based on the adaptive properties of the cerebellar microcomplex (Ito, 1984), its application in adaptive voluntary movements is detailed in the next part of this manuscript.

Part II

THE ROLE OF THE CEREBELLUM IN ADAPTIVE VOLUNTARY MOVEMENTS

Abstract

The cerebellum plays a major role in motor control. It is thought to mediate the acquisition of internal models of the body-environment interaction (Ito, 1984). In this study, the main processing components of the cerebellar microcomplex are modeled as a network of spiking neural populations. The model cerebellar circuit is shown to be suitable for learning both forward predictive and inverse corrective models. A new coupling scheme is put forth to optimize online adaptation and support offline learning. The proposed model is validated on a procedural task of rotation adaptation (Huber et al., 2004) and the simulation results are consistent with data from human experiments on adaptive motor control and sleep-dependent consolidation (Huber et al., 2004). This work corroborates the hypothesis that both forward and inverse internal models can be learned and stored by the same cerebellar circuit, and that their coupling favors online and offline learning of procedural memories.

Chapter 6

Introduction

As stated in the previous part, it is largely admitted that the cerebellum plays a major role in motor control, coordinating the movements, making them accurate and adapting the commands to different contexts (see Ito, 2002; Fine et al., 2002; Ito, 2006 for a review).

The fast and coordinated movements can not be executed using only the feedback information (Wolpert and Ghahramani, 2000; Shadmehr et al., 2010). Indeed, *(i)* the neuronal nerves send information at low speed, delaying the sensory feedbacks the brain can rely on to update and correct the movements; *(ii)* the neural computations often require tens of milliseconds, suggesting that most of these feedbacks might be integrated too late to be efficiently used and *(iii)* the sensory information is noisy, hence imprecise, and often incomplete (e.g., a task executed in the dark does not have visual feedback). To resolve these limitations, the internal model hypothesis has emerged, proposing that the brain — and more specifically the cerebellum — acquires internal models of the body and world interactions (Ito, 1970, 1984; Kawato et al., 1987).

In this chapter, we propose a new coupling scheme which supports both online and offline adaptations in voluntary movements.

6.1 The internal model hypothesis

In theory, an internal model can approximate the input-output relationship of almost any dynamical system. It could, for example, simulate the dynamics of a hand using a tool, the dynamics of the tool itself, and the controller of the hand — i.e. the areas of the CNS responsible for the hand

control. By extension, it is also suggested that an internal model could approximate the essential properties of our mental representations of the world (Ito, 2008). In practice, there is strong evidence coming from behavioral, fMRI and physiological studies, that some internal models can be created and stored in the cerebellum (Wolpert et al., 1998; Kawato et al., 2003; Ito, 2005; Pasalar et al., 2006). In motor control theory, they are generally divided into two groups identified as forward and inverse models.

The forward models appreciate the causal relationship between inputs to the system and its outputs. In motor control theory, it predicts the state and sensory outcome of a body part. A schematic representation of a forward model predicting the cinematics of a finger is presented in figure 6.1. It anticipates the next position and velocity of the limb and the expected sensory feedbacks given the current state of the motor apparatus and the motor command sent to the arm. A forward model can be integrated in a motor control architecture to form a close-loop control system. Such a system (as shown figure 6.2) can be used to optimize the selection of the best set of motor commands to perform efficiently in a specific motor task.

The forward models are thought to influence most of sensory-motor tasks, such as: motor learning and control (Ito, 1984; Miall et al., 1993; Wolpert and Miall, 1996; Jordan and Rumelhart, 1992), state and sensory estimations (Goodwin, 1984; Miall et al., 1993) or context predictions (Wolpert and Kawato, 1998). Evidences of existence of such models have been reinforced by experimentation (see for example Mulliken et al., 2008 for motor control, Miall, 1998 for state and sensory estimation, Bell et al., 1997 for sensory cancellation, and Eskandar and Assad, 1999 for context prediction) and robotic implementations (Laschi et al., 2008; Saegusa et al., 2009), validating the viability of such systems in complex environments.

The inverse models work in the opposite direction, providing the motor command that causes a desired change in the state of a system. In other words, an inverse model maps a desired target location to a set of torque commands (Kawato, 1999) and are therefore adapted to achieve some desired state transitions (see for example Contreras-Vidal et al., 1997; Schweighofer et al., 1998). A motor control system based on an inverse control scheme is presented in figure 6.3.

A derivative type of an inverse model is called feed-forward corrector (Kawato and Gomi, 1992). Instead of sending the whole motor command to the limb, it transmits a motor correction that will be added to the motor cortex command. This control system, presented in figure 6.4, is therefore

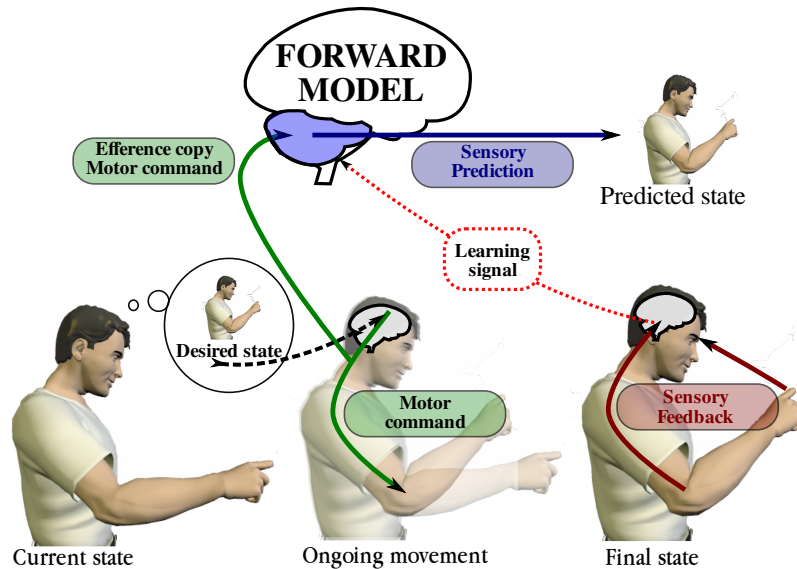


Figure 6.1: Forward Model architecture (Human model taken from Wolpert and Ghahramani, 2000). Schematic diagram of a forward model estimating the finger location during a simple movement. The steps are presented from left to right, showing the different phases of the movement and the sensory feedback along time. First, the finger is in the position 'current state' (left image). The desired position of the finger (inset of left image) is sent to the motor cortex that will calculate the motor command to be sent to the articulation to reach the desired position (middle image). An efference copy of the motor command is also conveyed to the cerebellum which predicts the future position of the finger (predicted state, top). Once the motor command has been realized, the actual state of the system — the position of the finger — is observed through a sensory system (here a combination of the proprioceptive information of the arm and the visual information) with a delay of tenths to hundreds of milliseconds. This signal is returned to the cerebellum, which will learn to closely mimic the motor apparatus of the finger and predict the sensory consequences and finger state expected after the execution of a motor command

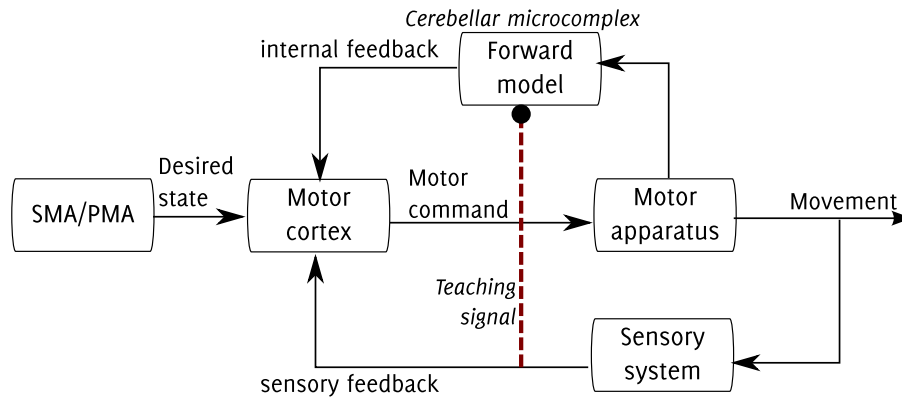


Figure 6.2: Close-loop motor control scheme using a forward model (adapted from Ito, 2005) The motor cortex can perform a precise movement using an internal feedback from the forward model instead of the external feedback from the real control object. SMA: Supplementary Motor Area / PMA: Pre-Motor Area

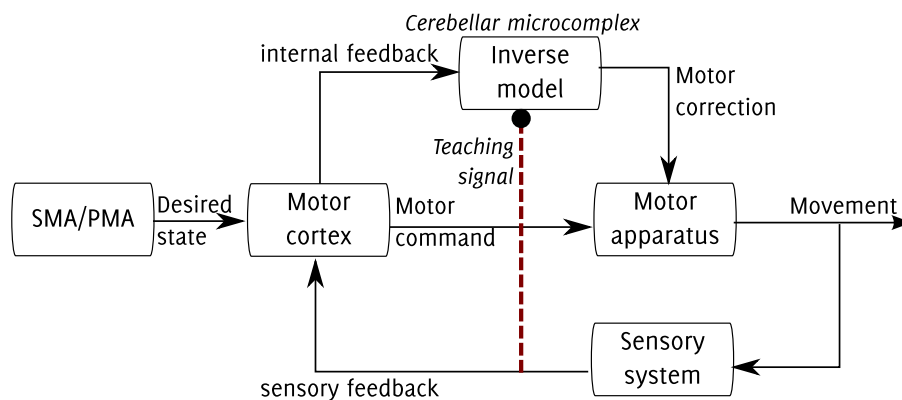


Figure 6.3: Open-loop motor control scheme using an inverse model (adapted from Ito, 2005) The inverse model control system is characterized by the convergence of cerebral and cerebellar outputs to a motor apparatus. Errors of motor command are thought to be complemented by accurate inverse model corrections. The convergence of cerebral and cerebellar pathways has been demonstrated in the rubrospinal and the reticulospinal tracts.

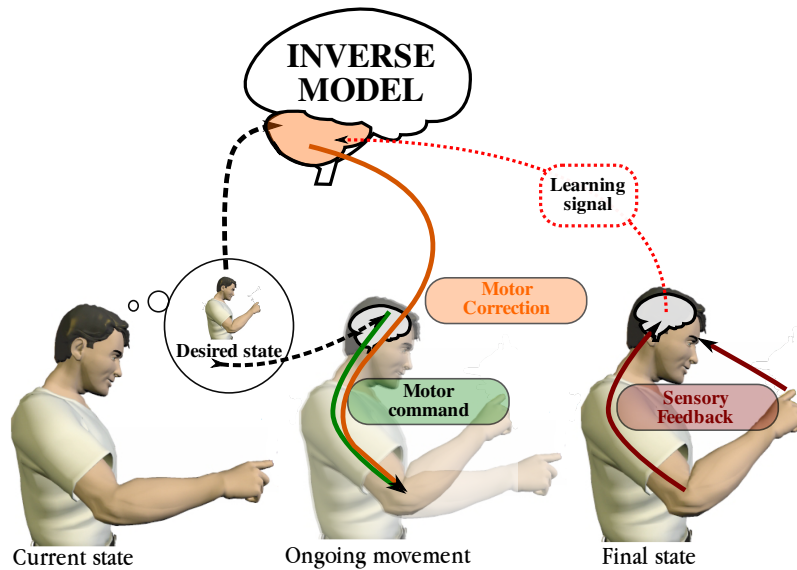


Figure 6.4: Feed-forward corrector (human model taken from Wolpert and Ghahramani, 2000). This figure presents a schematic diagram of an inverse model acting as a feed-forward corrector. The desired position of the finger is conveyed to the motor cortex and to the cerebellum which sends a predictive motor correction. This correction signal is summed up to the motor command calculated by the motor cortex. The resulting command is then sent to the articulation. By comparing the desired state and the actual state of the system (observed through the sensory system), the system can learn to gradually modify the order to reduce the error between the desired position and the current position of the finger.

characterized by the convergence of cerebral and cerebellar outputs to a motor apparatus. A recent study has used this type of model to control a robotic arm (Carrillo et al., 2008).

Both the forward and the inverse models depend on the dynamics of the motor system and of the controlled object. These dynamics can not be known a priori, and the motor system evolves through life: consequently, the internal models must adapt to new situations and change in pair with the motor apparatus (for a review, see Lalazar and Vaadia, 2008).

If a forward model can be obtained directly by comparing the predicted outcome of a motor command to its delayed sensory consequences, the inverse models and its derivatives need a more elaborate process to be learned since there will be no need for such models if the correct motor

command was already known.

An approach to solve this problem consists in converting the errors of the actual trajectory into motor command errors (see for example the distal supervised learning scheme introduced by Jordan and Rumelhart, 1992 and the feedback-error-learning model proposed by Kawato and Gomi, 1992); another solution proposes a direct inverse modeling (Kuperstein, 1988). Because inverse models are more complicated to learn, they are therefore slower to converge.

Although Darlot et al. (1996) suggested that a forward model would be first formed in the cerebellar cortex and then converted to an inverse model, most of the existing studies only look at the benefit of one system over the other, and debate which type of model is implemented in the cerebellum (e.g., Pasalar et al., 2006; Dean et al., 2010). Very few studies investigate the advantages of coupling internal models. We propose that such a coupling would bring offline learning capabilities to the system. This is supported by studies demonstrating that sleep — a major type of offline processing state — contributes to the consolidation and enhancement of motor adaptation tasks, and that the cerebellum is undoubtedly implied in procedural adaptive processes (e.g., Thach et al., 1992).

6.2 Coupling of internal models

To the best of our knowledge, the first study anticipating that forward models may be used to generate sensory error signals guiding the learning of inverse models has been presented by Jordan and Rumelhart (1992). In their work, the authors introduced a composite model where the internal models could be coupled to control an arm. They demonstrated that certain classical problems using a teaching signal could be solved by using two coupled internal models, a forward and an inverse, as the component of an adaptive system. Their contribution is a theoretical proof of the convergence of such a system.

The advantage of the model proposed here is that it uses a biologically plausible model of the cerebellar circuit. Also, each neural unit is modeled as a spiking neuron, thus improving the flexibility of the overall system. Moreover, we study the possible implication of the cerebellum in offline learning processes.

Following another idea, Miall et al. suggested that the cerebellum

might form two types of internal model working in parallel (Miall et al., 1993). In the proposed architecture, a forward predictive model of the motor apparatus gives a rapid prediction of the sensory consequences of each movement, and a second model delays this rapid prediction so it could be compared with actual sensory feedback from the movement. The result of this comparison is used both to correct both the errors of position and adapt the first model (Miall et al., 1993). If this scheme uses two internal coupled models, no inverse model is implemented; and therefore only the forward prediction is used to re-adapt the trajectory.

Another interesting work concerns the model presented by Wolpert and Kawato (1998). In their paper, they proposed an architecture based on multiple pairs of inverse and forward models. The MOSAIC model (for Modular Selection And Identification for Control) proposes that internal inverse (controllers) and forward (predictors) models can be coupled and used as a functional unit. Behaviors could be generated by combining the output of several units. The contribution of each unit is determined by calculating a “responsibility signal”: the predicted state made by the forward model is compared to the sensory consequences of a motor action and this comparison provides the degree of contribution of each module. Since a coupled unit can be used in different contexts, a large repertoire of behaviors can be generated with a limited number of modules. This view has been validated experimentally by analyzing functional magnetic resonance images during two tasks where the dynamics of a pointing device was changed (Imamizu et al., 2004). The authors observed that between 350 and 700 microzones could be implied in these tasks (Imamizu et al., 2003). Also, a change of dynamics seemed to dramatically influence the activated zone in the cerebellum, supporting the modular organization of internal models. The main contributions of these studies are focused on the benefits of using a modular approach for motor learning and control. In our architecture, presented in the next section, the forward model is not used to choose the appropriate inverse model for a given context but participates in both learning a feed-forward corrector and in influencing the motor policy by sending projections to the controller.

6.3 Our approach

We present a new way of coupling internal models to control the dynamic of a body part. Interactions between forward and inverse models are summarized in figure 6.5 where we present a general scheme showing the inputs and outputs of both models and the controller. To illustrate our architecture, we use a task where the system must control the dynamics of an arm. Figure 6.5a shows the on-line learning scheme. The controller of the arm receives a set of *desired states* in the form of coordinates and transform them into a set of motor commands (τ). Additionally, the *desired state* is sent to an inverse model that acts as a feed-forward corrector, and calculates the motor correction (τ_c) to be added to the motor command. The resulting command (τ_f) is then conveyed to the arm. By comparing the *desired state* and the *actual state* of the system — observed through the sensory system — the inverse corrector model learns to gradually modify the motor command to reduce the error between the desired position and the real position at each time step.

While the motor command τ_f has been sent to the arm, an efference copy of the command is also conveyed to the forward model that predicts the future position and velocity of the arm joints (*predicted state*) all along the trajectory. Then, the *actual state* sensed at the level of the sensory system is used to adapt the forward model — via the FM Learning module — to closely mimic the motor apparatus of the hand. The forward model predictions are also sent to the controller of the arm which can recalculate a new trajectory if the expected positions of the limbs differ from the predicted ones.

One of the main advantages of such a coupling scheme is to provide offline learning capabilities to the system, presented in figure 6.5b. When processing information offline, sensory feedback is no more available, and consequently, real state can not be used to adapt neither the forward model nor the inverse model. However, if the forward model is at least partially learned, the prediction of the model can be used in training the inverse model offline, replacing the *real state* input of the IM Learning module. This scheme makes the assumption that the whole sequence of actions — or at least desired states — could be replayed offline, as the input of the controller. The hypothesis is based on earlier animal investigations, that have explored the possibility that patterns of brain activity elicited during initial task training are replayed during subsequent sleep (Wilson

and McNaughton, 1994; Kudrimoti et al., 1999; Maquet et al., 2000, 2003).

6.4 Effect of sleep on motor learning

As we have seen in the previous section, an interesting aspect of coupling internal models is that it brings offline learning capability to the system ; providing an insight how memory is consolidated during sleep. In this chapter, we will consider sleep as an offline state where information could be reprocessed, without distinguishing different stages of sleep (see Schulz, 2008). The cerebellum is known to be implicated in procedural memories — that can be defined as non-conscious memories — in contrast to conscious declarative memories (Squire and Zola, 1996).

Most of human studies focusing on procedural memory showed that sleep has an important effect on performance and particularly in motor tasks (Stickgold, 2005). For example, Walker et al. (2002) have demonstrated that a night of sleep can trigger significant performance improvements in speed and accuracy on a sequential finger-tapping task, while equivalent periods of time during wake provide no significant benefit. More recently, in another motor learning paradigm using a rotation adaptation task Huber et al. (2004) demonstrated that the local increase in slow wave activity after learning correlated with the improved performance of the task after sleep. Many effective protocols have been developed in the last ten years to unveil the effect of sleep-dependent memory in motor control (Stickgold, 2005 for a review). The relative simplicity of some of the existing tasks allows us to transpose them in a simulated environment, that could lead to a better understanding of the sleep function. We propose that some of the memory consolidation and performance enhancement after sleep could be explained by the offline capability of our model, an issue that has not been addressed in theoretical studies so far.

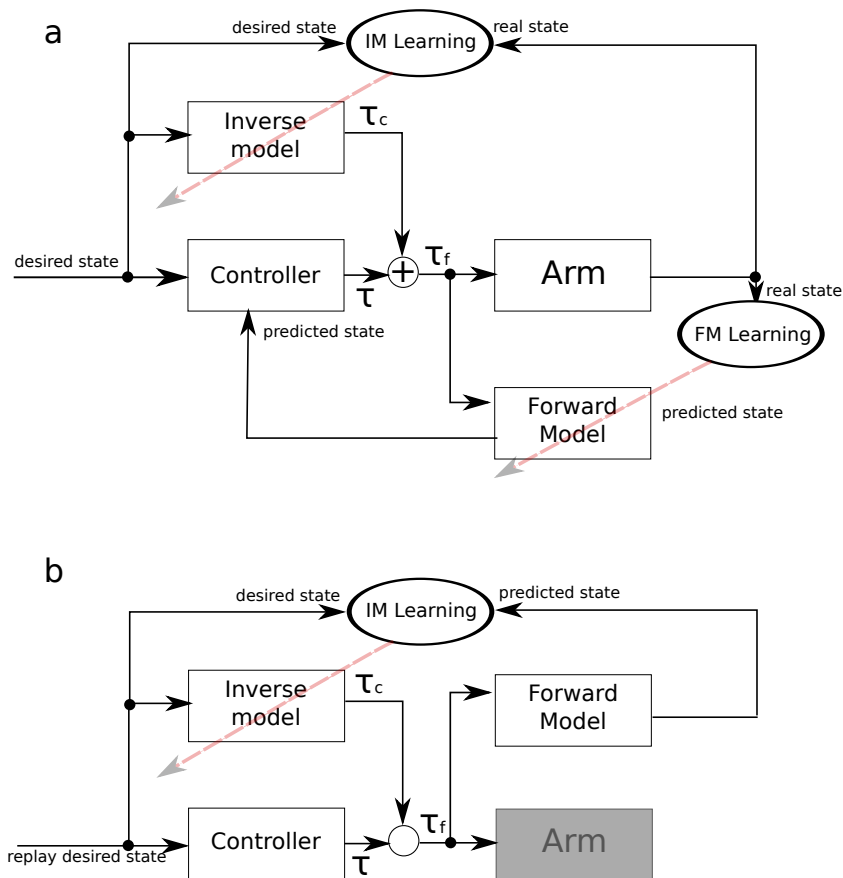


Figure 6.5: Model of the coupling scheme for on-line and offline learning. **(a)** The inverse model is used as a feed-forward corrector, using the desired state to predict the motor correction to send to the arm. At first, the inverse model produces no correction signals, the major source of control is provided by the controller. By using the predictions of the forward scheme, the controller can consequently recalculate the trajectory to account for the predicted error. Then, when the inverse model is learned, it produces torque corrections that allow the system to follow a desired trajectories with smaller error, thus, the role of the feedback controller should be diminished. **(b)** In the offline scheme, once the forward model is at least partially learned, the prediction of the forward model can be used in training the inverse model.

Chapter 7

Material and methods

The purpose of this study is to exploit the presented coupling model to control a two joints simulated arm in a task reproducing the rotation adaptation task used by Huber et al. (2004). In the following chapter, we first introduce the rotation task and detail the simulated version of the system. After presenting the global architecture, we describe our model of the cerebellar microcomplex and show how we use the system in the simulated protocol.

7.1 The Task

The task has been inspired from a rotation adaptation task performed by Huber et al. (2004) in human, and where the goal was to elicit the importance of sleeping for local learning in a procedural motor task. In this task, subjects had to move a handheld cursor on a digitizing tablet from a central starting point to one of eight targets displayed on a computer screen together with the cursor position. An opaque shield prevented subjects from seeing their arm and hand at all times. Targets were randomly highlighted at regular 1-s intervals. In the rotation adaptation task, unbeknown to the subjects, the cursor position was rotated anticlockwise relative to the hand position by a fixed angle (from 15 to 60 °, depending on the trial).

We implement a simulated version of this experiment that allows us to study the possible role of collaboration of internal models during online training and through an offline process.

7.2 Integrated model for adaptive voluntary movements

7.2.1 Overall model architecture

The global architecture of the generation of the arm movements is illustrated in figure 7.1. We use the architecture described by Carrillo et al. (2008) to control a 2 joints simulated arm in real time. First, a minimum jerk model is used to compute the desired smooth movement of the arm end-point toward the target positioned in (X, Y) . The desired trajectory is expressed in Cartesian coordinates for the defined time of movement Δt . This desired movement is then transformed into arm-related coordinates: $\theta_{des}(t) = (\theta_{s,des}, \theta_{e,des})$ are the desired angular position of the shoulder and elbow. These coordinates are the inputs of a crude inverse dynamic controller which extracts a set of torque commands $\tau = (\tau_s, \tau_e)$, then sent to the articulations with a time delay $\delta t = 50ms$. All mathematical solutions of minimum jerk, inverse kinematics and dynamics model have been taken from Carrillo et al., 2008. An error relative to the arm position has been added into the minimum jerk model, emulating a rotation of α degrees anticlockwise as done in experimentation.

In agreement with the Marr-Albus-Ito theory (Marr, 1969; Albus, 1971; Ito and Kano, 1982), we assume that the cerebellum can acquire internal models of complex sensorimotor interactions (Ito, 1970; Wolpert et al., 1998) and store them in multiple and coupled microcomplexes —the computational units of the cerebellum (Ito, 1984). We model a highly simplified cerebellar microcomplex circuit (figure 7.3) capable of adapting its input-output dynamics through online learning. We employ the same microcomplex model to learn two types of internal models, namely *inverse corrector* and *forward predictor*, consistently with experimental data (Bell et al., 1997; Miall, 1998; Wolpert et al., 1998; Eskandar and Assad, 1999; Wolpert et al., 1998; Imamizu et al., 2000; Miall et al., 2007; Mulliken et al., 2008).

In the inverse model scheme (IMS), the desired angular positions for both joints are sent to the cerebellum. The model then calculates corrective torque signals $\tau_c = (\tau_{s,c}, \tau_{e,c})$ that compensate the rotation error and dynamic perturbations during the realization of the movement. The torque commands applied to each articulation i is the sum of the torque τ_i com-

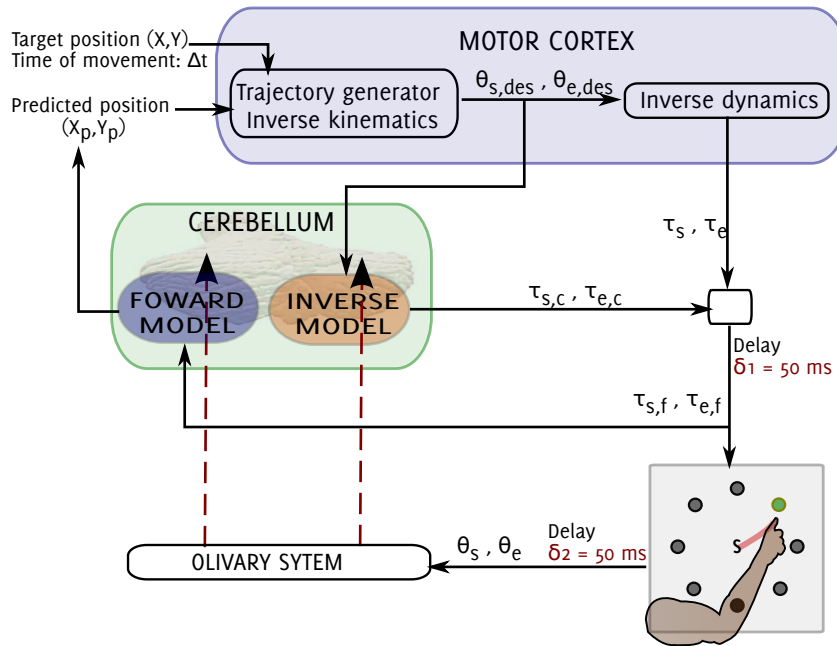


Figure 7.1: Overview of the biomimetic control architecture used to learn the rotation adaption task. Functional diagram of the controller: A desired trajectory to the highlighted target is computed by the trajectory generator and transformed in the joint-related reference frame by the inverse kinematics model. These desired shoulder and elbow states are used at each time step to compute a set of crude torque commands. The desired states are also sent to the inverse model correctors implemented in the cerebellum, whose outputs are the corrective torque commands to control the arm movements. The cerebellar forward model receives an efference copy of the motor command, and predicts the future state (position and speed) and sends it to the trajectory generator. In the coupling scheme, both type of internal models drive the system. The trajectory errors are sensed at the level of the limb and sent back to the system to compute the training signals. These signals are encoded by the olivary system and conveyed through the climbing fibers to both internal models.

puted by a basic inverse dynamics model according to the desired kinematic trajectory, and of the cerebellar corrections ($\tau_{i,c}$): $\tau_f = \tau + \tau_c$. These two commands are sent to the limbs with a delay $\delta 1 = 50$ ms. The error in the execution of the movement is computed at the level of the arm, and sent back to the system with a delay $\delta 2 = 50$ ms. This information is then used to determine the learning signal conveyed by the inferior olive and to teach the cerebellum to produce anticipative motor corrections.

In the forward model scheme (FMS), the simulated cerebellum receives information about the current state of each articulation — the angular position of elbow and shoulder $\theta(t) = (\theta_s, \theta_e)$ — and an efference copy of the torque commands $\tau_f = \tau_{s,f} + \tau_{e,f}$. Using this information, the model predicts the future positions and velocities of the articulations ($\theta(t) = (\theta_{s,est}, \theta_{e,est})$ and $\dot{\theta}(t) = (\dot{\theta}_{s,est}, \dot{\theta}_{e,est})$). The coordinates are then transformed into Cartesian coordinates and sent to the trajectory generator (X_p, Y_p). This prediction is compared to the expected position of the arm. If there is a discrepancy between the two positions, the whole movement from the current estimated place is recalculated by the minimum jerk model. Because this process is supposed to require important neuronal resources, we limit its use at once every 100 ms. We fix a duration of motor execution of 0.7 s for each movement, followed by a period of pause of 0.3 s where the joints positions are reset, and the activity of the models is allowed to get back to a basal level. Because of this short execution time and taking in consideration the delay of the sensory feedback, we assume that a high level motor correction — that is a recalculation of the whole trajectory — could not be performed in the absence of a prediction of the sensory feedback signal. Each internal model could be activated independently of the other, or both could be activated at the same time.

Figure 7.4 illustrates the correspondence between the analog input/output signals and the spiking activity of internal models.

7.2.2 Cerebellar microcomplex model

We model the basic elements of the cerebellar microcircuit (figure 12.1A) as a network of spiking neural populations (figure 12.1B). This network accounts for a set of mossy fibre (MF) inputs, a granular cell (GC) layer, a population of Purkinje cells (PCs), deep cerebellar nuclei (DCN), and climbing fibre inputs from the inferior olive (IO). We implement MF inputs as axons of a population of leaky integrate-and-fire neurones, whereas we

model GCs, PCs, and DCN as populations of conductance-based spiking units.

The mossy fibers (MFs) layer is composed of 1600 cells, 800 cells for the forward model region and 800 cells for the inverse model region. Forward model region receives afferent information about the current position of each joint ($\theta_{s/e}$) and an efference copy of the torque command for each joint ($\tau_{s,f/e,f}$). MFs of the inverse model convey signals related to the desired positions ($\theta_{s,des/e,des}$) and velocities ($\dot{\theta}_{s,des/e,des}$) of the shoulder and elbow joints along the trajectory. We compute the activity of MFs based on a family of radial basis functions spanning the input space uniformly.

MFs send excitatory projections to a population of 200 DCN units based on an all-to-all connection scheme. The forward model DCN layer is composed of 100 cells that estimate the future state - position $\theta_{s,estim/e,estim}$ and velocity $\dot{\theta}_{s,est/e,est}$ - of each joint (25 cells per variable) and the inverse models are composed of 100 DCNs cells that compute the torque corrections ($\tau_{s,corr/e,corr}$) to be sent to each joint (50 cells per variable).

MFs also excite a population of 10^4 GCs. The MF–GC connection probability is equal to $P_{MF-GC} = 0.04$, such that, on average, each MF innervates 400 GCs and each GC receives 4 MF afferents—in agreement with anatomical data (Eccles et al., 1967; Jakab and Hamori, 1988; Chadderton et al., 2004).

The model GC ensemble activity provides a sparse representation of MF inputs, optimizing encoding capacity and information transmission properties (D’Angelo and De Zeeuw, 2009). Each GC targets, on average, a subset of 150 PCs out of a population of 200. Thus, each PC receives on average 7500 parallel fiber (PF) excitatory afferents (i.e. GCs’ axons) and the connection probability is $P_{PF-PC} = 0.75$. In the model, each PC is also driven by the activity of a subset IO units mediated by a climbing fiber connection. A network of 20x200 IO units project onto 200 PCs (20:1 connections). The reason of such a convergence ratio of IO cells is explained in mini-page 7.2.

A Poisson spike-train generation process models the irregular firing of IO neurons. We then modulate the IO activity to encode error/teaching signals representing either the ongoing angular discrepancies between actual and desired movements (for the inverse corrector model) or the differences between inferred and actual result of movement execution (for the forward predictor model). Finally, the 200 PCs inhibit the population of 100 DCN units through one-to-one projections, such that each DCN neu-

IO neurons are known to have a very low discharge rate (≈ 1 to 2 Hz when recorded in vivo), and up to 10 Hz when excited with drugs (Gibson et al., 2004). In a network model where only 2 PCs target a DCN cell, and with a biological rate of 1:1 IO to PC connection, stabilization of learning is not assured. Consequently, our model has been designed so that each PC receives 20 IO projections. This non-biological simplification has been adopted to bypass a computational time issue: given that each PC of our model integrates the signal of thousands of GCs, we needed to have a small number of PCs, and thus to limit the PC per DCN ratio (real DCN is known to be targeted by tenths to hundreds of PCs, see Palkovits et al., 1977). Thus, we artificially increase the number IO neuron projections such as the resulting network would be functionally equivalent to the biological structure — in respect to the known input-output converge and divergence through the different layers. The correlation between the PC–DCN convergence and the stabilization of learning is further discussed in section 10.3, page 141.

Figure 7.2: Solving the low IO firing rate of IO cells.

ron receives afferents from two PCs. DCN neurons provide the output of the cerebellar microcomplex model. Their discharge encodes either a motor correction (inverse model corrector) or an estimate of the angular position and velocity of the shoulder and elbow (predictive forward model).

The modeled inhibitory action of PC activity onto DCN units primarily determines the response of the cerebellar model. In turn, PCs are principally driven by GC excitation mediated by PF–PC synapses. Therefore, modifying the strength of the PF–PC synapses results in shaping the input-output relation characterizing the cerebellar microcomplex. The model accounts for bidirectional long-term plasticity (i.e. LTP and LTD) at the level of PF–PC synapses. We implement LTP as a non-associative mechanism (Lev-Ram et al., 2002), such that every incoming PF spike triggers a synaptic efficacy increase. Conversely, we model LTD as an associative mechanism, such that the conjunctive inputs to the PCs from PFs and climbing fibres tend to depress PF–PC projections (Ito and Kano, 1982; Wang et al., 2000; Safo and Regehr, 2008).

As aforementioned, we employ the same microcomplex spiking network to realize both an inverse corrector model and a forward predictive model. Motor execution errors (for the inverse model) and next state pre-

diction errors (for the forward model) determine the IO teaching signals triggering LTD at PF–PC synapses. Thus, the inverse and forward models adapt their input-output dynamics online and learn, respectively, to anticipate the motor corrections and predict the next states of each joint. In the current implementation, four cerebellar microcomplex networks mediate the adaptive inverse corrector and four other microcomplexes learn the forward predictions.

In each internal model, Purkinje cells (PC), deep cerebellar nuclei cells (DCN) and inferior olive neurons (IO) are divided into functional microzones (inspired from the cerebellar microzone organization described by Oscarsson, 1976), each microzone representing the circuitry encoding a sensory information (forward model) or a torque correction signal (inverse model). A microzone of the forward model represents the predicted position or the velocity of a controlled joint. A microzone of the inverse model represents a virtual agonist ($\tau_{s,corr/e,corr}^+$) or antagonist ($\tau_{s,corr/e,corr}^-$) muscle of the two controlled joints (s and e for shoulder and elbow, respectively).

7.2.3 Neuronal models

We model each mossy fiber (MF) as the axon of a leaky integrate-and-fire neuron whose membrane potential $V(t)$ dynamics is defined as:

$$C \frac{dV(t)}{dt} = g_{leak} (V_{leak} - V(t)) - I(t) \quad (7.1)$$

where C denotes the membrane capacitance and g_{leak} the leak membrane conductance —i.e. $\tau = C/g_{leak}$ is the membrane time constant; V_{leak} is the resting membrane potential, and $I(t)$ the total synaptic drive. Whenever the membrane potential reaches a threshold V_{th} the neuron emits a spike. We used a time step $dt = 1$ ms for numerical integration.

Granule cells (GCs), Purkinje cells (PCs) and deep cerebellar nuclei (DCN) neurons are conductance based leaky integrate-and-fire units (similar to Carrillo et al., 2008) described by the following equation:

$$C \frac{dV(t)}{dt} = g_{leak}(t) (V_{leak} - V(t)) + g_{exc}(t) (V_{exc} - V(t)) + g_{inh}(t) (V_{inh} - V(t)) \quad (7.2)$$

where the membrane potential $V(t)$ depends on an excitatory synaptic conductance g_{exc} , an inhibitory conductance g_{inh} , and a leaky conductance

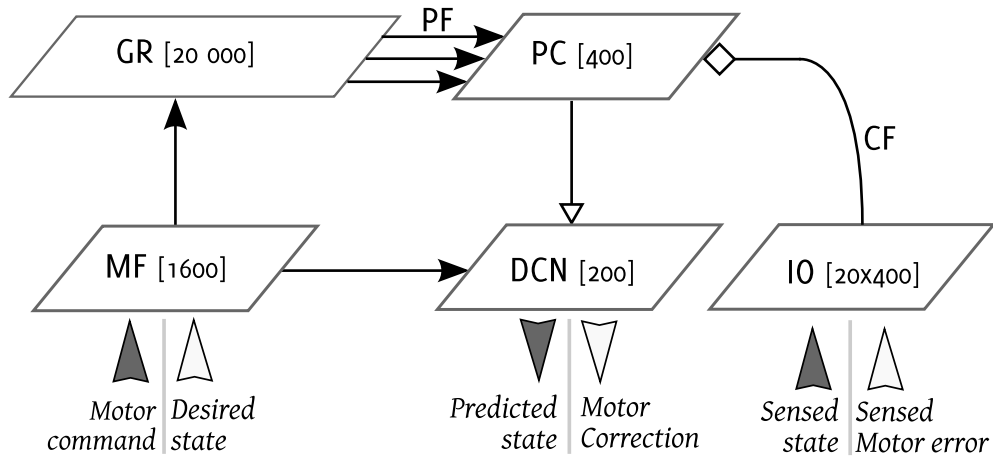


Figure 7.3: *Model of the cerebellum.* The microcomplex circuit is modeled as a network of populations of formal spiking neurons. Mossy fibers are implemented as axons of a population of 1600 leaky integrate-and-fire neurons separated in two regions, Forward and Inverse Model regions respectively. Their input currents are determined by using radial basis functions spanning uniformly the space of (1) the arm joint kinematics, and (2) the movements related details. Moreover, we divide each region in 8 clusters of 100 cells, each cluster representing a different target. Each cluster activates a cluster of 1250 granule cells (a whole region of MFs activated a population of 10000 GCs) producing a sparse representation of the input state. MFs excite a population of 200 neurons in the deep cerebellar nuclei (DCN) layer of the model. Each cluster of GC activates at its turn of a population of 200 PCs which send inhibitory projections onto the DCN neurons. The firing of DCN neurons provided the output of the model, the forward model cluster cells estimating the future state of each joint (position and velocity) and the inverse model cluster cells computing the torque correction to send to the system. The firing rate of DCN units are mainly determined by the inhibitory action of PCs, which in turn are principally driven by PF activity. Therefore, modifying the strength of the synapses between PFs and PCs result in changes of the input-output relation characterizing the cerebellar system. Bidirectional long-term plasticity (i.e., LTP and LTD) is modeled at the level of PF – PC synapses. Learning is conveyed by a population of 20x400 IO neurones.

g_{leak} , V_{leak} , V_{exc} , and V_{inh} are the corresponding resting potentials. Again, when $V(t)$ reaches a threshold V_{th} the cell emits a spike. All active conductances $g_{leak}(t)$, $g_{exc}(t)$, $g_{inh}(t)$ vary according to:

$$g(t) = \bar{g} \sum_j W_j \int_{-\infty}^t \exp\left(-\frac{t-t'}{\tau_c}\right) \delta(t-t') dt \quad (7.3)$$

where \bar{g}_c is the maximal conductance, $W_j \in [0, 1]$ is the efficacy of the projection from presynaptic neuron j , τ_c is the synaptic time constant, t' is the time of a presynaptic spike, and $\delta(t-t')$ is a Dirac function equal to 1 only when the presynaptic neuron emits a spike at time t' .

In the model, a discrete homogeneous Poisson spike-train generator produces the irregular discharge of inferior olive (IO) neurones. At each time step $dt = 1$ ms, we approximate the probability of emitting an IO spike as $P(1 \text{ spike during } dt) \approx r(t) \cdot dt$, with $r(t)$ denoting the mean firing rate. Let $\eta(t)$ be a random number uniformly distributed between 0 and 1. At each time interval dt , an IO cell discharges if-and-only-if:

$$\eta(t) \leq r(t) \cdot dt \quad (7.4)$$

As detailed in section. 7.2.7, error-related information modulates the firing rate $r(t)$, allowing IO activity to signal timed information about instantaneous error (Schweighofer et al., 2004).

Table 7.1 provides the parameter settings for all neuronal models used in our simulations.

7.2.4 Encoding MF cerebellar inputs

The mossy fibers (MFs) constitute the main input stage of the cerebellar microcomplex (Eccles et al., 1967). In the model, MFs carry sensory information (target position), an efference copy of the motor command (torque command for each joint), and the desired joint states (the position and velocity of the elbow and shoulder).

In both inverse and forward cerebellar models, a family of radial basis functions spans the input state space uniformly and generates the input currents $I(t)$ of MFs neurons (Eq. 7.1):

$$I(t) = \gamma + \exp\left(-\frac{(x(t) - \mu)^2}{2\sigma^2}\right) \quad (7.5)$$

Neuronal parameters		DCN	GR	PC	MF
V_{th}	mV	-60	-60	-60	-60
C	pF	2	2	2	2
g_{leak}	nS	2	2	2	2
V_{leak}	mV	-70	-70	-70	-70
g_{exc}	nS	0.1	0.2	60	-
V_{exc}	mV	0	0	0	-
g_{inh}	nS	2	-	-	-
V_{inh}	mV	-80	-80	-80	-
τ_{leak}	ms	20	20	20	20
τ_{exc}	ms	0.5	0.5	0.5	-
τ_{inh}	ms	10	-	-	-

Plasticity parameters		
Model	LTD (β)	LTP (α)
Forward	-0.5	1
Inverse	-0.025	0.1

Table 7.1: Parameter settings for neuronal and plasticity models.

Parameter	$R = [x_{min}, x_{max}]$	σ_x
$\theta_{s,des}$	[-80:40]	12
$\dot{\theta}_{s,des}$	[-180:170]	35
$\theta_{e,des}$	[30:170]	20
$\dot{\theta}_{e,des}$	[-220:170]	39
θ_s	[-80:40]	12
θ_e	[30:170]	20
τ_s	[-3000:3000]	240
τ_e	[-1000:1000]	80

Table 7.2: Input functions parameters

where μ and σ^2 are the center and the variance of the radial basis kernel associated to the MF neuron, respectively. In our simulations, the variance parameter ensures a small overlap of MF responses, the γ constant factor endows MF neurons with intrinsic spontaneous activity of about 5 Hz, and the parameters regulating the discharge of MFs limit their activity to 50 Hz. Input function parameters are given in tab 7.2.

For each region, the target information (see section 7.3) is used to divide the inputs into 8 clusters. Each cluster represents a different target. This clustering strategy is not biologically inspired (the differentiation and the context separation are thought to be made at the granular layer level Philipona and Coenen, 2004), however, it offers a simple way to (i) limit destructive interferences, and (ii) facilitate learning by providing a sparse representation of information (see section 9.3).

7.2.5 Decoding cerebellar outputs

Model deep cerebellar nuclei (DCN) provide the main cerebellar output. For the four inverse corrector models, the decoding of DCN activity must produce motor command adjustments —i.e. correction torque $\sigma_{e,corr}^+$ and $\sigma_{s,corr}^+$ for the agonist muscles of elbow and shoulder, respectively, and $\sigma_{e,corr}^-$ and $\sigma_{s,corr}^-$ for the antagonist muscles of elbow and shoulder, respectively.

For the four forward predictor models, the decoding of the DCNs activity must produce the estimated position and velocity of the limb —i.e. $\theta_{e,est}$, $\theta_{s,est}$ for the elbow and shoulder joints angular positions; and $\dot{\theta}_{e,est}$,

$\dot{\theta}_{s,est}$ for the elbow and shoulder joints angular velocities, respectively.

Decoding DCN activity in inverse corrector models. For each of the four inverse models, an average decoding scheme maps the DCN outputs into a torque adjustment signal. The scheme follows an agonist-antagonist muscle representation. For each articulation, one population called agonist codes for the positive correction torque $\sigma_{limb,corr}^+$ and one population called antagonist for the negative correction torque $\sigma_{limb,corr}^-$. The sum of both extracted correction represents the correction signal that is sent to the limb: $\sigma_{limb,corr} = \sigma_{limb,corr}^- + \sigma_{limb,corr}^+$. Limb represents either the shoulder or the elbow.

Each variable is extracted from the activity of the related population of DCNs, and follow the equation :

$$\sigma_{limb,corr}^{+/-} = A_{limb} \sum_{i=1}^N v_i(t) \quad (7.6)$$

with N the number of artificial neurons coding for the variable and $v_i(t)$ the activity of neuron i at time t . $v_i(t) = \frac{1}{N}$ if neuron i is active, 0 otherwise. Each neuron was considered active if it had fired at least 2 spikes in the last 25 *ms* — that is an instant firing rate of at least 80 *Hz*. A_{limb} is a joint-relative scaling factor and represents the maximum correction that can be applied by the inverse corrector model. In our simulation A_{limb} is set to 3000 and 1000 for the shoulder and elbow, respectively. An example of positive corrective signal of the elbow is shown in figure 7.5.

Decoding DCN activity in forward predictor models. A population decoding scheme computes the predictions of the forward models. Each forward model codes for a predicted position or velocity of a limb (shoulder or elbow) The decoding of each variable follows the equation:

$$\theta / \dot{\theta}_{limb,e} = \frac{\sum_{i=1}^N fr_i(t) * x_i / \dot{x}_i}{\sum_{i=1}^N fr_i(t)} \quad (7.7)$$

where $\theta_{limb,e}$ and $\dot{\theta}_{limb,e}$ represent the estimated position and velocity of the limb at time t , N is the number of output neurons coding for the variable, $fr_i(t)$ is the instantaneous firing rate of the neuron i at time t coding for the position of the limb. The frequency is extracted using a sliding rectangular window of 25 *ms*. x_i and \dot{x}_i represent the preferred position and

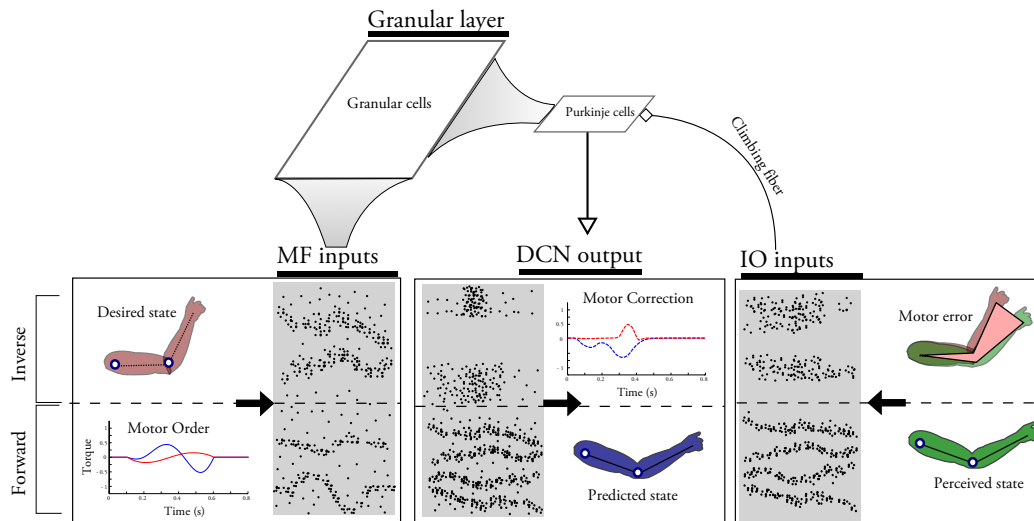


Figure 7.4: Activity of input and output layers. This figure presents an illustrative example of the correspondence between the analog input/output signals and the spiking activity of internal models. Each gray rectangle illustrates a raster plot of a particular layer of cells for both the set of inverse (higher part of the rectangles) and forward (lower part of the rectangles) models (separated by a dash line), through a 800 ms simulation. Time is represented horizontally, neurons vertically, each black dot symbolizes a discharge. The MF layer (left) receives the contextual signal, the desired state of the joints (inverse models) and the motor commands (forward models). The DCN layer (middle) encodes the output, that is the torque corrections (inverse models) and the predictions of the states of the limbs (forward models). IO layer (right) codes for the motor error (inverse model, the difference between the desired state and the perceived state) and for the perceived state of the limbs (forward model). The activity Purkinje cell layer is anti-correlated with DCN's spiking activity and is not illustrated in this image. Also, the sparse activity of the granule cells layer is later presented in figure 9.2.

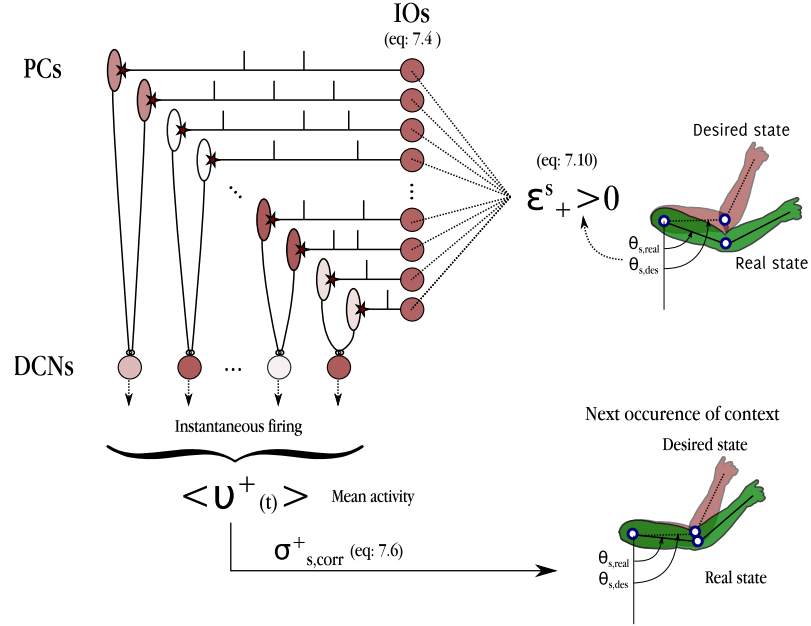


Figure 7.5: Coding scheme of the inverse corrector model. Example of error encoding and output decoding for the virtual agonist muscle of the shoulder joint. The same scheme applies for the positive and negative corrective systems of elbow and shoulder joints. The pictured microzone controls the virtual agonist muscle of the shoulder joints (positive correction, $\tau_{s,corr}^+$). In this example, once the motor command has been executed, the desired angular position of the shoulder (top-right image, $\theta_{s,des}$) is larger than the perceived one (top-right image, $\theta_{s,real}$): the teaching signal should hence favor an increase of the corrective signal controlling the shoulder joint ($\epsilon_{s,+} = \theta_{s,des} - \theta_{s,real} > 0$). Consequently, the IO neurons' spiking is increased for this microzone, which in turn depreciates the strength of PF-PC connections. Later, this reduces the activity of targeted PCs. Due to random initialization weights and the Poisson behavior of IO cells (suggested by a raster plot in each IO-PC connection), the PCs activity is different for each cell (symbolized by a different color opacity). However, it sequentially captures the error message and tunes the mean firing rate of the DCNs neurons to follow the direction of the desired correction. In this case, the PCs activity is depreciated, and thus the activity of DCNs' neurons is increased, amplifying $\tau_{s,corr}^+$. At the next occurrence of the same context, the observed position of the shoulder will be closer to the desired one, as pictured in the bottom-right image. The color opacity gives a visual indication of the activity of cells, and the equations to transform analog signals into currents/spiking activity (and vice-versa) are numbered in reference to the equations of this manuscript.

velocity, respectively, coded by the neuron i . For each variable, preferred position and velocity are evenly distributed over the output space. The range $R = [x_{min}, x_{max}]$ of each variable is given in table 7.2. An example of predictive signal for the angular position of the shoulder is described in figure 7.6.

7.2.6 Synaptic efficacy and plasticity rules

In the model, most connections of the microcomplex circuit are non plastic, except for parallel fiber–Purkinje cell (PF–PC) synapses —although other plasticity sites of the real cerebellar microcomplex have been reported (Hansel et al., 2001; Boyden et al., 2004; De Zeeuw and Yeo, 2005; Pugh and Raman, 2009). Non-plastic synaptic weights are tuned to generate mean firing rates consistent with experimental data. Recent GC in vivo recording experiments (Chadderton et al., 2004; Jörntell and Ekerot, 2006; Rancz et al., 2007; Arenz et al., 2008) have reported that joint-related movement inputs generate sustained GC activity at a frequency of about 150 Hz (Chadderton et al., 2004). Also, it is admitted that two or more input spikes from MF afferents are necessary to elicit one GC burst of spikes (Chadderton et al., 2004). We tuned GC neuronal parameters and MF–GC synaptic weights in order to fit these data. The model does not account for the very high transient GC activity induced by other types of sensory modalities. Model PC simple spikes occur at rates ≤ 150 Hz (Raman and Bean, 1999) when PC are activated by parallel fibers. PC complex spikes, caused by a single discharge of the afferent climbing fiber, correspond to learning triggering events —we do not simulate high frequency components of the bursts. Finally, DCN neurons have mean firing rates of about 20 Hz (Lamont, 2009). Since this average activity occurs while PCs send inhibitory signals to DCN cells, we assume that, in the absence of PC activity, DCN can have a stronger activity upper-bounded by 200 Hz.

Model PF–PC synapses undergo bidirectional long-term plasticity, i.e. both potentiation, LTP, and depression, LTD. We implement LTP as a non-associative weight increase triggered by each GC spike, consistent with the homosynaptic rule describe by Lev-Ram et al. (2002). The synaptic weight W_{PF-PC} of each PF–PC connection increases according to:

$$\Delta W_{PF-PC}(t) = \alpha \cdot \delta(t - t_{GC}) \quad (7.8)$$

where α denotes a gain factor and the delta function is $\delta > 0$ only when the presynaptic GC emits a spike at time t_{GC} .

We simulate LTD at PF–PC synapses as an associative weight decrease triggered by a spike from the IO. This principle is in agreement with the heterosynaptic plasticity mechanism described by Ito and Kano (1982). The weight W_{PF-PC} of each PF–PC synapse decreases as:

$$\Delta W_{PF-PC}(t) = -\beta \cdot \int_{-\infty}^{t_{IO}} f(t - t_{IO}) \delta(t - t_{GC}) dt \quad (7.9)$$

where β is a gain factor, and the temporal kernel function f correlates each IO spike with the past discharge of a GC (see figure 7.7 and Carrillo et al., 2008). In the model, the largest LTD amplitude occurs when the PC receives an IO spike approximately 100 ms after an input spike from a GC, consistent with Safo and Regehr (2008).

Table 7.1 provides the parameter settings for the implemented plasticity models.

7.2.7 Encoding of error/teaching signals

In both inverse corrector and forward internal models, IO neurons convey error/teaching signals via the climbing fibers that target PCs and mediate LTD at PF–PC synapses.

Teaching signal for inverse corrector model. For the four inverse models, the error signals must account for the discrepancies between the desired and executed motor commands. The teaching signal relies on the perceived motor error, which is the discrepancy between the desired position of each joints and their real position. The error signal, at time t , for the joint i is $\epsilon_i(t) = (\theta_{i,des}(t_1) - \theta_i(t_2))$, where $\theta_{i,des}(t_1)$ is the desired position of joint i at time t_1 and $\theta_i(t_2)$ is the real position appreciated by the sensory feedback system at time t_2 . We have to take into consideration that the signals were delayed in order to align them in time ($t_1 = t - (\delta_1 + \delta_2)$ and $t_2 = t - \delta_2$). Biologically, this could be explained by the processing time of each structure and the delay of the sensory feedback signals.

The error signal is then used to modulate the firing rate $r(t)$ of each IO cell (see eq. 7.4). To compute this value, we first extract the positive part of the error signal for joint i : $[\epsilon_i(t)]^+$ which is related to an error in

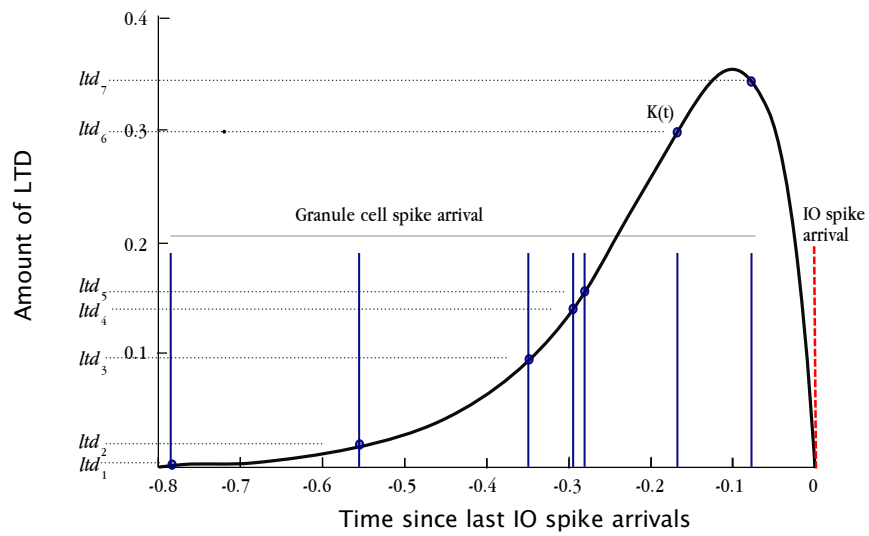


Figure 7.7: LTD Kernel (adapted from article Carillo et al. 2008.). Kernel ($K(t)$) used for a granule cell (GR) and Purkinje Cell (PC) synaptic long term depression. The kernel is convolved with the spike train of the afferent PF (all spikes emitted at time $t < 0$). This provides a trace of the past PF activity setting the eligibility of the synapse to depression when the IO neuron (afferent to the PC) emits a spike (at time $t = 0$). In this example the resulting LTD at the PF-PC synapse would be equal to $\sum_{i=1}^7 ltd_i$.

the corresponding agonist muscle, and the negative part $[\epsilon_i(t)]^-$ which is related to an error in the antagonist muscle.

For instance, the firing rate $r(t)$ of all IO neurons in the two microcomplexes correcting errors in the positive range ($\sigma_{s,corr}^+$) and negative range ($\sigma_{s,corr}^-$) of the torque command of the shoulder (σ_s) vary respectively according to:

$$r_{\sigma_s^+}(t) = k \cdot \mathcal{H}([\epsilon_s(t)]^+) \quad (7.10)$$

$$r_{\sigma_s^-}(t) = k \cdot \mathcal{H}([\epsilon_s(t)]^-) \quad (7.11)$$

where $k = 10$ is a scaling factor and \mathcal{H} is the Heaviside function defined such that $\mathcal{H}(0) = 0.1$.

According to Eqs. 7.10, 7.11 (and see also example in figure. 7.5):

- When the cerebellar output equals the output required for the shoulder, i.e. no torque change is needed and $\epsilon_s(t) = 0$, the mean IO firing rates are $r_{\sigma_s^+}(t) = r_{\sigma_s^-}(t) = 1 \text{ Hz}$, which make heterosynaptic LTD (Eq. 7.9) and homosynaptic LTP (Eq. 7.8) at PF–PC synapses to compensate each other in both microcomplexes —i.e. no adaptation takes place.
- When the cerebellar output undershot the output required for the shoulder, i.e. the torque of the shoulder must be increased and $\epsilon_s(t) > 0$, then $r_{\sigma_s^+}(t) = 10 \text{ Hz}$, which makes LTD to take over LTP in the active PF–PC synapses of the corresponding microcomplex. The consequent decrease of PF–PC synaptic efficacy reduces the inhibitory action of PCs onto DCN neurons the next time that the microcomplex receives the same contextual input —which activates the same PF–PC synapses and then the same PC responses. As a consequence, the population activity of DCN neurons increases, which reinforces the correction signal $\sigma_{s,corr}^+(t)$ (according to Eq. 7.6). In addition, for $\epsilon_s(t) > 0$, the mean IO firing rates $r_{\sigma_s^-}(t) = 0 \text{ Hz}$, which blocks LTD in the active PF–PC synapses of the corresponding microcomplex. Thus, LTP increases and strengthens future inhibitory actions of PCs onto DCN neurons in the presence of the same contextual input to the microcomplex. Then, the corrective signal $\sigma_{s,corr}^-(t)$ decreases over time. As a consequence, the resultant correction $\sigma_{s,corr}(t)$ tends to increase and become positive over training.

- Conversely, when the cerebellar output overshoot the output required for the shoulder — i.e. the torque command of the shoulder must be decreased and $\epsilon_s(t) < 0$ — the overall correction $\sigma_{s,corr}(t)$ tends to decrease and become negative over training.

During offline consolidation, the perceived motor error is calculated by using the prediction of the forward model. In this case, the error signal at time t , for joint i is given by $\epsilon_i(t) = (\theta_{i,des}(t) - \theta_{i,pred}(t))$ where $\theta_{i,pred}(t)$ is the predicted position for joint i at time t . When this information is not available, then the error is considered null and $r_{\sigma_s^+}(t) = r_{\sigma_s^-}(t) = r_{\sigma_e^+}(t) = r_{\sigma_e^-}(t) = 1 \text{ Hz}$ for all IO neurons.

Teaching signal for the forward predictor model. For the forward model, the teaching signal relies on the perceived state of each limb. The mean firing rates of IO cells in each microcomplex vary according to a set of radial basis functions spanning the state space uniformly.

For instance, in the microcomplex subserving the prediction of the shoulder angular position as described in figure 7.6, the mean firing rates of each IO cell i —i.e. $r_i(t)$ — varies as:

$$r_i(t) = k \cdot \exp\left(-\frac{(\theta - \theta_i)^2}{2\sigma_i^2}\right) \quad (7.12)$$

where $k = 10$ is a scaling factor, θ_i is the “preferred angle” of the cell, and σ determines the degree of overlap between adjacent IO responses. In this microcomplex, a group of 2×20 IO cells shares the same preferred angle. Each group of IO neurons targets two distinct PCs, which in turn inhibit the same DCN unit. The latter codes for the same portion of the θ state space (and has the same preferred angle θ_i) than the IO cells that modulate its inhibitory PC afferents. According to Eq. 7.12 and to the plasticity rules described in section 7.2.6:

- If the firing rate of the two IO cells with preferred angle θ_i is $r_i(t) \approx 1 \text{ Hz}$, then LTD and LTP at PF–PC synapses of the two PCs driven by these two IO cells compensate each other. No learning occurs.
- If the firing rate of the two IO cells with preferred angle θ_i is $1 < r_i(t) \leq 10 \text{ Hz}$, then LTD dominates LTP at the PF–PC synapses of the two PCs driven by these two IO cells. Thus, over training, the DCN unit whose preferred angle is close to θ_i tends to increase its

firing activity, whereas the other DCN units tend to either decrease or maintain their spike frequency. As a consequence, the decoding scheme used to readout the population activity of DCN neurons in the forward predictor model (Eq. 7.7) will tend towards an estimate of the next angular position close to θ_i .

- Conversely, if the firing rate of the two IO cells with preferred angle θ_i is $0 \leq r_i(t) < 1$ Hz, then LTP dominates and the corresponding DCN neuron tends to decrease its spike frequency. Thus, this DCN unit will not contribute to the population decoding scheme significantly.

7.3 Simulated environment

The simulated environment reproduces the experimental paradigm used by Huber et al. (2004) in a rotation adaptation task. It is defined by a central position S, and by eight targets equally set on a circle centered on the central position S. We define a trial as the succession of 90 movements. Each movement starts from the center S and consists in realizing a straight movement of the hand to one of the eight targets, randomly changed every second (1 s corresponds to the time length of an isolated movement in our simulation). The trajectory of the hand was precomputed by the minimum jerk model previously described, in which we added an error relative to the arm position. This error emulates a rotation anticlockwise as described in figure 7.8 and each subject had to adapt their movement to compensate for this error.

Since the trajectory of the hand depends on the torque sent to each joint (shoulder and elbow), correcting the error is not a trivial operation. The torque signals are not fixed during the movement: they are updated at each time step of the movement (every millisecond) by taking into account the expected position, velocity and acceleration of each joint. Furthermore, the optimized sets of motor torque commands to reach two different targets are independent, thus the adaptation to one target can not be generalized to another target. Similarly, an increase of the rotation error implies a new set of command independent of the previous one. This is illustrated in figure 8.3 in which we present target reaching for two symmetric targets, with a fixed angular error of 45° in four different configurations: (1)

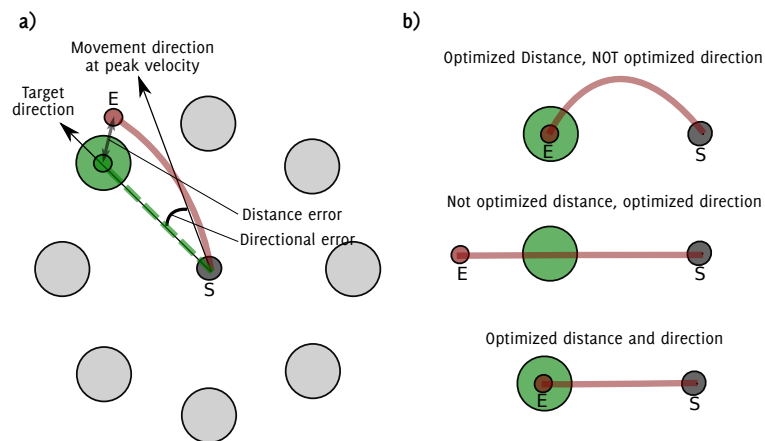


Figure 7.8: Experimental protocol and measures of performance. (a) The experimental protocol is made of eight targets (large circle) placed around a circle of center S . S corresponds to the starting position of the hand when initiating the movement, and, for each movement, the subject has to reach a random target (green circle) that changes randomly every second. The distance and directional errors are calculated when a subject stops its movement. The directional error corresponds to the angle between the line representing the target direction (dotted green line) and the line representing the movement at the peak outward velocity. The distance error corresponds to the distance between the position of the target (T) and the final position of the hand when movement stops (E). (red circle E). (b) Independence of directional and distance errors. Top: The distance error is null, but the directional error is high. Middle: The directional error is minimal, but the distance error is high. Bottom: Optimized trajectory with a null distance and directional error.

No adaptation, (2) an adaptation using the forward models, (3) an adaptation using the inverse models and (4) an adaptation using the coupling scheme.

7.4 Measures of performance

The performance is measured by monitoring two parameters: the directional and distance errors (see figure 7.8a). The directional error corresponds to the angle between the line from the initial hand position (S) to the central position of the target (T) (dotted green line) and the line to the position of the hand at the peak outward velocity (solid line). The red line represents the hand trajectory from its starting position (S) to its end (E). The distance error has been calculated as the distance between the position of the target (T) and the final position of the hand (E).

Both errors have been normalized. For example, if we add an angular deviation of 15° in the minimum jerk model, a directional error of 1 in our simulation corresponds to an error of 15° ; and a distance error of 1 corresponds to an error of 36 mm — that is the distance between E and T if the movement is not corrected. The two errors are independent, and we suppose that a trajectory is optimal when both the directional and distance errors are minimal (see figure 7.8 b)

Chapter 8

Simulations

In the following chapter, we present our simulation results and confront them with experimental data. First, we assess the capacity of the internal models to adapt their dynamics and compensate for the directional and distance errors by training them on a fixed angular deviation protocol. In a second section, we observe how the system behaves on a simulated version of the evolutive angular deviation protocol used by Huber et al. (2004). In the last section of this chapter, we present the consolidation of performance provided by the offline efficacy of the coupling scheme.

8.1 Fixed angular deviation protocol

We first tested capacity of the internal models - Inverse and Forward - to adapt their dynamics and compensate for directional and distance errors by training them on a fixed angular deviation protocol.

In this protocol, three groups (FM_g , IM_g and CM_g) of 10 artificial individuals were trained on a rotation adaptation task containing 6 trials, with a fixed angular deviation set to 15 degrees in the generation of movements.

The subjects of the FM_g group (for Forward Model) are allowed to adapt their trajectory using only the forward model scheme, i.e. they could only recalculate the whole trajectory to the target by using the predicted positions and velocities of the forward models. The subjects from the IM_g group (for Inverse Model) can adapt their movements using only the inverse model corrections, i.e. sending corrections to the limbs adapted to the ongoing contextual informations. The subjects from the CM_g groups (for Coupling Model) are allowed to change the dynamic of the arm us-

ing at the same time information from the forward models and from the the inverse models, taking advantage of the coupling solution presented previously in section 7.2.

The performance of the three groups are then compared (*i*) in order to highlight the specificities of each type of internal model and (*ii*) to account for the benefits of using the coupling scheme over the other methods.

8.1.1 Results

The results from the fixed angular error protocol are presented in figure 8.1 and 8.2. In figure 8.1, we show a sample of 3x8 trajectories at three different steps of the learning (end of trial 1, 2 and 5). This figure gives a visual feedback of what is learned by the three systems, and suggests that the coupling scheme (CMS) is able to surpass both the forward model (FMS) and the inverse model corrections (IMS) all along the training for the distance and directional measures. To attest for this, we present in figure 8.2 the normalized mean error for distance and direction for the three tested methods - forward, inverse and coupling. In the first iteration (one movement for each target), both distance and directional errors are maximum (36 mm and 15 °, respectively). Then, the mean distance and directional errors decrease through the training process for all three systems. Reflecting the fast adaptation capabilities of the forward models, the FMS adapts faster than the IMS, and reaches a plateau after the second trial; the IMS is slower to adapt, and decreases significantly the error between the first and second trial ($\approx 40\%$ for distance and directional errors). For the distance error (right), it reaches a peak of performance in the second trial (0.5 ± 0.1). We then observe an over-training and a slow decrease in performance. This decrease is also visible in figure 8.1-right-panel: the trajectories are well corrected during the first part of the movement but then deviate from the ideal trajectory, thereby increasing the distance between the target and the hand position by the end of the movement. In average, we notice that the FMS makes smaller errors of distance than the IMS, indicating that the forward predictive models are more indicated in correcting the final position of the controlled object. For directional errors, if the IMS adapts more slowly than the FMS, it then outdistances the FMS performance and still learns to optimize the trajectory up to the end of the learning session, to reach a minimum of 0.28 ± 1.2 at the end of trial 6. This indicates that the inverse model is more efficient in correcting the angular error (the global

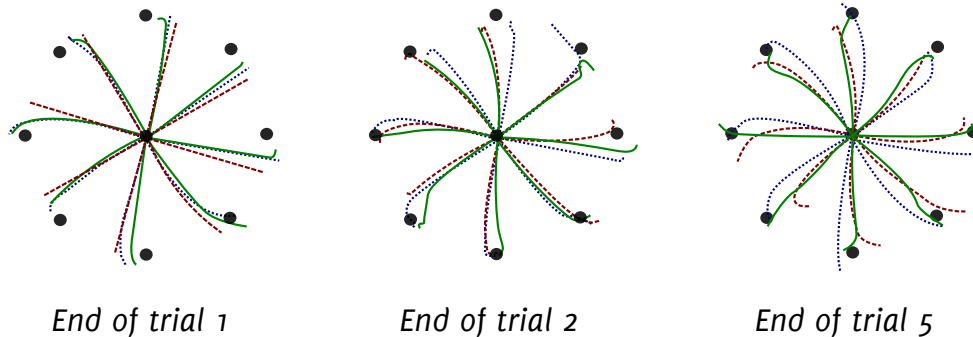


Figure 8.1: Example of trajectories at three steps of learning. Three different configurations for adapting the movement are used: the forward (FMS), inverse (IMS) or coupling model scheme (CMS). The hand starts from a central position and has to reach one of the eight targets represented with a black point. The target is chosen randomly and changed every second. The system has to adapt its dynamics to fit the ideal movement, which should be a straight line from the central position to the target. Adaptation using the forward model is shown in blue dotted line, the inverse model in red dotted line, and the coupling scheme in green plain line. One sample per target is shown. **A.** At the end of the first trial, the inverse model scheme, which has a slow learning dynamic, does not correct the trajectory which deviates of 15 degrees from the ideal one. The fast learning capabilities of the forward model, on its side, permits to adapt the trajectory on a smaller time scale, and shows a beginning of adaptation. The coupling model takes advantage of the forward model and shows similar performance. **B.** At the end of the second trial (middle), both the inverse and the forward models (IMS and FMS) are able to adapt the trajectory. The forward model scheme seems efficient enough to reach the target with a good accuracy but the shape of the trajectory is elliptic, far from being optimal. The inverse model seems to be more adapted to correct the shape of the movement to follow a direct path. The coupling scheme (CMS) seems to take advantages of both strategies, and shows a good accuracy in term of reaching the target and shaping the movement. **C.** At the end of the fifth trial (right), the forward model (FMS) learning seems to be stabilized, and performance appears to be equal compare to the previous one. Reaching is good but shaping is not optimal. The inverse model scheme (IMS) movements present a good shape from the start until the middle of the trajectory, but afterwards over-corrects the movement which drifts from the target, reflecting an over-training. Again, the coupling scheme (CMS) takes the best of each method and corrects the trajectory for it to fit accurately the ideal movement.

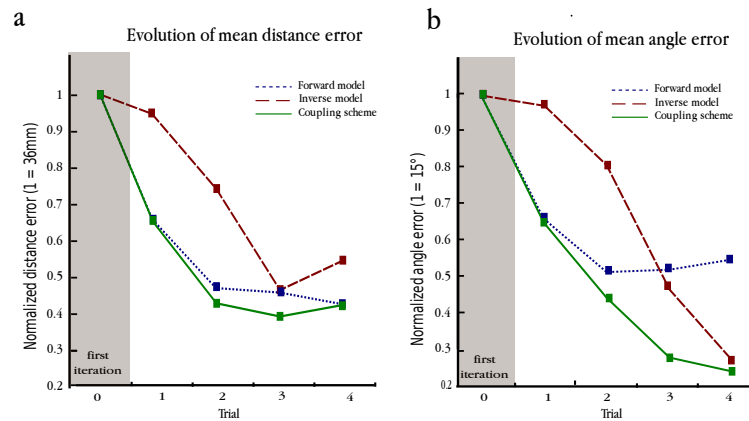


Figure 8.2: Evolution of angle and distance along training. Evolution of the distance (a) and the directional (b) errors along training, using three different configurations for adapting the movements: the FMS, IMS or CMS. Adaptation using the forward model scheme (FMS) is shown in blue dotted line, the inverse model scheme (IMS) in red dash line, and the coupling scheme (CMS) in green plain line. The first iteration corresponds to the base line and shows the performance of all three learning schemes before adaptation. Each trial corresponds to a session of 90 s and both errors are normalized.

shape of the trajectory during the realization of the movement).

The CMS, for both error measures, seems to initially benefit from the fast learning capabilities of the forward model and then takes advantage of both methods (forward and inverse) to surpass any correction capabilities of a forward or an inverse model could provide without coupling. Indeed from trial 1 to trial 6, we observe that the performance of the coupling method is better than that of a simple learning method for correcting the directional error. For the distance error, the CMS equals the FMS performance during the first three trials (except for trial 2 where distance error of the CMS is slightly higher), and surpasses the FMS capabilities in the three last trials of the training session.

8.2 Evolutive angular deviation protocol

Once we observed how each type of internal model was able to correct a precise component of motor error (directional error and distance error for the inverse and forward model, respectively), we implemented a more complex simulation reproducing the experimental protocol made by Hu-

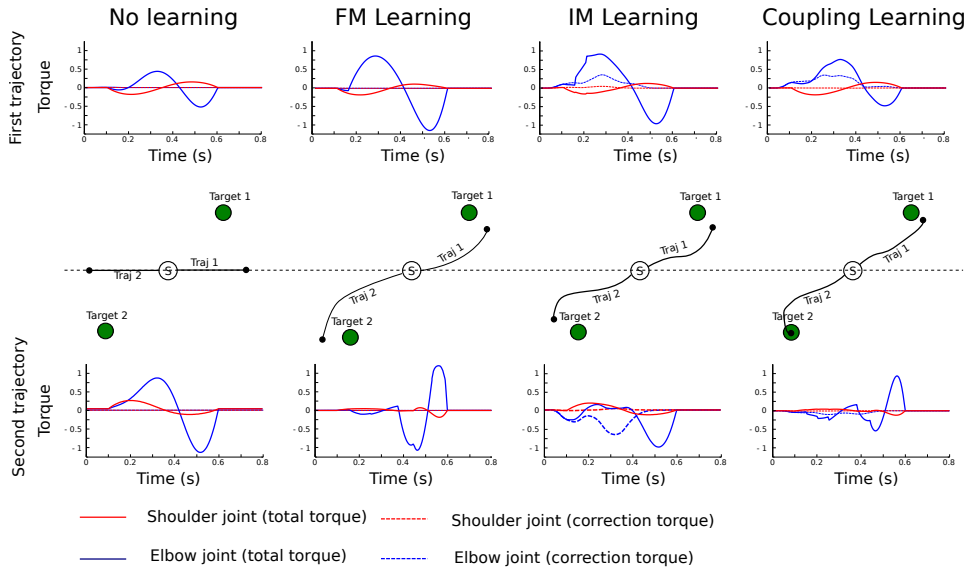
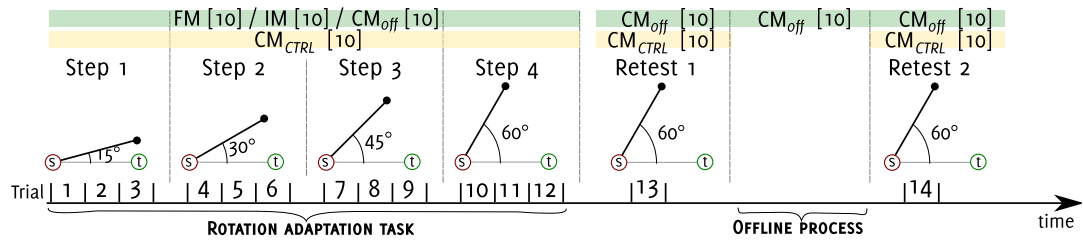


Figure 8.3: Example of torque commands and corrections. We show in this figure the torque commands and corrections sent to each joint to reach two symmetrical targets in four distinct configurations. Target 1 related torques are presented at the top and target 2 related torques at the bottom of the figure. For each target, four different configurations are presented from left to right: No adaptation, the FMS adaptation, the IMS adaptation and the CMS adaptation. For each figure, the torque commands sent to each articulation are represented along time in plain line (shoulder is in red and elbow in blue): Each movement is supposed to be realized in a time window of 700 ms. The correction torques are also represented in dashed line (same color scale), and torque values have been normalized. Three observations have to be made: (1) Torques sent to each articulation are not static during the movement generation, they dynamically change to achieve the desired movement. (2) Two symmetrical movements imply two sets of independent torque commands (compare first and second trajectory when no adaptation is permitted, left figures) (3) A correction of the angular deviation implies a new set of torque commands independent of those of the not corrected movement (compare for example torque commands sent in the No adaptation scheme and the CMS, in the case of the second target, insets 1 and 4 at the bottom).



*Figure 8.4: Groups and protocols. **Evolutionary angular deviation protocol*** Evolution of performances of three groups of ten subjects (FM , IM and CM_{off}) are compared. Each subject of each group is provided with a special scheme for learning. A simulated individual from the FM , IM and CM_{off} group can adapt its movement using the FMS, IMS and CMS, respectively. Training is realized over four sets of three trials of 90 s each. After each step, the angular deviation introduced in the minimum jerk model is increased by 15° , starting from an error of 15° in step 1 and ending with an error of 60° for step 4. For each step, we draw in black an uncorrected movement realized by an agent. The starting point S corresponds to the hand position at the beginning of the movement, t represents the target (desired position of the hand at the end of movement), and the black dot symbolizes the real position of the hand afterward. **Offline protocol** Two groups of ten subjects, CM_{off} and CM_{CTRL} , underwent rotation adaptation task as described in the evolutionary angular deviation protocol. The extent of the rotation adaptation is tested after the end of training using an imposed rotation of 60° (Trial 13 in Retest 1). Subjects from group CM_{off} then achieve an offline consolidation process composed of a series of 48 trials in offline mode. Subsequently, subjects from both groups are retested on a simple trial (Trial 14, retest 2) and performances of both group are compared.

ber et al. (2004).

8.2.1 The protocol

In this experiment, the angular deviation added to the generation of movement was allowed to evolve through the task. Similarly to Huber et al. (2004), the experimental protocol involves four incremental steps, for each of which the angular deviation (bias) is increased by 15° , within the range $[15^\circ, 60^\circ]$ (see figure 8.4). Every step is composed of three trials. Three groups (FM , IM , CM_{off}) of ten individuals each are trained on the rotation adaptation task. The FM group uses a pure forward model strategy

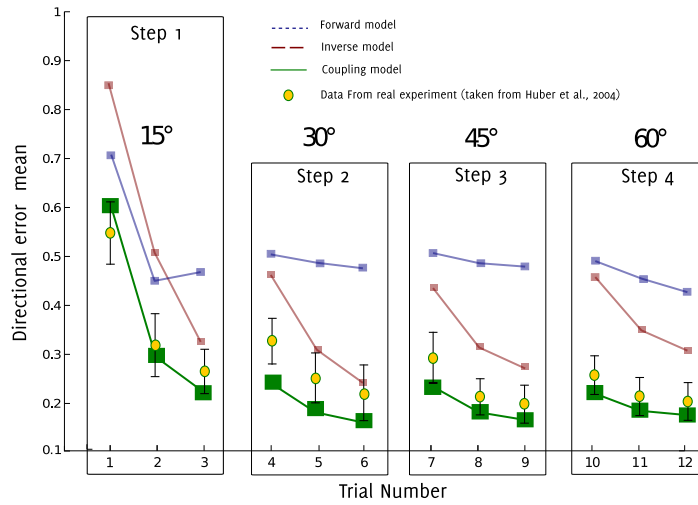


Figure 8.5: Variation of angular error in the evolutive angular deviation protocol. Evolution of directional error through learning. Only subjects from CM_{OFF} group (plain green line), using a coupling method to adapt trajectory, are able to reproduce experimental data, showed in yellow dot in the figure. Subjects from IM (pointed red line) show a slower learning process but present a higher level of performance once adapted to the task, Subjects from FM (dashed blue line) adapted faster but stabilize at a much higher error level.

to solve the task. The IM group employs a pure inverse model strategy to adapt the response to the unknown angular bias. The CM_{off} group uses the coupling scheme.

Following the four training steps, the extent of rotation adaptation of the CM_{off} group is tested using an imposed bias of 60° (Trial 13 in Retest 1). Then, simulated agents are enabled to undergo an offline consolidation process consisting of a series of 48 trials. Subsequently, subjects are retested on a simple trial (Trial 14, retest 2). To assess the benefit of an offline consolidation process against a pure online learning, performances of the CM_{off} group are compared to a group of control subjects (CM_{CTRL}) which do not perform offline consolidation.

8.2.2 Results

The results of the *Evolutive angular deviation protocol* are presented in figure 8.6 for the directional error and in figure 8.5 for the distance error, for the three system (the IMS , FMS and CMS).

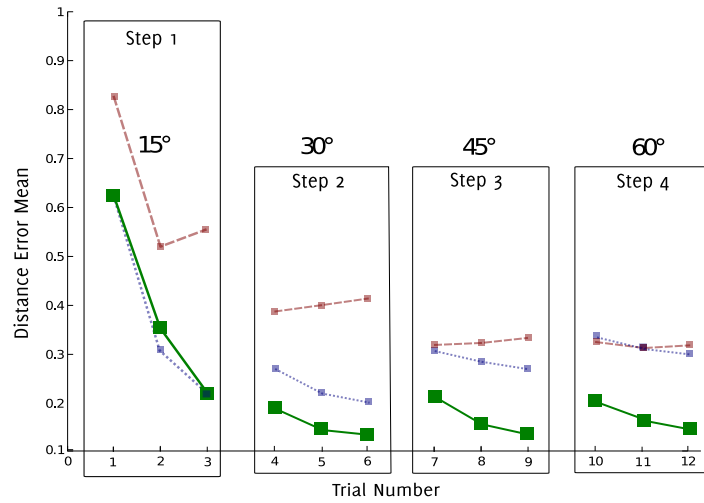


Figure 8.6: Evolution of distance error in the evolutive angular deviation protocol.

Directional error. As observed previously, the IMS (red dotted line) is slower to adapt and hence presents higher directional error at the beginning of the learning (trial 1 and 2), compared to the FMS. The IMS goes beyond the FMS performances in trial 3 and then outperforms it during the rest of the rotation task. The adaptation of the IMS is characteristic and stereotyped at each shift of the angular deviation (from 30 to 60°). When the fixed angular deviation is increased (trial 4, 7 and 10), the performance collapses and the directional error rises to a level contained between 0.43 and 0.47. This reflects the slow adaptation process of the inverse model while facing new contexts. In the course of the second and third trial of each step, the inverse model then adapts the trajectory and the directional error strongly decreases to an acceptable level by the end of each step ($Edir_{IMS}(6) = 0.25$, $Edir_{IMS}(9) = 0.27$ and $Edir_{IMS}(6) = 0.3$).

On the contrary, the FMS (blue dotted line) adapts the trajectory from the first trial and stabilizes its performances as soon as the end of the second trial, thanks to its fast learning capability ($Edir_{FMS}(2) = 0.46$). The error stays relatively stable until the end of the training process, oscillating from 0.43 in trial 12 to 0.5 in trial 7. The passage to a new step does not have a significant impact on performance and the error only slightly increases (+8% after step 1; +6% after step 2 and +2% after step 3), followed by a new slight decrease of error.

Eventually, we observe that the CMS shows better performance levels (green line) than the IMS and the FMS at any time of the training. The level

of optimization of the system rapidly increases in the first block of three trials, the directional error falling to a level of 0.25 by the end of the third trial. The error rises slowly for every change in the angular deviation and progressively decreases to stabilize at a good level of performance at the end of the steps ($e_{IMS}(6) = 0.17$, $e_{IMS}(9) = 0.17$ and $e_{IMS}(12) = 0.18$)

Additionally, only the CMS is able to reproduce the data we observed on real subjects (yellow dots). This suggests that a good collaboration between predictors and correctors is needed in the central system in order to optimize voluntary movements.

Distance error. As we previously observed, the FMS is more adapted to reduce the errors of distance than the IMS. At the beginning of step 1, due to a slow learning adaptation capability, the IMS only slightly corrects the distance error in trial 1. On the contrary, the FMS profits from fast learning capabilities, and reduces the error as soon as the first trial of step 1. The IMS then progressively reduces the distance error but stays most of the time behind the level of correction of the FMS. At some point in the learning - for example at step 1, trial 3 - we also observe that the system must have been overtrained and loses performance. Interestingly, the IMS better corrects distance error when the deviation is high (stabilizing at a level of 0.3), contrary to the FMS, which loses performance with an increase of the angular deviation. Consequently, the difference of performance based on distance error is reduced along training between the FMS and the CMS, and the discrepancy between the two models is no longer observable by step 4, when the angular deviation reaches 60° . Once again, we observe the benefits of using the CMS, which retains a higher level of performance for a majority of steps. In step 1, the system benefits from the fast learning capabilities of the forward model and equals the performance of the FMS. It then outperforms the FMS and the IMS models for each trial of the other steps, keeping a good level of performance all along training. As we observed for the directional error, each change of step induced a slight decrease in performance for the first trial of the new step (except from step 1 to 2), but the learning then stabilizes the distance error at a very low value by the end of each step (0.2, 0.14, 0.15, 0.16 for step 1, 2 3 and 4, respectively), revealing a very good adaptation of the model to all types of errors.

8.3 Offline consolidation

As we observed in the *Evolutionary angular deviation protocol*, a good collaboration between the forward and the inverse models can explain with a good accuracy online experimental recording obtained recently on a motor task adaptation (Huber et al., 2004). Furthermore, another main advantage of such a coupling scheme is to provide offline learning capabilities to the system if we make the assumption that the sequence of actions could be replayed offline. Hence, the purpose of the next section is to emphasize the offline learning capabilities of our model and compare our simulation results with experimental ones on a similar task.

8.3.1 Consolidation after a subsequent offline consolidation process

As aforementioned, another potential advantage of the coupling scheme is that it supports offline learning assuming that the sequence of actions executed during online training can be replayed offline (Maquet et al., 2003).

Protocol. In order to assess whether an offline consolidation process can further increase the system's performance — at the end of the online adaptation protocol — 2 groups of 10 simulated subjects are considered. Both groups consist of subjects adopting the coupling scheme (CM). However, one group (CM_{off}) is allowed to undergo offline learning, whereas the other (CM_{CTRL}) is not.

The figure. 8.4 shows the protocol. Both groups (CM_{off} and CM_{CTRL}) undertake the 12 online training trials. A first probe test (trial 13) is executed to evaluate the extent of the online rotation adaptation in both groups. Then, subjects from group CM_{off} undergo a simulated offline learning process consisting of a set of 48 trials (4320 trajectories randomly replayed) during which no sensory feedback is provided to the system. Therefore, the learning signal can only be computed based on the prediction provided by the forward model, and the inverse model can adapt its dynamics only when this teaching information is available. Finally, both groups CM_{off} and CM_{CTRL} undertake a second probe test (trial 14) and their performances are compared.

Once again, data obtained from our simulations were confronted with

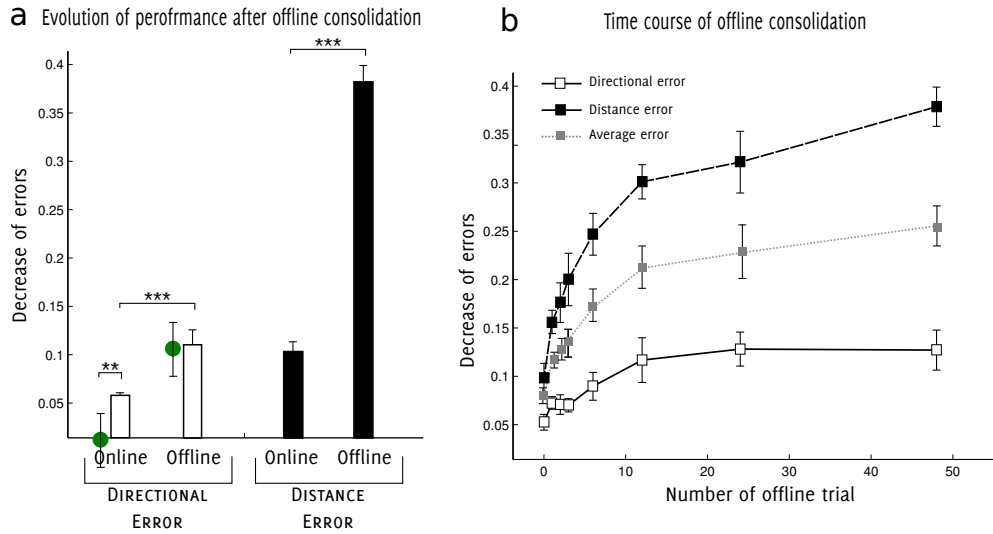


Figure 8.7: Post-offline process performance improvement. **A:** Post-offline performance improvement. An ANOVA test showed that the two groups had a similar performance when tested immediately after training; however, during a retest after an offline consolidation process, mean directional and distance error were highly reduced in the CM_{OFF} group, compared to the CM_{CTRL} group. Experimental results obtained on real subjects are shown in green dots, and taken from Huber et al. (2004). The two groups differ significantly in the extent of their test-retest performance change. **B:** Decrease of angular and distance errors compared to the offline process duration.

experimental data obtained on human subjects from recent behavioral experimentation (Huber et al., 2004).

Results. Figure 8.7a shows the results of this comparison both from our simulations and from experimental data obtained on human subjects (Huber et al., 2004). A repeated measure analysis of variance and post-hoc tests show that the two groups have similar performances during the first probe test (i.e. when tested immediately after online training, trial 13). On the other hand, the second probe test (trial 14) shows that the mean directional error and distance error of CM_{off} subjects is significantly reduced compared to control subjects. For the directional error, compared to the first probe test (trial 13), a performance enhancement of $12.7 \pm 2.1\%$ is reached by CM_{off} subjects. By contrast, the control subjects exhibit a lower performance improvement of $5.2 \pm 1\%$. For the distance error, compared to the first probe test (trial 13), a performance enhancement of $38 \pm 2\%$

is reached by CM_{off} subjects. By contrast, the control subjects exhibit a lower performance improvement of 9.8 ± 1.5 %. The small increase of performance of the control population (i.e. with no offline consolidation) reflects the learning occurring during the second probe test. Furthermore, the increase of performance related to angle error of simulated CM_{off} subjects is consistent to that observed experimentally on human subjects after a night of sleep (yellow data, $+11 \pm 3$ % (Huber et al., 2004)). Since all parameters were controlled in our simulation, the improvement we report could only be explained by the offline consolidation process, and not by other factors such as a circadian cycle. However, simulated control subjects appear to better perform during the probe test (trial 14) compared to human subjects tested again after 8 hours of wakefulness, who do not show any significant improvement. This discrepancy might be at least partially explained by random interferences during the 8 hours of wake on human subjects.

8.3.2 Time course and limit of offline consolidation

As observed in the last subsection, a sufficient time length of offline processing could lead to an improvement of overall performances for both monitored criteria. This observation, other than being consistent with real data, raises a fundamental question concerning the level of improvement one can achieve as a function of the duration of offline processes.

Protocol. To address this question, we performed a new set of simulations using 8 groups of 10 individuals. Each group was allowed to perform an offline consolidation process for a different given duration (0,1,2,3,6,12,24 or 48 trials). Prior to the consolidation process, subjects from all groups followed an initial training session of the rotation adaptation task as described in section 8.2 and a first test trial to measure the extent of rotation adaptation (trial 13 of the *Evolutionary angular deviation protocol*).

After the offline process, a second probe test (trial 14) was performed by all the subjects of all groups and the evolution in performance was measured for both monitored errors (the distance and the directional errors).

Results. Figure 8.7b shows the results of our simulations. As reported in the previous protocol, a repeated measure analysis of variance and post-

hoc tests show that the eight groups have similar performance when tested immediately after training (trial 13).

More interestingly, we observe that an increase in performance during the second probe test (trial 14) was highly dependent of (i) the monitored criteria and (ii) the time length of the offline process. We observe that the directional precision profits slightly from an offline processing ($12.7 \pm 2.1\%$ after 48 trials compared to $5.2 \pm 1\%$ with no offline learning), whereas the distance precision receives a high benefit from the offline consolidation process ($38 \pm 2\%$ compared to $9.8 \pm 1.5\%$ with no offline learning). Furthermore, the increase of performance based on directional error seems to stabilize after about 20 offline trials (passing from 24 to 48 offline trials does not decrease significantly the directional error). On the other hand, the distance error keeps taking advantage of the offline process until its end ($32 \pm 2\%$ versus $38 \pm 2\%$ after 24 and 48 trials, respectively). However, the benefit obtained between the 24th and the 48th trials does not appear to be statistically conclusive, indicating that offline learning can not optimize learning beyond a certain limit. Importantly, we do not observe a fall in performance when the system is over-trained, suggesting that our system is robust.

Chapter 9

Properties of the internal models

All the behavioral results we presented in the previous chapter do not only depend on the coupling scheme but also on the properties of the simulated internal models. Three intrinsic features of the simulated cerebellar microcomplexes play a major role in achieving good performances in the online and offline adaptation, and concern both the forward and inverse models: *(i)* first, the forward models need to be bistable (bistability being defined as the capacity to give an accurate prediction¹ when the forward model is active, and to stay silent otherwise); *(ii)* then, when performing offline, the inverse model has to keep its dynamic unchanged when the forward model is unable to give a good prediction of the state of the joints; *(iii)* eventually, granule cells have to optimize the neural information conveyed by the mossy fibers so that it facilitates learning at PF–PC’s synapses.

In this chapter, we detail why these properties are fundamentals and we quantify them in our network.

9.1 Bistability and performances of the forward model

The forward models are useful only if they are accurate. In our simulated system, accuracy is controlled by a bistability behavior of the forward model: it must provide a good prediction — i.e. make small errors — when it is active, and remains silent (i.e. below a threshold of activity)

¹Accuracy will be quantified in the next section

otherwise.

This bistability is fundamental in our simulations for two reasons; first, when working online, the simulated motor cortex uses incoming signal from the forward model to recompute the optimal trajectory. If the forward model conveyed erroneous positions and velocities of the limbs, then the new optimal trajectory would be calculated improperly, thus leading to catastrophic performances. Second, in the offline consolidation process, the predictive signal of the forward model is exploited to extract the teaching signal used to enhance performance of the feed-forward corrector. Again, a suboptimal prediction would lead to changes in non-adapted synapses and hence to destructive learning.

9.1.1 Bistability measures

We define three measures to account for the forward model bistability. First, we calculate the mean forward model angular error for each joint across the activity of the forward model $\gamma_{s, fm/e, fm}$. We then look at the error level occurrence probability when the forward model is active - i.e $\gamma_{s, fm/e, fm} > 5Hz$ - or inactive $\gamma_{s, fm/e, fm} \leq 5Hz$. In both measures, activity of the forward model for the shoulder and elbow is defined as $\gamma_{s, fm/e, fm}(t) = \sum_{i=1}^N \gamma_i(t)$, with N the number of neurons coding for the forward model of the joint, and $\gamma_i(t)$ is the discharge frequency of neuron i at time t , calculated using a sliding rectangular window of 25 ms. We finally measure the probability of response of the forward model over time, giving an indication of its learning time-course. Each value is averaged and presented in time bins of 15 s, showing learning evolution over a sequence of 300 s. All measures have been averaged over a population of 20 individuals who used only the forward models to change the movement dynamics.

9.1.2 Results

The results of the forward model bistability are presented in figure 9.1a-c.

In figure 9.1a, we show the mean error of the predicted angular position of the model as a function of its activity. When the forward model is inactive ($< 5 Hz$), the main prediction error is high (bigger than 20 degrees for both joints) compared to the case of an active forward model ($> 5 Hz$) where the angular position error is below 4 degrees for both joints.

Then, we also observe that the prediction quality depends on the model activity: the prediction improves proportionally to the forward model activity, with an average error below 3° for an activity of 180 Hz or higher. In figure 9.1b, we present the probability of occurrence for each angular error when the forward model is active (plain lines) or not (dotted lines), for both shoulder (shown in red) and elbow (shown in blue) joints. As expected, for both joints, the error is evenly distributed when the forward model is inactive. In comparison, when the forward model is active, an error smaller than 10 degrees for both joints is highly probable ($p = 0.78$ and $p = 0.92$ for shoulder and elbow, respectively). Furthermore, getting a prediction error of 30 degrees or more has a probability close to 0 for both joints.

Finally, another interesting dynamic of the forward model concerns its fast learning capability as it is presented in figure 9.1c. We present the learning performances of the forward model over time — i.e. the probability of response of the model — during the training process. We observe that after only one trial (90 s), the forward model is able to give a prediction 75 per cent of the time. This value stays relatively stable all along the training process, but since new contexts appear all along adaptation, our forward model increases the number of input-output patterns stored.

9.2 LTD-LTP compensation

Another essential feature of our internal models concerns how long-term potentiation and depression at PF–PC synapses could compensate each other. Given that LTP and LTD are not symmetrical (LTP is implemented as an homosynaptic process, and LTD as a heterosynaptic process), this compensation is not trivial and principally depends on the strength of LTP and LTD. However, it is a necessary condition to maintain the existing input–output relationship of the internal models when the learning signal could not be conveyed, and consequently, to avoid interferences with previous learnings. If this case is not supposed to occur when the learning is made online — learning signal is extracted from the sensory feedback signal — the learning signal is sometime unknown during an offline consolidation.

In the offline scheme, the sensory feedback signal is replaced by the predictions of the forward model. If the forward model is able to give

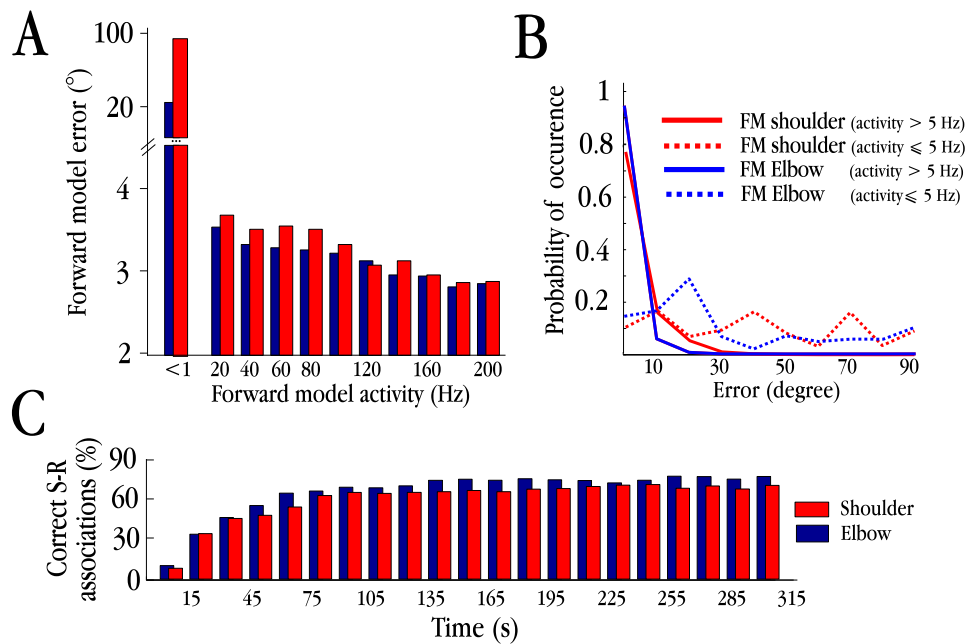


Figure 9.1: Performance of the forward model. **A.** Mean angular prediction error function of the forward model activity for elbow (blue rectangles) and shoulder (red rectangles) joints. **B.** Probability of error occurrence for the predicted angular position of the shoulder (red lines) and elbow (blue lines) when the forward model is silent (dot lines) and active (plain lines). **C.** Fast learning capabilities of the forward model is presented by showing the percentage of correct stimulus-response associations of the forward model for the shoulder (red rectangle) and the elbow (blue rectangle) over time (in seconds).

an accurate prediction for a high ratio of contexts, the existing dynamic in the inverse model needs to be kept intact when the forward model does not provide the learning information. Since LTP occurs before knowing whether the learning signal is available, this is not possible to freeze learning in such a case and we have to drive the learning signal in such a way that the heterosynaptic LTD between parallel fibers and Purkinje cells compensates perfectly the homosynaptic LTP.

9.2.1 Protocol

To account for an efficient LTD–LTP compensation, we implement a simple stabilization protocol where the input/output relationship of the network is supposed to stay unchanged during the whole simulation.

The protocol consists of one session of 1000 s during which we feed a subset of 100 mossy fibers with a constant current making them discharge at approximately 100 Hz. A null error signal is used to modulate the firing rate $r(t)$ of each IO cell (see eq. 7.4). Thus, each IO cell discharges at approximately 1 Hz following a Poisson process (we recall that 1 Hz is the firing rate of IO cell when no error is reported).

We record the output activity of the network (the firing frequency of the DCN) and monitor how stable is the mean frequency by calculating the standard deviation of the firing rate (calculated using a sliding rectangular window of 25 ms) over all trials. We average our results over a population of 10 subjects.

9.2.2 Results

The standard deviation of the mean frequency is $15.6 \pm 8\text{Hz}$. Also, the difference between the mean frequency reported during the first five seconds of the test and the whole simulation is very small ($6 \pm 2\text{Hz}$). These results indicate that LTD and LTP can compensate each other on a long time scale basis when neurons from the inferior olive conveys a null error signal (that is a firing rate of 1 Hz).

Yet, our cerebellar model has been designed so that each PC cell receives 20 IO projections. In a real cerebellum, each PC is actually targeted by only one climbing fiber. This dissimilarity in our model was motivated by a computational time issue: we needed to have a small number of Purkinje Cell, and thus to limit PC per DCN ratio. In a model where only 2 PCs

target a DCN cell, with 1:1 IO to PC connection, stabilization of learning could not be assured (mean std= $45 \pm 5Hz$). In a biological system, each DCN is thought to integrate information from tenth to hundreds of Purkinje cells (Palay, 1974). Since we could not increase the number of PCs in our model, we artificially duplicate the number of IO neurons connected to single PC, so emulating the in vivo convergence ratio of PC per DCN cell and solving the problem of stabilization. This point will be further discussed in the next chapter, in section 10.3, page 141.

9.3 Sparsification in the granular layer

It is thought that the granular layer of the cerebellum embeds half of the neurons of the entire brain (Palay, 1974). Due to this huge number, the role of these very small cells has long been discussed, and is still under debate.

One hypothesis emerged from early theories and considered GCs as a pool of neuronal resources capable of optimizing information by providing a sparse code of the input, thus facilitating learning at PF-PC synapses (e.g., Schweighofer et al., 2001).

In order to determine whether this is the case in our model, we implement two measures of sparseness, first a simple global activity analysis, and then a Kurtosis test.

9.3.1 Global activity

First, we measure the sparseness of the granular layer during a single movement (from starting position S to a fixed target T) using the average activity ratio. Results are presented in figure 9.2. We observe that 34 per cent of the granule cells of the target cluster are active at least once. Every 10 ms, an average of 35 ± 1 GR cells discharge. This represents 2.8% of the granular layer cluster (composed of 1250 cells) and 7% of the total active cluster cells. Visually, we observe that the neural representation of the movement is distributed over the entire cluster (see figure 9.2a). Furthermore, the cluster activity is clearly distinguishable at three different times of the movement, with a sparse activity at each time step (see figure 9.2b).

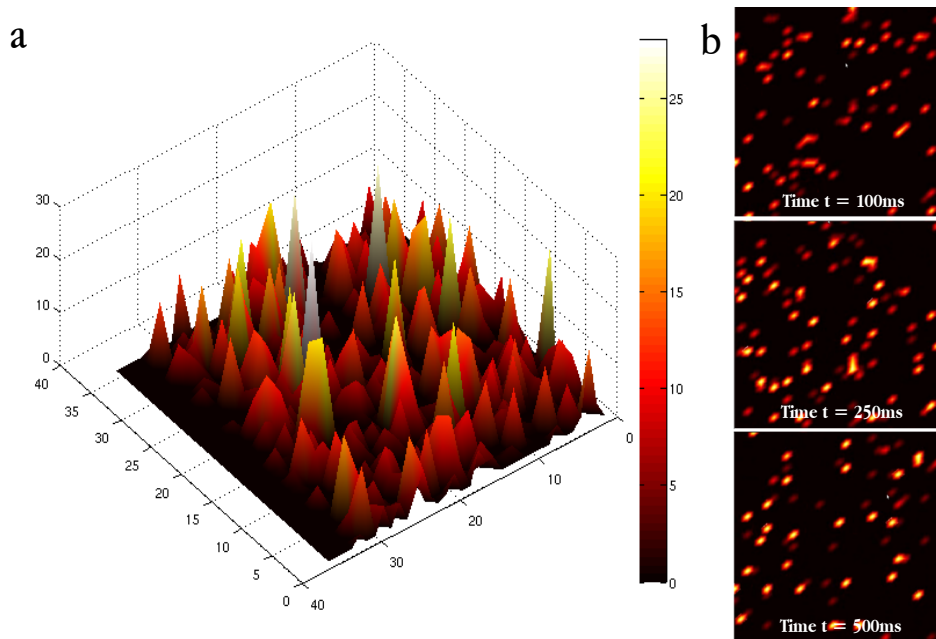


Figure 9.2: Activity of the granular layer during a trajectory. A. Global activity of the granular cells cluster of a forward model during a 1 s simulation (time length of a movement). The cluster is represented on a square array of 35 by 35 cells. z axis shows the number of spikes that the neuron of index (i, j) fired during the generation of the movement. **B.** State of the same granular layer cluster at three different times of the trajectory (100 ms, 250 ms and 500 ms). The cluster is again represented on a square array of 35 by 35 cells. Each red dot in the figure represents a neuron that spiked during the previous 20 ms. The neurons that discharged on a shorter time scale or with higher frequency appear brighter than others.

9.3.2 Kurtosis

We therefore conducted a more complete analysis using the kurtosis measure.

Methods. We feed the network with a set of 10,000 distinct patterns covering the input entry space uniformly. Each pattern is considered independent of the others and presented for 100 *ms* to the neural network. Sparseness is calculated separately for each individual activity pattern k . This measure is also known as population sparseness (Willmore and Tolhurst, 2001). Alternatively, we also measure the selectivity for each single neuron i across all patterns. This measure is known as lifetime sparseness (Willmore and Tolhurst, 2001). To quantify both sparsenesses, we used a kurtosis measure (Field, 1994). Kurtosis excess is defined as

$$K_k = \frac{\langle (x_i^k - \mu_k)^4 \rangle_i}{\sigma_k^2} - 3$$

where $\mu_k = \langle x_i^k \rangle_i$ and $\sigma_k = \langle (x_i^k - \mu_k)^2 \rangle_i$ are the expected value and the variance of x_i^k , respectively. Expectation is taken across all artificial neurons. The average population kurtosis is then $K_{pop} = \langle K_k \rangle_k$. The same measure adapted to lifetime kurtosis is calculated and defined by $K_{life} = \langle K_i \rangle_i$. We finally compare the sparseness of the mossy fiber layer to the granular layer's one and the gain we obtained by separating the input into 8 clusters (one cluster per target).

Results. Results are shown in figure 9.3. First, we observe the effect of the re-encoding process at the granular layer level by comparing the granular layer and the mossy fiber layer kurtosis. In the clustering model (each target is encoded in a distinct population of mossy fibers), the network gets almost no advantage of the re-encoding, as shown by the population kurtosis — which measures the global activity of the layer for each pattern. In the mossy fiber, $K_{pop,CMF} = 146$ while in the granular layer, $K_{pop,CGR} = 148$. However, if we now take into account the lifetime kurtosis — which measures the selectivity of each unit over the whole set of patterns — we observe a sparsification of the information when a signal is reprocessed in the granular cells ($K_{life,CMF} = 53$ and $K_{life,CGR} = 212$ in the mossy fiber layer and clustered granular layer, respectively)

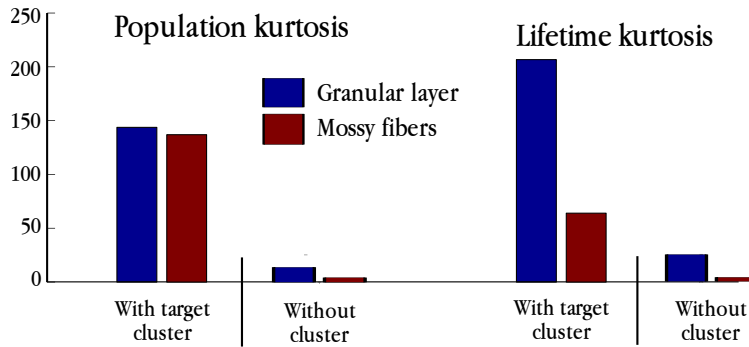


Figure 9.3: Sparsification of the network: Measure of Kurtosis. Population kurtosis (**left**) and lifetime kurtosis (**right**) for granular layer and mossy fibers layer. In both cases, kurtosis is presented when input signal is both clustered and not. With target clusters: each target is encoded in a distinct population of mossy fiber and granular cells. Without clusters: the eight targets are encoded in the same cluster of mossy fiber and granular cells..

If we remove clustering — i.e. all targets are now encoded in a single cluster of MFs and a single cluster of GCs —, we dramatically reduce the sparseness of the information for both layers, confirming that by manually clustering inputs, we favor an efficient separation of the contexts. Without clustering, population kurtosis and lifetime kurtosis are $K_{pop,GR} = 14$ and $K_{life,GR} = 24$ in the granular layer, and $K_{pop,MF} = 4$ and $K_{life,MF} = 4$ in the mossy fiber layer. In both cases, granular layer helps to sparsify information coming from mossy fibers, corroborating the idea of an optimization of the neural code in granular layer.

Chapter 10

Discussion

In this chapter, we discuss our results, define the limits of our system, and propose future directions of research. In the first section, we resume the main contributions of this study.

10.1 Contributions

The study presented in this part addresses the coupling of internal models in the cerebellum which aims at enhancing both online and offline learning capabilities in procedural tasks. The proposed connectionist architecture takes inspiration from the cerebellar microcomplex circuit and employs spiking neural populations to process information. Long-term synaptic plasticity (both LTP and LTD) was implemented to achieve adaptive motor control.

In the one hand, it was shown that the system can acquire representations of closed-loop sensorimotor interactions, suitable to adapt the behavioral response to changing sensory contexts. We then validated the coupling model on a rotation adaptation task proposed by Huber et al. (2004). The simulation results of the proposed architecture reproduced the experimental findings on the human procedural learning task both during a training phase (online) and after a night of sleep (offline consolidation). The sleep-dependent consolidation observed experimentally was mimicked by an offline learning phase during which a replay of the contextual information elicited during online training occurred (see section 10.2 for a discussion on the biological plausibility of such replays).

Furthermore, three properties of the cerebellar circuitry have been pro-

posed to play a major role in the adaptation of the procedural memory and in its consolidation during subsequent offline phases. First, we proposed that the forward models had to be bistable to allow good performances of the overall motor control scheme. We defined bistability as the capacity of giving good prediction when the model is active, and to stay silent otherwise. Second, we suggested that during offline processing, the inverse model had to keep its dynamic unchanged when the forward model was unable to predict the sensory consequences of a motor command. This assumption predicts that cerebellar LTP and LTD at PF-PC synapses could precisely compensate each other. Knowing that LTP and LTD are not symmetrical — LTP is a homosynaptic process whereas LTD is an heterosynaptic one — this compensation is not trivial and mainly depends on the strength of LTP and LTD. Eventually, as it was proposed by other authors (Marr, 1969; Schweighofer et al., 2001; Philipona and Coenen, 2004; Brunel et al., 2004), we suggested that the encoding at the granular layer should optimize the neural information conveyed by the mossy fibers so that it facilitates learning at PF-PC synapses. We proposed that a sparse encoding at the granular layer level might be the basis of such a mechanism.

10.2 Sleep and memory consolidation

Several studies have confirmed the beneficial effect of sleep on procedural memories in various tasks (Walker et al., 2003; Mednick et al., 2003; Stickgold et al., 2000b,a; Gais et al., 2002; Korman et al., 2007; Walker et al., 2003; Fischer et al., 2002; Plihal and Born, 1997). Although memory consolidation is mainly considered as a stabilization phase, there are many examples of procedural tasks where the performance of subjects retested the next morning had improved significantly relative to the last evening session (e.g., Huber et al., 2004; Walker and Stickgold, 2004). Hence, consolidation should also be thought as an enhancement stage of memories.

In our study, we proposed that a coupling architecture might account for such a beneficial effect in different procedural tasks. The offline consolidation process we implemented in our model is based on the assumption that the sequences of actions performed during online training could be replayed offline. The validity of this hypothesis and other related questions are discussed below.

Replay during sleep. Several studies suggested that the firing patterns observed in the hippocampal neuronal ensembles of rodents are reactivated during non rapid eye movement (NREM) sleep. These reactivations were demonstrated mainly in the hippocampal place cells after the realization of a spatial task (Wilson and McNaughton, 1994; Kudrimoti et al., 1999). Spike sequences had also been shown to be repeated in hippocampal cells during NREM sleep (Nadasdy et al., 1999), and the temporal order of place cells firing conserved during repetitive moves (Lee and Wilson, 2002). This offline replay of hippocampal cells has been proposed to be involved in the consolidation of newly encoded spatial information. One possibility is that spatial memory could be gradually translated from short-term hippocampal to long-term neocortical memory sites (Sutherland and McNaughton, 2000).

Based on these earlier animal investigations, several neuroimaging studies have explored the possibility that patterns of brain activities elicited during initial task training could be replayed during subsequent sleep in humans.

Using Positron Emission Tomography (PET) imaging, Maquet and colleagues (2000) have shown that activation patterns elicited during practice of a serial-reaction-time motor skill task prior to sleep reappear during subsequent REM sleep episodes, while no such activity is present in control subjects who received no day time training (Maquet et al., 2000).

In a more recent study, Maquet et al. (2003) developed another protocol where the effect of sleep was demonstrated. Two groups of subjects (one control and one sleep-deprived) were trained on a smooth pursuit task. In both groups, authors observed an increase in brain responses to the learned trajectory as compared with a new trajectory. More interestingly, when retested the following day, the authors observed behavioral and functional differences between the subjects of both groups. Compared to the sleep deprived group, subjects' performance of the sleep group was improved and an increased functional connectivity was observed between the superior temporal sulcus and the cerebellum (Maquet et al., 2003). These differences were interpreted as sleep-related plastic changes during motor skill learning in areas involved in smooth pursuit eye movements. Consequently, it is likely that such synaptic changes could occur in the cerebellum, known to participate in the control of smooth pursuit tasks.

In light of these experimental results, the replay hypothesis seems plausible. Thus, further studies using this coupling model could help in

gaining a better understanding of the computational mechanisms responsible for offline enhancement of memories.

For example, it could be elucidated how the benefits of offline learning would vary if the contextual information were only partially replayed. Indeed, in our simulations, to solve the rotation adaptation task, random sequences of entire trajectories were replayed when performing offline consolidation. This question is currently under investigation.

Time course of offline learning. Significant sleep benefits on memory are observed after 8 hours of night sleep, but also after shorter naps of 1 or 2 hours (Nishida and Walker, 2007; Korman et al., 2007; Mednick et al., 2003). For procedural memory, it appears that longer sleep durations yield greater improvements (Walker et al., 2003; Stickgold et al., 2000a); however, the optimal amount of sleep needed to benefit memory is unclear at present (Diekelmann and Born, 2010).

In our simulations, we observed that a sufficiently extended offline consolidation (i.e. 48 trials replayed offline) leads to an improvement of overall performances. The time course of the offline consolidation process have also been investigated using our model. We showed that an increase of performances on the second probe test (trial 14) was highly dependent on the monitored variable and on the time length of the offline process.

Consistently with experimental findings, we showed that benefits could be observed after a short offline consolidation process (several trials), but that a longer duration of simulated sleep led to a better performance at retest trial. Also, we observed that simulated offline consolidation can not optimize learning beyond a certain limit.

These results suggest that it exists an optimal time of offline processing — an optimal number of repetitions during an offline consolidation — which may depend on three parameters: (i) the learning task, (ii) the level of performance previously acquired on the task and (iii) the components of the task to be optimized.

It is possible that the CNS could extract the relevant parameters to adjust the duration of the offline consolidation. However, the neuronal processes responsible for such an estimation are still unclear. We propose that our coupling model could help to resolve such issues. First, the model should be employed in different procedural tasks to determine whether there exist some correlations between different parameters. Also, numerous analyses should be performed to determine the influence of the qual-

ity and quantity of the encoded information in both internal models on the quality of the subsequent consolidation. For example, it could be computationally observed how the quality of prediction — embedded in the forward model — could change the plateau or the time course of optimization. Thus, these analyses would help to design experimental protocols that should further validate or refute the proposed model.

The fact that offline learning might affect distinctively the different components of a procedural task is suggested by the difference of optimization after an offline consolidation process between the two observed variables — the error of distance and angle — in the simulated rotation adaptation task. Further analysis would be needed to identify why we observe an important decrease of distance error while we only have small decay of directional errors, and whether such differences are observed experimentally. In our simulation, it could be that *(i)* directional error had already been optimized during online training; or that *(ii)* offline learning is more adapted in reducing the distance error. An interesting property of our model could help answering the previous question. During the offline process, only the inverse model of the coupling scheme is updated (no sensory feedback can be used to teach the forward model). We observed that, when using an inverse model scheme online, reducing the distance error is problematic, and leads to an over-training that implies a degradation of performances. However, this phenomenon does not appear neither in the forward model scheme nor in the inverse model for the correction of the directional error. Hence, a possibility is that learning to correct the error of distance would not have converged to an optimal value during the online training compared to the directional error. Consequently, offline learning would allow an higher level of optimization on the distance error but convergence would take more time, because of the slow learning capability of the inverse model.

Sleeping phases. Sleep in humans has been classified into two distinct types; non-rapid eye movement (NREM) sleep and rapid eye movement (REM) sleep. NREM sleep is further divided into four stages (1-4) which correspond to increasing depth of sleep (Rechtschaffen and Kales, 1968). Stages 3 and 4 NREM are often grouped together under the term “slow wave sleep” (SWS) due to the occurrence of high amplitude waves in the delta range (0.5 – 4 Hz, Amzica and Steriade, 1995). Throughout these sleep stages, the brain also undergoes many neurochemistry and activity

alterations (see Walker et al., 2003 for a review).

The respective role of the various sleep stages in the consolidation of memory traces is still unsettled (for review, see Diekelmann and Born, 2010). Although both SWS and REM sleep may be involved in the processing of memory traces for several tasks, procedural learning seems particularly sensitive to REM sleep deprivation. Other studies suggest the necessity of ordered successions of NREM and REM sleep stages for a consolidation of memory traces (Gais et al., 2000; Stickgold et al., 2000a; Lee and Wilson, 2002).

Walker et al. (2003) proposed a framework to study the consolidation role of sleeping in procedural learning. According to their model, procedural learning consists of a first acquisition phase, followed by two specific stages of consolidation, one involving a process of stabilization, the other involving a delayed or latent phase of enhanced learning (Walker et al., 2003). The process results in additional performance improvements.

If initial acquisition and stabilization of procedural memories do not relate to sleep (see Walker et al., 2003; Diekelmann and Born, 2010 for review), the enhancing stage of consolidation appears to be sleep dependent.

In our study, we proposed a model that might account for the enhancing effect of sleep. However, we gave a highly simplified vision of sleep and gathered all stages in one simple replay process, which does not entirely reflect the reality. An evolution of our model should therefore integrate some of the electrophysiological, neurochemical and anatomic-functional properties highlighted during different sleeping stages.

Extension to other paradigms. As suggested in the previous paragraph, it is fundamental to evaluate our architecture in other procedural learning paradigms where sleep has been shown to enhance the performances.

So far, a simplified version of the coupling architecture has been validated on a second procedural paradigm (see Passot et al., 2010), a sequential finger tapping task proposed by Walker and Stickgold (2004). A brief account of the protocol and results are presented in annexe C.1 (page 279).

Validation of this second task corroborates the idea that the described coupling scheme may offer a plausible model to *(i)* combine the advantages of the fast online adaptation properties of the forward model and the accurate but slower convergence of the inverse model, and *(ii)* achieve

offline consolidation of procedural memories to enhance motor control capabilities. Also, a growing number of tasks have been proposed to elucidate the role of sleep in procedural memory (see Stickgold, 2005 for a review). The relative simplicity of some of the protocols and paradigms used in such tasks should allow modelers to simulate them in a virtual environment and compare the validity of the coupling model with experimental data.

10.3 Properties of cerebellar circuitry

Different properties of internal models have been investigated in this computational study. For the forward model, it has been suggested that the system, in order to guarantee usable feedback predictions, should be bistable and hold fast learning capabilities. For the inverse model, we advocated that stabilization of its dynamic should be assured in case the error signal can not be conveyed.

In this subsection, we discuss the biological and theoretical evidence of these properties.

PC-DCN's convergence. During offline consolidation, the inverse model has to keep its dynamics unchanged when the forward model is unable to predict the sensory consequences of a motor command. This assumption predicts that cerebellar LTP and LTD at PF-PC synapses can precisely compensate each other. However, LTP and LTD are not symmetrical — LTP is a homosynaptic process whereas LTD is a heterosynaptic one — this compensation is not trivial and depends on *(i)* the strength of LTP and LTD, *(ii)* the properties of discharge of the IO neurons, and *(iii)* the connection scheme of the cerebellar network — i.e. the input-output converge and divergence through different layers.

IO neurons are known to have a very low discharge rate (≈ 1 to 2 Hz when recorded in vivo), and up to 10 Hz when excited with drugs (Gibson et al., 2004). In a network model where only 2 PCs target a DCN cell, and with a biological rate of 1:1 IO to PC connection, stabilization of learning is not assured. Consequently, our model has been designed so that each PC receives 20 IO projections. This non-biological simplification has been adopted to bypass a computational time issue: given that each PC of our model integrates the signal of thousands of GCs, we needed

to have a small number of PCs, and thus to limit the PC per DCN ratio. Interestingly, real DCN is known to be targeted by tenths to hundreds of PC (Palkovits et al., 1977). The majority of cerebellar Purkinje cells synapse onto neurons in the DCN; 90% of DCN neurons are contacted by Purkinje cell terminals, with an estimated convergence ratio of 26:1 (Palkovits et al., 1977). We argue that this ratio might be used to convey a good distribution of the error on DCN even with a low frequency rate of the IO.

Figure 10.1 shows the stabilization of DCN frequency as a function of the number of connected PCs. We observe that, when there is a small number of PCs targeting each DCN, stabilization of the DCN frequency can not be obtained. Then, when the convergence ratio reaches higher values (≈ 25), firing frequency deviation of the DCN deviation is attenuated and heretosynaptic LTD is able to globally compensate homosynaptic LTP. Interestingly, the standard error of the mean standard deviation is also reduced when PC ratio is augmented.

Bistability of the forward model. The forward models are useful only if they are accurate (Shadmehr et al., 2010). In our simulated system, accuracy is controlled by a bistability behavior of the forward model: it must provide a good prediction — i.e. make small errors — when it is active, and stays below a threshold of activity otherwise. Bistability is fundamental in our simulation for two reasons; first, when working online, the simulated motor cortex uses incoming signal from the forward model to recompute an optimal trajectory. If the forward model gave erroneous position and velocity of the limbs, then the new optimal trajectory would be calculated improperly, thus leading to catastrophic performances. Second, in offline consolidation process, the predictive signal of the forward model is employed to extract the teaching signal used to enhance performance of the feed-forward corrector. Again, a suboptimal prediction would lead to changes in non-adapted synapses and hence to destructive learning.

Evidence suggests that the accuracy of a forward model is maintained through adaptive processes driven by sensory prediction errors (Shadmehr et al., 2010). This adaptation occurs once the forward model has already been formed, and little is known concerning the first step of learning of a forward model. It remains to be understood how the central nervous system decides whether or not the prediction can be used. We propose that this differentiation might be explained by a bistable behavior of the microcomplex system, thus suggesting that when a forward model

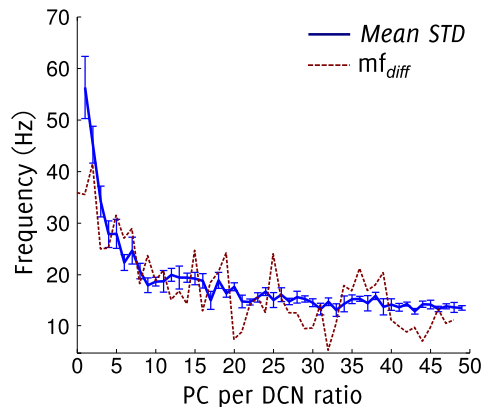


Figure 10.1: LTD-LTP compensation. Mean standard deviation of the firing frequency of DCN activity (msd) in blue and difference between the mean firing frequency of the first five seconds of the simulation and the mean firing frequency of the entire simulation (mf_{diff}) in dashed red. We report the evolution of msd and mf_{diff} as a function of PC-per-DCN ratio (i.e., the number of PCs connected to each DCN). For each ratio (1 to 50), we completed 10 simulations of 1000 seconds each. For each simulation, the protocol consisted of one session of 1000 s where we feed a subset of 100 mossy fibers with a constant current so that they fire at 100 Hz on average. Each IO is also fed with a constant current that makes it discharge at approximately 1 Hz (firing rate when no error is reported). Each PC is targeted by one and only one climbing fiber (1:1 ratio). For each PC per DCN ratio, LTD and LTP parameters were tuned such as they optimized the stabilization of the output signal. The output activity of the network is measured as the firing frequency of the DCN (computed with a rectangular sliding window of 25 ms).

becomes active, the prediction is supposed to be usable. To the best of our knowledge, no experimental study has intended to demonstrate this property.

Time-course of adaptation. This prediction raises questions on the time scale adaptation of the forward model. A recent example of visuomotor adaptation provides interesting data on on both time scale and the role of sensory prediction errors.

Mazzoni and Krakauer (2006) had people tested in a similar paradigm that the one used by Huber et al. (2004) presented in this study, but with a different protocol. After a baseline familiarization period of 40 movements, experimenters imposed a 45 ° counter-clockwise rotation. In the control group, the subjects gradually learned to move their hand in a way

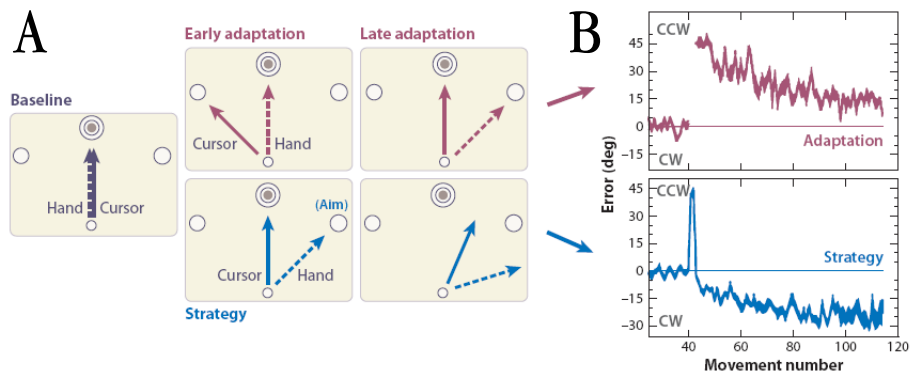


Figure 10.2: Learning from sensory prediction errors during visuomotor adaptation (from Mazzoni and Krakauer, 2006; Shadmehr et al., 2010) **A**. Subjects are asked to make an out-and-backward movement to one of eight targets. In the baseline condition, hand motion and cursor motion were congruent. In the adaptation condition, a 45° rotation is imposed to the motion of the cursor and the hand. In the adaptation group (top two plots), the subjects gradually learned to move their hand in a way that compensated for the rotation. In the strategy group (bottom two plots), after two movements, the subjects were told about the perturbation and asked to simply aim to the neighboring target. **B**. Endpoint errors in the adaptation and strategy groups. The strategy group immediately compensated for the endpoint errors, but the errors gradually grew. The rapid initial improvement is due to learning in the explicit memory system, whereas the following gradual learning is due to an implicit system.

that compensated for the rotation. After 80 movements, a normal subject would therefore make a very small error (within 5° of target, figure 10.2a, adaptation group).

In another group of subjects (the strategy group), after two movements with an imposed rotation of 45° , subjects were told about the perturbation and asked to simply aim to the neighboring target. On the next trial (movement 43), the error dropped to zero (see figure 10.2a strategy group). However, as the trials continued, the errors gradually grew with a rate of change which was comparable to the one observed in the regular adaptation paradigm.

These results suggest that the ability to predict the consequences of actions and the ability to use them improve at the same rate. They also give indication on the time course of estimation: in trial 43, whereas subjects of the strategy group had been explicitly told of the perturbation, there

was still a discrepancy between the predicted (implicit) and observed sensory consequences. The learning curve indicates how quickly a forward model is built and that the quality of estimation of the movement gradually grows over about 50 trials (closely matching the time course of normal adaptation, see figure 10.2b).

In our model, the quality of estimation is not only related to the error made when the forward model makes a prediction since this error is supposed to be relatively small. Rather, we argue that the quality of estimation must be derived from the rate of forward model prediction during movements. However, if the dynamic of the movement is changed (for example if the imposed rotation grows to 60°), then both parameters (the percentage of time during which the forward model gives a response and the mean prediction error) should be taken into consideration.

10.4 Limitations and future work

At this stage of our study, several limitations of the proposed architectures must be highlighted and future directions of research must be proposed.

A first series of questions relates to the implementation of the cerebellar microcircuitry, which is a highly simplified version of the biological structure. Indeed, in our study, we do not take into account all cerebellar cellular types (e.g., inhibitory interneurons) and only emulate PF-PC's LTD/LTP to account for the adaptive properties of the microcomplex.

A second question arises out of the relative simplicity of the simulated motor control and body system. We need to precise in which measures the control of a two joints simulated arm could be generalized to a biological limb.

Model description level. The microcomplex model proposed and tested in this study is a highly simplified version of the biological microcircuitry it emulates. First, we voluntarily omitted interneurons in our model (Golgi, stellate and basket cells). If these neurons could be important to lower the level of noise in the cerebellum (Hirano et al., 2002; Garrido et al., 2007), to provide timing information (Desmond and Moore, 1988; Fiala et al., 1996; Kistler et al., 2000; Yamazaki and Tanaka, 2007; Garrido et al., 2007), or to provide the biological resources for the implementation of the covariance learning rule (see Sejnowski, 1977; Dean et al., 2010 for review), interneu-

rons were not fundamental to present the concept of coupling. Moreover, they would not bring significant improvement in the simulated system where (1) the input noise is controlled algorithmically, (2) time related information could be conveyed by the mossy fibers layer and (3) a bidirectional long-term synaptic plasticity was used to adapt the internal models dynamics. However, we agree that future implementations of the coupling scheme should integrate such neuronal diversity to address timing and noise related issues.

Also, adaptation has been modeled by long term synaptic plastic changes between parallel fibers and Purkinje cells (LTD and LTP). Yet, other synaptic and intrinsic plasticities were not included in our model. As presented in chapter 4, many other synaptic plasticities have been reported so far, and it is likely that every connection undergoes plasticity mechanisms. One of the most controversial plasticity process concerns the functional role of the synaptic site between the mossy fibers and deep cerebellar nuclei (Zhang and Linden, 2006). This synaptic plasticity is thought to be triggered by an activity rebound of the DCN, following the high hyperpolarization level reached when a complex spike from a subset of connected PCs is received (Pugh and Raman, 2006). Functional implications are still undetermined. Memory may be acquired first in the cerebellar cortex and then be transferred to the cerebellar nuclei, a synaptic plasticity between MF and DCN would therefore contribute to the persistence of memories (Masuda and Ichi Amari, 2008); or the cerebellar cortex could store timing-related information whereas the deep cerebellar nucleus would be more important for storing the amplitude of the response (Medina and Mauk, 1999). Due to this uncertainty, and given that it was not fundamental for this study, we did not include a plasticity site between MF and DCN in our model. A further extension of this work should take into consideration this process and other synaptic sites to address their possible functions and consequences in the coupling scheme.

Motor control. Our study focused on the control of a simulated arm composed of 2 joints (shoulder and elbow). This simplified version circumvents many problems the central nervous system must face when trying to control a biological arm (see annexe A for an introduction on the neurocomputation of movements).

The curse of dimensionality, the redundancy and the inversion problem are some scenarios which are not supposed to occur in our simplified

system. In these conditions, one might argue that our results can not easily be generalized to a real arm.

We need to point out that the motor system of the human brain is extensive and, movement-related regions include the primary motor cortex, supplementary and presupplementary motor areas, premotor cortex, parietal cortex, dorsolateral prefrontal cortex, the basal ganglia, the thalamus, the cerebellum and most of the spinal cord. Reciprocal connections and communication pathways are found among these structures, which therefore interact to initiate and control voluntary movements (Pockett, 2006).

In the framework of optimal control theory, a mathematical optimization method for deriving control policies (largely used to explain the generation of voluntary movement in humans, see chapter A and Todorov, 2004), the cerebellum is thought to predict the sensory feedback; the parietal cortex is thought to estimate the current state by integrating predicted sensory feedbacks and the proprioceptive and visual information in order to form beliefs; the basal ganglia is thought to learn the costs and rewards associated with different sensory states and estimating the cost during the execution of a motor task; the primary motor cortex and the premotor cortices are thought to be related to the implementation of an optimal control policy which transforms our belief about proprioceptive and visual states into motor commands by minimizing a cost-reward function (for review, see Shadmehr and Krakauer, 2008).

In this study, we do not attempt to address all the issues related to the control of movements. Neither inversion nor state dimensional problems are thought to be related to the predictive or corrective functions of the cerebellum. Here, we focus on the advantages of coupling internal models and we argue that if the system to control is sufficiently simple, our study can highlight the most fundamental characteristics of the coupling scheme. However, a next step of this work would be to integrate our model in an extended neural architecture (e.g., the optimal control framework), in order to study how it can adapt to more complex dynamics.

Part III

THE ROLE OF THE CEREBELLUM IN SPATIAL COGNITION

In the context of motor control, we have studied how multiple cerebellar microcomplexes encoding internal predictive and corrective models might collaborate to efficiently participate to the adaptation of motor behaviors. In the next part of this thesis, we examine to what extent the framework of cerebellar internal models can be applied to spatial cognition. Our motivation is to highlight the cerebellar computations that might affect the procedural and declarative (episodic) memories involved in solving navigation tasks.

For the sake of clarity, the structure of this part follows the organization of the (nearly) submitted paper. We therefore put additional materials, methods — congruent with the previous study — and results in annexe chapters placed at the end of this part. Furthermore, compared to the paper version, the introduction and discussion sections have been extended.

Abstract

Complementing the extensive research on the role of the cerebellum in motor learning, recent experimental findings have begun to unravel the implication of the cerebellum in high-level functions such as spatial cognition (Burguière et al., 2005). We modeled the main information processing components of the cerebellar microcomplex and focus on behavioral genetic data suggesting that L7-PKCI mice (lacking LTD at parallel fiber–Purkinje cell synapses) are impaired in learning the procedural component of spatial navigation (Burguière et al., 2005). In order to validate this hypothesis, we compared the performance of simulated control and L7-PKCI mice in both Morris watermaze and the Sarmaze (Rondi-Reig et al., 2005) tasks. Our findings show that a purely local impairment of the procedural component cannot explain all the experimentally observed differences between the goal-searching behavior of mutants and controls (Burguière et al., 2005). We therefore put forth a new hypothesis according to which mutants' spatial learning impairment may reflect a deficit in trading-off exploration and exploitation strategies. Based on this assumption, we were able to reproduce the entire set of behavioral results (Burguière et al., 2005). Furthermore, we argued that the deficit in the exploration-exploitation balance might be due to suboptimal spatial representations in L7-PKCI mice, which would result in increased exploration in novel environments. We evaluated this assumption by coupling our cerebellar model to an existing model of hippocampal spatial learning (Arleo and Gerstner, 2000; Sheynikhovich et al., 2009). Our simulation results suggest that the cerebellum may play an important role in integrating proprioceptive information to infer future state variables such as body orientation and position (Wolpert et al., 1998). This ability might be impaired in L7-PKCI mutants, thus affecting hippocampal multisensory integration which mediates stable spatial representations learning (Arleo and Rondi-Reig, 2007). This work gave rise to a testable prediction on the

difference between the free exploratory behavior of control animals (Fonio et al., 2009) and L7-PKCI mutants.

Chapter 11

Introduction

Spatial cognition involves the ability of a navigating agent to acquire spatial knowledge (i.e. the spatio-temporal relations between environmental cues or events), organize it properly, and employ it to adapt motor responses to specific contexts. Similarly to other high-level functions, spatial cognition involves parallel information processing mediated by a network of brain structures. These structures interact to promote an efficient spatial behavior, that is the learning and use of different and flexible routines allowing the resolution of navigation tasks. A short introduction of spatial cognition is given in the annexe B. Also, Knierim (2006); Arleo and Rondi-Reig (2007) propose recent reviews.

Spatial cognition requires both declarative (episodic) and procedural learning in order to elaborate multimodal representations supporting spatial behavior (Arleo and Rondi-Reig, 2007). Declarative learning allows spatiotemporal relations between multiple cues or events to be encoded (O'Keefe and Nadel, 1978; Eichenbaum, 2001). Procedural learning mediates the acquisition of an ensemble of procedures to solve a navigation task (Whishaw and Mittleman, 1986; Whishaw, 1991, 1985). At a low level, procedural learning optimizes goal-directed trajectories (locally in space and time) through sensorimotor adaptations (Cain and Saucier, 1996). At a higher-level, it participates in inhibiting non-adaptive behavior that may impair navigation (e.g. thigmotaxic behavior; Mittelstaedt and Mittelstaedt, 1973; Whishaw et al., 1997; Petrosini et al., 1998, and in regulating the efficiency and flexibility of exploration strategies (Leggio et al., 1999; Mandolesi et al., 2003).

Although many experimental studies have provided a large amount of evidences on the role of hippocampus in mediating declarative spatial

learning (see section B.5 in annexes), the role of the cerebellum in spatial cognition is not fully understood.

Anatomically, due to its connectivity with many structures of the central nervous system and more precisely with motor and non motor areas of the cerebral cortex, it is likely that the cerebellum could be implied in both procedural and declarative memories. However, the existence of direct connections between the cerebellum and structures which are known to play a role in the relational learning of spatial cognition, such as the hippocampus, is still highly hypothetical.

Only a few studies have demonstrated a possible communication between these two structures. In one direction, it has been shown that a stimulation of the efferent pathways of the hippocampus activates the efferent pathway of the cerebellum (Saint-Cyr and Woodward, 1980). Inversely, responses of the hippocampal neurons have been shown to be modulated by the activation of neurons of the fastigial nucleus (Heath et al., 1978). However, these studies do not determine the exact pathway that might convey signals between the two structures.

Numerous studies on human and animal suggest a possible role of the cerebellum in navigation processes (Rondi-Reig et Burguière, 2005).

11.1 Spatial deficits in human

As described in section 3.3, a review of the literature concerning human cerebellar patients has shown many possible cerebellar roles in cognitive processes. Among them, it is suggested that the cerebellum might play a role in spatial cognition, and more precisely, impairments were observed in visuo-spatial functioning, sequential and timing processes that might be important in navigation tasks.

Patients with distinct cerebellar damages were tested in numerous neuropsychological studies, including an evaluation of the visuo-spatial functions. These functions were measured by the rey complex figure test, a task where patients are asked to reproduce a complex but visible figure (see figure 11.1), and later draw it from memory. It has been shown that cerebellar patients affected by Friedreich's ataxia or olivo-pontocerebellar atrophy were quantitatively and qualitatively impaired in this complex task, suggesting a deficit in visuo-spatial organization (qualitative evaluation) and location (quantitative evaluation, Botez-Marquard and Botez,

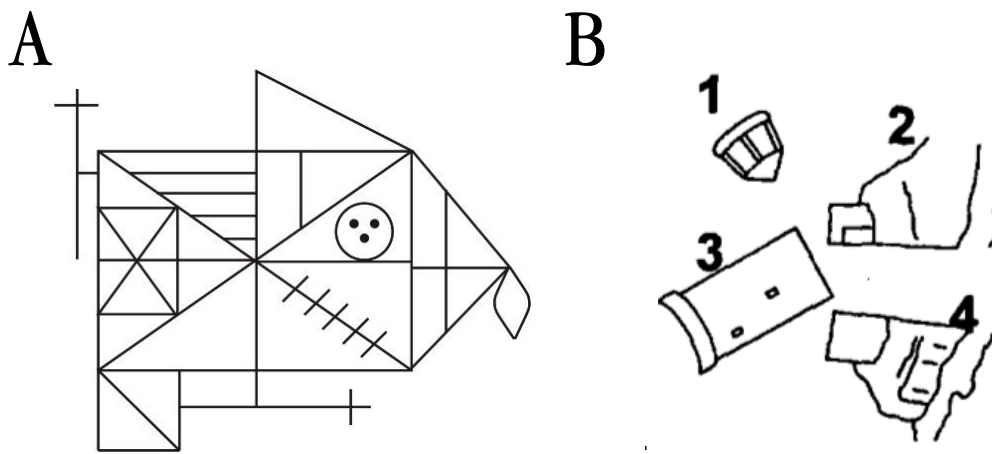


Figure 11.1: The rey complex figure and the Hooper tasks **A**. The Rey Complex Figure Test is a neuropsychological assessment which permits the evaluation of different functions, such as visuo-spatial abilities, memory, attention, planning, and working memory (executive functions). In this task, subjects are asked to reproduce a complicated line drawing, first by copying and then from memory. **B**. Sample of the “hooper task” (Hooper, 1983): in this test, subject have to mentally reconstruct an object cut into several pieces.

1992).

In another set of studies, neurological and psychological evaluations of patients affected by the cerebellar cognitive affective syndrome (Schmahmann and Sherman, 1997) demonstrated that they were impaired in the sequential drawing and the conceptualization of figures, in both the copy and memory version of the Rey complex figure task.

However, in an Hooper task (Hooper, 1983), a test where patients have to mentally reconstruct an object that has been cut in pieces and scattered on a page like parts of a puzzle, cerebellar patients were not significantly impaired. The authors hence suggested that the organization deficit observed in the Rey complex figure task was more related to the motor aspect of the latter task, rather than a cognitive problem. Nevertheless, it has been shown that the deficit in the Rey complex figure was not correlated with the severity of the dysmetria, thus suggesting that the observed deficit could not entirely be ascribed to motor problems, and reinforcing a possible non-motor role of the cerebellar function in spatial cognition (Schmahmann and Sherman, 1997).

Although the interpretation of these deficits remains unclear, experi-

mental findings on rodents' models have clarified the role played by cerebellar circuits in spatial-information processing (Petrosini et al., 1996, 1998; Burguière et al., 2005).

11.2 Spatial deficits in rodents' models

In the middle of the 1980s, Lalonde (1986) and his collaborators observed that weaver mutant mice — presenting a selective degeneration of cerebellar granule cells — performed poorly in the Morris watermaze task. They showed that weaver mutants made more errors and took a longer time to reach the platform (Lalonde and Botez, 1986). As this first study suggested a role of the cerebellum in navigation, the ataxia produced by cerebellar impairment was hardly convincing that the impairment could not only be ascribed to simple and isolated motor deficits ¹.

In another study using mutants mice with a degeneration of Purkinje cells, Goodlett et al. (1992) observed that mutants were deficient in finding an hidden platform compared to wild type, while they behaved as efficiently in a task where the goal was visible. Hence, they demonstrated that the spatial deficit in the 'not visible' case was not explained by a visuo-motor impairment (Goodlett et al., 1992). This conclusion was later reinforced by the work of Gandhi (2000) who found the same set of results by using a cerebellar model where the motor deficit was lacking (Gandhi et al., 2000).

While the use of cerebellar mutants demonstrated an implication of the cerebellum in navigation, it was still unclear if cerebellar lesions were affecting the procedural and/or the declarative components of spatial cognition.

We previously described spatial cognition as the integration and use of multiple sensory signals in an organized spatial representation (declarative memory) and the acquisition and use of a set of local and global procedures to optimally resolve the task. The respective role of the cerebellum in both types of memory remains to be elucidated.

¹Fortier et al. (1987) showed that swimming mazes are more suitable to study the role of the cerebellum in navigation task since motor deficits are less affected by cerebellar lesions during swimming than during walking (Fortier et al., 1987).

11.2.1 The cerebellum, procedural and declarative learning

In the late 90s, by using hemicerebellectomized rats, Petrosini and his collaborators demonstrated that cerebellar rats are impaired in developing efficient exploration strategies, but neither in building spatial maps nor in using localizing cues (Petrosini et al., 1996, 1998). This evidence was mainly based on the analysis of the behavior exhibited by these rats in performing classical spatial tasks. Rats with cerebellar damages, although not affected in swimming performance compared to their control littermates, displayed a characteristic impairment in executing complex and effective exploration. These results suggested that cerebellar learning was involved in the whole procedural component — local and global — of spatial learning.

More recently, a transgenic mice model has been used to investigate the cerebellar role in spatial cognition. L7-PKCI transgenic mice (De Zeeuw et al., 1998), lacking parallel fiber–Purkinje cell long-term depression were tested in two different mazes to dissociate the relative importance of declarative and procedural components of spatial navigation. In this study, the authors showed that the L7-PKCI mice were deficient in the acquisition of an adapted goal-oriented behavior, which is part of the procedural component of the task (Burguière et al., 2005). This supports the hypothesis that cerebellar LTD may subserve a local sensorimotor adaptation process shared by motor and spatial learning functions. This idea is also supported by Leggio and his collaborators, who stated that local procedural mnemonic processes permitting the fine tuning of navigation trajectories seem to involve the interaction between sub-cortical structures and the cerebellum (Leggio et al., 1999). It is worth mentioning that a declarative role of the cerebellum in spatial cognition has also been postulated (Hilber et al., 1998). By using lurcher mutant mice — which exhibit a massive loss of neurons in the cerebellar cortex and the inferior olivary nucleus — Hilber et al. (1998) suggested that cerebellar learning may play a crucial role in the retention of spatial information. However, these results could also be ascribed to the strong interaction between procedural and declarative learning (Lalonde and Botez, 1986; Gandhi et al., 2000; Joyal et al., 2001; Mandolesi et al., 2003). To stress the fact that declarative spatial learning requires appropriate procedural capabilities, Mandolesi et al. (2003) showed that hemicerebellar rats were not able to represent a new

environment because they could not explore it effectively, although they detected environmental changes as efficiently as control animals.

11.3 Unresolved questions

If the role of cerebellar learning in the procedural component of spatial cognition has been reported in multiple studies, a comprehensive interpretation of all experimental findings on the cerebellar role in spatial learning is still lacking. Among others, the following issues remain open: does a purely local adaptive motor control deficit (i.e. only impairing the low-level component of procedural learning) explain all the observed deficits in cerebellar subjects? Is the cerebellum also implied in the formation of more high-level procedural memories? Does (and if yes to what extent) cerebellar learning contribute to the declarative component of spatial cognition?

11.4 Our approach

Numerous computational models have investigated the cerebellar role in adaptive motor control and procedural learning (e.g. Fujita, 1982; Kawato et al., 1987; Schweighofer et al., 1996, 1998; Medina and Mauk, 2000; McKinstry et al., 2006). Yet, to the best of our knowledge, none of these studies has addressed the implication of the cerebellum in spatial cognition. In the following study, we will therefore examine in which measures the framework of cerebellar internal previously described and used to adapt voluntary movements can be applied to spatial cognition and help to resolve the previously stated question.

We hence propose to re-interpret available experimental data within a quantitative theoretical framework, in the attempt to shed light on the cerebellar role (either direct or indirect) in the multiple processing stages mediating spatial learning and goal-directed navigation. The rationale is to complete the existing behavioral observations with quantitative accounts testing specific hypotheses on the link between synaptic plasticity mechanisms, cell discharge properties, interstructure coupling, and behavioral responses.

To do so, we simulate a large-scale neural network (figure 11.2A) accounting for the functional coupling between cerebellum and hippocam-

pal formation. The modeled architecture also includes a putative cortical module for trajectory planning and inverse dynamics computation. The presented work focuses on the behavioral genetic findings reported by Burguière et al. (2005), which suggest that LTD at the parallel fiber-Purkinje cell (PF-PC) synapses is relevant to the adaptive tuning of navigation trajectories. We model the main information processing stages of the cerebellar microcomplex and we emulate the lack of LTD at PF-PC synapses of L7-PCKI transgenic mice (De Zeeuw et al., 1998). We simulate the experimental protocols employed by Burguière et al. (2005) to compare the learning performances of L7-PKCI mutants with those of control animals in two spatial navigation tasks: the Morris water maze (MWM, Morris, 1984; see simulated setup in figure 11.2B) and the Starmaze task (Rondi-Reig et al., 2005; figure 11.2C). In both setups, mice have to swim from random departure locations to a platform hidden below the surface of opaque water. Both tasks require declarative learning to building a spatial representation of the environment. Yet, in contrast to the MWM task, the Starmaze alleys guide movements, which eventually reduces the low-level procedural demand of the task. Thus, the use of these two paradigms allows the relative importance of the declarative and procedural components of navigation to be assessed (Burguière et al., 2005).

First, we quantify the impact of a purely local motor adaptation deficit on the overall goal-oriented behavior and we test this hypothesis against empirical observations (Burguière et al., 2005). Our results suggest an implication of the cerebellum in higher-level aspects of procedural spatial learning. In particular, our results show that L7-PKCI mutants are likely to be impaired in trading-off the exploration-exploitation balance and in inhibiting thigmotaxic (peripheral circling) behavior. Second, we test the working hypothesis that these two high-level procedural deficits may reflect a direct implication of the cerebellum in the integration of idiothetic (self-motion) cues —i.e. path integration or dead reckoning (Mittelstaedt and Mittelstaedt, 1980; Etienne et al., 1998; Etienne and Jeffery, 2004; McNaughton et al., 2006; Wiener et al., 2011)— and, consequently, an indirect implication of the cerebellum in declarative spatial learning. We characterize the encoding properties of hippocampal place cell activity as well as the functional time course of the learned place field representations. These analyses quantify the possible impact of cerebellar LTD deficits on the dynamics of hippocampal place coding. Our results show that the spatial mapping rate in L7-PKCI animals is impaired compared to con-

trols. They also suggest that the L7-PKCI hippocampal population code is less accurate—in terms of estimate of the location currently visited by the animal— than the one learned by control mice. A single unit analysis suggests an increased probability for L7-PKCI hippocampal place cells to exhibit multipeak receptive fields, which is likely to degrade the accuracy of the overall cognitive map. These results lead to a series of predictions—at the level of both single unit and neural population activity—that can be tested through extracellular electrophysiological recordings of L7-PKCI hippocampal place cells. At the behavioral level, our results suggest that the predicted path integration deficit of L7-PKCI mice would lead to observable differences in the free exploration patterns of mutants and controls during latent spatial learning in open-field environments (Drai et al., 2001; Fonio et al., 2009).

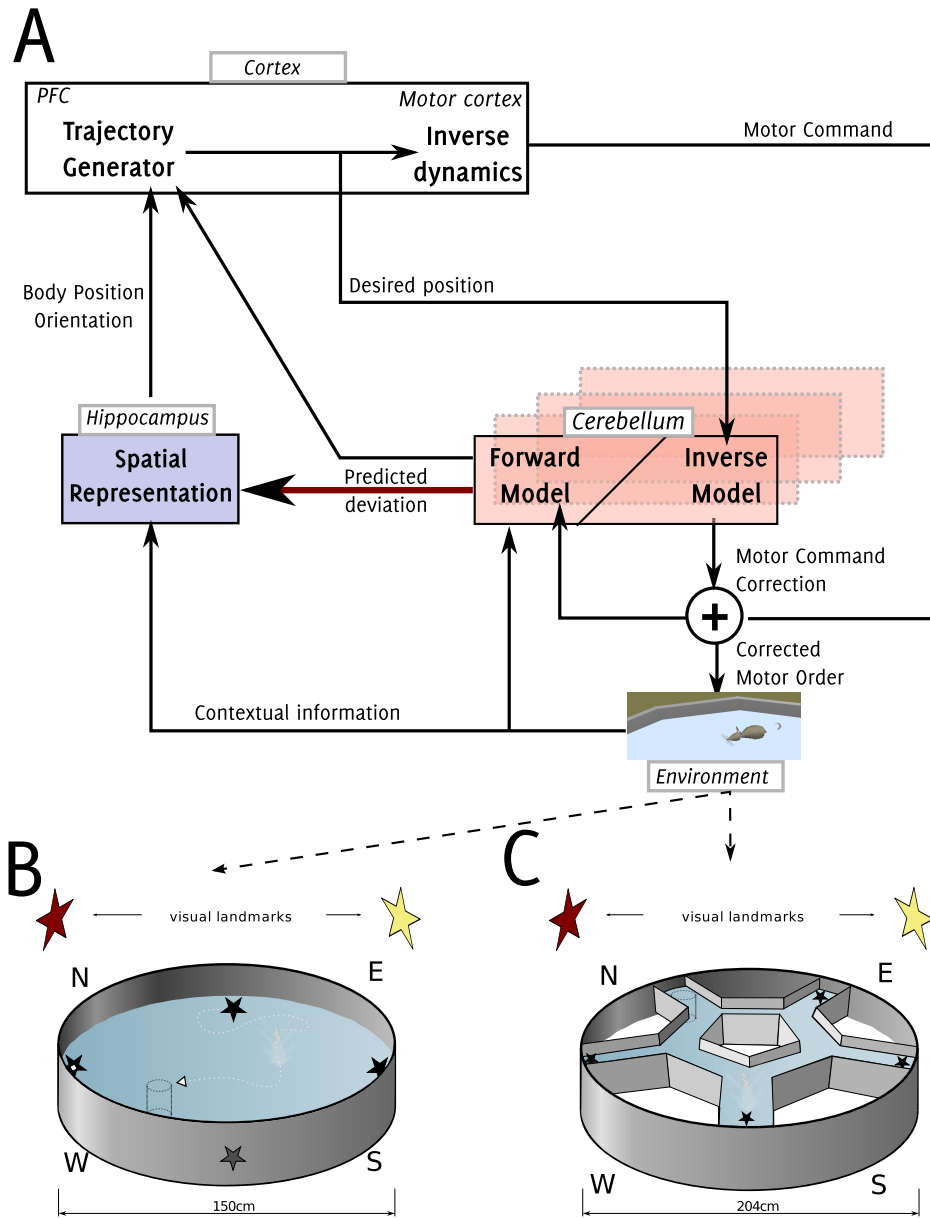


Figure 11.2: Overview of the model architecture and simulated navigation protocols. **A.** Overview of the biomimetic control architecture. **B.** The Morris watermaze (Morris, 1981) is a circular pool filled with water which has extensively been used in the study of spatial cognition. **C.** The Star maze (Rondi-Reig et al., 2005) consists of five alleys forming a central pentagonal ring and five alleys radiating.

Chapter 12

Material and methods

12.1 Integrated model of procedural and declarative spatial learning

12.1.1 Overall model architecture

Figure 11.2A shows an overview of the connectionist architecture developed for this study. The core of the model is the functional coupling between cerebellum and hippocampal networks, which allows the interplay between procedural and declarative components of spatial learning to be investigated.

In agreement with Marr-Albus-Ito theory (Marr, 1969; Albus, 1971; Ito and Kano, 1982), we assume that the cerebellum can acquire internal models of complex sensorimotor interactions (Ito, 1970; Wolpert et al., 1998) and store them in multiple and coupled microcomplexes—the computational units of the cerebellum (Ito, 1984). We model a highly simplified cerebellar microcomplex circuit (figure 12.1) capable of adapting its input-output dynamics through online learning. We employ the same microcomplex model to learn two types of internal models, namely *inverse corrector* and *forward predictor*, consistently with experimental data (Bell et al., 1997; Miall, 1998; Wolpert et al., 1998; Eskandar and Assad, 1999; Wolpert et al., 1998; Imamizu et al., 2000; Miall et al., 2007; Mulliken et al., 2008). The implemented internal models mediate low-level procedural spatial learning by encoding the causal relationships determining sensorimotor couplings during navigation. The inverse corrector model learns to map desired future positions into corrective commands compensating

for noisy inverse dynamics —and, consequently, for otherwise inaccurate movement execution (e.g. local drifts in swimming trajectories). The forward model learns to predict next states (egocentric translations and orientations) based on received motor command efference copies.

The spatial representation module consists of a hippocampal network adapted from our previous work (Arleo and Gerstner, 2000; Arleo et al., 2004; Sheynikhovich et al., 2009). The model integrates multimodal spatial information to establish and maintain hippocampal place field representations. The discharge properties of model hippocampal neurons are consistent with those of their biological counterpart (Sheynikhovich et al., 2009). Unsupervised Hebbian learning shapes the dynamics of the hippocampal network producing spatially-tuned hippocampal activity (O’Keefe and Conway, 1978). After training, the model hippocampal population coding supports place recognition and long-term spatial memory (Arleo and Gerstner, 2000; Sheynikhovich et al., 2009). A two-fold encoding process builds hippocampal representations on-line through active exploration. The simulated animal extracts spatiotemporal properties of the environment from visual inputs and elaborates an allothetic spatial code. Simultaneously, it encodes self-movement information through path integration (Mittelstaedt and Mittelstaedt, 1980; Etienne et al., 1998; Etienne and Jeffery, 2004) and builds an idiothetic spatial representation. Unsupervised learning binds the two encoding streams into a multimodal map in the proper hippocampus (CA1-CA3). We test the hypothesis that cerebellar procedural learning may influence path integration —and consequently the encoding of idiothetic cues in spatial memories. To do so, we employ the output of the cerebellar forward model (which predicts movement-related sensory feedback) to feed the idiothetic component of our hippocampal place code.

As shown in figure 11.2A, the model also includes a high-level module mediating cortical-like action selection and primary motor control. This module receives as inputs both an estimate of the current state from the hippocampal network and a prediction of the next state from the cerebellar forward model. It plans goal-directed trajectories and it locally maps desired positions onto motor commands through inverse dynamics computation. This module is purely algorithmic, since modeling goal-oriented navigation planning was out of the scope of this paper (see Martinet et al., 2011, for a recent model of action planning in a prefrontal cortical network model).

In the following, we provide brief descriptions of the cerebellar microcomplex and hippocampal models, focusing on connectivity layout and input-output functional relations. More comprehensive accounts — including neuronal model equations and parameter settings— can be found in Supplementary Information Sec. 15.1.

12.1.2 Cerebellar microcomplex model

We model the basic elements of the cerebellar microcircuit (figure 12.1A) as a network of spiking neural populations (figure 12.1B). This network accounts for a set of mossy fiber (MF) inputs, a granular cell (GC) layer, a population of Purkinje cells (PCs), deep cerebellar nuclei (DCN), and climbing fiber inputs from the inferior olive (IO). We implement MF inputs as axons of a population of leaky integrate-and-fire neurons, whereas we model GCs, PCs, and DCN as populations of conductance-based spiking units.

In the model, 100 MFs convey either egocentrically-encoded motor commands (for the inverse model corrector) or desired position inputs (for the predictive forward model). We compute the activity of MFs based on a family of radial basis functions spanning the input space —i.e. velocity vector or target location state space— uniformly. MFs send excitatory projections to a population of 100 DCN units based on an all-to-all connection scheme. MFs also excite a population of 10^4 GCs. The MF–GC connection probability is equal to $P_{MF-GC} = 0.04$, such that, on average, each MF innervates 400 GCs and each GC receives 4 MF afferents —in agreement with anatomical data (Eccles et al., 1967; Jakab and Hamori, 1988; Chadderton et al., 2004). The model GC ensemble activity provides a sparse representation of MF inputs, optimizing encoding capacity and information transmission properties (D’Angelo and De Zeeuw, 2009). Each GC targets, on average, a subset of 150 PCs out of a population of 200. Thus, each PC receives on average 7500 parallel fiber (PF) excitatory afferents (i.e. GCs’ axons) and the connection probability is $P_{PF-PC} = 0.75$. In the model, each PC is also driven by the activity of one IO unit mediated by a climbing fiber connection. A network of 200 IO units project onto 200 PCs (one-to-one connections). A Poisson spike-train generation process models the irregular firing of IO neurons. We then modulate the IO activity to encode error/teaching signals representing either the ongoing angular and translational discrepancies between actual and desired trajectories

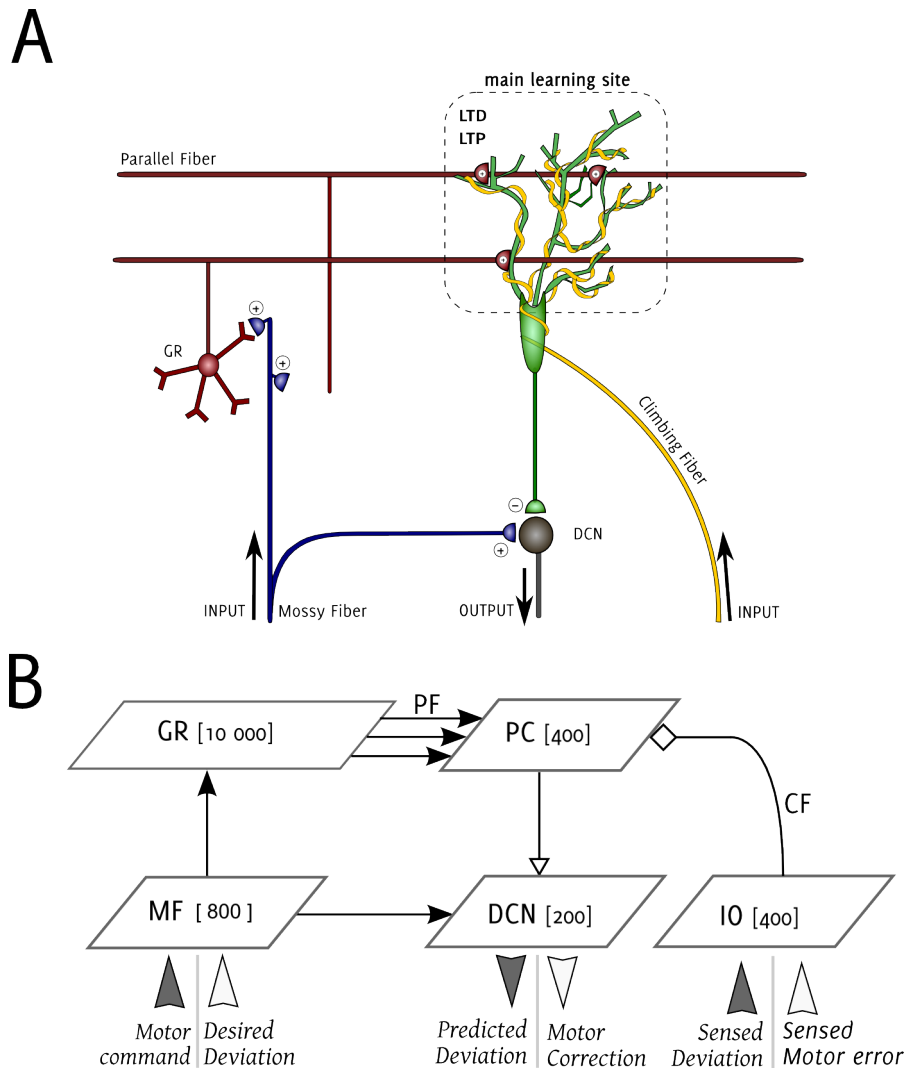


Figure 12.1: A. A simplified scheme of the cerebellar microcomplex (adapted from Medina et al., 2002) Afferent information enters the cerebellum via two neural pathways: the mossy fibers (MFs) and the climbing fibers (CFs). MFs convey multimodal sensorimotor signals whereas CFs are likely to transmit error-related information. Optimal sensorimotor representations and error-related signals converge onto the PC synapses, whose long-term modifications (i.e., long-term potentiation, LTP, and depression, LTD) constitute a suitable cellular mechanism for learning. B. The model cerebellar microcomplex circuit. Black and white arrows are excitatory and inhibitory synapses, respectively. The cerebellar model is divided into two regions, each one representing a set of internal forward (dark gray) and inverse (light gray) models. The number of simulated neurons is indicated for each layer. (MF: Mossy Fibers, GR: Granule Cells, PC: Purkinje Cell, IO: Inferior Olive, DCN: Deep cerebellar nuclei, Diamond-shaped: error signal)

(for the inverse corrector model) or the differences between inferred and actual result of movement execution (for the forward predictor model). Finally, the 200 PCs inhibit the population of 100 DCN units through one-to-one projections, such that each DCN neuron receives afferents from two PCs. DCN neurons provide the output of the cerebellar microcomplex model. Their discharge encodes either a motor correction (inverse model corrector) or an estimate of the deviation of the simulated animal (predictive forward model).

The modeled inhibitory action of PC activity onto DCN units primarily determines the response of the cerebellar model. In turn, PCs are principally driven by GC excitation mediated by PF–PC synapses. Therefore, modifying the strength of PF–PC synapses results in shaping the input-output relation characterizing the cerebellar microcomplex. The model accounts for bidirectional long-term plasticity (i.e. LTP and LTD) at the level of PF–PC synapses. We implement LTP as a non-associative mechanism (Lev-Ram et al., 2002), such that every incoming PF spike triggers a synaptic efficacy increase. Conversely, we model LTD as an associative mechanism, such that the conjunctive inputs to the PCs from PFs and climbing fibers tend to depress PF–PC projections (Ito and Kano, 1982; Wang et al., 2000; Safo and Regehr, 2008). In our simulation, we emulated L7-PKCI transgenic mutants by inactivating the LTD mechanism between PF and PC synapses.

As aforementioned, we employ the same microcomplex spiking network to realize both an inverse (corrector) model and a forward (predictive) model. Motor execution errors (for the inverse model) and next state prediction errors (for the forward model) determine the IO teaching signals triggering LTD at PF–PC synapses. Thus, the inverse and forward models adapt their input-output dynamics online and learn, respectively, to anticipate motor corrections and predict next states (i.e. location and orientation). In the current implementation, four cerebellar microcomplex networks mediate the adaptive inverse corrector and two other microcomplexes learn the forward predictor (see Sec. 15.1 in Supplementary Methods, for more details).

12.1.3 Hippocampal model

Figure 12.2 depicts a simplified view of the hippocampal model adapted from our previous work (Arleo and Gerstner, 2000; Arleo et al., 2004;

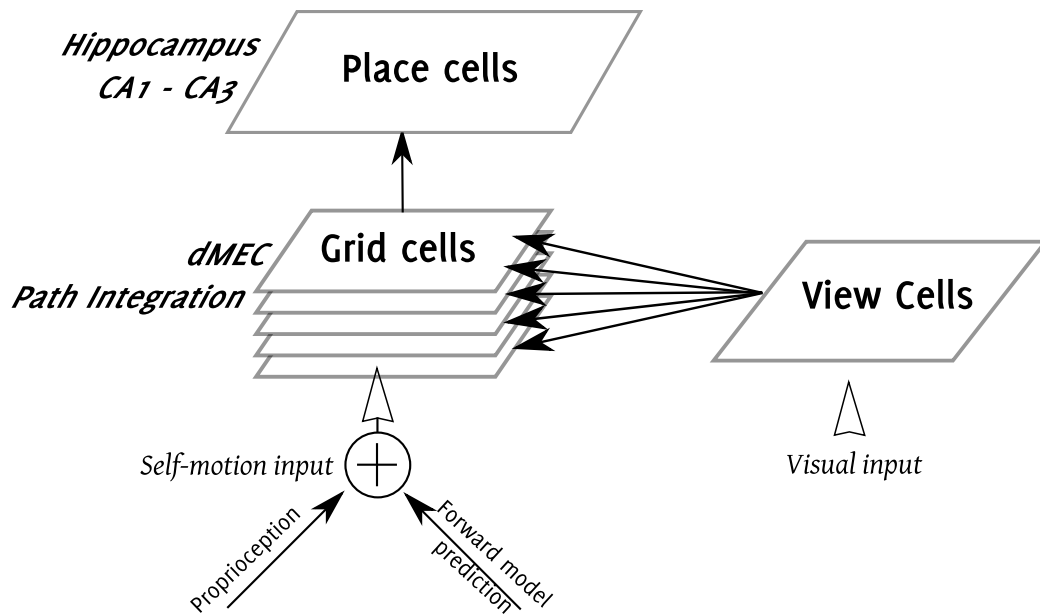


Figure 12.2: *Hippocampal Model Overview*. Visual input is processed by a set of filters (not shown) that project to hypothetical View cells. Grid cells in the dorsomedial entorhinal cortex (dMEC) receive self-motion input and visual input, preprocessed by the population of view cells. The grid cells connect to place cells in the hippocampal area CA1 and CA3. The place cells encode the spatial location.

Sheynikhovich et al., 2009). The model integrates allothetic (visual landmarks) and idiothetic (self-motion) information to establish and maintains hippocampal place fields. Model CA1 place cells receive feed-forward inputs from a population of grid cells in a simulated Layer II of the dorsomedial entorhinal cortex (Brun et al., 2002; Fyhn et al., 2004). Model grid cells discharge as function of self-motion cues over time (i.e. path integration). They also integrate visual landmark information encoded by a population of vision-based place cells (VC) (Sheynikhovich et al., 2009). Self-motion inputs encode the speed vector corresponding to the last movement. Visual inputs convey panoramic-like snapshots of the environment processed by a large set of orientation-sensitive visual filters (Arleo et al., 2004). As exploration of a novel environment proceeds, unsupervised Hebbian learning allows the hippocampal place field representation to be built incrementally.

Path integration is vulnerable to cumulative error (Etienne and Jeffery, 2004). Thus, maintaining allothetic and idiothetic representations consistent over time requires to bound dead-reckoning errors by occasionally resetting the path integrator (Arleo and Gerstner, 2000; McNaughton et al., 2006). The model simply assumes that the uncertainty on the location estimate provided by the path integrator grows linearly with time. Whenever the simulated mouse finds a previously visited location, it uses the learned allothetic spatial representation—encoded by the VC population activity—to localize itself and calibrate path integration (see Arleo and Gerstner, 2000; Arleo et al., 2004; Sheynikhovich et al., 2009, for a full account of the hippocampal model and its implementation details).

We assess the overall accuracy the spatial representation by means of two complementary measures, namely R and $\bar{\epsilon}$, which quantify the amount of information encoded in the hippocampus and the quality of this information (but see Sec. 12.2 and Supporting Methods Sec. 15.2, for more specific measures of unitary and population place code characteristics). Measure R estimates the percentage of the environment covered by the place field population and is calculated as the fraction of positions where the animal can self-localise (and then recalibrate its path integrator) with good accuracy (the accuracy threshold is set to 10 cm). Measure $\bar{\epsilon}$ quantifies the accuracy of the place code as the mean self-localisation error—i.e. the discrepancy between actual and estimated position obtained by population vector decoding of hippocampal activity Georgopoulos et al. (1986); Wilson and McNaughton (1993). See Supplementary Methods, Sec. 15.2,

for the definition of measures $\bar{\epsilon}$ and R .

12.1.4 Spatial behaviour policy

Simulated mice select actions (i.e. egocentric motion directions $\theta(t) \in [-\pi/4, \pi/4]$) based on a probabilistic policy. At each simulation step $\Delta t = 200$ ms, a probability P_{switch} makes the animal select one out of three possible behavioural responses:

- It can adopt a circling behaviour with probability P_{circ} , which exponentially decreases with training trials tr :

$$P_{circ}(tr) = C + e^{(-tr/\tau)} \quad (12.1)$$

in order to reflect top-down inhibition of this thigmotaxic response.

- It can select an exploratory (random) motion direction with constant probability $P_{explore}$.
- It can exploit the acquired spatial knowledge to perform goal-directed navigation with a probability $P_{exploit} = 1 - P_{explore}$. During exploitation, a trajectory planner estimates the direction to the hidden platform (goal) at each time step, based on the hippocampal place code.

Otherwise, with probability $1 - P_{switch}$, the simulated animal consolidates its current action —i.e. $\theta(t + \Delta t) = \theta(t)$.

The default values of these parameters are: $P_{switch} = 0.02$; $P_{explore} = 0.1$; and $C = 0$, $\tau = 5$. This tuning values allow the stochastic action selection policy to approximate the exploratory behaviour of control mice —in both the MWM and the Starmaze tasks described below. Note, however, that we modify these default settings in simulations aimed at evaluating the impact of cerebellar adaptation deficits of L7-PKCI mice on procedural spatial learning (Sec. 13.2) as follows: for mutants: $P_{explore} = 0.25$, $C = 0.075$, $\tau = 9$; for controls: unchanged. Importantly, we do not artificially affect the behavioural parameters of L7-PKCI mutants in simulations testing the possible cerebellar role in declarative spatial learning (Sec. 13.3). Rather, they are function of the accuracy of the spatial knowledge acquired at a given point in time. In particular, we take P_{circ} as:

$$P_{circ} = 1 - \left[R_{circ} - k \cdot \bar{\epsilon}_{circ} \right]^+ \quad (12.2)$$

where R_{circ} denotes the fraction of the 10-cm peripheral annulus properly encoded by the place cell population activity, and \bar{e}_{circ} is mean place code accuracy over the peripheral annulus (see Supplementary Methods, Sec. 15.2, Eqs. 15.21–15.22, for the definition of measures \bar{e} and R); k is a normalisation factor and $[f(x)]^+$ is the positive part operator —i.e. $[f(x)]^+ = \max(f(x), 0)$.

12.2 Spatial learning tasks and statistical analyses

12.2.1 Morris Water Maze and Starmaze tasks

We tested the model against experimental findings in two spatial learning paradigms: the Morris Water Maze (MWM, Morris, 1984) and the Starmaze task (Rondi-Reig et al., 2005) (Figs. 11.2B,C). In both tasks animals have to learn an allocentric spatial representation based on available allothetic cues (configuration of visual landmarks) and idiothetic (self-motion) information. Then, they can use this spatial map to locate and reach a hidden escape platform from any position in the maze. Thus, both paradigms require declarative spatial learning. However, the presence of alleys in the Starmaze constrains and guides the trajectories of mice, reducing the procedural demand of this task as compared to open-field navigation in the MWM.

We reproduce the experimental protocol used by Burguière et al. (2005) to assess to what extent simulated L7-PKCI transgenic mice are differentially impaired, compared to controls, in solving the MWM and the Starmaze. For each task, two groups of simulated mice ($n=15$ controls and $n=15$ mutants) undertake 40 training trials over 10 training days (with 4 trials per day). At the beginning of each trial the simulated animal is placed at a departure point randomly drawn from a set of four possible locations (Figs. 11.2B,C). Each trial ends either when the animal has reached the hidden platform or after a 90 s timeout —i.e. if the animal fails to locate and swim to the platform.

We simulate the MWM and the Starmaze experimental protocols in the Webots platform (Michel, 2004). The latter provides a realistic environment where simulated animals could process visual, proximity (whisker-like), and self-motion (proprioceptive-like) signals. Simulated mice move

at a speed within a range of $[0, 15]$ cm/s. Sensory feedback (e.g. visual, tactile and proprioceptive information) occur every 200 ms in order to process internal state variables and select actions. Prior action execution, an inverse dynamics module (figure 11.2A) translates actions into low-level motor commands. Stochastic noise affects the execution of each action, emulating unpredictable sensorimotor perturbations and/or drifts from desired swim trajectories.

12.2.2 Behavioral analysis

We compare the goal-oriented behavior of L7-PKCI and control mice by assessing the same set of parameters measured by Burguière et al. (2005): *(i)* the mean escape latency (s), i.e. the average time spent to reach the platform; *(ii)* the mean heading (deg), computed as the average angular deviation between ideal and actual trajectory to the goal; *(iii)* the mean circling time (s), i.e. the average time spent in a 10 cm peripheral annulus of the maze (Leggio et al., 1999); *(iv)* the ratio between time spent in the target quadrant and trial duration; *(v)* the mean distance-to-goal (cm), i.e. the average Euclidean distance between the animal and the platform; *(vi)* the mean distance swum by the animal (cm); *(vii)* the search score, characterizing the shape of a goal-oriented trajectory (Petrosini et al., 1996); *(viii)* the mean number of visited alleys (for the Starmaze only); *(ix)* the mean speed of the animal (cm/s). We average each parameter over all trials performed in one day by all subjects of a same group. An ANOVA analysis quantifies the statistical significance of the results ($P < 0.01$ is considered as significant).

12.2.3 Statistical analyses of unitary and population neural activities

We analyze the activity patterns of single and multi-unit discharges in terms of spatial encoding properties and time course of the spatial learning process. This analysis aims at elucidating the link between neural responses, network dynamics, and behavioral observations. We quantify: *(i)* the spatial selectivity properties of single cells by measuring the coherence (Hok et al., 2005), mean size, peak amplitude, and number of peaks of the receptive fields; *(ii)* the density —and other correlated measures such as

sparseness and redundancy— of the spatial population code; *(iii)* the reliability of neural representations (both at level of single cell and population code) in terms of spatial information content —i.e. how much it can be inferred about the animal’s position by observing neural responses only; *(iv)* the time course of the accuracy of the location estimate by population vector coding (Georgopoulos et al., 1986; Wilson and McNaughton, 1993); *(v)* the time course of the mean percentage of locations appropriately encoded by the spatial representation —i.e. the explored locations where the accuracy of the population vector estimate is above a fixed threshold. An ANOVA analysis measures the statistical significance of the results (again, $P < 0.01$ is considered as significant). See Supplementary Methods, Sec. 15.2, for details on the statistical measures and parameters employed for data analyses.

Chapter 13

Results

The logical flow of presented results is as follows: first, we assess the learning capabilities of forward predictor and inverse corrector models —both implemented by the same cerebellar microcomplex circuitry. Second, we characterize the spatial learning deficits of L7-PKCI mutants by isolating the local and global procedural components of navigation. Third, we verify the working hypothesis of a cerebellar role in path integration and, indirectly, in spatial information coding. To do so, we evaluate the possible impact of L7-PKCI learning deficits on the dynamics of hippocampal place representation —both at single unit and neural population levels. Finally, we derive possible behavioral correlates, at the level of spatial exploration strategies, of L7-PKCI synaptic plasticity deficits.

13.1 Adaptation in forward and inverse cerebellar models

Forward predictor models

We model two cerebellar microcomplexes to learn forward predictors of egocentric translations and orientations, respectively. The first microcomplex predicts traveled distances $d(t + \Delta t)$ based on current motor commands —i.e. mossy fiber (MF) inputs (figure 12.1B). The second learns online predictions of egocentric rotations $\theta(t + \Delta t)$. Henceforth, $\Delta t = 200$ ms. See Supplementary Methods, Sec. 15.1, for details.

Cerebellar forward models exhibit bistable responses. At the beginning of training, DCN cells tend to remain silent (baseline neuronal noise)

due to dominant inhibition from active Purkinje cells (PCs). Thus, the forward model provides no output and the prediction error is considered as infinitively large. Training modulates the inhibitory PC patterns to learn context (motor command) – response (next state) associations. As soon as DCN units start responding to a specific context, the prediction error becomes immediately small and converges after a few more context presentations (see Figure 13.1A for three examples of angular prediction errors as a function of motor command presentations). Figure 13.1B quantifies the mean number of presentations necessary to create context-response associations —by averaging over 100 different motor commands. Simulated control animals (white bar) need an average of 7.4 ± 1.02 (mean \pm s.e.) motor command presentations to reliably predict the corresponding angular displacements $\theta(t + \Delta t)$. By contrast, in simulated L7-PKCI mutants (black bar), DCN units remain inhibited over an infinite number of context presentations (i.e. no learning occurs). Similar findings hold for the prediction of traveled distances, $d(t + \Delta t)$, learned by the second cerebellar microcomplex implementing a forward model (not shown).

Figure 13.1C assesses the time-course of forward predictor learning in simulated mice trained in the Morris watermaze (MWM) task (see Sec. 12.2.1 for details on the protocol). Data points are averages over all animals ($n=15$ controls and $n=15$ mutants) and all trials ($n=4$) of a day. At day 1, simulated control animals learn to predict the outcome of about 30% of motor orders —i.e. to estimate *both* $\theta(t + \Delta t)$ and $d(t + \Delta t)$ before the execution of the motor commands. Performance increases monotonically over training and tends to stabilize around 70% at days 9 and 10. Figure 13.1C (right y-axis) also reports the absolute number of learned context-response associations over training. It suggests that the outcome of about 300 distinct motor commands is reliably predicted by the forward model after 10 days of training. As expected, simulated mutants do not establish any stimulus-response association over training. Figures 13.1D,E show the mean prediction errors (for linear and angular displacements, respectively) over the entire training session. In simulated control mice we observe a mean error of about 2.8 ± 1.7 mm for distances and of about 6 ± 0.8 degrees for rotations. In mutants, prediction errors are infinite.

Inverse corrector models

Four microcomplexes learn context-dependent correctors of inverse dynamics. Two of them compensate for movement execution errors online

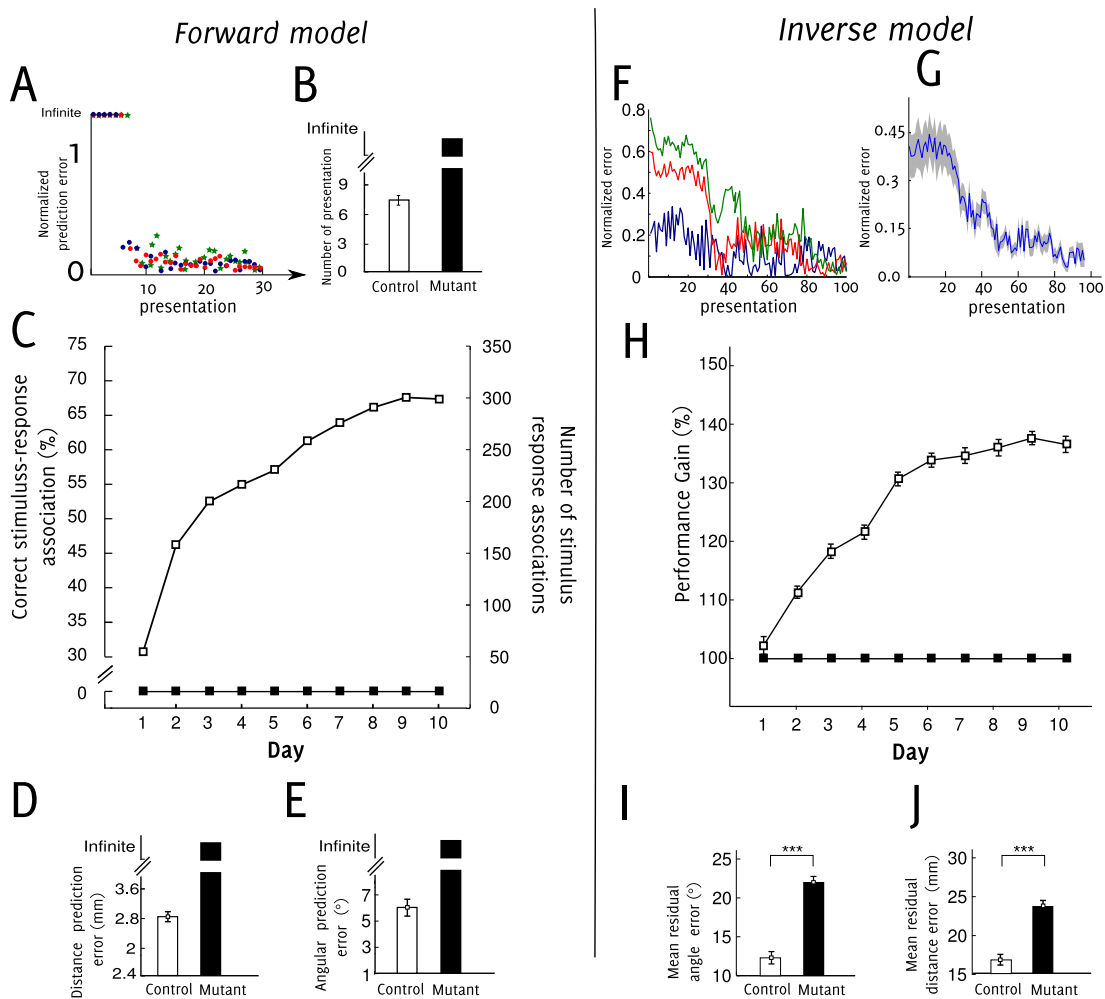


Figure 13.1: Learning performance of internal forward and inverse models. **(Left) Forward model properties.** **A.** Normalized prediction error for angular position in three different contexts. **B.** Mean number of presentations needed to create context-response associations. **C.** Time-course of forward predictor learning. To assess for the overall performance of forward model through learning, we report the correct stimulus-response association averaged over all animals at each day of training. **D.** Mean prediction error for linear displacement. **E.** Mean prediction error for angular displacement. **(Right) Inverse model properties.** **F.** Three samples of residual normalized angular error as a function of presentation. **G.** Mean normalized angular error averaged over 100 distinct desired states. **H.** Performance gain of controls vs mutants over training. **I.** Mean residual rotational error. **J.** Mean residual translational error. with $n=15$ animals and $m=4$ trials per day.

by correcting left-paw velocity commands (positive and negative ranges, respectively). The other two correct right-paw velocities (positive and negative ranges, respectively). See Supplementary Methods, Sec. 15.1, for details.

Figure 13.1F shows three samples of residual angular errors (i.e. differences between desired and actual orientations after the movement execution) as a function of the number of presentations of the corresponding (arbitrarily chosen) desired states (i.e. next positions and angles). Before training (0 input presentations), different commands lead to different residual errors. After convergence (100 presentations in this example), the inverse corrector models succeed in bounding post-execution angular errors. Figure 13.1G reports the mean angular errors (\pm s.e.) averaged over 100 distinct desired states. It suggests that inverse correctors converge significantly slower than forward predictors (e.g. figure 13.1A) and do not exhibit a bistable behavior.

Figure 13.1H quantifies the performance of control *vs.* mutant inverse corrector models over training in the MWM task. The mean performance accounts for both the distance and angular residual errors averaged over all animals ($n=15$ controls and $n=15$ mutants) and all trials ($n=4$) of a day. It is then normalized with respect to the mean value of mutants' performance to measure the relative gain obtained in the presence of adaptive cerebellar input-output dynamics. In simulated control mice, the performance gain significantly increases over training and converges to nearly 140% after 8 – 10 days. Figures 13.1H,I compare the mean rotational and translational errors averaged over all training trials for controls and mutants (white and black bars, respectively). Expectedly, the mean residual execution errors are significantly smaller in controls than mutants (ANOVA, $F_{1,28} = 64.01$, $P < 0.001$ for angular error; $F_{1,28} = 63.92$, $P < 0.001$ for distance error). After the movement execution, the control animals have a mean distance error of 17.2 ± 0.81 mm, whereas it is 23.8 ± 0.6 mm for mutants. Also, after each movement execution, controls deviate from the desired orientation of about $12 \pm 0.6^\circ$ *vs.* $21 \pm 0.7^\circ$ in mutants.

13.2 Cerebellar role in local *vs.* global procedural spatial learning

Here we assess the impact of cerebellar adaptation deficits in L7-PKCI mice on the procedural components of navigation behavior. The model allows the procedural bases of spatial navigation to be isolated by blocking the functional projection from the cerebellar network to the hippocampal network (figure 11.2A). As a consequence, we endow simulated control and mutant mice with equivalent spatial representation capabilities.

A local procedural deficit partially accounts for L7-PKCI spatial navigation impairments

First, we test the hypothesis of a purely *local* (i.e. low-level motor control) procedural deficit of L7-PKCI mice when solving both the MWM and the Starmaze (Sec. 12.2.1, Figs. 11.2 B,C, and also annexe B.4). Under this hypothesis, our simulation results reproduce the experimental data only partially —see details in Supplementary Results, Sec. 16.1. On the one hand, simulated L7-PKCI mutants are significantly impaired in terms of mean escape latency and heading-to-goal when solving the MWM (Supplementary Figs. 16.2 A,B, respectively). In the Starmaze we do not observe any significant difference between L7-PKCI and controls (Figs. 16.2 E,F). These results are consistent to experimental findings and suggest suboptimal navigation trajectories of L7-PKCI mice (compared to controls, figure 16.1) due to the lack of local minimizations of motor-command execution errors. On the other hand, our simulation results indicate that a purely local procedural deficit can not explain the coarser goal-search behavior of L7-PKCI reported by Burguière et al. (2005). Indeed, in contrast to experimental data, the simulated mutants neither spend significantly less time within the platform quadrant nor exhibit larger searching zones than the controls (Figs. 16.2 C,D).

A global procedural deficit accounts for all L7-PKCI spatial navigation impairments

Then, we test the hypothesis of a possible implication of the cerebellum in higher-level (*global*) procedural spatial learning. We assume a two-fold perturbation of the high-level action selection process of simulated L7-PKCI mice (Sec. 12.1.4). First, we artificially impair the mutants' abil-

ity to inhibit thigmotaxic behavior. To do so, we increase the time constant of the P_{circ} function, such that L7-PKCI mice are likely to perform peripheral circling over a larger number of training trials than controls (see details in Sec. 12.1.4). Note that adding a longer circling time to the purely local optimization of trajectories fails to account for all differences between L7-PKCI and control mice observed experimentally (not shown). Second, we artificially impair mutants' ability to balance the exploration-exploitation behavior compared to controls. We do so by increasing their exploration probability $P_{explore}$ over the entire training period (see details in Sec. 12.1.4).

We compare the spatial learning performance of simulated controls and mutants in both MWM and Starmaze tasks under this global procedural impairment hypothesis (figure 13.2). Consistent with experimental data (Burguière et al., 2005), in the MWM the simulated control mice improve their performance over training significantly better than mutants. Although the mean escape latency of controls and L7-PKCI is similar at the end of day 1, it decreases significantly faster and to a larger extent in controls over time (figure 13.2A, ANOVA, $F_{1,28} = 68.69$, $P < 0.001$). A similar result holds for the mean heading-to-goal measure (figure 13.2C, ANOVA, $F_{1,28} = 32.26$, $P < 0.001$), suggesting a deficit of simulated L7-PKCI in optimally orienting their locomotion toward the platform during navigation. Again, a difference of swimming speed is not responsible for the performance deficits of simulated mutants (not shown, ANOVA, $F_{1,28} = 1.5385$, $P > 0.1$). Importantly, the searching behavior of mutants is now impaired compared to controls—in contrast to the results under the purely local procedural scenario and in agreement with experimental data. The ratio between time spent within the platform quadrant and the trial duration is significantly larger in the simulated control animals over the entire training (figure 13.2D, ANOVA, $F_{1,28} = 44.16$, $P < 0.001$). Also, the search scores are larger in simulated mutants than in controls over training (figure 13.2A, right y-axis). As already reported by Burguière et al. (2005), search scores are highly correlated to escape latencies in both controls and mutants (figure 13.2B)—confirming that the longer time-to-goal needed by L7-PKCI mice is linked to a suboptimal searching behavior. Also, the mouse-to-platform distance measure demonstrates that on average mutants follow significantly longer goal pathways than controls (figure 13.2D, ANOVA, $F_{1,28} = 63.723$, $P < 0.001$). Expectedly, in accordance to the implemented P_{circ} functions for the model controls and mutants, the latter

exhibit a significantly larger amount of circling behavior over the entire training (figure 13.2F, ANOVA, $F_{1,28} = 59.60$, $P < 0.001$).

Altogether, the *global* procedural impairment hypothesis allows the entire set of experimental data in the MWM to be accounted (figure 13.2A-F) —in contrast to the *local* procedural deficit hypothesis (Supplementary Results, Sec. 16.1, figure 16.2). In addition, the mean intergroup differences in simulation and experiments —e.g. for the heading ϕ , we compute $\left\langle \phi^{WT} - \phi^{L7PKCI} \right\rangle_{n,m}$ by averaging over all $n = 15$ animals and all $m = 40$ training trials—, are comparable for all behavioral parameters (escape latency: ANOVA, $F_{1,18} = 0.0516$, $P > 0.5$; heading: ANOVA, $F_{1,18} = 2.987$, $P > 0.1$; ratio between time spent in the platform quadrant and trial duration: ANOVA, $F_{1,18} = 0.00005$, $P > 0.5$; distance to the platform: ANOVA, $F_{1,18} = 1.59$, $P > 0.1$; and circling: ANOVA, $F_{1,18} = 0.53$, $P > 0.25$).

Finally, results in the Starmaze task remain consistent with experimental data. We do not observe any statistical difference between controls and mutants in terms of either the mean number of alleys visited (figure 13.2G, ANOVA $F_{1,18} = 0.32$, $P > 0.5$), or the total distance swum (figure 13.2H, ANOVA $F_{1,18} = 0.45$, $P > 0.5$).

13.3 Cerebellar role in declarative spatial learning

The previous results point towards a joint effect of local motor adaptation deficits and a suboptimal exploration behavior in L7-PKCI mutants —which impair the fine and global tuning of goal-oriented trajectories, respectively.

But, how can the cerebellum influence the exploration/exploitation policy during spatial learning? An attractive hypothesis consists in relating the exploratory behavior to the accuracy of the acquired spatial knowledge. A recent study by Fonio et al. (2009) unfolds the free exploratory behavior of mice through time. They report that different strains of mice share stable and well-ordered behavioral pattern sequences when exploring open-field environments. Their results demonstrate that mice’s exploratory behavior consists of reiterated home-centered round-trips of increasing amplitude and “degrees of freedom”: first, mice explore a restricted area around their

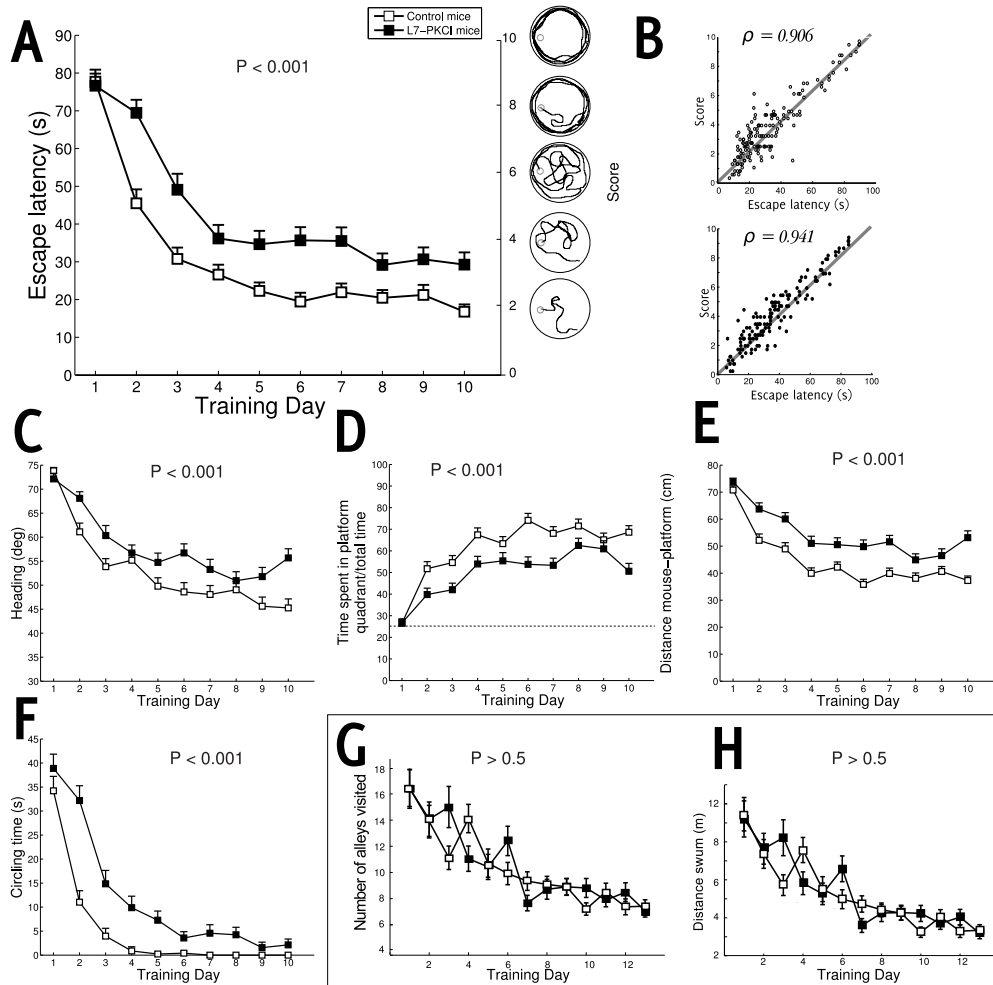


Figure 13.2: Results in the MWM (a-f) and in the Starmaze (g-h) under a procedural scenario.

MWM: **A.** Escape latency (left scale) and score (right scale) of simulated controls (white square) compared to mutants (black square). **B.** Correlation between the searching score and the escape latency for the simulated control (top) and mutant mice (bottom). **C.** Average angular deviation between ideal and actual trajectory to the goal **D.** Ratio of time spent in the platform quadrant over the total time of trial. **E.** Mean distance of the simulated mouse with the platform. **F.** Circling time. **Starmaze:** **G.** Mean number of alleys visited. **H.** Mean distance swum.

home base (dimension 0); second, they start moving along the wall of the environment (dimension 1; peripheral circling); third, they begin making incursions to the center of the environment (dimension 2) to fully explore it. Importantly, the exhaustion of a given spatial dimension is a necessary condition for the emergence of the next dimension in the sequence (Fonio et al., 2009). Here, we formulate the hypothesis that L7-PKCI mice may have impaired declarative spatial learning capabilities. This would reduce the rate of acquisition of spatial information in novel environments. Based on the observations by Fonio et al. (2009), this would therefore delay the exhaustion of each spatial dimension and then lead to a suboptimal exploratory behavior of cerebellar mutants compared to controls.

But, how can the cerebellum influence declarative spatial learning? Here we make the hypothesis that the cerebellum may play a role in path integration. It would indirectly provide the hippocampal formation—and in particular the medial entorhinal cortex—with self-motion related predictions suitable to refine the estimate of linear and angular displacements over time (see Discussion, Chapter. 14). Under this scenario, an impaired cerebellar processing would affect path integration and, consequently, the elaboration of hippocampal spatial representations.

To test this two-fold hypothesis, we enable the functional projection from the cerebellar network to the hippocampal network of the model (figure 11.2A). In particular, we connect the output of the forward predictor model to the path integrator module (figure 12.2). That is, we assume that the angular and linear displacements predicted by the forward models for each motor command are combined with sensory self-motion feedbacks (e.g. proprioceptive) to drive the enthorinal grid cell population of the model. As a consequence, the simulated control and L7-PKCI mice do not longer share equivalent spatial representation abilities mediated by the hippocampal formation—in contrast to previous simulations (Sec. 13.2). Additionally, we do not affect the searching behavior of mutants artificially as in previous simulations (Sec. 13.2). The circling behavior of simulated mice is now a function of the amount of encoded knowledge on a 10-cm annulus near the wall of the environment (see Sec. 12.1.4 for details). Also, the probability determining the exploring/exploiting trade-off is not differentiated a priori between mutants and controls (as in Sec. 13.2) but is initially equivalent for both groups. Therefore, differences in circling inhibition behavior and exploration-exploitation balance would rather reflect differences in spatial code accuracy in controls and mutants over training.

Cerebellar adaptation deficits reduce the rate of acquisition and accuracy of hippocampal place field representations

Figures 13.3A–C compare the time course of spatial information coding in the model hippocampal network of simulated controls and mutants solving the MWM. We quantify how the percentage R of the environment encoded by the place field representation evolves over training—see Sec. 12.2 and Supporting Methods Sec. 15.2 for the definition of measure R . Figure 13.3A measures the rate of acquisition of the spatial map over the entire MWM. It suggests that spatial learning converges at slower rate in L7-PKCI than controls, with significant time course differences during day 1-5 of training (ANOVA, $F_{1,28} = 10.24$, $P < 0.01$). This overall acquisition rate impairment results from the additive effect of delayed exhaustion of dimension 1 (circling) and dimension 2 (center of the environment) in simulated cerebellar mice (Figs. 13.3B and C, respectively).

Figures 13.3D–F quantify the time course of the mean position reconstruction error $\bar{\epsilon}$ of hippocampal population codes in L7-PKCI and controls—see Sec. 12.2 and Supporting Methods Sec. 15.2 for the definition of measure $\bar{\epsilon}$. Figure 13.3D shows that both simulated groups improve the accuracy of their spatial code over time. However, simulated mutants exhibit significantly larger self-localization errors than controls through the entire training (ANOVA, $F_{1,18} = 27.2$, $P < 0.001$). The bar diagram of Figure 13.3D (right) confirms this result by averaging over all training sessions (ANOVA, $F_{1,18} = 27.2$, $P < 0.001$). Expectedly, suboptimal place coding on the entire maze reflects the L7-PKCI impairment to encode dimensions 1 and 2 as accurately as controls (Figs. 13.3E, F).

Population place coding is suboptimal in L7-PKCI mice compared to controls

Figures 13.4A–C further characterize the properties of hippocampal population codes in both simulated groups. We observe that the mean spatial information content of controls' place field representation is significantly larger than in mutants (figure 13.4A; ANOVA $F_{1,18} = 15.9845$, $P < 0.001$). We then compare the redundancy of the spatial information content of the two neural population codes and find that, on average, they tend to be larger in mutants than in controls (figure 13.4B; ANOVA $F_{1,18} = 29.8529$, $P < 0.001$). The intergroup difference of mean spatial density of receptive fields confirms this observation (figure 13.4C; ANOVA $F_{1,18} = 23.6007$, $P < 0.001$). These results point towards suboptimal place field represen-

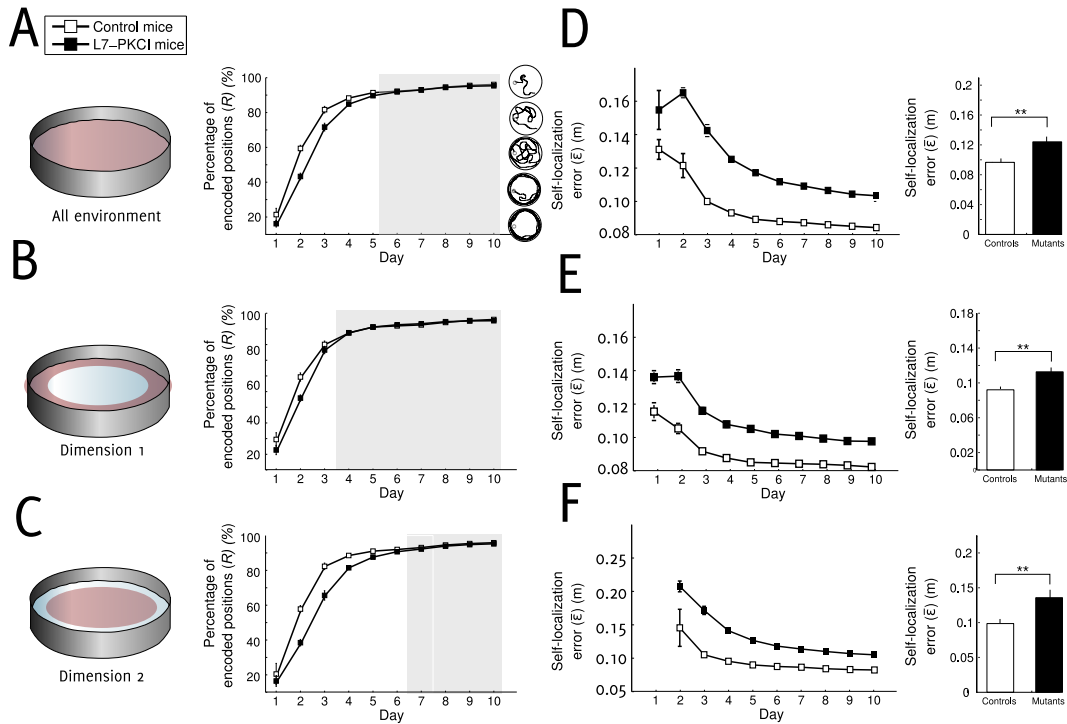


Figure 13.3: Accuracy of the spatial representation for both simulated populations. Accuracy is measured as the quantity and quality of information encoded in the hippocampal place cells for the whole environment (top: A,D), the peripheral area (middle: B,E) and the central region (bottom: C,F). A-C (left): Recording area of the MWM (red). A-C (right): Time course of the amount of information encoded. D-F (left): Time course of the quality of encoding. D-F (right): Mean self-localization error.

tations in mutants —i.e. encoding less spatial information despite a more redundant (dense) place code compared to controls. But where does this lack of optimality at the level of mutants' population code come from?

Unitary place fields of L7-PKCI mice are not impaired in terms of size, spatial coherence and information content

To address the above question we compare the spatial tuning properties of single hippocampal place cells in both simulated groups (again when solving the MWM). We observe that the size of hippocampal receptive fields is comparable, on average, in controls and mutants (figure 13.4D; ANOVA $F_{1,98} = 0.15, P > 0.5$). Similarly, the spatial coherence of mutants' place fields is not impaired compared to controls (figure 13.4E; ANOVA $F_{1,98} = 0.47, P > 0.1$). Also, there is no significant intergroup difference with respect to the amount of spatial information encoded by single hippocampal units (figure 13.4F; ANOVA $F_{1,98} = 0.01, P > 0.5$). Finally, mutant and control place cells are also statistically comparable in terms of mean firing rate (not shown, ANOVA $F_{1,98} = 0.56, P > 0.4$).

Multiple-peak place fields occur with higher probability in L7-PKCI compared to control mice

The above standard measures—which account for spatial tuning and accuracy of unitary hippocampal responses—fail to explain the subtle but significant difference observed at the level of population spatial selectivity in controls and L7-PKCI (Figs. 13.4A–C). We then further investigate the properties of model hippocampal single units by quantifying the unimodal *vs.* multimodal characteristic of their spatially tuned discharges. We apply the Hartigan DIP unimodality test (Hartigan and Hartigan, 1985) to classify the spatial firing distributions of single hippocampal units. Figure 13.5 shows some samples of hippocampal place fields “recorded” from simulated controls (left column) and mutants (right column) in the MWM. For each cell, we report the statistical significance of the Hartigan unimodality test (DIP test $P < 0.01$ indicates a multimodal receptive field). Figure 13.6A (first column) quantifies the ratio between unimodal and multimodal place fields for both simulated groups. Simulation results suggest that both groups have a majority of single-peak place cells—controls: 0.73 ± 0.02 , mutants: 0.51 ± 0.03 . However, they also indicate that, on average, controls' hippocampal units have a signif-

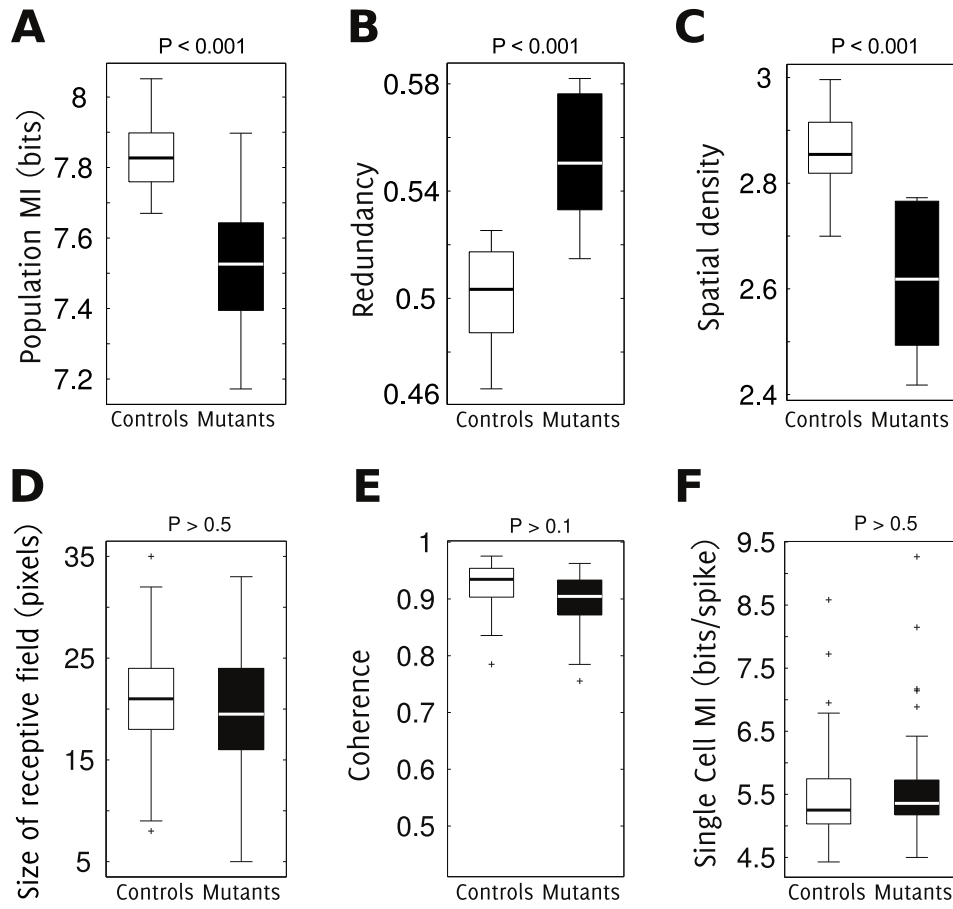


Figure 13.4: Information content of simulated place cells.

icantly larger fraction of single-peaked receptive fields compared to L7-PKCI mice (ANOVA $F_{1,198} = 50.49$, $P < 0.001$). Consistently, Figure 13.6A (second and third column) shows that mutants have a significantly larger ratio of double-peak and triple-peak place fields than controls (ANOVA $F_{1,198} = 20.52$, $P < 0.001$ and ANOVA $F_{1,198} = 15.91$, $P < 0.001$, respectively). By contrast, both groups have a negligible percentage of four-peak place fields (figure 13.6A, fourth column). Finally, we compare the mean number of peaks per hippocampal place field in controls and mutants (figure 13.6B). Consistent with previous results, we show that, on average, L7-PKCI place fields have a significantly larger number of peaks than controls (ANOVA $F_{1,198} = 7.1884$, $P < 0.01$).

The hypothesis of a global procedural deficit induced by a less accurate hippocampal place code in L7-PKCI mice accounts for all spatial navigation impairments in the MWM

Figures 13.7A–F present the behavioral results in the MWM under the L7-PKCI declarative deficit hypothesis. Both the mean escape latency and the search score of the simulated L7-PKCI mice are significantly impaired over training compared to controls (figure 13.7A; escape latency: ANOVA, $F_{1,28} = 56.16$, $P < 0.001$; search score: ANOVA, $F_{1,28} = 53.24$, $P < 0.001$). As already shown, these two behavioral measures are highly correlated for both groups of simulated animals (figure 13.7B; controls: Pearson’s product-moment coefficient $\rho = 0.936$, $P < 0.001$; mutants: $\rho = 0.94$, $P < 0.001$). This navigation impairment is not due to a deficit in swimming speed (not shown, ANOVA, $F_{1,28} = 1.47$, $P > 0.1$). Navigation trajectories of simulated L7-PKCI mice are also significantly less efficient than controls in terms of the heading-to-goal parameter —i.e. deviation between actual and direct trajectory to the platform (figure 13.7C, ANOVA, $F_{1,28} = 71.76$, $P < 0.001$). The intergroup differences of searching behavior are also corroborated by the ratio between time spent within the platform quadrant and trial duration, which shows a significant impairment of simulated L7-PKCI mice (figure 13.7D, ANOVA, $F_{1,28} = 34.22$, $P < 0.001$). Similarly, mutants’ spatial behavior leads to significantly longer mean distances-to-goal over training than controls (figure 13.7E, ANOVA, $F_{1,28} = 58.83$, $P < 0.001$). The circling time of simulated L7-PKCI mice is significantly larger over the entire training phase compared to wild type (figure 13.7F, ANOVA, $F_{1,28} = 83.12$, $P < 0.001$). Recall that in these simulations we do not artificially perturb the ability of simulated

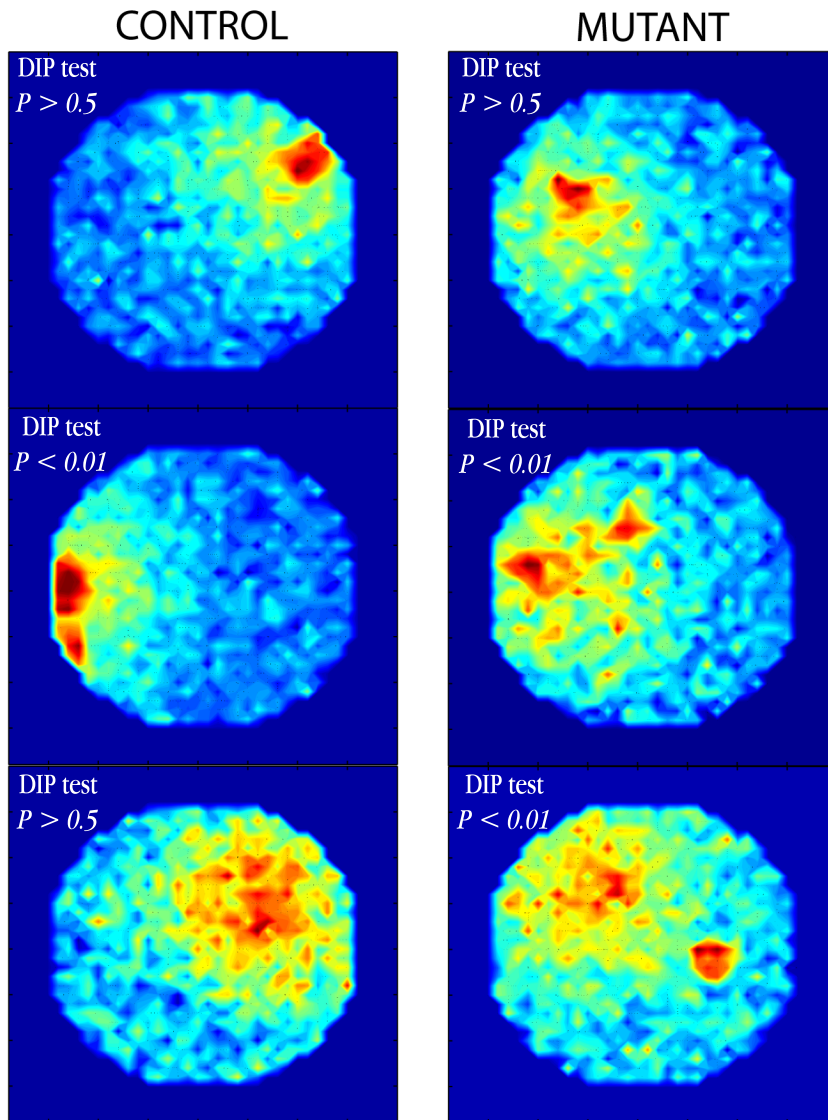


Figure 13.5: Samples of hippocampal simulated place fields recorded in the MWM. Sample of receptive field of three simulated place cells for a simulated control and mutant animal. The plots show the mean discharge of the neuron (red and blue denote peak and baseline firing rates, respectively) as a function of the animal position within the environment. Unimodality is accounted by a Hartigan DIP test ($P > 0.5$ indicates a unimodal receptive field, $P < 0.01$ indicates a multimodal receptive field).

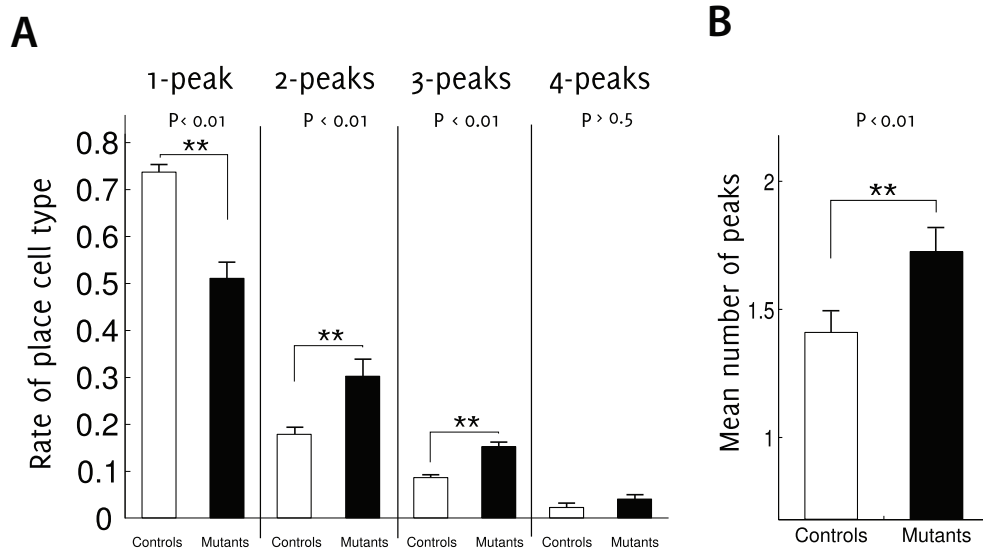


Figure 13.6: Quantification of uni-peak and multi-peaks simulated place cells **A**. Ratio between unimodal and multimodal place fields. **B**. Mean number of peaks per hippocampal place field.

mutants to inhibit their thigmotactic behavior. Thus, the observed intergroup difference in circling time indicates that mutants need significantly more time than controls to acquire an accurate spatial representation of the peripheral areas (dimension 1) of the environment. Finally, the occupancy grid plots of Figure 13.8 compare the searching behavior of controls and mutants qualitatively. They suggest that both simulated groups improve their spatial behavior through training and succeed in localizing and navigating to the platform from any starting location of the maze. Yet, consistently to the quantitative results of Figure 13.7, the simulated mutants exhibit a longer circling time and a wider spread in searching behavior than the simulated controls.

Altogether, these simulation results fully account for the navigation impairments of L7-PKCI in the MWM observed experimentally (Burguière et al., 2005). The mean intergroup differences in simulation and experiments are also consistent for all the measured behavioral parameters (escape latency: ANOVA, $F_{1,18} = 0.7535$, $P > 0.1$; heading: ANOVA, $F_{1,18} = 2.4892$, $P > 0.1$; ratio between time spent in the platform quadrant and trial duration: ANOVA, $F_{1,18} = 0.9144$, $P > 0.1$; distance to

the platform: ANOVA, $F_{1,18} = 0.7987, P > 0.1$; and circling: ANOVA, $F_{1,18} = 1.6411, P > 0.1$).

Finally, simulated mutants are not impaired in solving the Starmaze task compared to controls (Figs. 13.7G,H). There is no statistically significant intergroup difference in terms of mean escape latency (figure 13.7G, ANOVA, $F_{1,18} = 3.7960, P > 0.05$), mean distance swum to reach the platform (figure 13.7H, ANOVA, $F_{1,18} = 1.3031, P > 0.1$), and mean number of visited alleys (not shown, ANOVA, $F_{1,18} = 4.3505, P > 0.05$). These results are in agreement with experimental observations in the Starmaze (Burguière et al., 2005). However, in contrast to the interpretation drawn by Burguière et al. (2005), they point towards a slightly reduced declarative demand of the Starmaze task compared the MWM task (see Discussion, Sec. 14).

Cerebellar adaptation deficits impact the exploratory behavior of simulated L7-PKCI mice

The above results predict a behavioral incidence of suboptimal spatial coding capabilities of L7-PKCI mice. Here, we compare the exploratory behavior of simulated mutants and controls in the free exploration paradigm proposed by Fonio et al. (2009). This paradigm allows the exploration dynamics underlying latent spatial learning to be studied under reduced external constraints on the mouse's behavior (e.g. coercion by hunger, thirst, short session duration; Fonio et al., 2009).

We simulate a latent spatial learning task in a circular track (10 cm width) with no explicit goal. We let $n=15$ controls and $n=15$ mutants freely explore the maze from a fixed starting location (home base). During each trial, we sample the accuracy of the acquired hippocampal spatial code every 2' by quantifying the fraction of positions where self-localization error is less than a cutoff parameter (see Sec. 12.2 and Supporting Methods Sec. 15.2, for the definition of this measure, namely R , Eq. 15.22). Figure 13.9 compares the time necessary for the simulated controls and mutants to exhaustively explore the circular environment. This would correspond to the time necessary to exhaust dimension 1 (i.e. circling behavior) in Fonio et al. (2009), a necessary condition for the emergence of incursions into the center of an open-field environment (i.e. dimension 2). Our results show that both simulated animals significantly improve their hippocampal space code over time through a free exploratory behavior. Yet, the predicted declarative spatial learning deficit of simulated

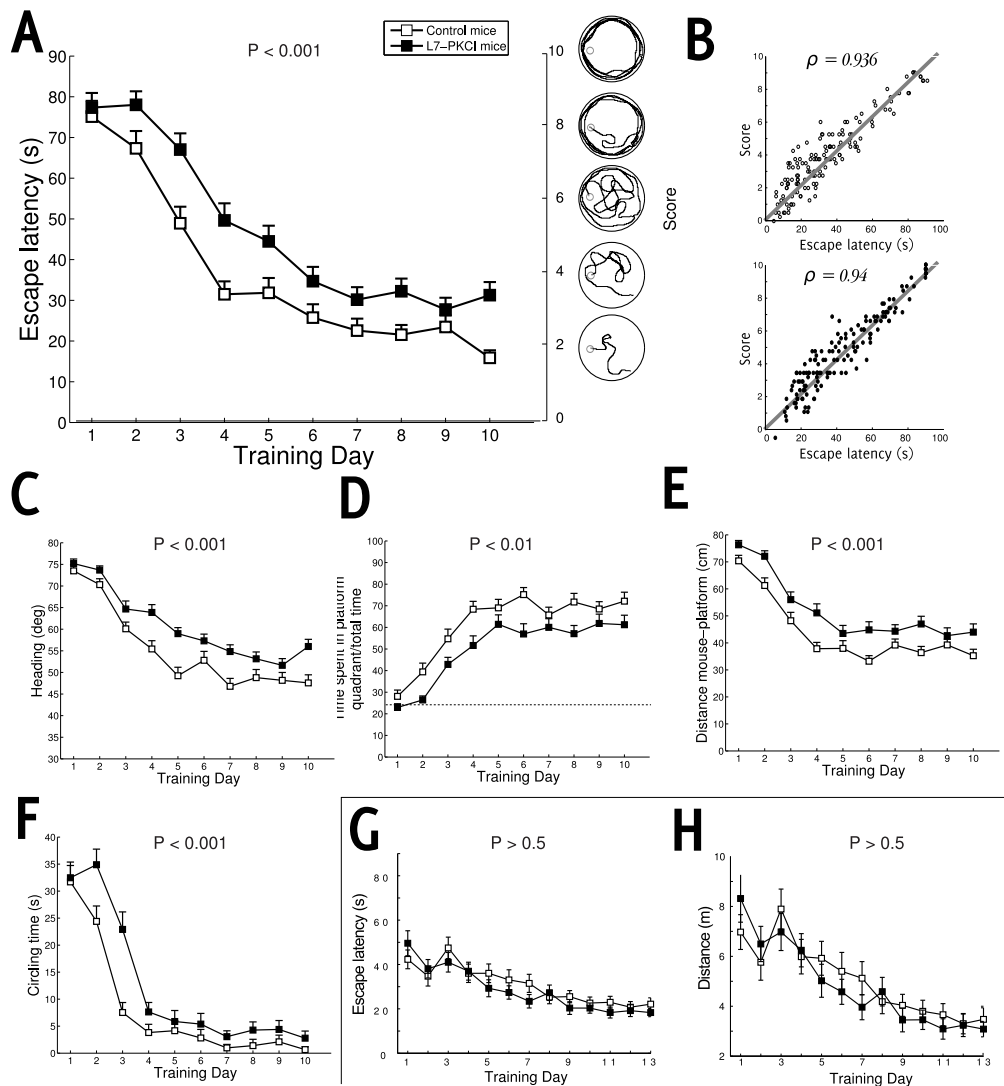


Figure 13.7: Results in the MWM (a-f) and in the Starmaze (g-h) under a declarative scenario **MWM:** **A.** Escape latency (left scale) and score (right scale) of simulated controls (white square) compared to mutants (black square). **B.** Correlation between the searching score and the escape latency for the simulated control (top) and mutant mice (bottom). **C.** Average angular deviation between ideal and actual trajectory to the goal **D.** Ratio of time spent in the platform quadrant over the total time of trial. **E.** Mean distance of the simulated mouse with the platform. **F.** Circling time. **Starmaze:** **G.** Mean number of alleys visited. **H.** Mean distance swum.

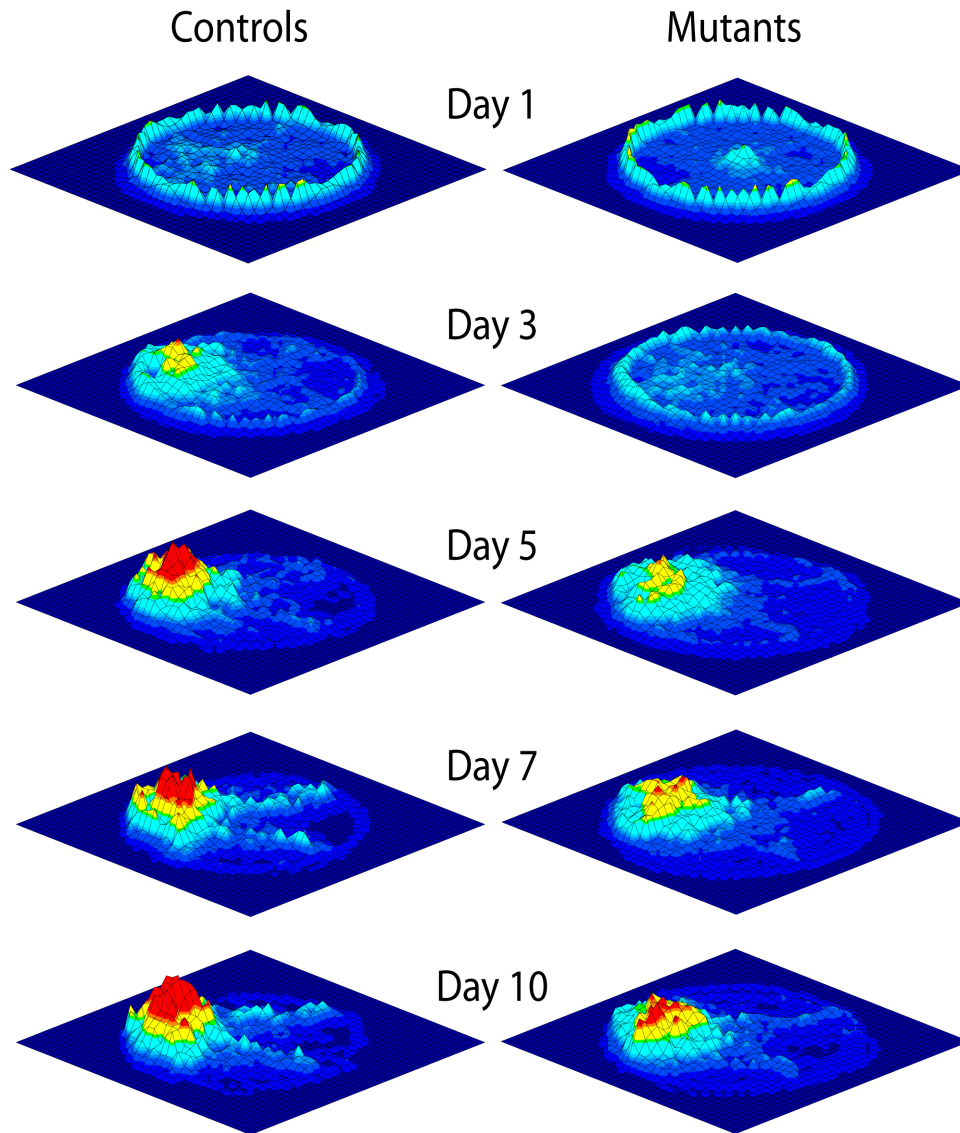


Figure 13.8: Occupancy map. Three-dimensional diagrams of the mean time spent by control and mutant mice at each location of the maze at different training phases. Qualitative representation of the time (z axis) spent on average by the two groups of animals in the different areas of the pool at different learning phases (days, 1, 3, 5, 7 and 10). These three dimensional plots show that, when solving the task, mutant mice tends to circle more than control (day 1 and 3) and had larger searching zone during the whole learning period.

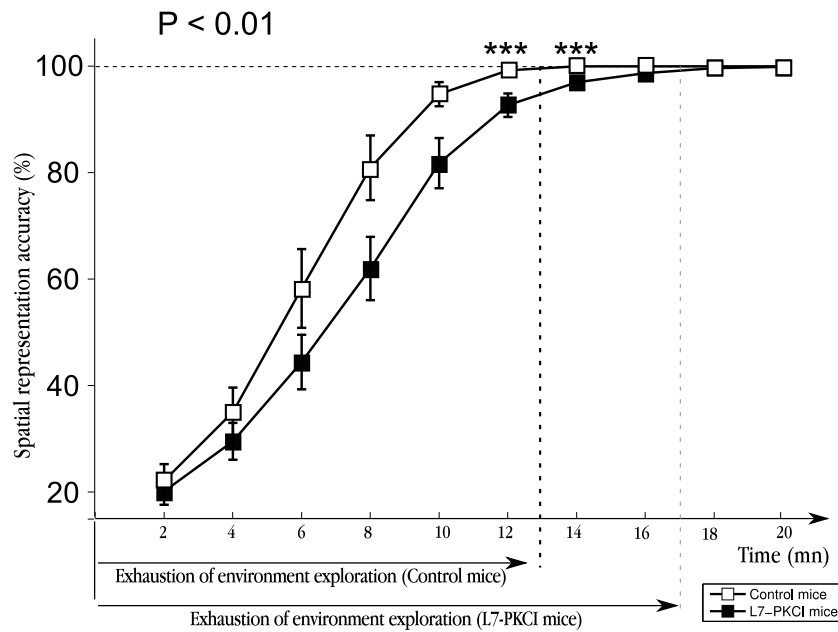


Figure 13.9: Time course of the spatial representation accuracy in a free-exploratory simulated task. Time necessary for simulated control animals (white) and a simulated mutant mice (black) to exhaustively explore the circular environment. Mutants need a significantly longer circling time than controls.

mutants (Figs. 13.9) makes them need a significantly longer circling time than controls (ANOVA, $F_{1,28} = 10.93$, $P < 0.01$). On average, the simulated controls exhaust dimension 1 within 15 – 35% less time than mutants (figure 13.9).

Chapter 14

Discussion

In this study, we examined the role of the cerebellum in navigation tasks by using a neurocomputational approach, bridging the gap between different levels of observation, from the discharge of neurons to the behavior of rodents. To the best of our knowledge, no theoretical study had addressed this question, and we are confident this methodology will help to get a comprehensive interpretation of different experimental findings. The rationale was therefore to complete these behavioral observations with quantitative accounts testing specific hypotheses on the link between synaptic plasticity mechanisms, cell discharge properties, interstructure coupling, and behavioral responses. The achievement of this work and related issues are discussed in this section. After a short summary of our contributions, we will review the biological and experimental evidence accounting for a cerebellar role in the integration of idiothetic cues. Then, we will address how our study could unify multiple experimental observations and we will conclude by presenting the possible future directions of research that arose from this work.

14.1 Contributions

In the presented study, we simulated a large-scale neural network accounting for the functional coupling between cerebellum and hippocampal formation. This framework is proposed to provide a comprehensive view of the role of the cerebellum in the multiple components and memory types associated with a spatial learning task.

We mainly focused on the behavioral genetic findings reported by Bur-

guière et al. (2005), which suggested that LTD at the parallel fiber-Purkinje cell synapses was a relevant mechanism for the adaptive tuning of navigation trajectories. We emulated the lack of LTD at PF–PC synapses of L7-PCKI transgenic mice. We simulated the experimental protocols employed by Burguière et al. (2005) to compare the learning performances of L7-PKCI mutants with those of control animals in two spatial navigation tasks: the Morris water maze and the Starmaze task. In both setups, mice had to swim from random departure locations to a platform hidden below the surface of opaque water. Both tasks required the declarative capability of building a spatial representation of the environment. Yet, in contrast to the Morris water maze task, the Starmaze alleys guided mice movements, which eventually reduced the low-level procedural demand of the task. Thus, the use of these two tasks made it possible to dissociate the relative importance of the declarative and procedural components of navigation.

First, we quantified the impact of a purely local motor adaptation deficit on the overall goal oriented behavior and we tested this hypothesis against empirical observations (Burguière et al. 2005).

On the one hand, the model reproduced some of the experimental findings obtained by Burguière et al. (2005) on the spatial learning impairments of L7-PKCI mice and corroborate the interpretation that cerebellar LTD plays a significant role in optimizing goal-directed trajectories through a continuous adaptation process that minimizes motor-command execution errors locally (Burguière et al., 2005).

On the other hand, because our modeling approach permitted to isolate the local procedural component of spatial cognition (we endowed control and mutant simulated mice with identical and effective declarative spatial learning), we provided a different interpretation of a part of the experimental data. Our findings suggested that a purely local procedural deficit could not explain *(i)* why real L7-PKCI mice exhibited coarser goal-searching behaviors than controls – i.e., they spent significantly less time within the target quadrant of the MWM and showed larger searching zones, *(ii)* the amplitude of differences of escape latency and heading between both population observed experimentally and *(iii)* why L7-PKCI mice tend to stay longer in peripheral areas compared to control animals.

Our results therefore suggested an implication of the cerebellum in higher-level (global) aspects of procedural spatial learning. In particular, our results showed that L7-PKCI mutants were likely to be impaired in trading-off the exploration-exploitation balance and inhibiting thigmo-

taxic (peripheral circling) behavior.

By modeling this deficit, our simulation results were consistent with the experimental data (Burguière et al., 2005), and they pointed towards the additive effect of a learning deficit in executing optimal goal-oriented behavior in mutants, paired with a suboptimal exploration behavior. It is important to note that adding a longer circling time to the purely local optimization of trajectories fails to account for all differences between L7-PKCI and control mice, as observed experimentally. Also, a small deficit in the exploration behavior of L7-PKCI mice does not statistically impair their performance in the Sarmaze compared to control animals, thus being consistent with experimental findings.

Second, we demonstrated that these two global procedural deficits may reflect the influence of the cerebellum in the integration of idiothetic cues — i.e. path integration or dead reckoning processes (Mittelstaedt and Mittelstaedt 1980; Etienne et al. 1998; Etienne and Jeffery 2004; McNaughton et al. 2006; Wiener et al. 2011) — and, consequently, an indirect implication of the cerebellum in the declarative spatial learning. By simulating the local procedural impairment and ineffective local estimations of the self-related movements in mutant animals, we reproduced all experimental data (Burguière et al., 2005). Our simulation results suggested that L7-PKCI mice could learn to locate the platform but did not encode information about their environment as efficiently as their control littermates.

In consequence, we propose a different interpretation of the observed deficit compared to Burguière et al. (2005), who considered that the declarative capabilities of L7-PKCI mice were not impaired. In their experimental work, the absence of a deficit in the Sarmaze — where the procedural demand is reduced — was considered as a proof of an intact declarative learning in L7-PKCI mice. We propose a different interpretation and suggest that declarative component could be affected in the MWM but not necessarily in the Sarmaze: in such environments where the movements are guided, the integration of the idiothetic information is facilitated. In simulation, we observed that simulated L7-PKCI mice do not present differences of performance compared to control animals.

We also characterized the encoding properties of hippocampal place cell activity as well as the functional time course of the learned place field representations. These analyses quantified the possible impact of cerebellar LTD deficits on the dynamics of hippocampal place coding. Our results showed that the spatial mapping rate in L7-PKCI animals is im-

paired compared to controls. They also suggested that the L7-PKCI hippocampal population code is less accurate—in terms of estimate of the location currently visited by the animal—than the one learned by control mice. A single unit analysis suggested an increased probability for L7-PKCI hippocampal place cells to exhibit multipeak receptive fields, which was likely to degrade the accuracy of the overall spatial representation. These results led to a series of predictions—at the level of both single unit and neural population activity. At the behavioral level, our results suggest that the predicted path integration deficit of L7-PKCI mice would lead to observable differences in the free exploration patterns of mutants and controls during latent spatial learning in open-field environments (Drai et al., 2001; Fonio et al., 2009).

14.2 Testable predictions emerging from the model

The results of this computational study lead to a set of predictions at multiple levels.

The first prediction addressed the neural activity of hippocampal place cells. We gave new insights on how a dysfunctional cerebellar plasticity could have an observable implication on the construction of the spatial map. We analyzed simulated place cells and we observed that the mean number of peaks was slightly higher in simulated mutants compared to simulated control animals. Consequently, we proposed that this discrepancy could be the main reason of a suboptimal population mutual information, a factor that would influence the quality of the spatial representation.

A way to experimentally test this prediction at the cellular level is to perform electrophysiological recordings of pyramidal cells in the hippocampal formation (CA1-CA3 place cells and entorhinal grid cells) from control and L7-PKCI mice in an open maze environment. In order to reinforce the need of idiothetic navigation, the maze should be sufficiently wide and circular, with no cues inside the maze that could help the animal to locate itself. Also, the experimentation should be realized in dim light.

The second prediction comes from the behavioral incidence of a suboptimal encoding of declarative memories. It focuses on the exploratory behavior of mutant mice compared to control animals in the protocol used

by Fonio et al. (2009). We propose to test mutants and controls in the same type of long lasting free exploration paradigm. In comparison to other paradigms performed in open field areas (such as the MWM), this protocol gives the experimentalist the opportunity to analyze the dynamics of occupancy without any other constraints imposed by the conditions of the experiment. The representation of this dynamic is well suited to point out differences between the exploratory behavior of the L7-PKCI and control groups, and define the cerebellar processes that could be responsible for them.

Our model suggests observable behavioral differences between L7-PKCI and their control litter-mates due to local procedural problems and a deficiency in integrating idiothetic movements. We predict that the duration of the first stage during which an animal explores the first dimension of a new environment (i.e. adopting a circling behavior, Fonio et al., 2009) should be extended for L7-PKCI mice compared to control animals. We expect to have significant differences when idiothetic cues are the main source of information for the animal (e.g. in the dark), while the discrepancy between both population should be lowered when allothetic information is predominant. If this prediction is validated by the experimental work proposed here, this would also demonstrate that a procedural learning could be influenced by the delay of formation of a coherent declarative representation. Our simulation results suggest that control should start to make incursion in the center of the environment in advance compared to mutants, and would exhibit a thigmotaxic behavior 15 to 35 % less.

14.3 The cerebellum and path integration

The simulated cerebellum was assumed to be implicated in predicting the consequences of movements by integrating idiothetic cues and receiving an efference copy of the motor command (Ito, 1970). By extension, it was supposed to play a role in the path integration system by sending predictive deviation to the simulated entorhinal grid cells.

If this holds true, cerebellar processing would influence the construction of an abstract representation of the environment, and a deteriorated sensorimotor association learned at the cerebellar level would delay the formation of a coherent declarative memory in the hippocampus. In turn, this would lead to longer exploration phases in mutants compared to con-

trols, and extend the thigmotaxic behavior of mutants at the beginning of learning, as suggested by Fonio et al. (2009).

It is largely accepted that the hippocampal formation can encode spatial locations by using the integration of self-motion related information without the need of external cues (McNaughton et al., 2006). This idiothetic information refers to proprioceptive, vestibular and optic flow signals as well as the motor efference copy (Arleo and Rondi-Reig, 2007). All types of signals are combined to determine the motion of the body and permit to integrate path linearly (Etienne and Jeffery, 2004; McNaughton et al., 2006). Theoretical and experimental findings have revealed that the medial entorhinal cortex might perform some of the essential neural computations underlying the path integrator and drive spatial firing patterns of place cells in the hippocampus (McNaughton et al., 2006). The idea of a role of the cerebellum in spatial orientation of rodents has already been proposed in the 1980s (e.g., Lalonde, 1987; Lalonde et al., 1988; Dahanoui et al., 1992a) and more recently, it has been shown that cerebellar lurcher mice showed some ineffective idiothetic navigation compare to wild type (Korelusova et al., 2007), thus giving the cerebellum a plausible role in building a coherent representation of the environment by using self-motion related signals.

Anatomofunctional evidence. Anatomical cues also suggest such a role of the cerebellum in integrating idiothetic signals. First, vestibular, proprioceptive and visual inputs are known to be implicated in cerebellar computations. The flocculonodular lobe (the vestibulocerebellum) has primary connections with the vestibular nuclei (Kotchabhakdi and Walberg, 1978; Compoin et al., 1997), and also receives visual inputs. The vestibulo-cerebellar tract carries information from the semi-circular canals of the inner ear to the cerebellum via the vestibular nucleus located in the lower pons and medulla. In addition, the reticulo-cerebellar tract conveys signals received by the reticular nuclei in various parts of the brain stem from the cortex, spinal cord, vestibular system and red nucleus. Then, the medial zone of the anterior and posterior lobes (which constitutes the spinocerebellum or paleocerebellum) receives proprioceptive inputs from the dorsal columns of the spinal cord and from the trigeminal nerve (Bosco and Poppele, 2001), as well as from visual and auditory systems (Ghez and Thach, 2000). It sends fibers to deep cerebellar nuclei that, in turn, project to both the cerebral cortex and the brain stem, thus providing modulation

of descending motor systems. The cerebellum is likely to encode dynamics of body limbs by using this idiothetic information and an efference copy of the motor command ¹. The cerebellum is strongly assumed to provide estimations of future state of the limbs by using this efference copy (Ito, 2005; Pasalar et al., 2006; Shadmehr et al., 2010). By extending this theory, it is likely that the cerebellum could provide estimation of the future state of the whole body (position, orientation, speed) to refine the estimation based on sensory feedback signals.

Experimental evidence. This hypothesis is also in agreement with recent experimental findings on monkeys demonstrating that the cerebellar circuit is implicated in acquiring and processing information necessary for spatial orientation and self-motion perception (Shaikh et al., 2004; Yakusheva et al., 2007; Angelaki et al., 2010).

Shaikh et al. (2004) proposed that a role of the cerebellum in spatial orientation could be to transform motion related signals in different reference frames usable to encode body motion. The authors demonstrated that activities of motion-sensitive neurons in the rostral fastigial nucleus have a distributed representation in different reference frames, whereas cells in the vestibular nuclei were primarily encoding motion in an egocentric reference frame. These results suggest that the cerebellum transforms body coordinates in different reference frames that might be usable to encode the body motion.

In a more recent study, Yakusheva et al. (2007) made a similar observation and showed that cerebellar cortical neuron activity in nodulus and uvula (lobules X and IX of the vermis) reflects the critical computations of transforming head-centered (egocentric) vestibular afferent information into world-centered (allocentric) self-motion and spatial orientation signals. More precisely, the authors showed that Purkinje cells of these areas encode inertial motion. The Purkinje cells in the nodulus and uvula appear to carry the world-horizontal component of a spatially transformed and temporally integrated rotation signals. This transformation appears critical for extracting the inertial linear accelerations during navigation, and thus providing the information to brain areas involved in the reten-

¹When a motor command is sent from the cortex to the lower motor neurons in the brain stem and spinal cord, a copy of this message is also sent to the cerebellum through the cortico-pontine-cerebellar tract (Ghez and Thach, 2000).

tion of spatial memories (Yakusheva et al., 2007; Angelaki et al., 2010).

In a distinct behavioral experiment, Korelusova et al. (2007) observed that in a group of Lurchers mice (suffering from a loss of Purkinje cells and a decreased number of granule cells and inferior olive neurons), the subjects which also presented a retinal degeneration were not able to use idiothetic navigation to solve a spatial orientation task. These results suggested that Lurchers animals can not integrate self-motion information, and thus reinforce the plausibility of our hypothesis.

14.4 Unifying multiple experimental observations

Consistent with the observations we made in our neurocomputational framework, most of the studies related to the role of the cerebellum in spatial cognition concluded on a cerebellar influence on the exploration behavior of rodents (Lalonde and Botez, 1986; Lalonde, 1987; Lalonde et al., 1988; Petrosini et al., 1996; Hilber et al., 1998; Leggio et al., 1999; Mandolesi et al., 2001, 2003; Rondi-Reig et al., 2002; Burguière et al., 2005; Korelusova et al., 2007).

Cerebellum and exploration behavior. The first indications of a role of the cerebellum in the navigational behavior have been proposed by Lalonde and Botez (1986); Lalonde (1987); Lalonde et al. (1988) who studied the navigation abilities of mutant weaver, staggerer and lurcher mice in comparison to control animals. The three types of mutants respectively had a selective degeneration of cerebellar granule cells; lose cerebellar Purkinje cells, granules cells and inferior olive neurons; and presented a degeneration of the olivo-cerebellar system. It was observed that all of them had deficits in the acquisition of maze learning, with different degrees of severity. Although procedural memory was suggested to be affected primarily (a simple stimulus association response was longer to be learned in lurcher mice Lalonde et al., 1988), these experiments failed to dissociate the relative importance of procedural and declarative memories in the observed deficits. Also, the cerebellar ataxia produced by such mutations and the subsequent visuo-motor deficits (lurcher mutants had difficulties in guiding themselves in the water toward a visible goal, see

Lalonde et al., 1988) made difficult the interpretation of the procedural components that might be affected by cerebellar learning. In the light of our results, we suggest that weaver, staggerer and lurcher mice may have developed local and global procedural impairments. Also, depending on the complexity of the task, mice could have suffered from a delay in the establishment of declarative memories compared to control animals. This would also explain the deficit observed experimentally in maze learning with staggerer mice (Lalonde, 1987).

Cerebellum and procedural learning. More recent studies using hemicerebellectomized (HCbed) rats also demonstrated that cerebellar specific lesions impaired the development of efficient exploration strategies. It therefore suggested that the cerebellum was more implicated in local and global component of procedural memories, that is respectively (i) a local optimization of the trajectory and (ii) the efficient learning and use of general procedures for optimally solving a spatial task (Leggio et al., 1999).

Leggio et al. (1999); Mandolesi et al. (2001); Foti et al. (2010) suggested that cerebellar networks might be involved in the acquisition of all procedural components necessary for an optimal behavior (Leggio et al., 1999), and in acquiring new behaviors and modifying them in relation to the context (Mandolesi et al., 2001). The influence of cerebellar lesions on the exploration of environments was also studied in different spatial distributions of multiple rewards. In all configurations, lesioned animals had their exploration behavior affected, suggesting that all components of the procedural memory were disturbed (Foti et al., 2010). These results are also consistent with the conclusion drawn by our neurocomputational study, proposing that both local and global components of spatial cognition should be influenced by cerebellar processing. However, the lack of flexibility in changing behaviors observed in HCbed rats (Leggio et al., 1999; Mandolesi et al., 2001) was not addressed by our study and will be discussed within the limits of our approach.

Cerebellum and declarative learning. It has been observed that HCbed rats succeeded in finding the platform even in a pure place paradigm (Petrosini et al., 1996). This result has often been considered as a line of evidence that cerebellum was not involved in building spatial maps (Leggio

et al., 1999; Mandolesi et al., 2001, 2003). However, it has been observed that this ability was acquired at a level significantly lower than controls (e.g., Petrosini et al., 1996). We suggest that an affected idiothetic navigation might account — in addition with local procedural impairment — for such a delay in the ability to learn the spatial map. We propose that the declarative impairment might only slightly affect rodents in tasks where idiothetic and allothetic information is available, but could be accentuated in tasks where self-position related signals are the main source of information, or in paradigms where both type of signals are conflicting. In the same direction, we also suggest that paradigms that reduce the procedural demand consequently facilitate declarative learning by simplifying the integration of idiothetic cues. Therefore, such environments should be used with caution when exploring small impairments in the formation of declarative memories.

Interaction between procedural and declarative learning. In another study, Mandolesi et al. (2003) analyzed the relationship between procedural and declarative spatial knowledge. Using HCbed rats, the authors pointed out that no declarative learning was possible without an appropriate procedural spatial learning: HCbed rats were not able to represent a new environment because they were not able to explore it appropriately (Mandolesi et al., 2003). Although this observation seems reasonable, we would like to call attention to a possible reverse interaction between procedural and declarative memories supported by data demonstrating the emergence of a stereotyped exploration behaviors in freely moving animals (Fonio et al., 2009). In the light of our results, we suggest that rodents could not appropriately explore the environment, unless they can efficiently represent the emerging dimensions of this environment. In the experimental observations drawn by Burguière et al. (2005), this is illustrated by longer thigmotaxic time for mutants compared to controls. In our neurocomputational framework, we advance that this difference can be understood thanks to the proposed interaction between declarative and procedural memories, suggesting that the inhibition of a circling behavior will be favored by a better knowledge of the near-wall portions of the environment. We therefore extend the observation made by Mandolesi et al. (2003), and propose that a deficit in procedural components when performing a navigation task should be taken carefully and would sometimes need to be discussed in term of a possible influence of the declarative

learning on procedural memories.

Sensorimotor associations in spatial tasks. More recently, Burguière et al. (2010) proposed that mutants L7-PKCI mice were able to acquire the stimulus-response associations, but exhibited a reduced optimization of their motor performances. They suggested that a LTD at PF-PC synapses was required for optimization of motor responses but not for learning a stimulus-response association. This result evokes the differential role of the cerebellar cortex and deep cerebellar nuclei in simple motor learning paradigms, such as eyeblink conditioning (Ito, 2006). In this task, it has been demonstrated that cerebellar cortex might not be essential for learning the eyeblink conditional response, but could have a significant contribution in expressing it optimally, notably in finely tuning the time response (Attwell et al., 2001). Similar conclusions could be drawn in stimulus-response associative learning performed in a spatial task. In such a task, the conditional response would be correctly learned, but the optimization of the response — illustrated by the trajectory of the animal — would not be optimal.

14.5 Limitations and future works

Role of cerebellar LTD. In our model, both LTD and LTP at PF-PC synapses allow the simulated cerebellar microcomplex to adapt and learn new sensorimotor associations.

The role of the cerebellar LTD in procedural learning has already been proposed to be required for cerebellar motor learning. For example, Ito (1998) has shown that in VOR adaptation, PF-PC LTD is likely to constitute the neural substrate of such an error-driven motor learning process (Ito, 1998). The hypothesis of a role of PF-PC LTD in the procedural component of navigation was derived from these results, since trajectories performed by the animal must be adapted to the spatial context, and optimized to reach optimally the goal. However, a recent reevaluation of the role of PF-PC LTD in cerebellar learning suggests that this synaptic plasticity would not be essential for motor learning (Schonewille et al., 2011). The authors showed that in different cerebellar coordination tasks, there isn't any visible motor learning impairment for three different types of mutant mice lacking PF-PC LTD. Alternatively, homosynaptic LTP at PF-PC synapses

has been recently shown to be critical. Schonewille et al. (2010b) observed that mutants mice for which long-term potentiation in Purkinje cells was abolished showed impaired adaptations in motor learnings such as the vestibulo-ocular reflex and the classical delay conditioning of the eyeblink response.

First, it should be observed that if LTD does not appear to be necessary for simple motor learning such as VOR and eyeblink conditioning, it is still unclear to what extent this result could be generalized for sensorimotor associative learning involved in spatial cognitive tasks. Second, as remarked by Schonewille et al. (2011), it is not excluded that other compensatory plasticity mechanisms could take over a deficient LTD at PF-PC synapses. Third, if LTD was demonstrated to have no functional implications in adaptation, the role of the cerebellum in building internal models would still be likely valid, although the mechanisms for an adaptation would need to be redefined. In other words, the results drawn by our model would still be pertinent.

Nevertheless, these recent reevaluation of LTD and LTP confirms the importance to include other plasticity sites in an extension of the presented model. Doing so, we could address their possible functions in motor and spatial learnings.

Other plausible functions of the cerebellum in navigation tasks. If the computational framework presented in this study gives a better understanding of the function of the cerebellum in navigation, some of the existing experimental data would need further developments to be consistently explained by the model.

First, a few findings suggest that the cerebellum might be implied in storing declarative spatial information (Hilber et al., 1998; Dahhaoui et al., 1992b), which was not addressed by our model. Hilber et al. (1998) observed that the cerebellum, although not necessary for learning a spatial task, plays a crucial role in its retention in mutant lurcher mice. The same conclusion was drawn by Dahhaoui et al. (1992b) who demonstrated that lesions of the afferent climbing fibers to the cerebellar cortex altered learning and retention of a spatial task.

Furthermore, our model does not take into account motivational and attentional aspects, which are likely to play a role in spatial cognition and to be impacted in cerebellar rodents (Marec et al., 1997; Caston et al., 1998). Caston et al. (1998) observed that lurcher mutant mice exhibit a

low level of exploration in part due to a decreased motivation to explore a novel environment. Marec et al. (1997) showed that rats with a cerebellar cortex made partially agranular, tended to develop an avoidance behavior. The authors proposed that the cerebellum could be hence linked to a decrease of anxiety, a lack of behavioral inhibition and/or attentional deficits. These aspects have not been addressed by our neurocomputational study since the main focus was to highlight potential procedural and declarative learning influenced by cerebellar processes.

Third, Leggio et al. (1999); Mandolesi et al. (2001) observed that HCbed animals present a lack of flexibility in changing exploration strategies. Lesioned rats showed a severe perseverative tendencies, which dramatically worsen their performances when the context of the experimentation was changed (Mandolesi et al., 2001; Foti et al., 2010). This absence of flexibility — in the use of procedures — could be addressed by studying the interaction of the cerebellum with areas known to be involved in working memory (e.g., the prefrontal cortex; Martinet et al., 2011).

Finally, recent data on sequential learning and navigation tasks indicated that the cerebellum seems to be involved in the automation of procedural rules related to a specific sequence of correct choices in a spatial task (Mandolesi et al., 2010). The authors proposed that the delay in sequential learning observed in the presence of a cerebellar lesion could be mainly related to a delay of the automation of the response. Such sequential learning might be of main importance in navigation behaviors and could be further investigated by using our neural architecture.

Chapter 15

Supplementary Methods

15.1 Cerebellar microcomplex model

Circuit model

The cerebellar microcomplex model (figure 11.2B in the main text) captures the main processing stages and connectivity layout (e.g. convergence/divergence ratios) of its biological counterpart (see Ito, 2006 for a recent review). In the model, the mossy fibers (MF) layer consists of 100 cells' axons. MFs activate a population of 10^4 granule cells (GCs), which produce a sparse representation of the input state space. Each MF is connected to a GC with a probability $P_{MF-GC} = 0.04$. Thus, each GC receives an average 4 MF inputs and each MF projects onto approximately 400 GCs. GCs activate in turn a population of 200 Purkinje Cells (PCs). Each GC can create a connection to a PC with a probability $P_{GC-PC} = 0.75$. Thus, each PC can receive about 7500 input connections from parallel fibers (PFs), i.e. the GCs' axons. MFs also excite a population of 100 neurons in the deep cerebellar nuclei (DCN) layer according to an all-to-all connection layout ($P_{MF-DCN} = 1$). The discharge of each DCN unit is also modulated by the inhibitory action of 2 afferent PCs. DCN activity constitutes the output of the cerebellar microcomplex model. A bidirectional long-term plasticity rule modifies the strength of PF-PC synapses, changing the input-output relationship of the circuit. Learning is primarily determined by the activity of a population of 400 inferior olive (IO) neurons, whose axons (climbing fibers) project onto PCs (1:1 connection scheme). Our highly simplified microcomplex model does not account for cerebel-

lar interneurons, i.e. Golgi, Stellate and Basket cells. These neurons are likely to be involved in denoising neurotransmission in the cerebellum (Hirano et al., 2002), conveying timing information (Desmond and Moore, 1988; Yamazaki and Tanaka, 2007; D’Angelo and De Zeeuw, 2009), and providing the biological substrate for the implementation of covariance-based learning rule (Sejnowski, 1977; Dean et al., 2010).

As mentioned in the main text, we employ multiple instances of the same microcomplex model to learn both inverse corrector models and forward predictor models. The former map desired positions onto motor commands correcting local drifts in swimming trajectories. The latter predict next egocentric translations and orientations based on current motor commands. Simulated mouse locomotion results from the differential contribution of two velocities $v_l(t)$ and $v_r(t)$ corresponding to left and right fore-and-hind paws, respectively. The cerebellar architecture includes:

- Four microcomplexes implementing inverse corrector models. Two of them learn to correct errors in the positive and negative ranges of left paw velocities, $v_l^+(t)$ and $v_l^-(t)$, respectively. The other two correct errors in the positive and negative ranges of right paw velocities, $v_r^+(t)$ and $v_r^-(t)$, respectively.
- Two microcomplexes implementing forward models. The first learns to predict the distance $d(t + \Delta t)$ traveled by the animal based on current motor velocity commands. The second learns to predict the next angular deviation $\theta(t + \Delta t)$.

15.1.1 Neuronal models

We model each mossy fiber (MF) as the axon of a leaky integrate-and-fire neuron whose membrane potential $V(t)$ dynamics is defined as:

$$C \frac{dV(t)}{dt} = g_{leak} (V_{leak} - V(t)) - I(t) \quad (15.1)$$

where C denotes the membrane capacitance and g_{leak} the leak membrane conductance —i.e. $\tau = C/g_{leak}$ is the membrane time constant; V_{leak} is the resting membrane potential, and $I(t)$ the total synaptic drive. Whenever the membrane potential reaches a threshold V_{th} the neuron emits a spike. We used a time step $dt = 1$ ms for numerical integration.

Granule cells (GCs), Purkinje cells (PCs) and deep cerebellar nuclei (DCN) neurons are conductance based leaky integrate-and-fire units (similar to Carrillo et al., 2008) described by the following equation:

$$C \frac{dV(t)}{dt} = g_{leak}(t)(V_{leak} - V(t)) + g_{exc}(t)(V_{exc} - V(t)) + g_{inh}(t)(V_{inh} - V(t)) \quad (15.2)$$

where the membrane potential $V(t)$ depends on an excitatory synaptic conductance g_{exc} , an inhibitory conductance g_{inh} , and a leaky conductance g_{leak} . V_{leak} , V_{exc} , and V_{inh} are the corresponding resting potentials. Again, when $V(t)$ reaches a threshold V_{th} the cell emits a spike. All active conductances $g_{leak}(t)$, $g_{exc}(t)$, $g_{inh}(t)$ vary according to:

$$g(t) = \bar{g} \sum_j W_j \int_{-\infty}^t \exp\left(-\frac{t-t'}{\tau_c}\right) \delta(t-t') dt \quad (15.3)$$

where \bar{g}_c is the maximal conductance, $W_j \in [0, 1]$ is the efficacy of the projection from presynaptic neuron j , τ_c is the synaptic time constant, t' is the time of a presynaptic spike, and $\delta(t-t')$ is a Dirac function equal to 1 only when the presynaptic neuron emits a spike at time t' .

In the model, a discrete homogeneous Poisson spike-train generator produces the irregular discharge of inferior olive (IO) neurons. At each time step $dt = 1$ ms, we approximate the probability of emitting an IO spike as $P(1 \text{ spike during } dt) \approx r(t) \cdot dt$, with $r(t)$ denoting the mean firing rate. Let $\eta(t)$ be a random number uniformly distributed between 0 and 1. At each time interval dt , an IO cell discharges if-and-only-if:

$$\eta(t) \leq r(t) \cdot dt \quad (15.4)$$

As aforementioned, error-related information modulates the firing rate $r(t)$, allowing IO activity to signal timed information about instantaneous error (Schweighofer et al., 2004).

Table 15.1 provides the parameter settings for all neuronal models used in our simulations.

15.1.2 Encoding MF cerebellar inputs

Mossy fibers (MFs) constitute the main input stage of the cerebellar micro-complex (Eccles et al., 1967). In the model, they carry information about motor commands and desired future states (egocentric positions). In both

Neuronal parameters		DCN	GR	PC	MF
V_{th}	mV	-60	-60	-60	-60
C	pF	2	2	2	2
g_{leak}	nS	2	2	2	2
V_{leak}	mV	-70	-70	-70	-70
g_{exc}	nS	0.1	0.2	60	-
V_{exc}	mV	0	0	0	-
g_{inh}	nS	2	-	-	-
V_{inh}	mV	-80	-80	-80	-
τ_{leak}	ms	20	20	20	20
τ_{exc}	ms	0.5	0.5	0.5	-
τ_{inh}	ms	10	-	-	-

Plasticity parameters		
Model	LTD (β)	LTP (α)
Forward	-0.5	1
Inverse	-0.025	0.1

Table 15.1: Parameter settings for neuronal and plasticity models.

inverse and forward cerebellar models, a family of radial basis functions spans the input state space uniformly and generates the input currents $I(t)$ of MFs neurons (Eq. 15.1):

$$I(t) = \gamma + \exp\left(-\frac{(x(t) - \mu)^2}{2\sigma^2}\right) \quad (15.5)$$

where μ and σ^2 are the center and the variance of the radial basis kernel associated to the MF neuron, respectively. In our simulations, the variance parameter ensures a small overlap of MF responses, the γ constant factor endows MF neurons with intrinsic spontaneous activity of about 5 Hz, and the parameters regulating the discharge of MFs limit their activity to 50 Hz.

15.1.3 Decoding cerebellar outputs

Model deep cerebellar nuclei (DCN) provide the main cerebellar output. For the four inverse corrector models, the decoding of DCN activity must produce motor command adjustments —i.e. $\Delta v_r^+(t)$, $\Delta v_r^-(t)$, $\Delta v_l^+(t)$, $\Delta v_l^-(t)$. For the two forward predictor models, the decoding of DCN activity must produce next state estimates —i.e. $\hat{d}(t + \Delta t)$ and $\hat{\theta}(t + \Delta t)$, with $\Delta t = 200$ ms.

Decoding DCN activity in inverse corrector models. For each of the four inverse models, a an average decoding scheme maps DCN outputs into a velocity adjustment signal. For instance, as shown in figure 15.1, for the microcomplex correcting positive right paw velocities, we take:

$$\Delta v_r^+(t) = \frac{A}{v_{max}} \cdot \left\langle v_i(t) \right\rangle_{i \in DCN} \quad (15.6)$$

where $v_i(t)$ denotes the instantaneous spike frequency of a DCN neuron i , calculated by averaging over a rectangular sliding window of 50 ms; the normalization term $v_{max} = 200$ Hz is the maximum spike frequency of model DCN cells; the scaling factor A determines the maximum correction amplitude. Similarly, the output the microcomplex devoted to negative right velocities produces a decoded signal $\Delta v_r^-(t)$. Then, the overall correction for the right fore-and-hind paws is simply:

$$\Delta v_r(t) = \Delta v_r^+(t) + \Delta v_r^-(t). \quad (15.7)$$

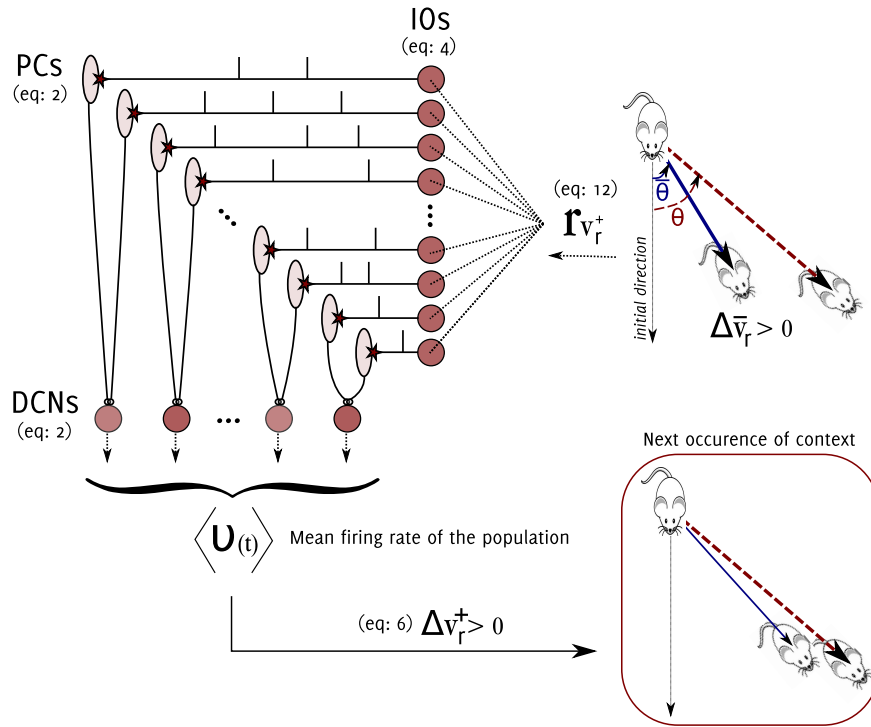


Figure 15.1: Coding scheme of the inverse corrector model. Example of error encoding and output decoding for the positive correction of the right paw. The color opacity gives a visual indication of the activity of cells, and the equations to transform analog signals into currents/spiking activity (and vice-versa) are numbered in reference to the equations of this manuscript.

A similar decoding scheme maps the outputs of the two microcomplexes correcting left fore-and-hind paw velocities into a signal $\Delta v_l(t)$.

Decoding DNC activity in forward predictor models. As shown in figure 15.2, a population decoding scheme computes the predictions $\hat{d}(t + \Delta t)$ and $\hat{\theta}(t + \Delta t)$ based on the DNC activities of the two forward models, respectively:

$$\hat{d}(t + \Delta t) = \frac{\sum_i v_i(t) \cdot d_i}{\sum_i v_i(t)} \quad (15.8)$$

$$\hat{\theta}(t + \Delta t) = \frac{\sum_i v_i(t) \cdot \theta_i}{\sum_i v_i(t)} \quad (15.9)$$

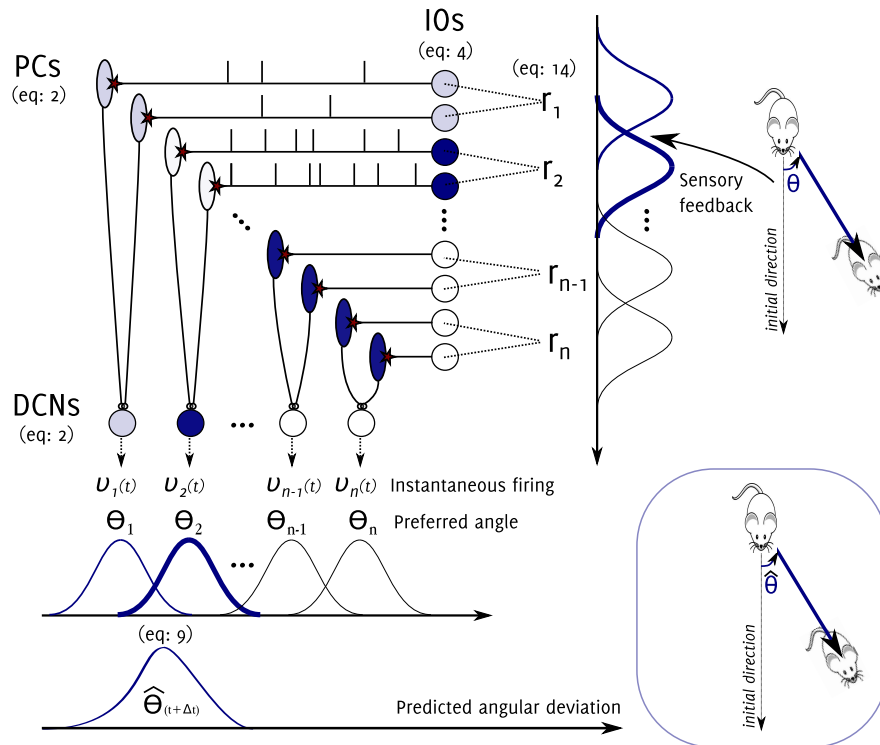


Figure 15.2: Coding scheme of the forward predictive model. Example of error encoding and output decoding for the angular position of the simulated mouse. The color opacity gives a visual indication of the activity of the cells, and the equations to transform analog signals into currents/spiking activity (and vice-versa) are numbered in reference to the equations of this manuscript.

where $v_i(t)$ indicates again the instantaneous spike frequency of a DCN neuron i , whereas d_i denotes the preferred distance encoded by a DCN neuron i in the first forward model and θ_i denotes the preferred angular displacement of a DCN neuron i in the second forward model —positive angles are defined counterclockwise. Both preferred distance and angle values are evenly distributed over the output space (figure. 15.2).

15.1.4 Synaptic efficacy and plasticity rules

In the model, most connections of the microcomplex circuit are non plastic, except for parallel fiber–Purkinje cell (PF–PC) synapses —although other plasticity sites of the real cerebellar microcomplex have been reported

(Hansel et al., 2001; Boyden et al., 2004; De Zeeuw and Yeo, 2005; Pugh and Raman, 2009). Non-plastic synaptic weights are tuned to generate mean firing rates consistent with experimental data. Recent GC *in vivo* recording experiments (Chadderton et al., 2004; Jörntell and Ekerot, 2006; a Rancz et al., 2007; Arenz et al., 2008) have reported that joint-related movement inputs generate sustained GC activity at a frequency of about 150 Hz (Chadderton et al., 2004). Also, it is admitted that two or more input spikes from MF afferents are necessary to elicit one GC burst of spikes (Chadderton et al., 2004). We tuned GC neuronal parameters and MF–GC synaptic weights in order to fit these data. The model does not account for the very high transient GC activity induced by other types of sensory modalities. Model PC simple spikes occur at rates ≤ 150 Hz (Raman and Bean, 1999) when PC are activated by parallel fibers. PC complex spikes, caused by a single discharge of the afferent climbing fiber, correspond to learning triggering events—we do not simulate high frequency components of the bursts. Finally, DCN neurons have mean firing rates of about 20 Hz (Lamont, 2009). Since this average activity occurs while PCs send inhibitory signals to DCN cells, we assume that, in the absence of PC activity, DCN can have a stronger activity upper-bounded by 200 Hz.

Model PF–PC synapses undergo bidirectional long-term plasticity, i.e. both potentiation, LTP, and depression, LTD. We implement LTP as a non-associative weight increase triggered by each GC spike, consistent with the homosynaptic rule describe by Lev-Ram et al. (2002). The synaptic weight W_{PF-PC} of each PF–PC connection increases according to:

$$\Delta W_{PF-PC}(t) = \alpha \cdot \delta(t - t_{GC}) \quad (15.10)$$

where α denotes a gain factor and the delta function is $\delta > 0$ only when the presynaptic GC emits a spike at time t_{GC} .

We simulate LTD at PF–PC synapses as an associative weight decrease triggered by a spike from the IO. This principle is in agreement with the heterosynaptic plasticity mechanism described by Ito and Kano (1982). The weight W_{PF-PC} of each PF–PC synapse decreases as:

$$\Delta W_{PF-PC}(t) = -\beta \cdot \int_{-\infty}^{t_{IO}} f(t - t_{IO}) \delta(t - t_{GC}) dt \quad (15.11)$$

where β is a gain factor, and the temporal kernel function f correlates each IO spike with the past discharge of a GC (Carrillo et al., 2008). In the model, the largest LTD amplitude occurs when the PC receives an IO spike

approximately 100 *ms* after an input spike from a GC, consistent with Safo and Regehr (2008).

Table 15.1 provides the parameter settings for the implemented plasticity models.

15.1.5 Encoding of error/teaching signals

In both inverse corrector and forward internal models IO neurons convey error/teaching signals via the climbing fibers that target PCs and mediate LTD at PF–PC synapses.

Teaching signal for the inverse corrector model. For the four inverse models, error signals must account for discrepancies between desired and executed motor commands. After the execution of each movement, we compute the translational error $\varepsilon_d = d(t) - \bar{d}(t)$ and the angular error $\varepsilon_\theta = \theta(t) - \bar{\theta}(t)$, where d and \bar{d} (θ and $\bar{\theta}$) indicate desired and actual traveled distances (angular displacements), respectively. The error signals ε_d and ε_θ allow the direction of change of left and right paw velocities to be inferred:

$$\begin{aligned} \varepsilon_d > 0, \varepsilon_\theta > 0 &\implies v_r > \bar{v}_r \implies \Delta\bar{v}_r > 0 \\ \varepsilon_d < 0, \varepsilon_\theta < 0 &\implies v_r < \bar{v}_r \implies \Delta\bar{v}_r < 0 \\ \varepsilon_d > 0, \varepsilon_\theta < 0 &\implies v_l > \bar{v}_l \implies \Delta\bar{v}_l > 0 \\ \varepsilon_d < 0, \varepsilon_\theta > 0 &\implies v_l < \bar{v}_l \implies \Delta\bar{v}_l < 0 \end{aligned}$$

As aforementioned, error related information modulates the activity of IO cells, which in turn determines synaptic plasticity changes at model PF–PC synapses (Sec. 15.1.4). For instance, the firing rate $r(t)$ (Eq. 15.4) of all IO neurons in the two microcomplexes correcting errors in the positive and negative range of $v_r(t)$, respectively, vary according to:

$$r_{v_r^+}(t) = k \cdot \mathcal{H}(\Delta\bar{v}_r) \quad (15.12)$$

$$r_{v_r^-}(t) = k \cdot \mathcal{H}(-\Delta\bar{v}_r) \quad (15.13)$$

where $k = 10$ is a scaling factor and \mathcal{H} is the Heaviside function defined such that $\mathcal{H}(0) = 0.1$. According to Eqs. 15.12, 15.13 (and see also example in figure. 15.1):

- When no speed change is needed, i.e. $\Delta\bar{v}_r = 0$, the mean IO firing rates are $r_{v_r^+}(t) = r_{v_r^-}(t) = 1$ Hz, which make heterosynaptic LTD

(Eq. 15.11) and homosynaptic LTP (Eq. 15.10) at PF–PC synapses to compensate each other in both microcomplexes —i.e. no adaptation takes place.

- When the velocity of right fore-and-hind paws must increase, i.e. $\Delta\bar{v}_r > 0$, then $r_{v_r^+}(t) = 10$ Hz, which makes LTD to take over LTP in the active PF–PC synapses of the corresponding microcomplex. The consequent decrease of PF–PC synaptic efficacy reduces the inhibitory action of PCs onto DCN neurons the next time that the microcomplex receives the same contextual input —which activates the same PF–PC synapses and then the same PC responses. As a consequence, the population activity of DCN neurons increases, which reinforces the correction signal $\Delta v_r^+(t)$ (according to Eq. 15.6). In addition, for $\Delta\bar{v}_r > 0$, the mean IO firing rates $r_{v_r^-}(t) = 0$ Hz, which blocks LTD in the active PF–PC synapses of the corresponding microcomplex. Thus, LTP increases and strengthens future inhibitory actions of PCs onto DCN neurons in the presence of the same contextual input to the microcomplex. Then, the corrective signal $\Delta v_r^-(t)$ decreases over time. As a consequence, the resultant correction $\Delta v_r(t)$ (Eq. 15.7) tends to increase and become positive over training.
- Conversely, when the velocity of right paws must decrease, i.e. $\Delta\bar{v}_r < 0$, the overall correction $\Delta v_r(t)$ tends to decrease and become negative over training.

Teaching signal for the forward predictor model. For the two forward models, error signals must encode the difference between estimated and actual next state —i.e. $d(t + \Delta t) - \hat{d}(t + \Delta t)$ for the microcomplex predicting translational changes, and $\theta(t + \Delta t) - \hat{\theta}(t + \Delta t)$ for the microcomplex predicting angular displacements.

As shown in figure 15.2, the mean firing rates of IO cells in the microcomplex subserving angular change predictions vary according to a set of radial basis functions spanning the θ state space uniformly. That is, the mean firing rate $r_i(t)$ (Eq. 15.4) of an IO cell i varies as:

$$r_i(t) = k \cdot \exp\left(-\frac{(\theta - \theta_i)^2}{2\sigma_i^2}\right) \quad (15.14)$$

where $k = 10$ is a scaling factor, θ_i is the “preferred angle” of the cell, and σ determines the degree of overlap between adjacent IO responses. In this microcomplex, groups of two IO cells share the same preferred angles (Supplementary figure 15.2). Each group of two IO neurons targets two distinct PCs, which in turn inhibit the same DCN unit. The latter codes for the same portion of the θ state space (and has the same preferred angle θ_i) than the two IO cells that modulate its inhibitory PC afferents.

According to Eq. 15.14 and to the plasticity rules described above:

- If the firing rate of the two IO cells with preferred angle θ_i is $r_i(t) \approx 1$ Hz, then LTD and LTP at PF–PC synapses of the two PCs driven by these two IO cells compensate each other. No learning occurs.
- If the firing rate of the two IO cells with preferred angle θ_i is $1 < r_i(t) \leq 10$ Hz, then LTD dominates LTP at the PF–PC synapses of the two PCs driven by these two IO cells. Thus, over training, the DCN unit whose preferred angle is close to θ_i tends to increase its firing activity, whereas the other DCN units tend to either decrease or maintain their spike frequency. As a consequence, the decoding scheme used to readout the population activity of DCN neurons in the forward predictor model (Eq. 15.8) will tend towards an estimate of the next angular displacement close to θ_i .
- Conversely, if the firing rate of the two IO cells with preferred angle θ_i is $0 \leq r_i(t) < 1$ Hz, then LTP dominates and the corresponding DCN neuron tends to decrease its spike frequency. Thus, this DCN unit will not contribute to the population decoding scheme significantly.

15.2 Statistical analyses of neural activities

To quantify spatial-related correlates of neural activity, we discretize the continuous two-dimensional input space into a grid of 5 x 5 cm square regions (pixels). Let S denote the set of stimuli —i.e. the set of pixels s visited by the simulated animal while solving the task.

Place field area. For each neuron, we compute the mean firing rate associated to each pixel s by dividing the spike count associated to s by the time spent by animal in s . We then estimate the size of a receptive (place)

field as the number of adjacent pixels with a firing rate above the grand mean rate —i.e. total spike count divided by the total time spent moving in the maze— plus the standard deviation (similarly to Muller et al., 1987; Hok et al., 2005).

Spatial coherence. We assess the local smoothness of place fields as the z-transform of the correlation between the firing rate in each element of the positional firing rate array and the aggregate rate in the eight nearest pixels (Hok et al., 2005).

Peak amplitude. For each neuron, we calculate the peak amplitude as the maximum firing rate of the neuron in the place field area.

Multimodality and number of peaks of receptive fields. We assess the statistical significance of unimodality *vs.* multimodality property of spatial receptive fields by means of the Hartigan DIP test (Hartigan and Hartigan, 1985). We estimate the number of peaks of a receptive field as the number of distinct activity blobs with a firing rate above the grand mean rate plus the standard deviation.

Spatial density of receptive fields. To assess the redundancy level of a spatial code —i.e. the average number of units encoding a spatial location $s \in S$ — we use the following density measure:

$$D_S = \left\langle \sum_{j \in J} \mathcal{H}(r_j(s) - \eta) \right\rangle_{s \in S} \quad (15.15)$$

where $r_j(s)$ is the response of a neuron $j \in J$ when the animal is visiting the location $s \in S$, η denotes the noise level activity, and \mathcal{H} is the Heaviside function.

Spatial information content of the spatial code. An information theoretical analysis quantifies how much information the neural responses $r \in R$ conveyed about spatial locations $s \in S$. We compute the *Shannon mutual information* $I(R; S)$ (Shannon, 1948; Bialek et al., 1991) between neural responses R and spatial locations S :

$$I(R; S) = \sum_{s \in S} p(s) \sum_{r \in R} p(r|s) \cdot \log_2 \left(\frac{p(r|s)}{p(r)} \right) = \sum_{s \in S} p(s) \cdot I(R; s) \quad (15.16)$$

where $p(r|s)$ indicates the conditional probability of recording a response r while having the simulated rat visiting a region s ; $p(s)$ the a priori probability computed as the ratio between time spent at place s and the total time; $p(r) = \sum_{s \in S} p(s) \cdot p(r|s)$ the marginal probability of observing a neural response r ; and $I(R; s)$ is the *stimulus-specific surprise* (DeWeese and Meister, 1999). We discretize the continuous output space of a neuron $R = [0, 1]$ by means of a binning procedure (bin-width equal to 0.1). We subtract a correcting term C to mutual information to limit the sampling bias (Panzeri and Treves, 1996):

$$C = \frac{\sum_s R_s^+ - R^+ - (|S| - 1)}{2N \ln(2)} \quad (15.17)$$

where $R_s^+ = \sum_{r \in R} \mathcal{H}(p(r|s))$ denotes the number of response bins in which the occupancy probability $p(r|s) > 0$; $R^+ = \sum_{r \in R} \mathcal{H}(p(r))$ denotes the number of response bins where $p(r) > 0$; $|S|$ is the number of stimuli; N is the number of stimulus-response pairs (s, r) .

We compute mutual information by considering both the responses of single units j , $I_j(R; S)$, and the neural population responses, $I_{pop}(R; S)$. The ratio:

$$I^*(R; S) = \frac{I_{pop}(R; S)}{\sum_{j \in J} I_j(R; S)} \quad (15.18)$$

measures the “information sparseness” of a population code, or, conversely, the redundancy level of the spatial information content of a neural code.

Mutual information quantifies the mean information content over the whole environment, but it does not quantifies the specificity of the neuronal discharges. Thus, we employ an additional measure, namely the information per spike I_{spike} (Skaggs et al., 1993) defined for a neuron j as:

$$I_{spike}(j) = \sum_{s \in S} \frac{r_j(s)}{\bar{r}_j} \cdot \log_2 \left(\frac{r_j(s)}{\bar{r}_j} \right) \cdot p(s) \quad (15.19)$$

Accuracy of the population space code. To assess the quality of a hippocampal place map, we measure the mean accuracy of the population vector coding estimate (Georgopoulos et al., 1986; Wilson and McNaughton, 1993). Let $r_i(s)$ denote the activity of a neuron i at position s , and s_i be the center of its place field. The population vector \vec{s} is the center

of mass of the ensemble activity:

$$\tilde{s} = \frac{\sum_i r_i(s) \cdot s_i}{\sum_i r_i(s)} \quad (15.20)$$

The mean localization error is simply taken as the mean Euclidean distance between actual positions s and estimates \tilde{s} :

$$\bar{\varepsilon} = \langle \varepsilon(s) \rangle_{s \in S'} = \left\langle \sqrt{\frac{\sum_n (\tilde{s}_n - s_n)^2}{n}} \right\rangle_{s \in S'} \quad (15.21)$$

where $S' \subseteq S$ is the set of positions where \tilde{s} is well defined (i.e. $\sum_i r_i(s) \neq 0$).

Percentage of recognized locations. We measure the fraction of the environment encoded with high accuracy by the population activity of simulated place cells as:

$$R = \left\langle \mathcal{H}(\xi - \varepsilon(s)) \right\rangle_{s \in S} \quad (15.22)$$

where $\varepsilon(s)$ is the place recognition error when the animal is actually visiting the location $s \in S$, ξ is the error threshold below which the estimate is considered accurate, and \mathcal{H} is the Heaviside function.

Chapter 16

Supplementary Results

16.1 Cerebellar role in *local* procedural spatial learning

Here we study the impact of a purely local motor adaptation deficit in simulated L7-PKCI mice on spatial navigation behavior. We validate this hypothesis against experimental findings by Burguière et al. (2005). In the model, we isolate the procedural role of the cerebellum by blocking the functional projection from the cerebellar forward predictor network to the hippocampal network (red projection in figure 11.2A). Thus, we assume that simulated control and L7-PKCI mice have equivalent spatial representation capabilities.

Figure 16.2 compares simulation and experimental behavioral data in both MWM and Starmaze tasks. In the MWM, the mean escape latency of simulated L7-PKCI mice is significantly larger compared to control subjects over the entire training period (figure 16.2 A, ANOVA, $F_{1,28} = 18.92$, $P < 0.001$). Similarly, simulated mutants are significantly impaired in reducing the (local) angular deviation between actual and ideal trajectory to the platform (figure 16.2 B, ANOVA, $F_{1,28} = 23.57$, $P < 0.001$). The difference of performance between simulated controls and mutants is not due to a difference of swimming speeds (ANOVA, $F_{1,28} = 2.5$, $P > 0.05$). Figure 16.2 A,B also show that both controls and mutants improve their spatial navigation performances over training, with a tendency to stabilization after day 7. These simulation results are qualitatively consistent with experimental findings (insets of Figure 16.2 A,B; from Burguière et al., 2005). However, if we compare the mean intergroup differences in simula-

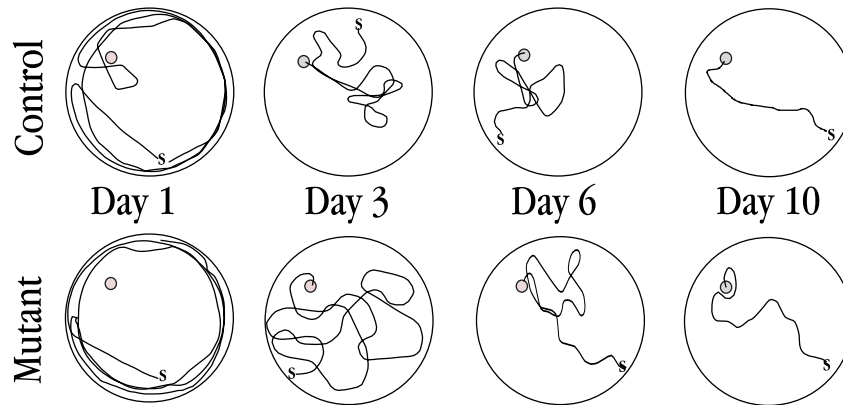


Figure 16.1: *Samples of trajectories.* Examples of trajectories in the MWM for a control (top) and a mutant (bottom) animal at 4 steps of the training.

tions and experiments for both behavioral parameters —e.g. for the heading ϕ , we compute $\langle \phi^{WT} - \phi^{L7PKCI} \rangle_{n,m}$ by averaging over all $n = 15$ animals and all $m = 40$ training trials—, we find significantly smaller values in simulation data (for escape latency: ANOVA, $F_{1,28} = 10.93$, $P < 0.001$; for heading: ANOVA, $F_{1,28} = 14.65$, $P < 0.001$).

In contrast to experimental observations, the difference between goal-searching behavior in simulated controls and mutants is not statistically significant under the pure local procedural hypothesis (figure 16.2C). We find that the ratio between time spent within the platform quadrant and trial duration increases over training for both simulated groups with no significant intergroup differences (ANOVA, $F_{1,28} = 3.1$, $P > 0.05$). Furthermore, contrariwise to experimental data, the mean distance-to-goal parameter is not significantly impaired in simulated mutants (figure 16.2D; ANOVA, $F_{1,28} = 3.7$, $P > 0.05$).

In the Starmaze task, simulated mutants and controls exhibit comparable performances over training in terms of both mean escape latency (not shown, ANOVA $F_{1,18} = 1.11$, $P > 0.25$), mean heading to goal (not shown, ANOVA $F_{1,18} = 2.01$, $P > 0.1$), number of visited alleys (figure 16.2E; ANOVA $F_{1,18} = 0.19$, $P > 0.5$), and mean distance swum to reach the target (figure 16.2F; ANOVA $F_{1,18} = 0.20$, $P > 0.5$). These findings are consistent to experimental observations by Burguière et al., 2005 (insets of figure 16.2E,F).

Morris water-maze

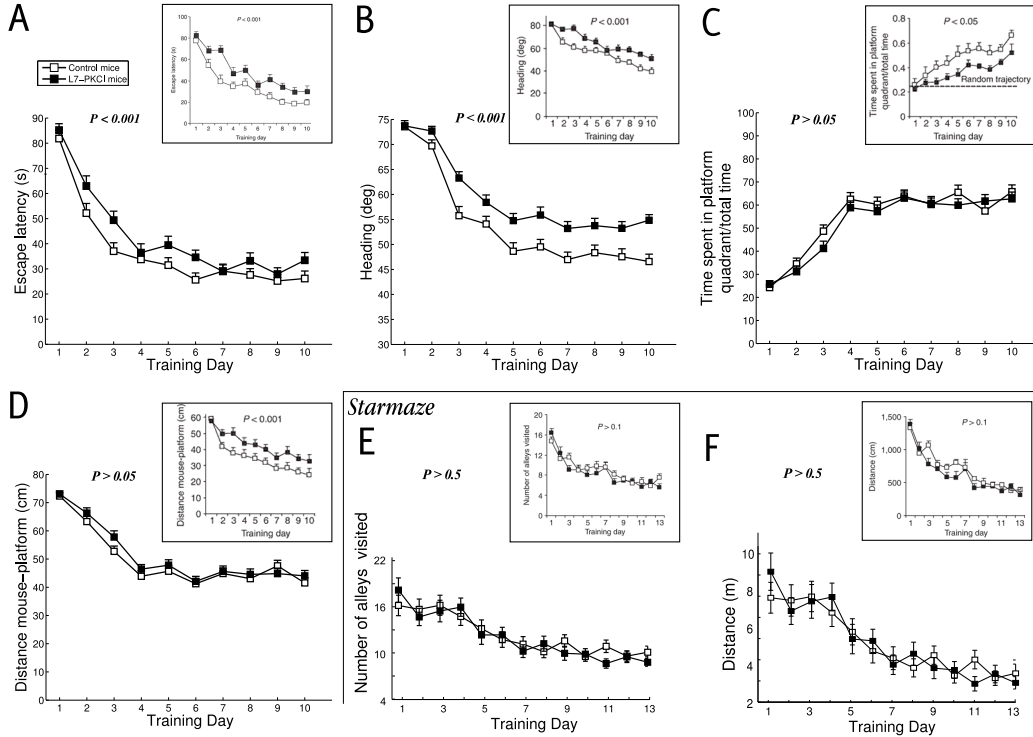


Figure 16.2: Results in the MWM (a-d) and in the Starmaze (e-f) under a purely local procedural scenario **MWM: A.** Escape latency of simulated controls (white square) compared to mutants (black square). **B.** Average angular deviation between ideal and actual trajectory to the goal **C.** Ratio of time spent in the platform quadrant over the total time of trial. **D.** Mean distance of the simulated mouse with the platform. **Starmaze: E.** Mean number of alleys visited. **F.** Mean distance swum. For each parameter, the corresponding experimental results are shown in an inset.

Chapter 17

General discussion and conclusion

In the context of this thesis, we focused on the neurocomputational principles underlying the functions of the cerebellum in both motor and cognitive processes. More precisely, we first concentrated on the role of the cerebellum in the adaptation of voluntary movements, and second, we sharpened our study on the theoretical role of this structure in spatial cognition.

As stated in the introduction, the synaptic organization of the cerebellar microcomplex is remarkably uniform, suggesting that it processes information with a single and characteristic computational principle. Based on this working hypothesis, the main objective of this thesis was to unveil the neurocomputational rules implemented in the cerebellar circuitry that could explain its function in both motor control and spatial cognition.

In the context of motor control, we study how multiple cerebellar microcomplexes encoding internal predictive and corrective models might collaborate to efficiently participate to the adaptation of motor behaviors. Then, we examine to what extent this framework of cerebellar internal models could be applied to navigation, and help to get a better understanding of the cerebellar computational properties in both procedural and declarative memories implied in spatial cognition.

In this chapter, we first summarized the main results and contributions of our studies. In a second section, we discuss the achievement of the main objective. Eventually, we give future directions of research.

17.1 Main results and contributions

17.1.1 Cerebellum and adaptive motor behavior

In the first part of my thesis, we considered the procedural learning mechanisms of the cerebellar circuitry in the context of adaptive voluntary movements. Using a neurocomputational approach, we investigated how cerebellar microcomplexes could implement both predictive and corrective internal models with the same neural architecture and how these models could work cooperatively to promote efficient online adaptation and offline consolidation mechanisms.

We proposed a novel scheme to couple internal cerebellar models, this connectionist architecture took inspiration from the cerebellar microcomplex circuit. Long-term synaptic plasticity (both LTP and LTD) at the parallel fiber Purkinje cell's synapses was implemented to achieve adaptive motor control.

We proposed that this coupling scheme may offer a plausible model to combine the advantages of fast online adaptation properties of forward models and accurate but slower convergence of inverse corrective models, and achieve offline consolidation of procedural memories to enhance motor control capabilities.

The architecture was validated on a closed-loop architecture to control the dynamics of a robotic arm: we assessed its learning capabilities on the rotation adaptation task used by Huber et al. (2004) to study motor learning (both online and offline) in humans.

Contributions

Behavioral results. First, our numerical simulations investigated the benefits of using both internal models to improve online learning capabilities. The system was shown to acquire representations of closed-loop sensorimotor interactions, suitable to adapt the behavioral responses to changing sensory contexts. The coupling model reproduced the experimental findings on human procedural learning during the rotation adaptation task proposed by Huber et al. (2004).

Offline consolidation. Then, we evaluated to what extent the proposed coupling scheme could explain the experimental findings on offline learn-

ing occurring during sleep. The sleep-dependent consolidation observed experimentally was mimicked here by an offline learning phase during which a replay of the contextual information elicited during online training occurs. This assumption was corroborated by several experimental studies: for example, it has been shown that patterns of activity recorded during online practice of a motor skill task reappear during episodes of REM sleep, while such activity is not seen in control subjects (Maquet et al., 2000).

Properties of the cerebellar processing. Three major properties of the cerebellar circuitry were highlighted and proposed to play a major role in the adaptation of procedural memory and in its offline consolidation. First, we showed that forward models needed to be bistable to achieve good performances. Bistability was defined as the capacity to give a good prediction when the model was active, and to stay silent otherwise. Second, we proposed that during offline processing, the inverse model had to keep its dynamic unchanged when the forward model was unable to predict the sensory consequences of a motor command. This presumed that cerebellar long term potentiation and depression at parallel fiber-Purkinje cell's synapses could compensate each other. Knowing that LTP and LTD are not symmetrical (LTP is a homosynaptic process and LTD is an heterosynaptic process), this compensation is not trivial and mainly depends on the strength of LTP and LTD. Eventually, we confirmed that encoding at the granular layer should optimize the neural code conveyed by the mossy fibers so that it facilitates learning at PF-PC synapses. We proposed that a sparse recoding might be the key of such a process.

17.1.2 Cerebellum and spatial cognition

In the second part of my thesis, we integrated the previously described model of the cerebellar microcomplex in an extended neural architecture in order to study the potential role of the cerebellum in the procedural and declarative components of spatial learning.

We simulated a large-scale neural network accounting for the functional coupling between cerebellum and hippocampal formation. The modeled architecture also included a putative cortical module for trajectory planning and inverse dynamics computation. The presented work focused on the behavioral genetic findings reported by Burguière et al.

(2005), which suggested that LTD at the parallel fiber-Purkinje cell's synapses was a relevant mechanism for the adaptive tuning of navigation trajectories. We emulated the lack of LTD at PF-PC synapses of L7-PCKI transgenic mice (De Zeeuw et al. 1998). We simulated the experimental protocols employed by Burguière et al. (2005) to compare the learning performances of L7-PKCI mutants with those of control animals in two spatial navigation tasks: the Morris water maze (Morris et al. 1984) and the Starmaze task (Rondi-Reig et al. 2005). In both setups, mice had to swim from random departure locations to a platform hidden below the surface of opaque water. Both tasks required the declarative capability of building a spatial representation of the environment. Yet, in contrast to the Morris water maze task, the Starmaze alleys guided mice movements, which eventually reduced the low-level procedural demand of the task. Thus, the use of these two tasks made it possible to dissociate the relative importance of the declarative and procedural components of navigation (Burguière et al. 2005).

Contributions

Behavioral results. First, we quantified the impact of a purely local motor adaptation deficit on the overall goal oriented behavior and we tested this hypothesis against empirical observations (Burguière et al. 2005). Our results suggested an implication of the cerebellum in higher-level (global) aspects of procedural spatial learning. In particular, our results showed that L7-PKCI mutants were likely to be impaired in trading-off the exploration-exploitation balance and inhibiting thigmotaxic (peripheral circling) behavior. Second, we demonstrated that these two global procedural deficits may reflect a direct implication of the cerebellum in the integration of idiothetic (selfmotion) cues — i.e. path integration or dead reckoning (Mittelstaedt and Mittelstaedt 1980; Etienne et al. 1998; Etienne and Jeffery 2004; McNaughton et al. 2006; Wiener et al. 2011) — and, consequently, an indirect implication of the cerebellum in declarative spatial learning.

Characterization of the spatial code. We performed a series of statistical and information theoretical analyses to characterize the encoding properties of hippocampal place cell activity as well as the functional time course of the learned place field representation. These analyses quantified the

possible impact of cerebellar LTD deficit on the dynamics of hippocampal place coding. Our results showed that the simulated L7-PKCI spatial mapping rate was slower compared to controls. They also suggest that the L7-PKCI hippocampal population code was less accurate — in terms of estimate of the location currently visited by the animal — than the one learned by control mice. A single unit analysis suggested an increased probability for L7-PKCI hippocampal place cells to exhibit multiple peak receptive fields, which could degrade the accuracy of the overall spatial representation.

Predictions. These results led to a series of predictions at the level of single unit (higher rate of cells with multiple peaks) and neural population activity (less accurate). Also, at the behavioral level, our results suggested that the predicted path integration deficit of L7-PKCI mice would lead to observable differences in the free exploration patterns of mutants and controls during latent spatial learning in open-field environments (Drai et al. 2001; Fonio et al. 2009), with an extended time spent in the periphery of the environment for mutants.

17.2 Limitations and perspectives

Throughout this dissertation we have already discussed several important points that need to be addressed in order to ameliorate the soundness of our approach; the issues listed below are potential future directions of researches that emerged from this thesis.

17.2.1 Studying inter-structure interactions in the generation of movements

If our model helps to get a better understanding on how the cerebellum can achieve local motor corrections to unexpected disturbances, we need to take into consideration that the movement is the reflection of an interaction of cortical and sub-cortical structures. By coupling our model with neuro-mimetic models of such structures, we hope to gain new insights on those interactions implicated in the correction of movements. Although the structures implied in the generation and control of voluntary movements are numerous, we are particularly interested in the role of cerebellar

interactions with the basal ganglia and the parietal cortex.

The cerebellum and the basal ganglia. The basal ganglia and the cerebellum are two major structures that influence the generation of voluntary movements. Recent findings have shown that there is an anatomical substrate for a substantial two-way communication between the cerebellum and the basal ganglia (Bostan et al., 2010). Thus, the two structures may be linked together to form an integrated functional network. A next step of our work would be to build a system that models these interactions to reveal how both structures specialize in the planning and correction of movements. In addition to gain core knowledge on the way the movements are processed inside the brain, this project has clear medical implications. For example, it has recently been shown that patients with Parkinson's disease have an hyper-activation of the cerebellum and motor cortex, and an hypo-activation of the basal ganglia (Yu et al., 2007). However the relationship between the two has not been clearly established. A model integrating both structures would help to understand the underlying mechanisms.

The cerebellum and the parietal cortex. The parietal lobe is known to be implicated in target reaching tasks, and more generally in motor prediction processes. The differential roles in prediction of the cerebellum and the parietal lobe are still under debate, and it is highly possible that these two structures work as a functional loop for predicting the sensory consequences of movements and making adequate corrections. It has been previously suggested that one of the distinctions between these two structures may be that, contrary to the predictions made by the cerebellum, those of the parietal cortex would be made available to awareness (Blakemore and Sirigu, 2003). A complementary view stresses the fact that the parietal cortex could be more involved in the comparison between sensory and motor information by maintaining the anticipated sensory consequences of a movement, this prediction being made by forward models located inside the cerebellum (MacDonald and Paus, 2003). An extended version of the coupling scheme should integrate a model of the parietal lobe, which could help to dissociate the role of both structures during on-line and offline adaptation.

17.2.2 Consolidation of learning during sleep

Consolidation of procedural memory. In our simulations to solve the rotation adaptation task, entire trajectories were randomly replayed when performing offline consolidation. We proposed that the global architecture was switched to an offline mode, such as learning of the inverse model would be driven by the predictions of the forward models. Nevertheless, we did not address how such a process is supposed to occur.

Also, several other issues related to the enhancement of procedural memory could be investigated by using our model. For example following questions could be addressed: *(i)* How the benefits of the offline learning would vary if contextual information were only partially replayed (which is likely, as shown in hippocampal recordings, see Gupta et al., 2010)? *(ii)* Does the brain have the capacity to extract the best sequences to be replayed to optimally enhance procedural memory? *(iii)* How the brain decides which task must be consolidated during sleep? Does it even have this capacity? *(iv)* Is there an optimal number of repetitions that could be determined internally? *(v)* Finally, could we extract the best way to enhance procedural memory, by using an efficient arrangement of online training and sleep consolidation stages? This last questions could have some nice practical implications in tasks where enhancement of procedural memory is at the core of the observed performance, such as playing an instrument or mastering a sport. It should be mentioned that such questions are currently debated and investigated in tasks where the declarative memory is primarily involved (e.g., Gupta et al., 2010).

Consolidation of spatial memories. In the context of spatial cognition, research studies have demonstrated that neural patterns reflecting previously acquired information, are replayed during sleep (e.g., Benchenane et al., 2010). We propose that our model could be used to determine in which measures the forward model could operate during offline consolidation in order to enhance or stabilize declarative memories.

Our modeling approach could also be employed to interpret available experimental data and to study how and when replays should occur to optimize learning. For example, we could study if replays should better favor remote experiences so that they are not forgotten or if it should focus on recent experiences so that they are learned faster (e.g., Gupta et al., 2010).

Implicit memories and insight. Insight denotes a mental restructuring that leads to a sudden gain of explicit knowledge. Recent scientific discoveries suggest that insights can be gained through sleep. For example, in an experiment where subjects performed a cognitive task, Wagner et al. (2004) have shown that many subjects gained insight into an hidden rule after sleep, compared to subjects who followed the same protocol but with nocturnal or daytime wakefulness. Authors concluded that sleep, by restructuring new memory representations, facilitates extraction of explicit knowledge (Wagner et al., 2004). Also, a recent study has suggested that an interaction between working memory related structures (e.g., the prefrontal cortex) and the cerebellum could play a role in intuition (Vandervert et al., 2007). During my Phd, I developed a simple prototype of a task that might help to elucidate if sleep can (i) enhance performances in procedural tasks where the motor sequence to consolidate has been hidden — and hence not been made available to awareness — in random noise, and (ii) provide insights on this hidden sequence. More importantly, this task is proposed to relate the role of the cerebellum in sleep consolidation processes. The task and expected results are presented in annexe C.2, page 281.

17.2.3 Validating the hypotheses/predictions derived by the model

Eventually, a next step of this work will be to validate the predictions derived by the model. In the study of spatial cognition, our results led to a series of predictions that can be tested through extracellular electrophysiological recordings of L7-PKCI hippocampal place cells. Because the encoding of hippocampal place cells has been demonstrated to relate to the projection of layers of hippocampal grid cells, further analyses and recording should be performed in hippocampal grid cells.

Finally, at the behavioral level, we predicted observable differences in the free exploration patterns of mutants and controls during latent spatial learning in open-field environments (Fonio et al., 2009). This prediction is being currently tested in our laboratory.

17.3 Toward a unified principle for motor and non motor tasks

I would like to finish this manuscript by discussing the hypothetical common functions of the cerebellum in motor and non-motor tasks, and to examine other views emerging in the neuroscience community.

The couple of studies we presented proposes a consistent interpretation of the function of the cerebellum in both motor and non-motor tasks, but does not extend the purely sensorimotor role of the structure (the influence on spatial cognition being the consequence of a sensorimotor function). The idea of a single computation principle implemented in the cerebellar circuitry, independently of the type of data being processed, has been advanced by other authors and is addressed in this section. This common representation implies that the function of the cerebellum has to be observed in terms of computations performed, rather than in the behaviors involved.

For example, Doya (2000) argued that the cerebellum could be a device associated with supervised learning, in contrast to the basal ganglia, which would achieve reinforcement learning, and the cerebral cortex, which is suggested to perform unsupervised learning. In his theory, Doya postulates that adaptation may be driven by a teaching signal conveyed by the climbing fiber, consistent with Marr-Albus-Ito's model. Some authors refuted this postulated role of the inferior olive's neurons, and proposed that the general purpose of the cerebellum could be to provide an internal clock (e.g., Lamarre and Mercier, 1971; Llinás and Yarom, 1986; Keele and Ivry, 1990).

This timing idea was first advocated by Braintenberg and Atwood (1958). Since then, there has been a continuous debate as to whether the role of the cerebellum in motor and non-motor tasks could be directly derived from a timing function, or if the cerebellar circuitry implements adaptive internal models of the body-environment interactions.

17.3.1 Are timing and internal model's theories mutually exclusive?

At first sight, the two proposed views, by postulating two distinct functions of a single cellular substrate can appear mutually exclusive. How-

ever, both theories are defensible because they explain consistently distinct subsets of experimental data. If it seems unlikely that the cerebellum only act as a timing operator, many evidences indicate that olivary neurons convey such type of information (see De Zeeuw et al., 2011 for a recent review). Therefore, it should be envisaged that both theories could be embedded in a more complete and coherent view of the cerebellar function, still to be developed.

Addressing the question of the temporal firing properties in cerebellar assemblies might help to unified the two debated theories on the function of the climbing fiber. Indeed, recent findings suggest that olivary neurons could convey a teaching signal *and* a timing information.

Mathy et al. (2009) stressed the fact that the phase and amplitude of oscillation in inferior olive neurons is highly correlated with the number of climbing fiber axonal spikes, which in turn influences the shape of Purkinje cell's complex spike and modulates the plasticity at parallel fiber-Purkinje cell's synapses (Mathy et al., 2009). This striking result is a first step toward an integration of both learning and timing theories related to the climbing fiber function. Also, this result demonstrates the need of gaining a better understanding of the neural code embedded in the different cerebellar cell's assemblies.

17.3.2 Neural code of cerebellar cell assemblies

Recent findings suggested that the cerebellum could use different strategies to encode and communicate information between its neural assemblies and to other parts of the central nervous system.

A very recent review focuses on the spatiotemporal firing patterns in the cerebellum, and unveils how patterns in complex and simple spikes might be generated in the Purkinje cells, and later read out by the cerebellar and vestibular nuclei (De Zeeuw et al., 2011). Interestingly, the review proposes that the olivocerebellar system is in principle optimally designed to create and employ these patterns. The authors also suggest that the role of the climbing fiber could be multiple. For example, in motor control, it could be used as a switch to engage a different program, or it could send a signal to speed up the current program.

Recent evidences suggest that characteristic spatiotemporal patterns can occur in Purkinje cells in the complex-spikes activity, in the simple-spikes activity, and in interaction between both type of action potentials

(see De Zeeuw et al., 2011 for review).

Still, a better description of subserving mechanisms is necessary. Many questions related to simple-spikes firing need to be addressed: How simple-spike patterns are generated? What is the role the intrinsic activity, and of the synaptic excitation and inhibition? How the configuration of the parallel fibers might shape and tune the patterns? What is the content of information conveyed by the inter-spike intervals?

Also, (i) the electrical coupling, and (ii) the subthreshold oscillations of olivary neurons are two mechanisms likely to generate synchrony and rhythmicity and hence characteristic spatiotemporal patterns in Purkinje cell's complex-spikes. However, their related properties need to be defined more clearly (De Zeeuw et al., 2011).

Furthermore, it is demonstrated that the patterns of complex spikes and simple spikes in the Purkinje cells can influence one another. For example, it has been observed that a climbing fiber discharge induces a pause in simple-spike generation, succeeded by a simple-spike facilitation phase (20-40 *ms*), immediately followed by a simple-spike suppression (see De Zeeuw et al., 2011 for review and references). The role of these dynamics are still not fully understood.

Finally, the spatiotemporal patterns generated at the level of the Purkinje cells can only have a significant importance if neurons of cerebellar nuclei are able to read out their content. Since a single cerebellar nucleus neuron integrates the information of tenths to hundreds of Purkinje cells, there should be some sort of coherence in the code of Purkinje cells so that a cerebellar nucleus cell can decrypt it. It therefore remains to be determine how spatiotemporal patterns may be read out by cerebellar and vestibular nuclei; and to depict the impact of complex spikes, simple spikes and mossy fibers collaterals on cerebellar nucleus neurons.

17.3.3 The internal mental models hypothesis

If studying the neural code of the cerebellar units is fundamental, observation at a higher structuro-functional level might provide further insights on the cerebellar role in both motor and non-motor functions.

The idea of cerebellar internal models, largely developed in the sensorimotor domain, has been extended to the cognitive functions, and it is suggested that the cerebellum could also encode internal models of our thoughts, known as internal mental models.

Thoughts engage both explicit and implicit manipulations. If an explicit process is supposed to occur in the cerebral cortex, the implicit process has been suggested to be inherent to other subcortical structures, such as the basal ganglia and the cerebellum (Ito, 2008).

Based on this working hypothesis, Ito (2008) described a potential mechanism for implicit thought handling. He proposed that the cerebellum might encode internal models which reflect the essential properties of mental representations — supposed to be formed in the cerebral cortex — the same way it represents internal models of sensorimotor dynamics. Ito therefore extends the internal model theory to cognition. The internal-model hypothesis implies that, during repeated trials of a thought that uses a particular mental model, an internal model (either forward or inverse) that mimics this mental model would be formed. It is important to note that this hypothesis goes further than our results. Indeed, in our navigation study, we presented how a sensory predictive function of the cerebellum is likely to influence the establishment of an abstract representation.

If the hypothesis of existence of cerebellar internal models for mental action is still highly speculative, this is a promising framework that could help to get a better understanding of the possible mechanisms involved in a wide range of cognitive tasks (e.g., intuition, creativity and implicit thoughts as described below). Also, this framework could account for some of the symptoms that are exhibited by psychiatric patients (Ito, 2008).

According to the presented theory, a forward model would replace the mental model as the object to be manipulated and an inverse model would substitute the prefrontal cortex as the controller. During manipulation of the forward model, an individual would not be aware of the content of the thought, since this operation would be taking place in the cerebellum. Also, during the control of a task by a cerebellar inverse model, the whole process would not be made available to awareness.

Neuromimetic architectures including forward and inverse models have been recently used to address the manipulation of symbolic thoughts. Vandervert et al. (2007) described how creativity and innovation could result from the repetitive processes of working memory learned as cognitive internal models in the cerebellum. These cognitive models are thought to be composed of multiple paired forward and inverse internal mental models, coupled in an architecture derived from Wolpert and Kawato's MOSAIC and hierarchical MOSAIC models (Wolpert and

Kawato, 1998; Haruno et al., 2001, 2003), generally used to describe the generation of voluntary movements in different contexts (e.g., Imamizu et al., 2003). This MODular Selection and Identification for Control's system explores and tests possible problem-solving requirements. When a solution to a new problem is found, it is implemented into a set of new internal models in the cerebellum.

The resulting newly formed predictor/controller models are proposed to be fed back to the prefrontal cortex to complete the thought. The authors suggested that this process could lead to creative and innovative problem solving and might explain how a person could have the feeling of solving a problem with immediate insight without reason (also called "intuition"). If an inverse model is used, this should provide a person with the possibility to proceed entirely implicitly.

The internal mental model hypothesis could thus explain implicit and intuitive aspects of thought and newly developed electromagnetic inverse techniques could be used in complement to functional brain imaging studies to further establish the validity of the theory (Vandervert et al., 2007).

Annexes

Appendix A

Neurocomputation of voluntary movement

We have the ability to control and adapt our movements with a great precision, and to perform efficiently in many different tasks. While this capability does not surprise us on everyday basis, even a simple arm-hand movement to reach for an object is theoretically puzzling. Indeed, we are able to reproduce this simple movement in many different contexts and we master this task without thinking of the constraints we are confronted to (see Shadmehr et al., 2010 for review): *(i)* our muscles are sensitive to fatigues and their response from one movement to the next is different; *(ii)* the neuronal nerves send information at low speed, delaying the sensory feedbacks we could rely on to update and correct our movement; *(iii)* neural computations often require tens of millisecond, suggesting that most of these feedbacks might be integrated too late to be efficiently used; *(iv)* the sensory information is noisy, hence imprecise, and often incomplete (e.g., a task executed in the dark does not have visual feedback); and *(v)* our body slowly changes through life, and consequently, the properties of our limbs and muscles are not static. All these limitations suggest that our nervous system has been designed to adapt to these constraints and compensate for them (Shadmehr et al., 2010).

In this context, the neuroscience of movement relates to the study of the capacity of the human brain to map an abstract task into a set of control laws (i.e., motor commands). Also, the neurocomputational field of movement neuroscience tries to unveil the properties of sensory-motor signals and to highlight the structures responsible for distinct functions related to

movement (see Shadmehr and Krakauer, 2008 for a recent review)

So far, many different theoretical approaches have provided a large amount of knowledge and made numerous predictions that have been validated (see Wolpert and Ghahramani, 2000; Todorov, 2002 for review). Still, a complete framework needs to be proposed, and many questions and computational problems stay with no consistent responses.

In this chapter, I will give a short introduction of the main neurocomputational approaches and theories related to the neuroscience of movement, and define which questions are still debated.

A.1 Computational properties of movement

A.1.1 The curse of dimensionality

Considering the high number of muscles the brain can control in the human body, and the number of possible levels of contraction for a single fiber, the encoding of all configurations would need a nearly infinite storage space; moreover, the calculation related to these configurations would also increase the resource needed. Or, it appears that the brain must deal with a finite number of computational units (the neurons) and hence storage space; this makes impossible to built up a simple correspondence between a simple correspondence between a configuration of all sensory related signals and a motor command, and vice versa, as it has been early remarked by Bellmann (1957), and referred as the “curse of dimensionality” problem ¹.

A.1.2 The state and the context

This limitation highly suggests that the central nervous system extracts a compact representation of the body (physical or psychological properties), gathering the relevant information needed to predict and control the system. This compact representation is termed the *state* (Wolpert and Ghahramani, 2000). At a low level, a state can be the synergies of a group muscle; also, it can define the position and velocity of a body part. At an even

¹Bellmann pointed out that the calculation and storage of all possible motor commands and response cannot be handled easily, and grows exponentially with the number of muscles to control (Bellman, 1957)

more abstract level, a state can be a motivational aspect. It is important to note that the fact that the representation of the state can be defined at different scales suggests the existence of some hierarchy in planning and control (shortly presented next subsection).

In voluntary movement, the state is by definition updated along the realization of the movement and is changing rapidly, in comparison with other key parameters defining *the context* (Wolpert and Ghahramani, 2000). The context changes in a discrete manner and is supposed to stay constant during the completion of the task. For example, when hitting a tennis ball with a racket, the static properties of the racket we are using (e.g., its size and weight) refer to contextual signals, as these information should not evolve during the realization of the movement. However, the use of a different racket would change the dynamic of the task, and the control policy — the calculation of a motor command — should therefore take into consideration these changes.

A.1.3 The notion of hierarchy

As mentioned earlier, sensorimotor function can be seen as the integration of multiple feedback controls that act at different hierarchical levels. This notion of hierarchy was first introduced by Bernstein (1947) who suggested four different levels, from the simple regulation of muscles tones to the organization of complex actions to resolve abstract actions.

Hence, the choice of a goal, often considered as the first step of a task, can be described at different levels. For example, when reaching for a glass of water, the purpose of task might be *(i)* to sate one's thirst; or *(ii)* to get the hand to the glass, or *(iii)* to rotate the shoulder and elbow joints in order to get the hand to the glass, or *(iv)* to activate sequentially the muscles to get the shoulder rotated and elbow joints in position.

In most of the existing schemes, the hierarchy is thought of in terms of planned trajectory representations in the brain in different spaces (abstract, Cartesian, joint and torque spaces). In optimal control, hierarchy must be seen as a subset of distinct control policies that act on distinct state estimates (Todorov, 2004).

From a purely anatomical view, this hierarchical organization is suggested by the multiple feedback loops operating at different time scales (e.g. Nichols and Houk, 1976). For example, the spinal cord generates very fast neural feedbacks but does not have the same adaptable capabil-

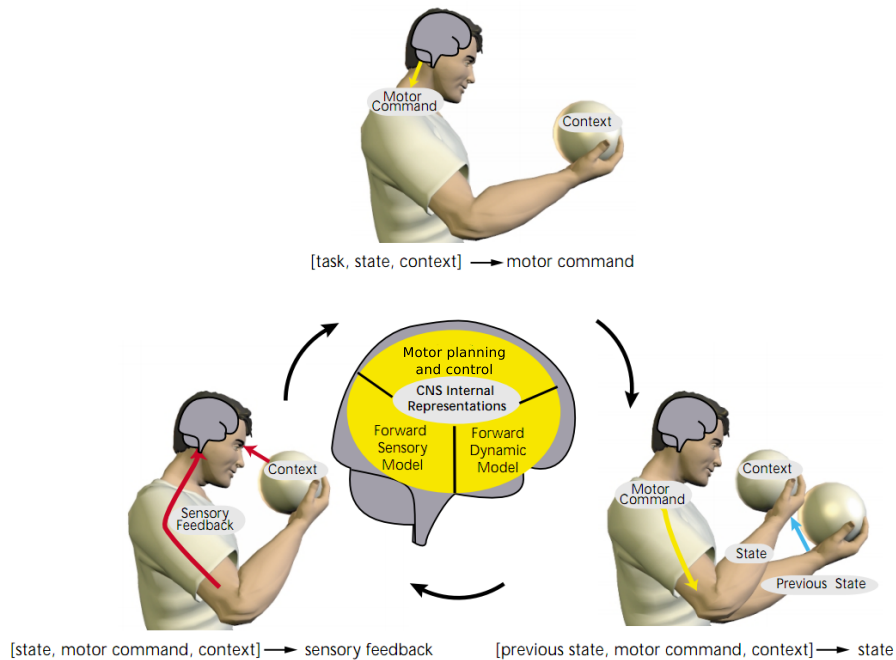


Figure A.1: Sensorimotor loop (from Wolpert and Ghahramani, 2000)

ities of more subtle loops such as a visuomotor feedback which involves the parietal cortex (Todorov, 2004).

A.1.4 The sensorimotor loop

As defined by Wolpert and Ghahramani (2000), processing a voluntary movement can be divided into three stages forming a sensorimotor loop. The first stage correspond to the generation of the motor command given a particular context, a state and an objective (stage 1); the second stage determines the change in the body and in the environment produced by the motor command (stage 2); and the third stage specifies the sensory feedback according to the new state of the system (stage 3).

Although the physical world implements the transformation function between the motor commands and the sensory consequences of these motor commands (stage 2 and 3), it has also been suggested that this transformation might be represented internally, in neuronal systems called forward internal models implemented inside the CNS (see Shadmehr et al., 2010 for review). More precisely, stage 2 is thought to be predicted by a

forward dynamic model, and stage 3 by a forward sensory model. We will see later that the cerebellum and the parietal cortex are likely to implement these neuronal systems. Also, the transformation between sensory and motivational inputs (stage 1) relies on models that first determines the next desired state (motor planning), and then the transformation from this desired state to the motor command (motor control). This motor control module can also be represented in an *inverse model*. However, in some framework such as the optimal feedback control (OFC), the distinction between motor planning and motor control disappears and both systems can be embedded in a single controller (see subsection A.2.2).

Motor control and motor planning (Stage 1)

Transforming a desired state into a set of muscles activation (for example, a combination of torque commands to be applied to the joints) is the objective of a motor control system. The first proposal was that the CNS specified spatial parameters and relied on the spring-like properties of muscles and reflex loops to move the limb (Hogan, 1984; Bizzi et al., 1984). For example, it was suggested that a set of muscle activations could define a stable equilibrium position of a body part in space and that movement was achieved via a succession of equilibrium positions along a desired trajectory (Flash, 1987). However, it is unlikely that the CNS uses such a strategy to control movement (Gomi, 1996): muscle gain are low, which prohibit this kind of control.

A more appealing proposition is that an inverse model is built and maps a set of desired states into motor commands. For inverse model control, the equations of motions are solved and the forces are applied in order to generate the desired acceleration, speed, and state transition (Kawato et al., 1987).

Both approaches (equilibrium position and inverse model) require a detailed description of how the desire goal should be accomplished. Indeed, they explain how a reference trajectory can be used to guide limb movements, but doesn't say how the reference trajectory can be found by the CNS. Thus, these theories assume the existence of a motor planning stage which determines the trajectory of a movement represented in a non-motor reference frame. Different frameworks have been proposed to resolve this task and the most elegant and promising one relates to optimal control theories, and will be presented in section A.2.

State and context estimation (Stage 2 and 3)

Estimation of the state To optimally control an object, it is fundamental for the motor system to accurately estimate the current state of the controlled object (being a body part, a tool, or their combination). It has been shown that our beliefs (state estimations) are not based on our observation only and must depend on a combination of two quantities: (i) a prediction and (ii) an observation (Vaziri et al., 2009; Körding et al., 2004).

While an observation comes from the sensory system that provides a measure of the state changes, a prediction comes from an internal forward model, a model that emulates the existing relation between a motor command and its sensory consequences (e.g., Kawato et al., 2003). In more abstract tasks, a forward model is defined as a model that appreciates the causal relationship between the inputs to a system and its outputs. Although a state estimation could be achieved without the implementation of a forward model, the combination of feedback signals and predictive inference might help to compensate for intrinsic sensorimotor delays and noises, as well as for incomplete sensory feedbacks. This combination is often referred to *an observer*. In 1960, Kalman proposed an algorithm that can be used to combine the two sources of information in a way that minimizes the variance of the estimation, building up an optimal observer. Importantly, the resulting estimation also incorporates a measure of confidence for each type of information (feedback and prediction). In a pointing task, Körding and Wolpert (2004) demonstrated that the CNS was integrating information in such a Bayesian process. This Bayesian integration also accounts for other experimental results such as the feedback responses to force perturbation and the estimation of the kinetic in the presence of noise (Muller et al., 2001; Muller et al., 1987; Granon et al., 1994; Körding et al., 2004).

Estimation of the context. A Bayesian approach has also been used to estimate the probability of a specific context, this estimation uses two distinct quantities known as the prior and the likelihood (Wolpert and Ghahramani, 2000).

The prior is defined as an estimation of this context before the execution of the movement (how likely a context is) while the likelihood of a particular context is defined as the probability of receiving a sensory feedback given this particular context. Sensory forward predictors can be

used in parallel in order to determine the relative likelihood of different contexts.

The likelihood and the prior are supposed to be optimally combined: while the prior is used to define the initial strategy to be used, the set of predictors corrects for erroneous priors. Importantly, Bayes' rule allows a quick correction to the appropriate control online.

Wolpert and Kawato (1998) demonstrated that internal models could be coupled to achieve this task, in a modular architecture for selection and identification of control (MOSAIC). In their model (Wolpert and Kawato, 1998), the contribution of each unit is determined by calculating a responsibility signal: the predicted state made by the forward model is compared to the sensory consequences of a motor action and this comparison provides the degree of contribution of each module. Since a coupled unit could be used in different contexts, a large repertoire of behaviors can be generated with a limited number of modules.

A.2 Optimal control theories

In the first part of this chapter, the different stages of motor control and the related concepts have been defined. In this section, we present theories that unified these concepts, based on optimal performance. In a few words, optimal control is a framework for dealing with the selection of the best possible movement to achieve a desired objective (see Todorov, 2004 for a recent review). In order to work efficiently, optimal control methods need a cost-reward criterion — i.e. a measure of performance — describing the goal of the task. Later, it automatically determines the best trajectory and/or control policy that achieves the best possible performance (that is the highest reward and the lowest cost). At the same time, it addresses questions that are intrinsically related with the generation of voluntary movements in human, such as redundancy². Also, it can explain behavioral observations on multiple level of analysis: limb trajectories, joint torques, interaction forces, muscle activation (e.g., Nelson,

²The redundancy is related to the fact that the same final state can be the result of an abundant number of different trajectories. In most of the tasks we perform, the redundancy problem lays on choosing one out of all possible solutions. If this is a benefit for sensory motor system (there would always be an optimal solution for two different tasks), it has been a big challenge to understand how we make the choice of one trajectory over the other.

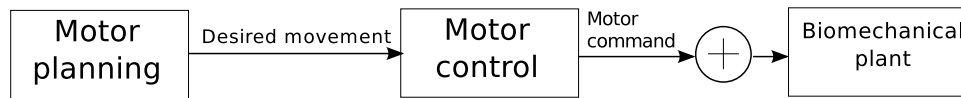


Figure A.2: Open loop motor control

1983; Uno et al., 1989; Kuo, 1995; Todorov and Jordan, 1998; Harris and Wolpert, 1998; Nakano et al., 1999; Shimansky, 2000; Todorov and Jordan, 2002; Todorov, 2002; Fagg et al., 2002; Crevecoeur et al., 2009).

The most fundamental distinction between existing models using the framework of optimal control concerns the type of control law being used (Todorov, 2004). The first category of models uses an open loop control scheme: they plan the best sequence of muscle activations, ignore feedback, and usually presume a deterministic dynamic. The second category of models uses a closed loop control scheme, this type of model constructs the sensory-motor transformation (also called feedback control law) that yields the best possible performance in the presence of motor noise, sensory feedback uncertainty and delays (Todorov, 2002). Finally, some hybrid models, such as the predictive control model, have been developed (e.g., Hoff and Arbib, 1993).

A.2.1 Open-loop motor control

The first category of models focuses on open-loop controls; they plan the best sequence of muscle activation and ignore the role of online sensory feedbacks. They therefore usually assume deterministic dynamic. Many models using an open loop control scheme have been implemented to control a wide variety of movements and predict averaged behaviors (e.g. Nelson, 1983; Uno et al., 1989; Todorov and Jordan, 1998; Harris and Wolpert, 1998). Figure A.2 shows an open loop motor control scheme.

Models using open loop control scheme differ from the cost function they optimize. In biomechanics, most models minimize the energy used by the muscles (see for example Rasmussen et al., 2001). For example, a relatively recent model has determined the optimal sequence of muscle activations, joint torque and body postures using this cost function in the gait cycle, in a biological model incorporating 54 muscles and 23 degrees of freedom (Anderson and Pandy, 2001). In other movements, such as arm-hand motions, it appeared that a cost function based on energy is not relevant to resolve the task, and that a function based on smoothness is

more adapted. For example, the minimum jerk model — often used to model the trajectory of reaching (Hogan, 1984) and grasping movement (Smeets and Brenner, 1999) — uses a cost function that penalizes the time-derivative of hand (for reaching) and finger (for grasping) acceleration (termed jerk). Such an open loop control scheme provides detailed and accurate prediction of behavior averaged over multiple repetitions of a task (see Todorov, 2004 for review). Two limitations have to be pointed out in such systems: first, it fails to reproduce the high variability of movement from trial to trial, as it has been observed experimentally; and second, it does not usually take into account noise that is inherent to the system to be controlled³. Furthermore, in the open loop control scheme, sensori-motor control is seen as a static transformation, which is highly unlikely to be the case. Also, whereas the nervous system has obvious reasons for minimizing the energy, it is not understood why CNS should care about smoothness.

A second category of systems takes into account the motor noise as well as the sensory uncertainty and delays in the optimization phase. The big advantage of such models is that they solve a control problem repeatedly rather than repeat a solution, and are therefore the most adapted system in the presence of noise, delays and unpredictable change in the system and environment (the context). This category of models uses a closed loop control scheme as defined below.

A.2.2 Close-loop motor control

In optimal control, close loop models construct the sensory-motor transformation (also called feedback control law) that yields the best possible performance in the presence of motor noise, sensory feedback uncertainty and delays (Todorov, 2002). The most promising framework is the Optimal feedback control (OFC) which has recently unified a wide range of concepts and observations into a coherent theoretical framework. In no particular order, and without being exhaustive, OFC has provided consistent explanations and predictions in the kinematic regularities, the motor

³Note that open loop control models which take into consideration the presence of noise in the system have been proposed (e.g, Harris and Wolpert, 1998). In those systems, an adaptable feedforward corrector is thought to integrate feedback information and desired state to cancel (or at least minimize) the instantaneous deviations between the desired state and the actual state of the system.

synergies, the structured variability on impedance control and the speed accuracy trade-off. A good review and reference for papers is presented in Shadmehr and Krakauer 2008.

Like other theories based on optimality, the notion of cost and reward is at the core of OFC. That is, even for a simple task of reaching, all the calculations are based on the response to a simple question: what are the costs and rewards of the task?

Once a response for this problem has been clearly defined, the framework of optimal feedback control builds a consistent system able to find the best way to get the maximum reward with the minimum effort (or cost). In other words, it defines the best set of motor commands to achieve the specific goal. The other major difference with open loop systems resides in the fact that motor planning and motor control are not defined as two different processes. Instead, they are merged into a single controller, transforming the state of the body and the world into a set of control signals (also called feedback gains). A complete description of the framework and the mathematical definition can be found in Shadmehr and Krakauer 2008. A simplified description of modules and of the flow of information in OFC is given in caption of figure A.3.

A.2.3 Predictive control models

Eventually, some hybrid models have been developed in the context of optimal control theory. For example, predictive control models use an open loop optimization control law such as the minimum jerk model to determine the best trajectory toward a goal; then, at each point in time, they take into consideration the sensory feedback and prediction to update the controller and recalculate the whole trajectory from the current state to the goal (Hoff and Arbib, 1993). This transformation from an open loop control scheme to a close loop system is referred as predictive control models. While this approach is difficult to comprehend, it provides a degree of flexibility to the system. For example, it is possible to use both a feedforward corrector *i* to cancel small deviations from the desired trajectory when the inverse controller is not optimal and *ii* to use the state estimator to provide a recalculation of the optimal trajectory if the deviation is too important.

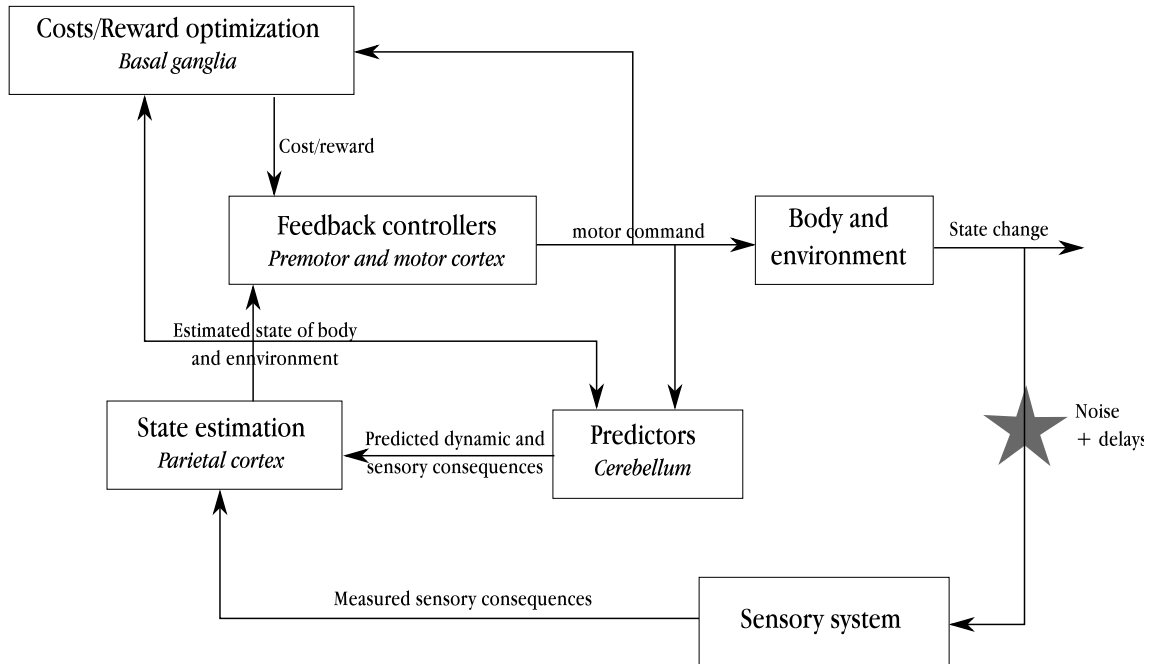


Figure A.3: *Optimal feedback control* At step 1 of the task, the objective is to get to a specific reward at a minimal cost. It is postulated that the reward of the task and the cost are two predefined functions. At a precise time t , there are many possible actions, and each action is associated with a cost and a reward, being associated with a sensory state. If we choose to get to a specific reward, we need to know how our motor commands change the state of the system (e.g., the position and speed of the body limbs and the state of the surrounding objects): this step is called system identification and postulates the existence of a forward dynamic model. Then, in order to be optimal, we need to produce the motor commands that minimize the costs and maximize the reward (Todorov, 2002, 2004). The result of this minimization is a feedback control policy (that is a set of motor command, or feedback gain) that we should apply to the sensory states. Once motor commands are generated and performed, we integrate the observation with the prediction we make about sensory consequences of motor actions and this integration leads to a new state of the system, which is later used to determine the next action to perform, closing the sensorimotor loop.

A.2.4 Limitations

The current understanding and data collection related to motor control suggest that methods related to optimal control might explain how the central nervous system processes information about movement. However, some issues remain unsolved. The main drawback of the theory is that it does not say how the costs and rewards associated to a specific task might be discovered and implemented in the CNS (Shadmehr and Krakauer, 2008). Is there a generic and powerful algorithm that might unveil the best cost and reward function for each task? At the present time, no consistent answer has been given (but see Körding et al., 2004 for a paper related to determining cost functions).

Another unanswered question concerns the timescale of optimization (the calculation of the new optimal trajectory in open loop control or in the feedback gain in OFC). An experiment shows that timescale could be longer than a single trial, and that optimization is not computed at each reaction time of the trial. In a reaching experiment, Jax and Rosenbaum (2007) demonstrated that reaching around an obstacle affects the subsequent trial when there is no obstacle. This result might suggest that the optimization process has a cost which has to be taken into consideration in the optimization process itself (indeed, the numerical methods used to approximate optimal feedback controller are computationally expensive). Or, it could be that the system identification module (predictor) might influence the optimization phase of the next trial, by suggesting the presence of an obstacle due to the previous trial. This possibility raises new interrogation concerning the time scale of predictive systems.

Another question concerns the formation of internal forward models. In optimal control theory, the control can theoretically be optimal only if the internal predictor model is accurate. In other terms, we cannot maximize the reward and limit cost optimally unless the prediction agrees with sensory feedback. The implication of this relationship between learning better sensory prediction and learning better commands is that both processes cannot be dissociated in time. In fact, building an accurate forward model must prevail or go hand in hand with the process of optimization: this prediction has still to be tested (Shadmehr et al., 2010).

Finally, the OFC makes no prediction about an internal inverse corrector model, i.e. a feedforward correction signal that would optimally correct movement when it is automated. Or, it appears that such a strat-

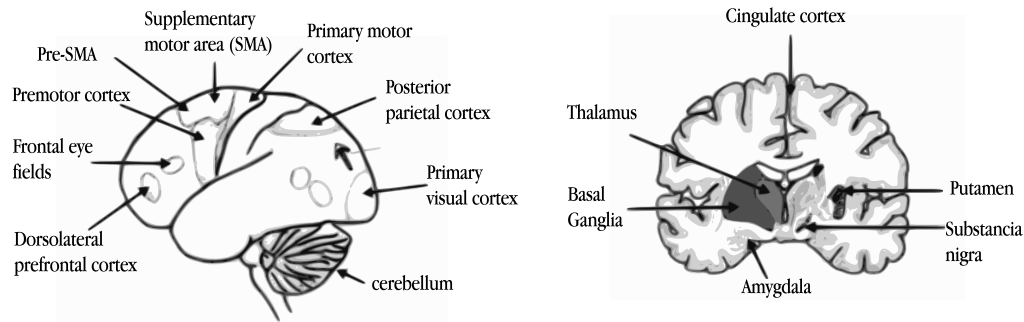


Figure A.4: Location of brain areas involved in movement (taken from Pockett, 2006). Left: Surface of left hemisphere. Right: Transverse section in region of SMA.

egy is used by the CNS in certain condition of motor learning (for example in VOR adaptation task, see Ito, 2006). Other evidences of the existence of inverse models can be found in (Ito, 2006), it could hence be considered that such a strategy is used in voluntary movement.

A.3 Structures involved in voluntary movement

The motor system of the human brain is extensive and, without being exhaustive, movement-related regions include the primary motor cortex, supplementary and presupplementary motor areas, premotor cortex, parietal cortex, dorsolateral prefrontal cortex, the basal ganglia, the thalamus, the cerebellum and most of the spinal cord. Reciprocal connection and communication pathways are found among these structures, which therefore interact to initiate and control voluntary movement (Pockett, 2006).

Note that the purpose of this section is not to review the functional role of each cortical and subcortical regions implicated in voluntary movements. Rather, we briefly relate the functional unit described in optimal control theory with a potential part of the brain that might implement the function. As a consequence, we will not address the identification of structures related to the initiation of movement, neither the areas involved in abstract representation of the task. Furthermore, we won't debate which structure might be related to a "conscious" thought of movement, and which may process information "unconsciously". A short review addressing the current knowledge on these issues has been written by Pocket (2006).

In the framework presented in figure A.3, role has been proposed for the cerebellum in system identification (i.e., predicting the changes in state as a result of a motor command). The parietal cortex is thought to estimate the state by integrating the predicted sensory feedback and the proprioceptive and visual information in order to form beliefs. The basal ganglia is thought to learn the costs and rewards associated with different sensory states and to estimate the cost during the execution of a motor task. The primary motor cortex and the premotor cortices are thought to be related to the implementation of an optimal control policy which transforms our beliefs about proprioceptive and visual states into motor commands by minimizing the cost function (Shadmehr and Krakauer, 2008).

Cost and reward in the basal ganglia. Experiments on action selection in rodents provide insights into the question of the site of localization of the rewarding nature of a task. It appears that the ability to associate a reward to a stimuli, regardless of its spatial location, must depend on the basal ganglia (Packard and McGaugh, 1992). More precisely, it has been proposed that striatal damage might have a dramatic impact on the assessment of movement cost and reward. In the context of OFC, Mazzoni et al. (2007) presented an experimental demonstration of the contribution of energy cost to speed selection, independent of spatial accuracy. Authors suggested that the basal ganglia could provide the motor motivation signal, which would be used to compute the “cost-to-go” value (Packard and McGaugh, 1992).

Control policy and the motor cortex. The implementation of an efficient control policy is thought to be located in the premotor and motor cortex. The role of the primary motor cortex and premotor cortices would be to implement a motor planning and control system in open loop control, or an optimal control policy in the framework of OFC (Shadmehr and Krakauer, 2008).

State estimation by the parietal cortex. Evidence from physiological studies in non human primates and patients have demonstrated that the parietal cortex might be involved in state estimation, by integrating prediction and observation information. For example, Rushworth et al. (1997) demonstrated that there is a double dissociation between the areas of pos-

terior parietal cortex required for reaching under visual control and the areas required for proprioceptive control (Rushworth et al., 1997). In optimal control theories, this state estimation might be used to produce a desired trajectory (open loop control scheme) or to be directly multiplied by a gain to generate motor commands (Optimal Feedback Control). In both cases, the sensory motor transformation is achieved by a strong interaction between the parietal cortex and the frontal motor areas. It has also been shown that parietal cortex might also be related to the estimation of the position of the goal. Indeed, parietal patients do not perform efficiently when the goal state was changing when performing a target reaching task (Desmurget et al., 1999).

Predicting sensory consequences of motor commands and compensating error in the cerebellum. As mentioned in chapter 3 of this manuscript, the cerebellum has been shown to participate to the generation and adaptation of complex voluntary movements, and more precisely in predicting the sensory consequences of motor commands. Some movements are so fast that they leave no time for the sensory system to play a role. For example, the brain must control the amplitude and velocity of the eye saccade without the presence of usable sensory feedbacks (the saccade movement is too brief, 50 – 80 ms, for visual feedback to be integrated). To compensate for this slow feedback, a solution the brain might use is to internally estimate of the state of the eye. Numerous studies proposed that the cerebellum might implement this internal feedback (Optican, 2005; Hopp and Fuchs, 2004; Girard and Berthoz, 2005).

If the implementation of a forward estimator for the control of eye saccade in the cerebellum is well documented, it is also thought that the cerebellum might implement feedback estimator during the control of voluntary movements. In a behavioral experiment, Nowak et al. (2007) asked subjects to hold a force transducer that measures grip force and to drop a ball into a basket attached to the transducer. Experimenters showed that in healthy individuals, the brain can predict the release of the ball and those subjects anticipate the fall of the ball to the basket by squeezing the basket handle (force transducer) right before the ball impacts the basket. However, in patients who did not have a cerebellum, this anticipatory adjustment could not be made (Nowak et al., 2007). Therefore, two hypotheses can be made on the role of the cerebellum in this precise task. Either the cerebellum is required for the ability to predict the sensory consequences

of the motor commands and send these predictions to other motor areas that decide of the action to be performed (squeezing), or, it could be that the cerebellum could directly send a motor command to control the hand and finger squeeze, in anticipation of the impact of the ball to the basket. These two interpretations of this simple result suggest that the cerebellum might implement either a forward model of the sensory consequences of our movement, an inverse model, or a feedforward corrector for the predictive correction of our movement.

Thus far, it is still debated whether the cerebellum implements a forward or an inverse model of our limbs.

Appendix B

Spatial cognition: a short introduction

Spatial cognition involves the ability of a navigating agent to acquire spatial knowledge (i.e. the spatio-temporal relations between environmental cues or events), organize it properly, and employ it to adapt motor responses to specific contexts. Similarly to other high-level functions, spatial cognition involves parallel information processing mediated by a network of brain structures, interacting to promote an efficient spatial behavior: the setup of different and flexible routines allowing the resolution of different navigation tasks (see Knierim, 2006; Arleo and Rondi-Reig, 2007 for a recent review).

Spatial cognition can roughly be observed at two distinct levels: the sensory and the action-selection level. At the sensory level, different perceptual modalities provide the animal with a description of the currently experienced spatial context. At the action selection level, navigating from one point to another involves multiple and parallel processes and requires the subject to adapt its strategy to the complexity of the task and the available contextual information (see Arleo and Rondi-Reig, 2007 for review).

B.1 Multisensory integration

A fundamental component of spatial cognition relates to the integration of multimodal signals into a coherent representation.

B.1.1 Type of information

The variety of sensory modalities related to spatial cognition can be divided into two groups, namely *idiothetic* and *allothetic* information (or cues), which have complementary properties.

Allothetic information Allothetic information are signals related to the external environment and which describe the static spatial relations between environmental cues. Allothetic signals include visual, olfactory, auditory and somatosensory cues. A spatial location can be encoded by a specific pattern of allothetic cues. By memorizing the configuration of these patterns, a agent can recognize a place and hence locate itself (McNaughton et al., 1991; Arleo and Rondi-Reig, 2007). agent can recognize a particular place according to the configuration of one or more cues.

Idiothetic information dynamic of the movement Idiothetic cues are self-motion related signals which provide the animal with the ability to perceive the kinetic of its movement and hence the ongoing changes of its body position and orientation in the environment. Idiothetic stimuli refer to vestibular, proprioceptive, optic flow signals as well as the motor efference copy (Arleo and Rondi-Reig, 2007). system structures give informative signal related to the orientation in multiple plans, as well as linear and angular acceleration of the head (Berthoz et al., 1995); proprioception detects the range and direction of movements of the limbs by using sensory information received from muscles (joints and tendons); and optic flow describes the pattern of apparent motion of visual scene components (objects, surfaces, and edges) caused by the relative motion between the eye of the observer and the scene (Gibson, 1950). determine how the optic flow could convey information on self-movement (Vidal 2002 for review).

The capacity to infer one's localization by using idiothetic information is called path integration (Redish, 1999) and has been observed in most animals (see Etienne et Jeffery, 2004). Different types of idiothetic information can be used independently but are generally combined to determine the motion of the body and allow to integrate path linearly (Etienne and Jeffery, 2004).

Reference frame Allothetic and idiothetic information can be encoded in different reference frames, either egocentrically — i.e. centered on the sub-

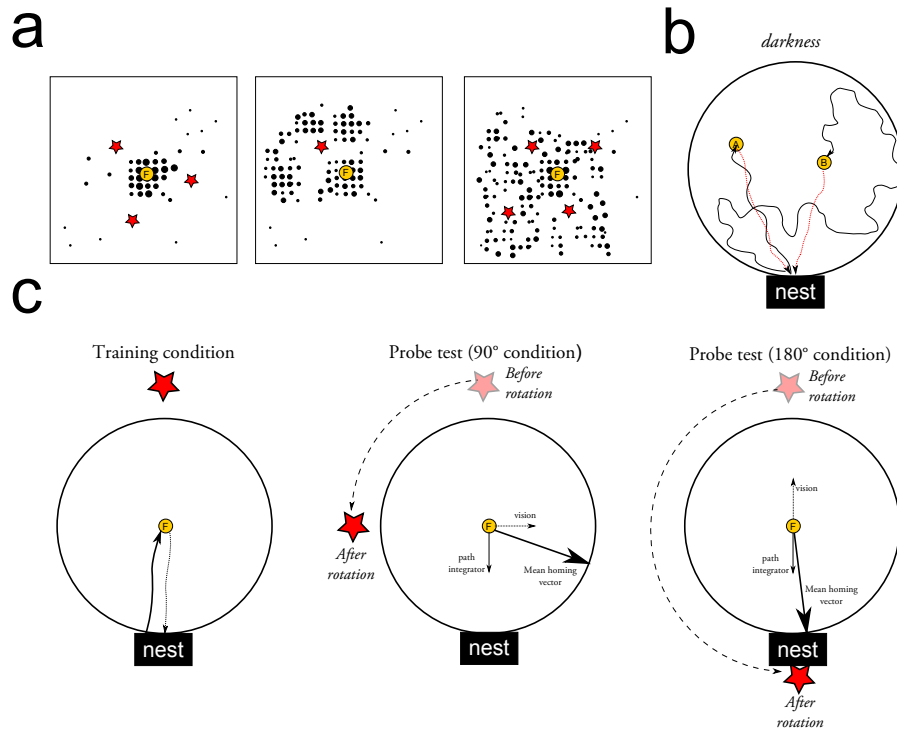


Figure B.1: Exploitation and interactions of allothetic and idiothetic signals (a) Exploitation of allothetic cues: Searching food using distal spatial cues. Rodents are trained to look for food (yellow circle) and use distal cues (red star). After learning (left image), the searching zone (black dots) is restrained to the food localization. By removing two distal cues (middle), animals extend their searching zone. When a new cue is added, animals perceive similar configurations at distinct localizations of the environment and the searching zone becomes confuse (adapted from Collett et al. 1986) (b) Exploitation of idiothetic signals: homing vector and path integration (PI). Hamsters have been shown to be able to integrate path linearly (i.e. integrate translations and rotations over time). Two examples of homing behavior are presented. After having been guided by a bait from the nest (black box) to two distinct locations (A and B, yellow circles), two hamsters return home following direct trajectories (red lines). Experiment was performed in the dark (from Etienne and Jeffery 2004) (c) Cooperation between allothetic and idiothetic signals in conflicting situation. During training (left image), animal use a stable distal landmark (spotlight, red star). In the probe trials, unknown by the animal, the landmark is rotated by either 90° (middle image) or 180° (right image). The rotation creates a conflict between self-motion and visual information. In case of 90° conflict (middle), allothetic signal dominates over idiothetic signals, whereas for a 180° mismatch (right), the path integration component becomes predominant (adapted from Etienne et al., 1998; Arleo and Rondi-Reig, 2007).

ject — or allocentrically — i.e. centered on the position of an object. Ego-centric coding might be easier to build but it varies as the animal moves in the environment, and is therefore not flexible. On the contrary, information encoded in an allocentric reference frame is more complex to build up, but has the advantage of being invariant with respect to the subject's position and orientation.

Interaction between idiothetic and allothetic informations Allothetic and idiothetic signals have complementary strengths and weaknesses. While the localization based on external landmark is stable over time, visual cues are not always available and, due to the specificities of an environment, ambiguous state might occur (i.e. two areas of the environment might be characterized by a equivalent pattern of allothetic signals (see figure B.1a). Also, path integration, which depends on idiothetic signals, allows a subject to self localize from the very first exploring excursion, and is suitable for all types of environment. Furthermore, path integration helps an animal to go back quickly to a safe home base location (see figure B.1b). However, path integration is highly sensitive to cumulative errors, and, if not recalibrated, the path integration process drifts dramatically and becomes useless (Etienne et al., 1998; Etienne and Jeffery, 2004; Arleo and Rondi-Reig, 2007).

Hence, we observe that idiothetic and allothetic cues are not sufficient if taken independently to build reliable spatial memories (see O'Keefe and Conway 1978; Jeffery and O'Keefe 1999; Berthoz and Viaud-Delmon 1999). The combination of the two signals into a unified representation overcomes the limits of both systems (Arleo and Rondi-Reig, 2007). The integration of idiothetic and allothetic information has been largely investigated (e.g., Etienne et al. 1990; Krichmar et al. 2005) and a simple example is presented in figure B.1c.

B.2 Interaction between multiple spatial strategies

Efficient spatial navigation calls upon the ability of the subject to select the appropriate strategy according to the complexity of the task (Trullier et al., 1997; Arleo and Rondi-Reig, 2007).

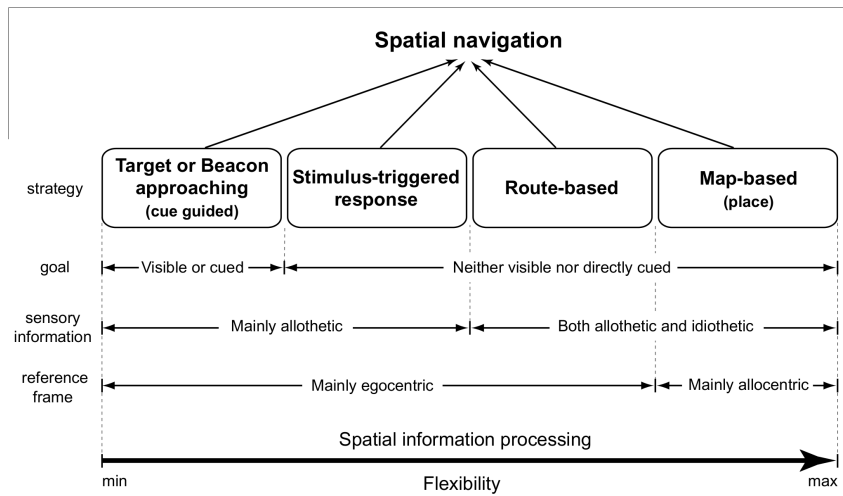


Figure B.2: Taxonomy of spatial navigation strategies

Navigation strategies are generally organized in terms of complexity and flexibility. Four types of navigation strategies have been identified, from the most simple acquisition of stereotyped stimulus-response associations, until the establishment of an elaborated representation by using the spatio-temporal relationships between cues of the environment (Trullier et al., 1997). Strategies are described in figure B.2. Target or Beacon approaching is the most simple strategy, it consists in moving towards a visible goal and needs a simple reactive behavior. It requires limited spatial information processing and refers to the acquisition of a single egocentric stimulus response association. Then, if the target is not visible, an animal can employ a stimulus-triggered response strategy to resolve the task. It consists in learning and using a set of motor Pavlovian associations. More complex, but also more flexible, the route-based strategy is defined as the ability to sequence a set of stimulus-triggered response to resolve a task. It provides the animal with the capability to anticipate the subsequent stimuli. Finally, the map-based navigation requires complex processing and needs the creation of an abstract representation of the environment. It allows the subject to perform with an high flexibility: it might be used to plan new or alternative trajectories, inferring shortcuts, and solving multiple goal tasks.

B.3 Memory used in spatial cognition

Mnesic processes implied in navigation tasks are at the core of the strategies used to resolve a navigation task (for example reach an hidden platform); A taxonomy gathering the results of psychological and neuroscience studies has been proposed by Squire to classify the different types of memory (Squire et al., 1993). In this taxonomy, long-term memory is often divided into two further main types: declarative (or explicit) memory and procedural (or implicit) memory.

Declarative memory (“knowing what”) is the memory of facts and events, and refers to those memories that can be consciously recalled. Declarative memory is sometimes referred to as explicit memory, because it consists of information explicitly stored and retrieved. Procedural memory (“knowing how”) is the unconscious memory of skills and “how to do things”, particularly the use of objects or movements of the body, such as playing a instrument or hitting a ball with a tennis racket. Procedural memory is sometimes referred to as implicit memory, because previous experiences are used when performing a task without explicit and conscious awareness of these previous experiences.

Spatial cognition requires both declarative and procedural learning in order to elaborate multimodal representations supporting spatial behavior (Arleo and Rondi-Reig, 2007). Declarative learning allows spatiotemporal relations between multiple cues or events to be encoded (O’Keefe and Conway, 1978; Eichenbaum, 2001). Procedural learning mediates the acquisition of an ensemble of procedures to solve a navigation task (Whishaw, 1985; Whishaw and Mittleman, 1986; Whishaw, 1991). At a low level, procedural learning optimises goal-directed trajectories (locally in space and time) through sensorimotor adaptation (Cain and Saucier, 1996). At a higher-level, it participates in inhibiting non-adaptive behaviours that may reduce navigation efficiency (e.g. thigmotaxic behaviour; Mittelstaedt and Mittelstaedt, 1973; Leggio et al., 1999), and regulating the exploration-exploitation balance for optimal strategy selection (Leggio et al., 1999; Mandolesi et al., 2003). In a navigation task, declarative and procedural memories permits respectively to answer the questions “where is the goal” and “how to optimally reach it”. The two types of memory are acquired simultaneously during the execution of a task.

The expression of both type of memories in navigation tasks has been demonstrated in many studies. For example, Morris et al. (1982) observed

that rats are able to retrieve a specific location from any departure point in the environment, only by using distal cues (allothetic information). This strategy calls upon the declarative memory (Morris, 1984; Morris et al., 1982). Furthermore, Whishaw and Mittleman (1986) showed that animals performing a navigation task have a tendency to reproduce a set of stereotyped actions during the realization of a trajectory, thus suggesting the use of procedural memory (Whishaw and Mittleman, 1986).

These findings and many others demonstrate that declarative and procedural memories are fundamental to spatial cognition. Depending on the task being performed, the type of information available, and the strategy used, one memory can be privileged over the other: the four types of strategies previously described engage the procedural and declarative memories at different levels.

On the one hand, target or beacon approaching strategy is more related to procedural memory since it results from simple stimulus-response associations that lead to an adapted sensory-motor response. On the other hand, map-based navigation strategy needs the encoding of a cognitive map (an abstract map of the environment where spatial cues are related one to each other) and hence calls upon declarative memory. Importantly, in this latter strategy, the procedural component is implicated at both local and global level. Locally, procedural memory might help to optimally correct the movements of the navigating agent, and globally it drives the exploration behavior of the animal to optimally resolve the task. It is important to note that route-based strategy does not require the implementation of a cognitive map, but needs to encode spatio-temporal relations between the procedural learned associations and is therefore related to declarative memory (see Trullier et al., 1997; Arleo and Rondi-Reig, 2007 for review).

B.4 Paradigms and protocols

Many experimental protocols have been developed and used to study spatial cognition in rodents; for example to determine the navigation strategy used by animals. Some of the most used paradigms are the cross maze (Tolman et al., 1946), the radial maze (Olton and Samuelson, 1976), and the Morris watermaze (Morris, 1981)

The use of these paradigms have demonstrated that animals could use a combination of previously described strategies to resolve a navigation

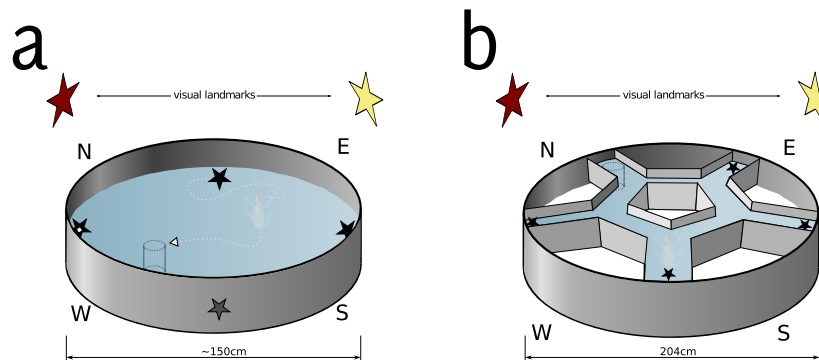


Figure B.3: Example of paradigms used in the study of spatial cognition **a**. The Morris watermaze (Morris, 1981) is a circular pool filled with water which has extensively been used in the study of spatial cognition, for example to demonstrate that rodents encode allothetic spatial cues in a cognitive map and use it to resolve a navigation task. **b**. The starmaze (Rondi-Reig et al., 2005) The starmaze consists of five alleys forming a central pentagonal ring and five alleys radiating. This paradigm has been used to characterize the different navigation strategies involved during a spatial behavior.

task and that different strategies can be encoded simultaneously (see for example Whishaw and Mittleman, 1986).

Since the description of each protocol goes beyond the scope of this chapter, the next section will concentrate only on two paradigms that have been implemented in my modeling study, for which the main properties and advantages will be defined.

B.4.1 The Morris watermaze

The Morris watermaze is a circular pool (usually between 1 or 2 meters of diameter) filled with water where an escape platform is hidden a few millimeters below the surface (see figure B.3a). The water can be made opaque by the addition of a non toxic colorant. A rat or mouse is placed into the pool and must swim around the pool while searching for an exit. The need of swimming reinforces the animal desire to quickly find the platform. Generally, animals are trained for several trials. In the typical paradigm, the starting point is chosen randomly at the beginning of each trial from a set of 4 different locations. Morris (1982) has proposed that animals can locate the platform with the use of external cues, and can gradually learn to reach the hidden platform through the most direct trajectory

even if the starting point is changed after each trial. Thus, he argued that animals use a map based strategy as it was earlier suggested by Tolman in its classical task (Tolman et al., 1946; Tolman, 1948). Many parameters, such as the time spent in each quadrant of the pool, the time taken to reach the platform (latency), and the total distance traveled can be recorded to account for the behavior and learning. Many variants of the task have also been developed (e.g., Morris, 1984; Brandeis et al., 1989; Stewart and Morris, 1993), its interpretation has been contested (e.g., Sutherland et al., 1987) and later reinforced (e.g., Matthews et al., 1995). Also, the Morris water-maze is one of the most robust paradigm used to study spatial cognition in rodents.

B.4.2 The starmaze

In 2006, Rondi-Reig and his collaborators developed a new specific maze in order to characterize the different navigation strategies used during a spatial behavior (Rondi-Reig et al., 2005). The entire maze (see figure B.3b) is inscribed in a circle and all the alleys are filled with water made opaque. To solve the task, subjects have to swim to a platform located at the end of one of the alleys and hidden below the water surface. In order to learn and then perform the optimal trajectory to the goal, animals can either use distal visual cues, follow a sequence of intra-maze cues, or use a sequence of self-movements

There are two main versions of the starmaze: the *multiple strategies* version and the *allocentric* version.

The multiple strategies version of the starmaze task uses the distal visual cues and the intra-maze cues, and is embedded with two components: (i) the training component assesses the animal learning abilities, and (ii) the probe test, is designed to identify the strategy used by an animal during the training part of the task.

The allocentric version was designed in order to evaluate the ability of animals to learn a spatial navigation task using exclusively the distal visual cues. In order to learn this task and use the optimal trajectory from each departure points, animals need to encode an allocentric representation of the environment. Similar to the Morris water maze, solving this version of the starmaze task implies the ability to find a hidden platform from different starting points. However, here animals are constrained to swim in alleys that guide their movements, which permits a detailed anal-

ysis of the animals' trajectories and reduce the procedural demand of the task (Burguière et al., 2005). The allocentric version of the starmaze has been used in the presented neurocomputational study.

B.5 Structures involved in spatial cognition

The declarative and procedural components of spatial cognition are widely interrelated and involve multiple brain areas (Arleo and Rondi-Reig, 2007 for recent review). A large body of experimental work has provided evidence for a role of the hippocampal formation in declarative spatial learning (O'Keefe and Conway, 1978; Kolb et al., 1983; Eichenbaum et al., 1990; Eichenbaum, 1992; McDonald and White, 1994). Complementing the well-documented implication of basal ganglia in procedural spatial memory (Hartley and Burgess, 2005; Balleine et al., 2007; Mizumori et al., 2009), some studies have begun to elucidate the contribution of the cerebellum to this component of spatial navigation (Lalonde and Botez, 1986; Petrosini et al., 1996, 1998; Leggio et al., 1999; Gandhi et al., 2000; Joyal et al., 2001; Mandolesi et al., 2001; Burguière et al., 2005). The precise known role of the cerebellum in spatial cognition will be explained in details in the next chapter.

Other brain areas are also important for navigation; the prefrontal cortex plays a role in planning (Hok et al., 2005), the amygdala is involved in the processing of emotional and motivational information (Aggleton, 1992); finally, the parietal cortex mediates visuo-motor transformations and egocentric spatial representations (Andersen, 1995; Andersen et al., 1997; Nitz, 2006).

A clear description of each of these structures goes behind the scope of this manuscript. However, since a key role of my study is to unveil the possible implication of the cerebellum on the declarative encoding, we will discuss the main anatomical and functional properties of the hippocampus, which is thought to be involved in declarative spatial memory and high-level processing of relational spatial information.

B.5.1 The hippocampus

Subdivisions

The hippocampal formation includes the dentate gyrus (DG), the subiculum (SC) and the hippocampus proper (or cornu ammonis, CA) composed of four subfields CA1-CA4 (usually only CA1 and CA3 are considered), see figure B.4A. The hippocampus occupies a large volume in rodent brains.

Connectivity

Hippocampal afferences and efferences Two major types of input enter the hippocampal formation: (i) Inputs from neocortical areas converge through the entorhinal cortex via the perforant path. These signals carry information coming from associative areas, which process multimodal sensory information (Rolls, 1995). (ii) Inputs from subcortical areas reach the hippocampus via the fornix fiber bundle. Signals from the thalamus, the hypothalamus, the brainstem, and the amygdala, are thought to convey arousal, emotional, and autonomic information (Burgess et al., 1999). The SC forms the major output of the hippocampal formation (Amaral and Witter, 1989; Witter, 1993). Until the mid-1970s it was thought that the hippocampal output was predominantly carried by the fornix. More recent studies have shown that an important pathway for the hippocampal outflow consists of the non-fornical projection to the deep layers of the entorhinal cortex (dEC). From dEC, information is sent to a variety of cortical areas (Witter, 1993; Insausti et al., 1997).

Intrinsic hippocampal circuit The highly processed information from neocortical areas reaches the entorhinal cortex (EC). Entorhinal cells, via the perforant path, project to DG granule cells, CA3/CA1 cells, and subicular cells (figure B.4B). Furthermore, EC exhibits intrinsic recurrent connectivity. The dentate gyrus sends efferents to CA3 via the hippocampal mossy fibers and each hippocampal granule cell (Hgc) projects approximately onto 14 pyramidal cells only (Amaral, 1993). DG has also intrinsic projections: Hgcs generate collateral synapses that terminate on the polymorphic DG region (Amaral and Witter, 1989). CA3 pyramidal cells form a recurrent network through the Shaffer collaterals, but the latter fiber bundle is also used to synapse CA1 and subicular cells. CA1 neurons send

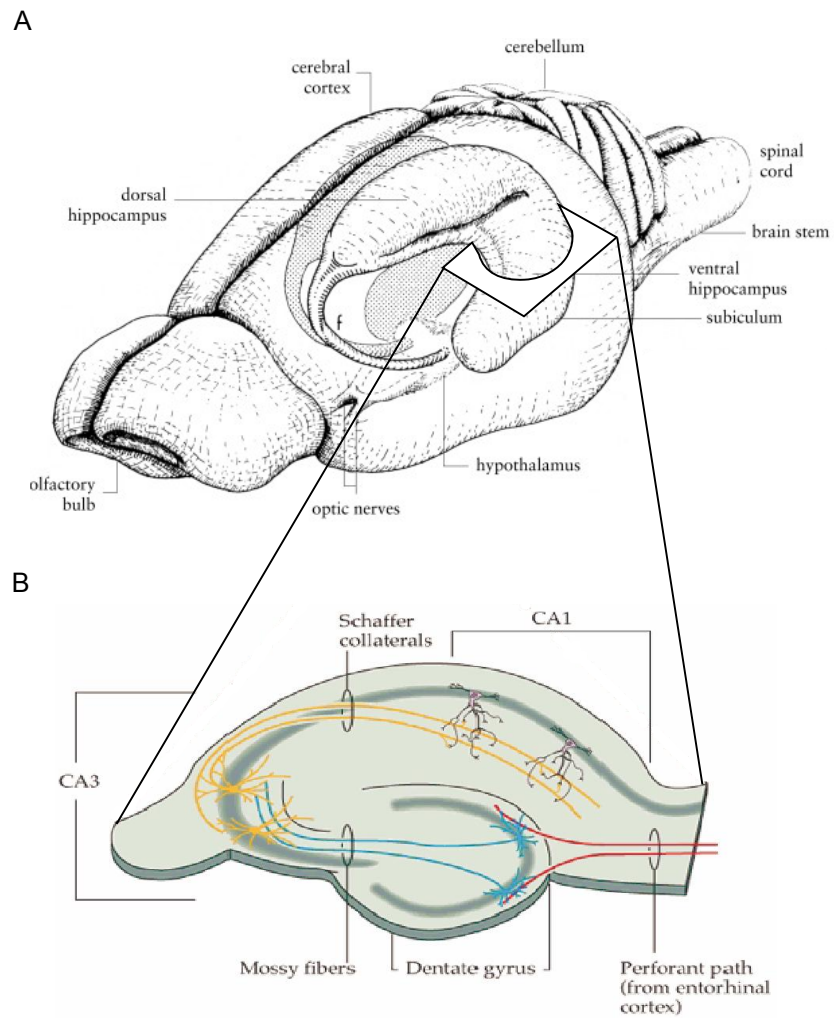


Figure B.4: Hippocampus of the rat from (Cheung and Cardinal, 2005). **(A)** Position of the hippocampus within the brain. **(B)** Circuitry of the hippocampus. Transversal section.

their output to entorhinal as well as subicular cells via the angular bundle (Amaral et al., 1991). Finally, SC projects onto the EC. The hippocampal circuit can be approximated by a feed-forward loop (Amaral and Witter, 1989): information enters the loop via EC, proceeds towards DG, then to CA3 and CA1, and finally arrives to SC which closes the loop by projecting to EC.

B.6 Cellular bases of spatial cognition

B.6.1 Hippocampal place cells

An extensive body of experimental work has investigated the neural bases of spatial learning capabilities. In particular, extracellular single-cell recordings have largely focused on the properties of pyramidal neurones in the hippocampal formation. This limbic region has been thought to mediate spatial memory functions ever since location-sensitive cells, called *place cells*, were found in the hippocampus of freely moving rats (O'Keefe and Dostrovsky, 1971; see also place cell recordings in humans Ekstrom et al., 2003). A typical hippocampal place cell discharges strongly when the animal crosses a cell-specific region of the environment, the *place field* of the cell, and is usually silent elsewhere in the environment (see figure B.5). The place cell population represents a large part of the hippocampal cells, estimated between 40 and 70 % over 1000000 neurons (Muller et al., 2001). These place cells can be found in the CA1 and CA3 subfields of the dorsal hippocampus (O'Keefe and Dostrovsky, 1971), as well as the ventral hippocampus (even if the spatial selectivity is coarser there, Poucet et al., 1994; Jung et al., 1994).

Essential place field properties. Several important properties of place fields can be pointed out (see Arleo and Gerstner, 2000; Alvernhe, 2010 for more details). In a small and simple open field environment, a typical place field can be approximated by a two-dimensional single-peak Gaussian surface (Muller et al., 1991; Burgess et al., 1999), but they may also exhibit multi-peak fields within a single environment (O'Keefe and Conway, 1978), particularly in larger scale environments (Fenton et al., 2008; Henriksen et al., 2009). Also, Kjelstrup et al. (2008) have recently shown a scale gradient of place fields. This gradient property may support the

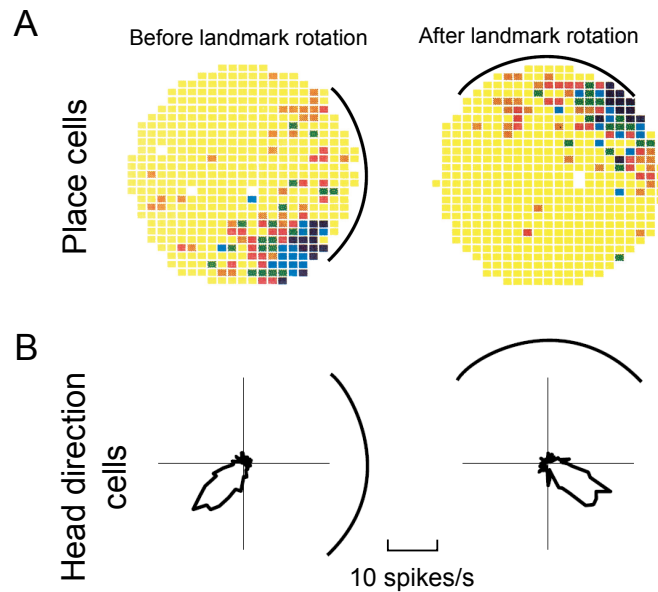


Figure B.5: Hippocampal place fields and head-direction cells (from Arleo and Rondi-Reig, 2007) (A) Sample of receptive field of a place cell recorded from the rat hippocampus. The plots show the mean discharge of the neuron (blue and yellow denote peak and baseline firing rates, respectively) as a function of the animal position within the environment (a cylindrical arena with a cue card attached to inner wall). The location-selective response of the cell is controlled by the cue card in that rotating the card by 90° induces an equivalent rotation of the receptive field. Adapted from Muller et al. (1987). (B) Sample of tuning curve of a head direction cell recorded in the rat anterodorsal thalamic nucleus. The polar plots indicate that the cell has a unique “preferred” direction and that the response of the cell is controlled by the visual landmark. Data by Arleo and Wiener.

representation of spatial contexts at different scales, to adapt the spatial code to the size and/or the complexity of the environment. Establishing a place field representation in a novel environment takes a relatively short time from a few minutes to 30 minutes (Austin et al., 1993; Wilson and McNaughton, 1993), with a difference between CA1 and CA3 place cells (Lee et al., 2004).

A dense population code. It is important to note that hippocampal spatial code is a population code. Place fields are generally a few times larger than the animal's size (Burgess et al., 1999), which do not provide a precise single-cell coding. Also, the activity of individual place cells can be extremely variable from one run through the firing field to another, a phenomenon referred to as *overdispersion* (Fenton and Muller, 1998). However, the proportion of active and location-selective pyramidal cells in the CA1 subfield in a given environment is very large, about 30 – 40 % (Wilson and McNaughton, 1993). This results in highly overlapping place fields, uniformly distributed over the environment (O'Keefe and Conway, 1978; Thompson and Best, 1989), which is usually referred to as a *dense* spatial representation (Willmore and Tolhurst, 2001). As a consequence, accurate space decoding may be achieved by taking into account the ensemble, rather than single-cell, firing activity (Muller et al., 1987; Wilson and McNaughton, 1993; Brown et al., 1998). Two properties of the place cell population are also interesting to mention. First, place cells are not topographically organized: two cells coding for neighboring locations do not seem to be anatomically adjacent (O'Keefe and Conway, 1978; Thompson and Best, 1989). Second, the spatial relationships between place cells are not preserved across environments: two cells coding for neighboring locations in one environment may not code for neighboring locations in another environment (O'Keefe and Conway, 1978; Thompson and Best, 1989).

Main determinants of place cells activity. Hippocampal place fields strongly depend on distal visual cues (O'Keefe and Conway, 1978) but to a lower extent on local landmarks (Cressant et al., 1997; Lenck-Santini et al., 2005). Also, the more stable an allothetic cue is perceived by the animal, the higher its influence upon place cell dynamics (Knierim et al., 1995). The geometry of an environment, such as its scale (Muller et al.,

1987; Kjelstrup et al., 2008) and its shape (O'Keefe and Burgess, 1996), seems to influence hippocampal place cell activity directly. Despite their dependence on allothetic signals, place cells exhibit clean location selectivity even when external cues are absent (e.g. in darkness, Quirk et al., 1990) or ambiguous (e.g. symmetric environment, Sharp et al., 1990). This suggests that hippocampal cells are also influenced by idiothetic signals, such as vestibular as well as optical flow signals (Sharp et al., 1995).

B.6.2 Grid and head direction cells.

Place cells are not the only examples of neurons with spatial-related discharge properties. Recent electrophysiological findings have brought evidence for a key contribution of the entorhinal cortex (within the hippocampal formation) to the spatial memory function (Hafting et al., 2005). Indeed, neurons in the medial entorhinal cortex have been found that exhibit spatially-selective discharges with multiple receptive fields (in contrast to most place cells) that cover the environment with regularly spaced hexagonal patterns. It has been suggested that these neurones, termed *grid cells*, could mediate the encoding of spatial metric information necessary for the path integration process (see McNaughton et al., 2006 for a review). Complementing the allocentric place responses of hippocampal neurones, *head direction cells* provide an allocentric representation of the orientation of the animal (see Wiener and Taube, 2005 for a review). The discharge of these neurones is highly correlated with the direction of the head of the animal in the azimuthal plane, regardless of the orientation of the head relative to the body, of the animal's ongoing behaviour and of its spatial location. Each head direction cell is selective for one specific 'preferred' direction, and the preferred directions of a population of head direction cells tend to be evenly distributed over 360 degrees.

Appendix C

Sleep consolidation in procedural tasks

C.1 Simulated finger tapping task

A simplified version of the coupling architecture has been validated on a second procedural paradigm (see Passot et al., 2010), a sequential finger tapping task proposed by Walker and Stickfold (2004). A brief account of the protocol and results are presented in this section

C.1.1 Protocol

This task requires subjects to press four numeric keys on a standard computer keyboard with the fingers of their non-dominant hand. A five elements sequence, 4-1-3-2-4, must be repeated as quickly and accurately as possible for a period of 30 s. Each 30 s trial is then scored according to the number of complete sequences achieved. The entire training consists of 12 trials (with 30 s rest periods between trials). The score from the first training trial is taken as a baseline, while the score from the final trial is taken as the post-training performance. 30 simulated subjects were allocated into 2 groups (A and B). Group A undergoes online adaptation only, whereas group B undergoes both online and offline learning.

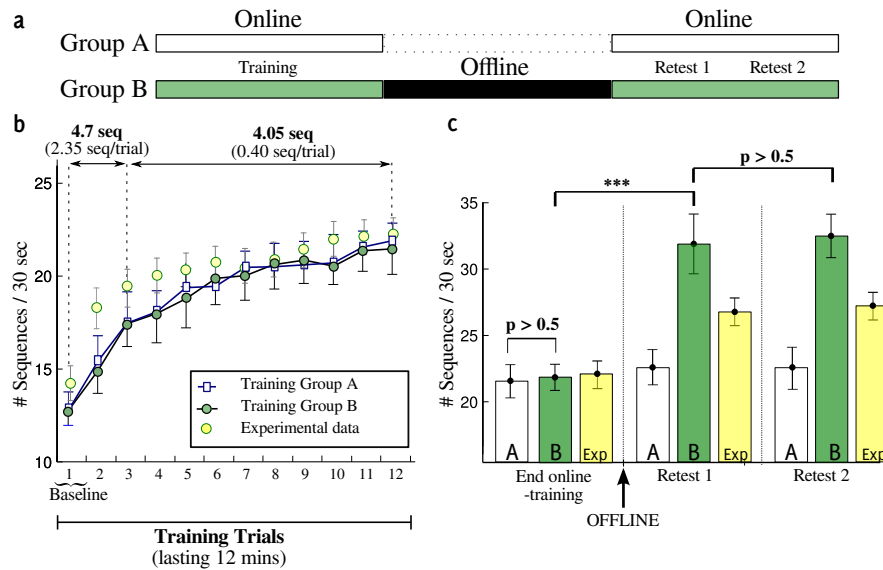


Figure C.1: Sequential finger tapping task. (a) Experimental protocol. (b,c) Simulation and experimental results (from (Walker and Stickgold, 2004)).

C.1.2 Results

The protocol and results are presented in Figs. C.1a, and b,c, respectively. Subjects from groups A and B show similar performance improvement across the 12 training trials, with a non significant difference of 4.8% observed at the end of training (Figs. C.1b). Overall performances improved by about 64% across the 12 training trials, with 40% occurring across the first three trials, and the remaining 24% occurring at a slower but relatively constant rate across the final ten trials. Figs. C.1c illustrates the effect of offline learning and consolidation. It is shown that subjects from group B, after offline training, exhibit a significant improvement compared to control group A (probe test 1). They display no further significant improvement with additional online training (probe test 2).

Figs. C.1b,c also show the correspondence between simulation results and experimental data obtained on human subjects (Walker and Stickgold, 2004).

C.2 A new task to elucidate the role of sleep in procedural learning

Recent scientific discoveries suggest that insights — a mental restructuring that leads to a sudden gain of explicit knowledge — can be gained through sleep. For example, in an experiment where subjects performed a cognitive task, Wagner et al. (2004) have shown that many subjects gained insight into an hidden rule after sleep, compared to subjects who followed the same protocol but with nocturnal or daytime wakefulness. Authors concluded that sleep, by restructuring new memory representations, facilitates extraction of explicit knowledge (Wagner et al., 2004). Also, a recent study has suggested that an interaction between working memory related structures (e.g., the prefrontal cortex) and the cerebellum could play a role in intuition (Vandervert et al., 2007).

I propose here a task to elucidate if sleep can (*i*) enhance performances in procedural tasks where the motor sequence to consolidate has been hidden — and hence not been made available to awareness — in random noise, and (*ii*) provide insights on this hidden sequence. More importantly, this task is proposed to relate the role of the cerebellum in sleep consolidation processes.

C.2.1 Protocol

This task is inspired from Walker et al. (2002)'s finger tapping task, that has been used to demonstrate the enhancing role of sleep in procedural memory. Our task requires subjects to press four numeric keys on a standard computer keyboard with the fingers of their non-dominant hand. During phase 1, numbers are presented to each subject who must type the corresponding key as quickly and accurately as possible for a period of 30 s. Each 30 s trial is then scored according to the number of key accurately typed. The entire training consists of 12 trials (with 30 s rest periods between trials). The score from the final trial is taken as the post-training performance. A second phase (phase 2) is performed after 8 hours. All the subjects are tested only one trial in which they must repeat a predefine sequence of key (e.g., 4-1-3-2-4). Importantly, subjects are not aware of the sequence before the trial starts. Subjects are scored according to the number of complete sequences achieved.

Control Groups			
Group A	random Phase 1	Sleep	sequence Phase 2
Group B	random Phase 1	Wakefulness	sequence Phase 2
Group C	rdm - seq - rdm Phase 1	Sleep	sequence Phase 2
Group D	rdm - seq - rdm Phase 1	Wakefulness	sequence Phase 2
Cerebellar Groups			
Group E	rdm - seq - rdm Phase 1	Sleep	sequence Phase 2
Group F	rdm - seq - rdm Phase 1	Wakefulness	sequence Phase 2

Figure C.2: Protocol of the proposed finger-tapping task. At phase 1, a filled green oval indicates that the numbers to be typed are generated randomly, a filled orange oval indicates that the predefined sequence key of phase 2 (e.g., 4-1-3-2-4) is inserted during the random generation of numbers. In phase 2, all subjects are tested only one trial in which they must repeat a predefined sequence of key (e.g., 4-1-3-2-4). Groups A, C and E are allowed to sleep, whereas group B, D and F have to stay awake in order to exclude sleep consolidation. (rdm = random numbers, seq: sequence)

In the experiment, subjects are proposed to be allocated into 4 groups (A, B, C and D). Whereas for groups A and B, the numbers to be typed are generated randomly, in group C and D, we insert, during the random generation of numbers, the predefined sequence of key the subject will have to type during phase 2 (in our example, 4-1-3-2-4). The number of apparition of the sequence in a trial should be chosen judiciously: it should appear as often as possible but without being perceptible to the subject.

Phase 1 is followed by 8 h of nocturnal sleep for groups A and C, and by 8 h daytime (or nighttime) wakefulness for groups B and D.

A prototype of the test (with instructions in French) is available at the following address: <http://anc.snv.jussieu.fr/test/>. For each participant, the group is determined randomly and is unknown to the subject.

C.2.2 Expected results

If we expect to have similar performances for groups A B C and D at the end of the first phase, we are more interested at the intergroup performance at phase 2. If the hypothesis of an implicit extraction and consoli-

dation of an unaware repetitive experience during sleep holds to be true, we expect the following results for phase 2:

- group C should have better performance than group A.
- group D should have better performance than group B.
- group C should have better performance than group D.
- group B should have better performance than group A.

We could also support the role of sleep in insight by addressing the following question: is a participant of group C, resp. D, able to tell the sequence that has been inserted (*i*) at the end of phase 1 (time t_1), (*ii*) before the start of phase 2 (time t_2)? If subjects from group C can intuit the sequence at t_2 (but not at t_1), whereas subjects of group D can not at both time t_1 and t_2 , this will give additional material for the "insight" role of sleep.

Other questions could be addressed with this simple protocol. For example, we would like to study if the explicit knowledge of the sequence could alter the consolidation process during sleep. This could be tested by adding two groups (one sleep and one sleep-deprived), at which we tell the instruction and sequence of phase 2 at the end of phase 1.

Also, we would like to address the role of the cerebellum in sleep consolidation process by using such a protocol. More precisely, we ask the following questions: (*i*) Could the enhancement of performance in procedural tasks involve the cerebellum? (*ii*) If so, is this consolidation the reflexion of an additional learning taking place in internal models located in the cerebellum? (*iii*) Eventually, if an insight role of sleep is validated, could this insight role be dependent of a forward model located in the cerebellum? To answer these questions, the same task should be extended by testing two more groups of cerebellar patients (E and F) in the same condition than group C and D, respectively.

We expect to have similar performances for group E and F at the end of stage 1. However, both groups should converge to lower level compare to group A,B,C and D, due to the postulated role of the cerebellum in procedural tasks. Furthermore, if the cerebellum plays an important role in consolidating the procedural memory during sleep, we expect for group E and F to have similar performances at the end of phase 2, or with a gain substantially reduce compared to the one observed between group C and

D. Eventually, supposing that the insight role of sleep is validated in our protocol using subjects from group C, we expect that subjects from group E and F could not intuit the sequence. This would favor a role of the cerebellum in intuitive process, as suggested by Vandervert et al. (2007) and more recently by Ito (2008).

Bibliography

- E. a Rancz, T. Ishikawa, I. C. Duguid, P. Chadderton, S. Mahon, and M. Häusser. High-fidelity transmission of sensory information by single cerebellar mossy fibre boutons. *Nature*, 450(7173):1245–8, 2007.
- H. Ackermann, K. Mathiak, and A. Riecker. The contribution of the cerebellum to speech production and speech perception: clinical and functional imaging data. *Cerebellum (London, England)*, 6(3):202–213, 2007.
- E. Adrian. Discharge frequencies in the cerebral and cerebellar cortex. *The Journal of Physiology*, 83:33, 1935.
- J. Aggleton. *The amygdala: neurobiological aspects of emotion, memory, and mental dysfunction*. Wiley-Liss New York, 1992.
- C. D. Aizenman and D. J. Linden. Rapid, synaptically driven increases in the intrinsic excitability of cerebellar deep nuclear neurons. *Nat. Neurosci.*, 3(2):109–111, 2000.
- C. D. Aizenman, P. B. Manis, and D. J. Linden. Polarity of long-term synaptic gain change is related to postsynaptic spike firing at a cerebellar inhibitory synapse. *Neuron*, 21(4): 827–835, 1998.
- J. S. Albus. A theory of cerebellar function. *Math. Biosci.*, 10(1-2):25–61, 1971.
- G. Allen and E. Courchesne. Differential effects of developmental cerebellar abnormality on cognitive and motor functions in the cerebellum: an fMRI study of autism. *The American Journal of Psychiatry*, 160(2):262–273, 2003.
- G. I. Allen and N. Tsukahara. Cerebrocerebellar communication systems. *Physiological Reviews*, 54(4):957–1006, 1974.
- J. Altman and S. A. Bayer. Time of origin and distribution of a new cell type in the rat cerebellar cortex. *Experimental Brain Research*, 29(2):265–274, 1977.
- A. Alvernhe. *Codage de la topologie de l'espace dans l'hippocampe: approches comportementale et électrophysiologique*. PhD thesis, Université de Provence, Marseille, 2010.
- D. Amaral. Emerging principles of intrinsic hippocampal organization. *Curr. Opin. Neurobiol.*, 3(2):225–229, 1993.

- D. Amaral and M. Witter. The three-dimensional organization of the hippocampal formation: a review of anatomical data. *Neuroscience*, 31(3):571–591, 1989.
- D. Amaral, C. Dolorfo, and P. Alvarez-Royo. Organization of ca1 projections to the subiculum: a pha-l analysis in the rat. *Hippocampus*, 1(4):415–435, 1991.
- D. G. Amaral, C. M. Schumann, and C. W. Nordahl. Neuroanatomy of autism. *Trends Neurosci.*, 31(3):137–145, 2008.
- F. Amzica and M. Steriade. Short- and long-range neuronal synchronization of the slow (≈ 1 Hz) cortical oscillation. *J Neurophysiol*, 73(1):20–38, 1995.
- R. Andersen. Encoding of intention and spatial location in the posterior parietal cortex. *Cerebral Cortex*, 5(5):457–469, 1995.
- R. Andersen, L. Snyder, D. Bradley, and J. Xing. Multimodal representation of space in the posterior parietal cortex and its use in planning movements. *Annu. Rev. Neurosci.*, 20:303–330, 1997.
- F. C. Anderson and M. G. Pandy. Dynamic Optimization of Human Walking. *Journal of Biomechanical Engineering*, 123(5):381, 2001.
- G. Andersson and O. Oscarsson. Projections to lateral vestibular nucleus from cerebellar climbing fiber zones. *Experimental Brain Research*, 32(4):549–564, 1978.
- N. C. Andreasen and R. Pierson. The role of the cerebellum in schizophrenia. *Biological Psychiatry*, 64(2):81–88, 2008.
- D. E. Angelaki, T. A. Yakusheva, A. M. Green, J. D. Dickman, and P. M. Blazquez. Computation of egomotion in the macaque cerebellar vermis. *Cerebellum*, 9(2):174–182, 2010.
- E. Aoki, R. Semba, and S. Kashiwamata. New candidates for GABAergic neurons in the rat cerebellum: an immunocytochemical study with anti-GABA antibody. *Neurosci. Lett.*, 68(3):267–271, 1986.
- R. Apps and M. Garwicz. Anatomical and physiological foundations of cerebellar information processing. *Nat. Rev. Neurosci.*, 6(4):297–311, 2005.
- R. Apps and R. Hawkes. Cerebellar cortical organization: a one-map hypothesis. *Nat. Rev. Neurosci.*, 10(9):670–681, 2009.
- A. Arata and M. Ito. Purkinje cell functions in the in vitro cerebellum isolated from neonatal rats in a block with the pons and medulla. *Neuroscience Research*, 50(3):361–367, 2004.
- A. Arenz, R. A. Silver, A. T. Schaefer, and T. W. Margrie. The contribution of single synapses to sensory representation in vivo. *Science*, 321(5891):977–80, 2008.
- A. Arleo and W. Gerstner. Spatial cognition and neuro-mimetic navigation: a model of hippocampal place cell activity. *Biological Cybernetics*, 83(3):287–299, 2000.

- A. Arleo and L. Rondi-Reig. Multimodal sensory integration and concurrent navigation strategies for spatial cognition in real and artificial organisms. *Journal of Integrative Neuroscience*, 6(3):327–366, 2007.
- A. Arleo, F. Smeraldi, and W. Gerstner. Cognitive navigation based on nonuniform Gabor space sampling, unsupervised growing networks, and reinforcement learning. *IEEE T. Neural. Networ.*, 15:639–652, 2004.
- S. Armano, P. Rossi, V. Taglietti, and E. D’Angelo. Long-term potentiation of intrinsic excitability at the mossy fiber-granule cell synapse of rat cerebellum. *J. Neurosci.*, 20(14):5208–5216, 2000.
- C. Assisi, M. Stopfer, G. Laurent, and M. Bazhenov. Adaptive regulation of sparseness by feedforward inhibition. *Nat. Neurosci.*, 10(9):1176–1184, 2007.
- P. Attwell, S. Cooke, and C. Yeo. Cerebellar function in consolidation of a motor memory. *Neuron*, 34(6):1011–1020, 2002.
- P. J. E. Attwell, S. Rahman, and C. H. Yeo. Acquisition of eyeblink conditioning is critically dependent on normal function in cerebellar cortical lobule HVI. *J. Neurosci.*, 21(15):5715–5722, 2001.
- K. Austin, L. White, and M. Shapiro. Short- and long-term effects of experience on hippocampal place fields. In *Society for Neuroscience Abstracts*, page 19:263, 1993.
- J. Babinski. De l’asynergie cerebelleuse. *Reviews in Neurology*, 7:806–816, 1899.
- B. W. Balleine, M. R. Delgado, and O. Hikosaka. The role of the dorsal striatum in reward and decision-making. *J. Neurosci.*, 27(31):8161–8165, 2007.
- M. F. Bear. Bidirectional synaptic plasticity: from theory to reality. *Philosophical Transactions of the Royal Society of London Series B Biological Sciences*, 358(1432):649–655, 2003.
- C. Bell, D. Bodznick, J. Montgomery, and J. Bastian. The generation and subtraction of sensory expectations within cerebellum-like structures. *Brain, Behavior and Evolution*, 50 Suppl 1:17–31, 1997.
- R. Bellman. *Dynamic Programming*, volume 11 of RAND CORPORATION. *Research studies*. Princeton University Press, 1957.
- K. Benchenane, A. Peyrache, M. Khamassi, P. L. Tierney, Y. Gioanni, F. P. Battaglia, and S. I. Wiener. Coherent theta oscillations and reorganization of spike timing in the hippocampal- prefrontal network upon learning. *Neuron*, 66:921–936, 2010.
- F. Bengtsson and G. Hesslow. Cerebellar control of the inferior olive. *The Cerebellum*, 5(1):7–14, 2006.
- A. Berthoz and I. Viaud-Delmon. Multisensory integration in spatial orientation. *Curr. Opin. Neurobiol.*, 9(6):708–712, 1999.

- A. Berthoz, I. Israël, P. Georges-François, R. Grasso, and T. Tsuzuku. Spatial memory of body linear displacement: what is being stored? *Science*, 269(5220):95–98, 1995.
- W. Bialek, F. Rieke, R. R. De Ruyter Van Steveninck, and D. Warland. Reading a neural code. *Science*, 252(5014):1854–1857, 1991.
- E. Bizzi, N. Accornero, W. Chapple, and N. Hogan. Posture control and trajectory formation during arm movement. *J. Neurosci.*, 4(11):2738–2744, 1984.
- S.-J. Blakemore and A. Sirigu. Action prediction in the cerebellum and in the parietal lobe. *Experimental brain research. Experimentelle Hirnforschung. Expérimentation cérébrale*, 153(2):239–45, 2003.
- T. A. Blenkinsop and E. J. Lang. Block of inferior olive gap junctional coupling decreases Purkinje cell complex spike synchrony and rhythmicity. *J. Neurosci.*, 26(6):1739–1748, 2006.
- G. Bosco and R. E. Poppele. Proprioception from a spinocerebellar perspective. *Physiological reviews*, 81(2):539–68, 2001.
- A. C. Bostan, R. P. Dum, and P. L. Strick. The basal ganglia communicate with the cerebellum. *Proc. Natl. Acad. Sci. U. S. A.*, 107(18):8452–8456, 2010.
- T. Botez-Marquard and M. I. Botez. Visual memory deficits after damage to the anterior commissure and right fornix., 1992.
- E. S. Boyden, A. Katoh, and J. L. Raymond. Cerebellum-dependent learning: the role of multiple plasticity mechanisms. *Annu. Rev. Neurosci.*, 27(1):581–609, 2004.
- V. Braintenberg and R. P. Atwood. Morphological observations on the cerebellar cortex. *Journal of Comparative Neurology*, 109(1):1–33, 1958.
- R. Brandeis, Y. Brandys, and S. Yehuda. The use of the Morris Water Maze in the study of memory and learning. *International Journal of Neuroscience*, 48(1-2):29–69, 1989.
- P. Brodal. The corticopontine projection in the rhesus monkey. Origin and principles of organization. *Brain: A journal of neurology*, 101(2):251–283, 1978.
- V. B. Brooks and W. T. Thach. *Cerebellar control of posture and movement*, pages 877–946. Am.Physiol.Soc., 1981.
- D. M. Broussard and C. D. Kassardjian. Learning in a Simple Motor System. *Learning Memory*, pages 127–136, 2004.
- E. Brown, L. Frank, D. Tang, M. Quirk, and M. Wilson. A statistical paradigm for neural spike train decoding applied to position prediction from ensemble firing patterns of rat hippocampal place cells. *J. Neurosci.*, 18(18):7411, 1998.

- V. H. Brun, M. K. Otnass, S. Molden, H.-A. Steffenach, M. P. Witter, M.-B. Moser, and E. I. Moser. Place cells and place recognition maintained by direct entorhinal-hippocampal circuitry. *Science*, 296(5576):2243–2246, 2002.
- N. Brunel, V. Hakim, P. Isope, J.-P. Nadal, and B. Barbour. Optimal information storage and the distribution of synaptic weights: perceptron versus Purkinje cell. *Neuron*, 43(5):745–757, 2004.
- D. Bullock, J. C. Fiala, and S. Grossberg. A Neural Model of Timed Response Learning in the Cerebellum. *Neural Networks*, 7(6/7):1101–1114, 1994.
- N. Burgess, K. Jeffery, and J. O’Keefe. Integrating hippocampal and parietal functions: a spatial point of view. In K. Jeffery, N. Burgess, and J. O’Keefe, editors, *The Hippocampal and Parietal Foundations of Spatial Cognition*, page 3–29. Oxford University Press, 1999.
- N. Burgess, E. A. Maguire, and J. O’Keefe. The human hippocampus and spatial and episodic memory. *Neuron*, 35:625–641, 2002.
- E. Burguière, A. Arleo, M. reza Hojjati, Y. Elgersma, C. I. De Zeeuw, A. Berthoz, and L. Rondi-Reig. Spatial navigation impairment in mice lacking cerebellar LTD: a motor adaptation deficit? *Nat. Neurosci.*, 8(10):1292–4, 2005.
- E. Burguière, A. Arabo, F. Jarlier, C. I. D. Zeeuw, and L. Rondi-Reig. Role of the cerebellar cortex in conditioned goal-directed behavior. *J Neurosci*, 30(40):13265–13271, 2010.
- D. P. Cain and D. Saucier. The neuroscience of spatial navigation: focus on behavior yields advances. *Reviews in the Neurosciences*, 7(3):215–231, 1996.
- D. Cantelmi, T. A. Schweizer, and M. D. Cusimano. Role of the cerebellum in the neurocognitive sequelae of treatment of tumours of the posterior fossa: an update. *The lancet oncology*, 9(6):569–576, 2008.
- R. R. Carrillo, E. Ros, C. Boucheny, and O. J. D. Coenen. A real-time spiking cerebellum model for learning robot control. *Biosystems*, 94(1-2):18–27, 2008.
- J. Caston, C. Chianale, N. Delhay-Bouchaud, and J. Mariani. Role of the cerebellum in exploration behavior. *Brain Res*, 808(2):232–237, 1998.
- P. Chadderton, T. W. Margrie, and M. Häusser. Integration of quanta in cerebellar granule cells during sensory processing. *Nature*, 428(6985):856–60, 2004.
- T. Cheung and R. Cardinal. Hippocampal lesions facilitate instrumental learning with delayed reinforcement but induce impulsive choice in rats. *BMC Neurosci*, 13:6–36, 2005.
- E. Chorev, Y. Yarom, and I. Lampl. Rhythmic episodes of subthreshold membrane potential oscillations in the rat inferior olive nuclei in vivo. *The Journal of Neuroscience: The Official Journal of the Society for Neuroscience*, 27(19):5043–52, 2007.

- K. M. Christian and R. F. Thompson. Neural substrates of eyeblink conditioning: acquisition and retention. *Learning & Memory*, 10(6):427–455, 2003.
- E. Clarke and C. D. O'Malley. *Chapter 11 - Cerebellum*, page 951. Norman Publishing, 1996.
- D. M. Clower, R. P. Dum, and P. L. Strick. Basal ganglia and cerebellar inputs to 'AIP'. *Cerebral Cortex*, 15(7):913–920, 2005.
- M. Coesmans, J. T. Weber, C. I. De Zeeuw, and C. Hansel. Bidirectional parallel fiber plasticity in the cerebellum under climbing fiber control. *Neuron*, 44(4):691–700, 2004.
- T. S. Collett, B. A. Cartwright, and B. A. Smith. Landmark learning and visuo-spatial memories in gerbils. *Journal of Comparative Physiology A*, 158(6):835–851, 1986.
- C. Compoint, C. Buisseret-Delmas, M. Diagne, P. Buisseret, and P. Angaut. Connections between the cerebellar nucleus interpositus and the vestibular nuclei: an anatomical study in the rat. *Neurosci. Lett.*, 238(3):91–94, 1997.
- J. L. Contreras-Vidal, S. Grossberg, and D. Bullock. A neural model of cerebellar learning for arm movement control: cortico-spino-cerebellar dynamics. *Learning & Memory*, 3(6):475–502, 1997.
- R. Courtemanche and Y. Lamarre. Local field potential oscillations in primate cerebellar cortex: synchronization with cerebral cortex during active and passive expectancy. *Journal of Neurophysiology*, 93(4):2039–2052, 2005.
- R. Courtemanche, J.-P. Pellerin, and Y. Lamarre. Local field potential oscillations in primate cerebellar cortex: modulation during active and passive expectancy. *Journal of Neurophysiology*, 88(2):771–782, 2002.
- R. Courtemanche, Y. Lamarre, L. Melloni, C. Molina, M. Pena, D. Torres, and W. Singer. Local Field Potential Oscillations in Primate Cerebellar Cortex. *Journal of Neurophysiology*, 93(December 2004):2039–2052, 2010.
- V. Coutinho, H. Mutoh, and T. Knöpfel. Functional topology of the mossy fibre-granule cell–Purkinje cell system revealed by imaging of intrinsic fluorescence in mouse cerebellum. *European Journal of Neuroscience*, 20(3):740–748, 2004.
- F. Crepel, J. Mariani, and N. Delhaye-Bouchaud. Evidence for a multiple innervation of Purkinje cells by climbing fibers in the immature rat cerebellum. *Journal of Neurobiology*, 7(6):567–578, 1976.
- A. Cressant, R. Muller, and B. Poucet. Failure of centrally placed objects to control the firing fields of hippocampal place cells. *J. Neurosci.*, 17(7):2531–2542, 1997.
- F. Crevecoeur, J.-L. Thonnard, and P. Lefèvre. Optimal integration of gravity in trajectory planning of vertical pointing movements. *Journal of Neurophysiology*, 102(2):786–96, 2009.

- M. Dahhaoui, J. Lannou, T. Stelz, J. Caston, and J. M. Guastavino. Role of the cerebellum in spatial orientation in the rat. *Behavioral and Neural Biology*, 58(3):180–189, 1992a.
- M. Dahhaoui, T. Stelz, and J. Caston. Effects of lesion of the inferior olivary complex by 3-acetylpyridine on learning and memory in the rat. *J Comp Physiol A*, 171(5):657–664, 1992b.
- E. D’Angelo and C. I. De Zeeuw. Timing and plasticity in the cerebellum: focus on the granular layer. *Trends Neurosci.*, 32(1):30–40, 2009.
- E. D’Angelo, P. Rossi, S. Armano, and V. Taglietti. Evidence for NMDA and mGlu receptor-dependent long-term potentiation of mossy fiber-granule cell transmission in rat cerebellum. *Journal of Neurophysiology*, 81(1):277–87., 1999.
- E. D’Angelo, P. Rossi, D. Gall, F. Prestori, T. Nieus, A. Maffei, and E. Sola. Long-term potentiation of synaptic transmission at the mossy fiber-granule cell relay of cerebellum. *Progress in Brain Research*, 148:69–80, 2005.
- C. Darlot, L. Zupan, O. Etard, P. Denise, and A. Maruani. Computation of inverse dynamics for the control of movements. *Biological Cybernetics*, 75(2):173–186, 1996.
- E. De Schutter. Using realistic models to study synaptic integration in cerebellar Purkinje cells. *Reviews in the Neurosciences*, 10(3-4):233–245, 1999.
- E. De Schutter and J. M. Bower. An active membrane model of the cerebellar Purkinje cell II. Simulation of synaptic responses. *Journal of Neurophysiology*, 71(1):401–419, 1994.
- C. I. De Zeeuw and C. H. Yeo. Time and tide in cerebellar memory formation. *Curr. Opin. Neurobiol.*, 15(6):667–74, 2005.
- C. I. De Zeeuw, C. Hansel, F. Bian, S. K. Koekkoek, A. M. Van Alphen, D. J. Linden, and J. Oberdick. Expression of a protein kinase C inhibitor in Purkinje cells blocks cerebellar LTD and adaptation of the vestibulo-ocular reflex. *Neuron*, 20(3):495–508, 1998.
- C. I. De Zeeuw, F. E. Hoebeek, L. W. J. Bosman, M. Schonewille, L. Witter, and S. K. Koekkoek. Spatiotemporal firing patterns in the cerebellum. *Nat. Rev. Neurosci.*, 12 (June), 2011.
- P. Dean, J. Porrill, C.-F. Ekerot, and H. Jörntell. The cerebellar microcircuit as an adaptive filter: experimental and computational evidence. *Nature reviews. Neuroscience*, 11(1): 30–43, 2010.
- J. E. Desmond and J. W. Moore. Adaptive timing in neural networks: the conditioned response. *Biological Cybernetics*, 58(6):405–415, 1988.
- M. Desmurget, C. M. Epstein, R. S. Turner, C. Prablanc, G. E. Alexander, and S. T. Grafton. Role of the posterior parietal cortex in updating reaching movements to a visual target. *Nat. Neurosci.*, 2(6):563–567, 1999.

- M. R. DeWeese and M. Meister. How to measure the information gained from one symbol. *Network*, 10(4):325–340, 1999.
- M. R. Diño, F. H. Willard, and E. Mugnaini. Distribution of unipolar brush cells and other calretinin immunoreactive components in the mammalian cerebellar cortex. *Journal of Neurocytology*, 28(2):99–123, 1999.
- M. R. Diño, A. A. Perachio, and E. Mugnaini. Cerebellar unipolar brush cells are targets of primary vestibular afferents: an experimental study in the gerbil. *Experimental Brain Research*, 140(2):162–170, 2001.
- S. Diekelmann and J. Born. The memory function of sleep. *Nat. Rev. Neurosci.*, 11(2): 114–126, 2010.
- S. Dieudonne and A. Dumoulin. Serotonin-Driven Long-Range Inhibitory Connections in the Cerebellar Cortex. *J. Neurosci.*, 20(5):1837–1848, 2000.
- K. Doya. Complementary roles of basal ganglia and cerebellum in learning and motor control. *Curr. Opin. Neurobiol.*, 10:732–739, 2000.
- D. Drai, N. Kafkafi, Y. Benjamini, G. Elmer, and I. Golani. Rats and mice share common ethologically relevant parameters of exploratory behavior. *Behavioural Brain Research*, 125:133–140, 2001.
- J. C. Eccles, M. Ito, and J. Szentágothai. *The Cerebellum as a Neuronal Machine*, volume 6. Springer-Verlag, 1967.
- H. Eichenbaum. The Hippocampal System and Declarative Memory in Animals. *Journal of Cognitive Neuroscience*, 4(3):217–231, 1992.
- H. Eichenbaum. The hippocampus and declarative memory: cognitive mechanisms and neural codes. *Behavioural Brain Research*, 127(1-2):199–207, 2001.
- H. Eichenbaum, C. Stewart, and R. G. M. Morris. Hippocampal representation in spatial memory. *J. Neurosci.*, 10:3531–3542, 1990.
- H. Eichenbaum, P. Dudchenko, E. Wood, M. Shapiro, and H. Tanila. The hippocampus, memory, and place cells: is it spatial memory or a memory space? *Neuron*, 23:209–226, 1999.
- C. F. Ekerot and H. Jörntell. Parallel fibre receptive fields of Purkinje cells and interneurons are climbing fibre-specific. *European Journal of Neuroscience*, 13(7):1303–1310, 2001.
- C. F. Ekerot and B. Larson. Branching of olivary axons to innervate pairs of sagittal zones in the cerebellar anterior lobe of the cat. *Experimental Brain Research*, 48(2):185–198, 1982.
- A. D. Ekstrom, M. J. Kahana, J. B. Caplan, T. A. Fields, E. A. Isham, E. L. Newman, and I. Fried. Cellular networks underlying human spatial navigation. *Nature*, 425:184–188, 2003.

- E. N. Eskandar and J. A. Assad. Dissociation of visual, motor and predictive signals in parietal cortex during visual guidance. *Nat. Neurosci.*, 2(1):88–93, 1999.
- A. S. Etienne and K. J. Jeffery. Path integration in mammals. *Hippocampus*, 14(2):180–192, 2004.
- A. S. Etienne, E. Teroni, C. Hurni, and V. Portenier. The effect of a single light cue on homing behaviour of the golden hamster. *Animal Behaviour*, 39:17–41, 1990.
- A. S. Etienne, R. Maurer, J. Berlie, B. Reverdin, T. Rowe, J. Georgakopoulos, and V. Séguinot. Navigation through vector addition. *Nature*, 396(6707):161–164, 1998.
- G. J. O. Evans. Synaptic signalling in cerebellar plasticity. *Biology of the cell / under the auspices of the European Cell Biology Organization*, 99(7):363–78, 2007.
- A. H. Fagg, A. Shah, and A. G. Barto. A computational model of muscle recruitment for wrist movements. *Journal of Neurophysiology*, 88(6):3348–3358, 2002.
- A. Fenton and R. Muller. Place cell discharge is extremely variable during individual passes of the rat through the firing field. *Proc. Natl. Acad. Sci. U.S.A.*, 95(6):3182–3187, 1998.
- A. Fenton, H. Kao, S. Neymotin, A. Olypher, Y. Vayntrub, W. Lytton, and N. Ludvig. Unmasking the ca1 ensemble place code by exposures to small and large environments: more place cells and multiple, irregularly arranged, and expanded place fields in the larger space. *J. Neurosci.*, 28(44):11250–11262, 2008.
- J. C. Fiala, S. Grossberg, and D. Bullock. Metabotropic glutamate receptor activation in cerebellar purkinje cells as substrate for adaptive timing of the classically conditioned eye-blink response. *The Journal of Neuroscience: The Official Journal of the Society for Neuroscience*, 16(11):3760–3774, 1996.
- D. J. Field. What is the goal of sensory coding? *Neural Computation*, 6(4):559–601, 1994.
- J. A. Fiez, S. E. Petersen, M. K. Cheney, and M. E. Raichle. Impaired non-motor learning and error detection associated with cerebellar damage. *Brain*, 115:155–178, 1992.
- E. J. Fine, C. C. Ionita, and L. Lohr. The history of the development of the cerebellar examination. *Semin Neurol*, 22:375–384, 2002.
- S. Fischer, M. Hallschmid, A. L. Elsner, and J. Born. Sleep forms memory for finger skills. *Proc. Natl. Acad. Sci. U. S. A.*, 99(18):11987–11991, 2002.
- T. Flash. The control of hand equilibrium trajectories in multi-joint arm movements. *Biological Cybernetics*, 57(5):257–274, 1987.
- K. Fliessbach, P. Trautner, C. M. Quesada, C. E. Elger, and B. Weber. Cerebellar contributions to episodic memory encoding as revealed by fMRI. *NeuroImage*, 35(3):1330–1337, 2007.

- P. Flourens. *Recherches Expérimentales Sur Les Propriétés Et Les Fonctions Du Système Nerveux, Dans Les Animaux Vertébrés*. Chez Crevot, 1824.
- P. Földiák. Forming sparse representations by local anti-Hebbian learning. *Biological Cybernetics*, 64(2):165–170, 1990.
- E. Fonio, Y. Benjamini, and I. Golani. Freedom of movement and the stability of its unfolding in free exploration of mice. *Proc. Natl. Acad. Sci. U. S. A.*, 106(50):21335–21340, 2009.
- P. A. Fortier, A. M. Smith, and S. Rossignol. Locomotor deficits in the mutant mouse, Lurcher. *Experimental Brain Research*, 66(2):271–286, 1987.
- F. Foti, L. Mandolesi, D. Cutuli, D. Laricchiuta, P. De Bartolo, F. Gelfo, and L. Petrosini. Cerebellar damage loosens the strategic use of the spatial structure of the search space. *Cerebellum (London, England)*, 9(1):29–41, 2010.
- C. A. Fox and J. W. Barnard. A quantitative study of the purkinje cell dendritic branchlets and their relationship to afferent fibres. *Journal of Anatomy*, 91(Pt 3):299–313, 1957.
- Y. Fuhrman, M. A. Thomson, G. Piat, J. Mariani, and N. Delhay-Bouchaud. Enlargement of olivo-cerebellar microzones in the agranular cerebellum of adult rats. *Brain Res.*, 638(1-2):277–284, 1994.
- M. Fujita. Adaptive filter model of the cerebellum. *Biological Cybernetics*, 45(3):195–206, 1982.
- R. K. Fulbright, A. R. Jenner, W. E. Mencl, K. R. Pugh, B. A. Shaywitz, S. E. Shaywitz, S. J. Frost, P. Skudlarski, R. T. Constable, C. M. Lacadie, K. E. Marchione, and J. C. Gore. The cerebellum's role in reading: a functional MR imaging study. *Ajnr American Journal Of Neuroradiology*, 20(10):1925–1930, 1999.
- M. Fyhn, S. Molden, M. P. Witter, E. I. Moser, and M.-B. Moser. Spatial representation in the entorhinal cortex. *Science*, 305(5688):1258–1264, 2004.
- S. Gais, W. Plihal, U. Wagner, and J. Born. Early sleep triggers memory for early visual discrimination skills. *Nat. Neurosci.*, 3(12):1335–1339, 2000.
- S. Gais, M. Molle, K. Helms, and J. Born. Learning-dependent increases in sleep spindle density. *J. Neurosci.*, 22(15):6830–6834, 2002.
- C. C. Gandhi, R. G. Wiley, and T. J. Walsh. Impaired acquisition of a Morris water maze task following selective destruction of cerebellar purkinje cells with OX7-saporin. *Behavioural Brain Research*, 109(1):37–47, 2000.
- K. S. Garcia and M. D. Mauk. Pharmacological analysis of cerebellar contributions to the timing and expression of conditioned eyelid responses. *Neuropharmacology*, 37(4-5):471–480, 1998.

- A. Garenne and G. A. Chauvet. A discrete approach for a model of temporal learning by the cerebellum: in silico classical conditioning of the eyeblink reflex. *Journal of Integrative Neuroscience*, 3(3):301–318, 2004.
- J. Garrido, E. Ros, R. R. Carrillo, and E. D’Angelo. Noise reduction and time slicing facilitated by local network topologies in the cerebellum granular layer network. *in preparation*, 2007.
- A. P. Georgopoulos, A. B. Schwartz, and R. E. Kettner. Neuronal population coding of movement direction. *Science*, 233(4771):1416–1419, 1986.
- C. Ghez and W. T. Thach. *The Cerebellum*, pages 832–851. McGraw-Hill Medical, 2000.
- A. Gibson, K. Horn, and M. Pong. Activation of climbing fibers. *The Cerebellum*, 3(4): 212–221, 2004.
- J. J. Gibson. *The Perception of the Visual World*, volume 98. Houghton Mifflin, 1950.
- B. Girard and A. Berthoz. From brainstem to cortex: computational models of saccade generation circuitry. *Progress in Neurobiology*, 77(4):215–251, 2005.
- M. Glickstein. What does the cerebellum really do? *Curr. Biol.*, 17(19):R824–7, 2007.
- M. Glickstein and K. Doron. Cerebellum: connections and functions. *Cerebellum (London, England)*, 7(4):589–94, 2008.
- M. Glickstein, J. G. May, and B. E. Mercier. Corticopontine projection in the macaque: the distribution of labelled cortical cells after large injections of horseradish peroxidase in the pontine nuclei. *Journal of Comparative Neurology*, 235(3):343–359, 1985.
- H. Gomi. Equilibrium-point control hypothesis examined by measured arm stiffness during multijoint movement. *Science*, 272(5258):117–120, 1996.
- A. Gonshor and G. M. Jones. Extreme vestibulo-ocular adaptation induced by prolonged optical reversal of vision. *The Journal of Physiology*, 256(2):381–414, 1976.
- C. R. Goodlett, K. M. Hamre, and J. R. West. Dissociation of spatial navigation and visual guidance performance in Purkinje cell degeneration (pcd) mutant mice. *Behavioural Brain Research*, 47(2):129–141, 1992.
- G. C. Goodwin. *Adaptive filtering prediction and control*. English. Prentice-Hall, (Englewood Cliffs, N.J), 1984.
- B. Gottwald, B. Wilde, Z. Mihajlovic, and H. Mehdorn. Evidence for distinct cognitive deficits after focal cerebellar lesions. *Journal of Neurology, Neurosurgery & Psychiatry*, 75 (11):1524–1531, 2004.

- T. J. Gould, L. L. Sears, and J. E. Steinmetz. Possible CS and US pathways for rabbit classical eyelid conditioning: electrophysiological evidence for projections from the pontine nuclei and inferior olive to cerebellar cortex and nuclei. *Behavioral and Neural Biology*, 60(2):172–185, 1993.
- S. Granon, C. Vidal, C. Thinus-Blanc, J. P. Changeux, and B. Poucet. Working memory, response selection, and effortful processing in rats with medial prefrontal lesions. *Behavioral Neuroscience*, 108(5):883–891, 1994.
- D. A. Grant, C. McFarling, and I. Gormenazo. Temporal conditioning and the effect of interpolated UCS presentations in eyelid conditioning. *The Journal of general psychology*, 63:249–257, 1960.
- G. Gundappa-Sulur, E. De Schutter, and J. M. Bower. Ascending granule cell axon: An important component of cerebellar cortical circuitry. *The Journal of Comparative Neurology*, 408(4):580–596, 1999.
- A. S. Gupta, M. A. A. van der Meer, D. S. Touretzky, and A. D. Redish. Hippocampal replay is not a simple function of experience. *Neuron*, 65(5):695–705, 2010.
- T. Hafting, M. Fyhn, S. Molden, M.-B. Moser, and E. I. Moser. Microstructure of a spatial map in the entorhinal cortex. *Nature*, 436(7052):801–806, 2005.
- H. E. Halverson, I. Lee, and J. H. Freeman. Associative plasticity in the medial auditory thalamus and cerebellar interpositus nucleus during eyeblink conditioning. *J. Neurosci.*, 30(26):8787–8796, 2010.
- C. Hansel and D. J. Linden. Long-term depression of the cerebellar climbing fiber–Purkinje neuron synapse. *Neuron*, 26(2):473–482, 2000.
- C. Hansel, D. J. Linden, and E. D’Angelo. Beyond parallel fiber LTD: the diversity of synaptic and non-synaptic plasticity in the cerebellum. *Nat. Neurosci.*, 4(5):467–475, 2001.
- D. L. Harrington, R. R. Lee, L. A. Boyd, S. Z. Rapcsak, and R. T. Knight. Does the representation of time depend on the cerebellum? *Brain*, 127(3):561–574, 2004.
- C. M. Harris and D. M. Wolpert. Signal-dependent noise determines motor planning. *Nature*, 394(6695):780–784, 1998.
- J. A. Hartigan and P. M. Hartigan. The Dip Test of Unimodality. *The Annals of Statistics*, 13(1):70–84, 1985.
- T. Hartley and N. Burgess. Complementary memory systems: competition, cooperation and compensation. *Trends Neurosci.*, 28(4):169–170, 2005.
- M. J. Hartmann and J. M. Bower. Oscillatory activity in the cerebellar hemispheres of unrestrained rats. *Journal of Neurophysiology*, 80(3):1598–1604, 1998.

- M. J. Hartmann, J. M. Bower, E. Galliano, P. Mazzarello, E. D. Angelo, L. C. Hoffmann, S. D. Berry, H. Ros, R. N. S. Sachdev, Y. Yu, N. Sestan, D. A. McCormick, M. J. Russo, H.-J. Yau, M.-G. Nunzi, E. Mugnaini, M. Martina, L. Forti, E. Cesana, and J. Mapelli. Oscillatory Activity in the Cerebellar Hemispheres of Unrestrained Rats conditioning. *Journal of Neurophysiology*, pages 1598–1604, 2010.
- M. Haruno, D. M. Wolpert, and M. Kawato. Mosaic model for sensorimotor learning and control. *Neural computation*, 13(10):2201–20, 2001.
- M. Haruno, D. M. Wolpert, and M. Kawato. Hierarchical MOSAIC for movement generation. *International Congress Series*, 1250:575–590, 2003.
- R. J. Harvey and R. M. Napper. Quantitative study of granule and Purkinje cells in the cerebellar cortex of the rat. *Journal of Comparative Neurology*, 274(2):151–157, 1988.
- K. Hashimoto and M. Kano. Functional differentiation of multiple climbing fiber inputs during synapse elimination in the developing cerebellum. *Neuron*, 38(5):785–796, 2003.
- M. Häusser and B. A. Clark. Tonic synaptic inhibition modulates neuronal output pattern and spatiotemporal synaptic integration. *Neuron*, 19(3):665–678, 1997.
- R. Hawkes and N. Leclerc. Purkinje cell axon collateral distributions reflect the chemical compartmentation of the rat cerebellar cortex. *Brain Res.*, 476(2):279–290, 1989.
- S. Haykin. *Neural Networks: A Comprehensive Foundation*, volume 13. Prentice Hall, 1999.
- R. G. Heath, C. W. Dempsey, C. J. Fontana, and W. A. Myers. Cerebellar stimulation: effects on septal region, hippocampus, and amygdala of cats and rats. *Biological Psychiatry*, 13(5):501–529, 1978.
- E. Henriksen, M. Moser, and E. Moser. Megaspace recording from hippocampal place cells and entorhinal grid cells. In *Society for Neuroscience Abstracts*, page 101.10/FF52, 2009.
- P. Hilber, F. Jouen, N. Delhay-Bouchaud, J. Mariani, and J. Caston. Differential roles of cerebellar cortex and deep cerebellar nuclei in learning and retention of a spatial task: studies in intact and cerebellectomized lurcher mutant mice. *Behavior Genetics*, 28(4): 299–308, 1998.
- T. Hirano, D. Watanabe, S. Kawaguchi, I. Pastan, and S. Nakanishi. Roles of inhibitory interneurons in the cerebellar cortex. *Annals of the New York Academy of Sciences*, 978: 405–412, 2002.
- B. Hoff and M. A. Arbib. Models of trajectory formation and temporal interaction of reach and grasp. *Journal of Motor Behavior*, 25(3):175–192, 1993.
- N. Hogan. An organizing principle for a class of voluntary movements. *J. Neurosci.*, 4 (11):2745–2754, 1984.

- V. Hok, E. Save, P. P. Lenck-Santini, and B. Poucet. Coding for spatial goals in the pre-
limbic/infralimbic area of the rat frontal cortex. *Proc. Natl. Acad. Sci. U. S. A.*, 102(12):
4602–4607, 2005.
- G. Holmes. The Cerebellum of Man. *Brain*, 62(1):1–30, 1939.
- H. Hooper. *Hooper visual organization test (VOT)*. 1983.
- J. J. Hopp and A. F. Fuchs. The characteristics and neuronal substrate of saccadic eye
movement plasticity. *Progress in Neurobiology*, 72(1):27–53, 2004.
- V. Houten. Compound and Tests After for Excitation in Early Extinction Acquisition of
Prolonged Conditioned. *Learning*, pages 246–258, 1972.
- R. Huber, M. F. Ghilardi, M. Massimini, and G. Tononi. Local sleep and learning. *Nature*,
430(6995):78–81, 2004.
- H. Imamizu, S. Miyauchi, T. Tamada, Y. Sasaki, R. Takino, B. Pütz, T. Yoshioka, and
M. Kawato. Human cerebellar activity reflecting an acquired internal model of a new
tool. *Nature*, 403(6766):192–5, 2000.
- H. Imamizu, T. Kuroda, S. Miyauchi, T. Yoshioka, and M. Kawato. Modular organization
of internal models of tools in the human cerebellum. *Proc. Natl. Acad. Sci. U. S. A.*, 100
(9):5461–5466, 2003.
- H. Imamizu, T. Kuroda, T. Yoshioka, and M. Kawato. Functional magnetic resonance
imaging examination of two modular architectures for switching multiple internal
models. *J. Neurosci.*, 24(5):1173–1181, 2004.
- R. Insausti, M. Herrero, and M. Witter. Entorhinal cortex of the rat: cytoarchitectonic
subdivisions and the origin and distribution of cortical efferents. *Hippocampus*, 7(2):
146–183, 1997.
- P. Isope and B. Barbour. Properties of unitary granule cell–Purkinje cell synapses in
adult rat cerebellar slices. *J. Neurosci.*, 22(22):9668–9678, 2002.
- M. Ito. Neurophysiological basis of the cerebellar motor control system. *International
Journal of Neurology*, 7(2):162, 1970.
- M. Ito. *Control mechanisms of cerebellar motor system*, pages 293–303. MIT Press, 1974.
- M. Ito. *The Cerebellum and Neural Control*. Raven Press, New York, 1984.
- M. Ito. Cerebellar learning in the vestibulo-ocular reflex. *Trends in Cognitive Sciences*, 2(9):
313–321, 1998.
- M. Ito. Cerebellar long-term depression: characterization, signal transduction, and func-
tional roles. *Physiological reviews*, 81(3):1143–95, 2001.

- M. Ito. Historical review of the significance of the cerebellum and the role of purkinje cells in motor learning. *Annals of the New York Academy of Sciences*, 978:273–288, 2002.
- M. Ito. Bases and implications of learning in the cerebellum—adaptive control and internal model mechanism. *Progress in Brain Research*, 148:95–109, 2005.
- M. Ito. Cerebellar circuitry as a neuronal machine. *Progress in Brain Research*, 78:272–303, 2006.
- M. Ito. Control of mental activities by internal models in the cerebellum. *Nat. Rev. Neurosci.*, 9:304–313, 2008.
- M. Ito and M. Kano. Long-lasting depression of parallel fiber-Purkinje cell transmission induced by conjunctive stimulation of parallel fibers and climbing fibers in the cerebellar cortex. *Neurosci. Lett.*, 33(3):253–258, 1982.
- M. Ito and T. Myashita. The effects of chronic destruction of the inferior olive upon visual modification of the horizontal vestibulo-ocular reflex of rabbits. *Neurosci. Lett.*, 8:283–287, 1975.
- M. Ito and M. Yoshida. The cerebellar-evoked monosynaptic inhibition of Deiters' neurones. *Experientia*, 20(9):515–516, 1964.
- M. Ito, N. Nisimaru, and M. Yamamoto. Specific patterns of neuronal connexions involved in the control of the rabbit's vestibulo-ocular reflexes by the cerebellar flocculus. *The Journal of Physiology*, 265(3):833–854, 1977.
- R. B. Ivry and S. W. Keele. Timing functions of the cerebellum. *Journal of Cognitive Neuroscience*, 1(2):136–152, 1989.
- R. B. Ivry and R. M. C. Spencer. The neural representation of time. *Curr. Opin. Neurobiol.*, 14(2):225–32, 2004.
- R. B. Ivry, S. W. Keele, and H. C. Diener. Dissociation of the lateral and medial cerebellum in movement timing and movement execution., 1988.
- C. B. Jaeger, R. Kapoor, and R. Llinas. Cytology and organization of rat cerebellar organ cultures. *Neuroscience*, 26(0306-4522 (Print) LA - eng PT - Journal Article RN - EC 1.11.1.- (Horseradish Peroxidase) SB - IM):509–538, 1988.
- D. Jaeger and J. M. Bower. Synaptic control of spiking in cerebellar Purkinje cells: dynamic current clamp based on model conductances. *J. Neurosci.*, 19(14):6090–6101, 1999.
- R. L. Jakab and J. Hamori. Quantitative morphology and synaptology of cerebellar glomeruli in the rat. *Anatomy and Embryology*, 179:81–88, 1988.
- K. J. Jeffery and J. O'Keefe. Learned interaction of visual and idiothetic cues in the control of place field orientation. *Experimental Brain Research*, 127(2):151–161, 1999.

- M. I. Jordan and D. E. Rumelhart. Forward Models: Supervised Learning with a Distal Teacher. *Cognitive Science*, 16(3):307–354, 1992.
- H. Jörntell and C.-F. Ekerot. Properties of somatosensory synaptic integration in cerebellar granule cells in vivo. *The Journal of Neuroscience: The Official Journal of the Society for Neuroscience*, 26(45):11786–97, 2006.
- H. Jörntell, M. Garwicz, and C. F. Ekerot. Relation between cutaneous receptive fields and muscle afferent input to climbing fibres projecting to the cerebellar C3 zone in the cat. *European Journal of Neuroscience*, 8(8):1769–1779, 1996.
- C. C. Joyal, C. Strazielle, and R. Lalonde. Effects of dentate nucleus lesions on spatial and postural sensorimotor learning in rats. *Behavioural Brain Research*, 122(2):131–137, 2001.
- M. Jung, S. Wiener, and B. McNaughton. Comparison of spatial firing characteristics of units in dorsal and ventral hippocampus of the rat. *J. Neurosci.*, 14(12):7347–7356, 1994.
- M. Kahlon and S. G. Lisberger. Changes in the responses of Purkinje cells in the floccular complex of monkeys after motor learning in smooth pursuit eye movements. *Journal of Neurophysiology*, 84(6):2945–2960, 2000.
- S. G. Kalinichenko and V. E. Okhotin. Unipolar brush cells—a new type of excitatory interneuron in the cerebellar cortex and cochlear nuclei of the brainstem. *Neuroscience and Behavioral Physiology*, 35(1):21–36, 2005.
- M. Kano, U. Rexhausen, J. Dreessen, and A. Konnerth. Synaptic excitation produces a long-lasting rebound potentiation of inhibitory synaptic signals in cerebellar Purkinje cells. *Nature*, 356(6370):601–604, 1992.
- M. Kawato. Internal models for motor control and trajectory planning. *Curr. Opin. Neurobiol.*, 9(6):718–727, 1999.
- M. Kawato and H. Gomi. The cerebellum and VOR/OKR learning models. *Trends Neurosci.*, 15:445–453, 1992.
- M. Kawato, K. Furukawa, and R. Suzuki. A hierarchical neural-network model for control and learning of voluntary movement. *Biological Cybernetics*, 57:169–185, 1987.
- M. Kawato, T. Kuroda, H. Imamizu, E. Nakano, S. Miyauchi, and T. Yoshioka. Internal forward models in the cerebellum: fMRI study on grip force and load force coupling. *Progress in Brain Research*, 142:171–188, 2003.
- V. B. Kazantsev, V. I. Nekorkin, V. I. Makarenko, and R. Llinás. Self-referential phase reset based on inferior olive oscillator dynamics. *Proc. Natl. Acad. Sci. U. S. A.*, 101(52):18183–18188, 2004.
- J. G. Keating and W. T. Thach. Nonclock behavior of inferior olive neurons: interspike interval of Purkinje cell complex spike discharge in the awake behaving monkey is random. *Journal of Neurophysiology*, 73(4):1329–1340, 1995.

- J. G. Keating and W. T. Thach. No clock signal in the discharge of neurons in the deep cerebellar nuclei. *Journal of Neurophysiology*, 77(4):2232–2234, 1997.
- S. W. Keele and R. Ivry. Does the cerebellum provide a common computation for diverse tasks? A timing hypothesis. *Annals of the New York Academy of Sciences*, 608(0077-8923 (Print) LA - eng PT - Journal Article PT - Review SB - IM):179–211, 1990.
- E. J. Kehoe. A layered network model of associative learning: learning to learn and configuration. *Psychological Review*, 95(4):411–433, 1988.
- R. M. Kelly and P. L. Strick. Cerebellar loops with motor cortex and prefrontal cortex of a nonhuman primate. *J. Neurosci.*, 23(23):8432–8444, 2003.
- G. T. Kenyon. A model of long-term memory storage in the cerebellar cortex: A possible role for plasticity at parallel fiber synapses onto stellate basket interneurons. *Proc. Natl. Acad. Sci. U. S. A.*, 94(25):14200–14205, 1997.
- W. M. Kistler, J. L. van Hemmen, and C. I. D. Zeeuw. Time window control: a model for cerebellar function based on synchronization, reverberation, and time slicing. *Progress in Brain Research*, 124:275–297, 2000.
- S. Kitazawa and D. M. Wolpert. Rhythmicity, randomness and synchrony in climbing fiber signals. *Trends Neurosci.*, 28(11):611–619, 2005.
- S. Kitazawa and P.-B. Yin. Prism adaptation with delayed visual error signals in the monkey. *Experimental Brain Research*, 144(2):258–261, 2002.
- K. Kjelstrup, T. Solstad, V. Brun, T. Hafting, S. Leutgeb, M. Witter, E. Moser, and M. Moser. Finite scale of spatial representation in the hippocampus. *Science*, 321(5885):140–143, 2008.
- J. Knierim, H. Kudrimoti, and B. McNaughton. Place cells, head direction cells, and the learning of landmark stability. *J. Neurosci.*, 15(3 Pt 1):1648–1659, 1995.
- J. J. Knierim. Neural representations of location outside the hippocampus. *Learning & Memory*, 13(4):405–415, 2006.
- S. K. E. Koekkoek, H. C. Hulscher, B. R. Dortland, R. A. Hensbroek, Y. Elgersma, T. J. H. Ruigrok, and C. I. De Zeeuw. Cerebellar LTD and learning-dependent timing of conditioned eyelid responses. *Science*, 301(5640):1736–1739, 2003.
- B. Kolb, R. J. Sutherland, and I. Q. Whishaw. A comparison of the contributions of the frontal and parietal association cortex to spatial localization in rats. *Behavioral Neuroscience*, 97(1):13–27, 1983.
- S. Kondo and A. Marty. Synaptic currents at individual connections among stellate cells in rat cerebellar slices. *The Journal of Physiology*, 509(Pt 1):221–232, 1998.

- K. P. Körding, I. Fukunaga, I. S. Howard, J. N. Ingram, and D. M. Wolpert. A Neuroeconomics Approach to Inferring Utility Functions in Sensorimotor Control. *PLoS Biol.*, 2 (10):e330, 2004.
- I. Korelusova, J. Cendelin, and F. Vozéz. Motor and visuospatial abilities in a model of olivocerebellar and retinal degeneration—Lurcher mutant mice of C3H strain. *Prague Medical Report*, 108(1):37–48, 2007.
- M. Korman, J. Doyon, J. Doljansky, J. Carrier, Y. Dagan, and A. Karni. Daytime sleep condenses the time course of motor memory consolidation. *Nat. Neurosci.*, 10(9):1206–1213, 2007.
- N. Kotchabhakdi and F. Walberg. Cerebellar afferent projections from the vestibular nuclei in the cat: an experimental study with the method of retrograde axonal transport of horseradish peroxidase. *Experimental Brain Research*, 31(4):591–604, 1978.
- J. L. Krichmar, D. A. Nitz, J. A. Gally, and G. M. Edelman. Characterizing functional hippocampal pathways in a brain-based device as it solves a spatial memory task. *Proc Natl Acad Sci U S A*, 102(6):2111–2116, 2005.
- H. S. Kudrimoti, C. A. Barnes, and B. L. McNaughton. Reactivation of hippocampal cell assemblies: effects of behavioral state, experience, and EEG dynamics. *J. Neurosci.*, 19 (10):4090–4101, 1999.
- A. D. Kuo. An optimal control model for analyzing human postural balance. *IEEE T. Bio-Med. Eng.*, 42(1):87–101, 1995.
- M. Kuperstein. An adaptive neural model for mapping invariant target position. *Behavioral Neuroscience*, 102(1):148–162, 1988.
- H. Lalazar and E. Vaadia. Neural basis of sensorimotor learning: modifying internal models. *Curr. Opin. Neurobiol.*, 18(6):573–81, 2008.
- R. Lalonde. Exploration and spatial learning in staggerer mutant mice. *Journal of Neurogenetics*, 4(6):285–291, 1987.
- R. Lalonde and M. I. Botez. Navigational deficits in weaver mutant mice. *Brain Res.*, 398 (1):175–177, 1986.
- R. Lalonde, Y. Lamarre, and A. M. Smith. Does the mutant mouse lurcher have deficits in spatially oriented behaviours? *Brain Res.*, 455(1):24–30, 1988.
- Y. Lamarre and L. A. Mercier. Neurophysiological studies of harmaline-induced tremor in the cat. *Can. J. Physiol. Pharmacol.*, 49(12):1049–1058, 1971.
- M. Lamont. An electrophysiological analysis of deep cerebellar nuclei, with particular focus on Kv3 channels. *Bioscience Horizons*, 2(1):55–63, 2009.
- I. Lampl and Y. Yarom. Subthreshold oscillations and resonant behavior: two manifestations of the same mechanism. *Neuroscience*, 78(2):325–341, 1997.

- E. J. Lang. Organization of olivocerebellar activity in the absence of excitatory glutamatergic input. *J. Neurosci.*, 21(5):1663–1675, 2001.
- Larsell. The morphogenesis and adult pattern of the lobules and fissures of the cerebellum of the white rat. *Journal of Comparative Neurology*, 97(2):281–356, 1952.
- O. Larsell and J. Jansen. *The comparative anatomy and histology of the cerebellum*. U. Minnesota P., 1970.
- C. Laschi, G. Asuni, E. Guglielmelli, G. Teti, R. Johansson, H. Konosu, Z. Wasik, M. C. Carrozza, and P. Dario. A bio-inspired predictive sensory-motor coordination scheme for robot reaching and preshaping. *Autonomous Robots*, 25(1-2):85–101, 2008.
- D. G. Lavond, T. L. Hembree, and R. F. Thompson. Effect of kainic acid lesions of the cerebellar interpositus nucleus on eyelid conditioning in the rabbit. *Brain Res.*, 326(1):179–182, 1985.
- D. G. Lavond, B. J. Knowlton, J. E. Steinmetz, and R. F. Thompson. Classical conditioning of the rabbit eyelid response with a mossy-fiber stimulation CS: II. Lateral reticular nucleus stimulation. *Behavioral Neuroscience*, 101(5):676–682, 1987.
- D. G. Lavond, J. J. Kim, and R. F. Thompson. Mammalian brain substrates of aversive classical conditioning. *Annual Review of Psychology*, 44:317–342, 1993.
- A. K. Lee and M. A. Wilson. Memory of sequential experience in the hippocampus during slow wave sleep. *Neuron*, 36(6):1183–1194, 2002.
- I. Lee, G. Rao, and J. Knierim. A double dissociation between hippocampal subfields: differential time course of ca3 and ca1 place cells for processing changed environments. *Neuron*, 42(5):803–815, 2004.
- M. G. Leggio, P. Neri, A. Graziano, L. Mandolesi, M. Molinari, and L. Petrosini. Cerebellar contribution to spatial event processing: characterization of procedural learning. *Experimental Brain Research*, 127(1):1–11, 1999.
- H. C. Leiner, A. L. Leiner, and R. S. Dow. The human cerebro-cerebellar system: its computing, cognitive, and language skills. *Behavioural Brain Research*, 44(2):113–128, 1991.
- P. Lenck-Santini, B. Rivard, R. Muller, and B. Poucet. Study of ca1 place cell activity and exploratory behavior following spatial and nonspatial changes in the environment. *Hippocampus*, 15(3):356–369, 2005.
- V. Lev-Ram, S. T. Wong, D. R. Storm, and R. Y. Tsien. A new form of cerebellar long-term potentiation is postsynaptic and depends on nitric oxide but not cAMP. *Proc. Natl. Acad. Sci. U. S. A.*, 99(12):8389–8393, 2002.
- V. Lev-Ram, S. T. Wong, D. R. Storm, and R. Y. Tsien. A new form of cerebellar long-term potentiation is postsynaptic and depends on nitric oxide but not cAMP. *Proc. Natl. Acad. Sci. U. S. A.*, 99(12):8389–93, 2002.

- J. S. Lincoln, D. A. McCormick, and R. F. Thompson. Ipsilateral cerebellar lesions prevent learning of the classically conditioned nictitating membrane/eyelid response. *Brain Res.*, 242(1):190–193, 1982.
- S. G. Lisberger. Neural basis for motor learning in the vestibuloocular reflex of primates. III. Computational and behavioral analysis of the sites of learning. *Journal of Neurophysiology*, 72(2):974–998, 1994.
- S. G. Lisberger. Internal models of eye movement in the floccular complex of the monkey cerebellum. *Neuroscience*, 162(3):763–76, 2009.
- R. Llinás and Y. Yarom. Electrophysiology of mammalian inferior olivary neurones in vitro. Different types of voltage-dependent ionic conductances. *The Journal of Physiology*, 315(0022-3751 SB - IM):549–567, 1981.
- R. Llinás and Y. Yarom. Oscillatory properties of guinea-pig inferior olivary neurones and their pharmacological modulation: an in vitro study. *The Journal of Physiology*, 376(0022-3751 SB - IM):163–182, 1986.
- R. Llinas, R. Baker, and C. Sotelo. Electrotonic coupling between neurons in cat inferior olive. *Journal of Neurophysiology*, 37(3):560–571, 1974.
- R. R. Llinás. Inferior olive oscillation as the temporal basis for motricity and oscillatory reset as the basis for motor error correction. *Neuroscience*, 162(3):797–804, 2009.
- Y. Loewenstein, S. Mahon, P. Chadderton, K. Kitamura, H. Sompolinsky, Y. Yarom, and M. Hausser. Bistability of cerebellar Purkinje cells modulated by sensory stimulation. *Nat. Neurosci.*, 8(2):202–211, 2005.
- L. Luciani. Il Cervelleto; nuovi studi di fisiologia normale e pathologica. *Journal of anatomy and physiology*, 26(Pt 4):568–573, 1892.
- W. Maass, T. Natschläger, and H. Markram. Real-time computing without stable states: a new framework for neural computation based on perturbations. *Neural Comput*, 14(11):2531–2560, 2002.
- P. A. MacDonald and T. Paus. The role of parietal cortex in awareness of self-generated movements: a transcranial magnetic stimulation study. *Cerebral Cortex*, 13(9):962–967, 2003.
- K. Maekawa and J. L. Simpson. Climbing fiber responses evoked in vestibulocerebellum of rabbit from visual system. *Journal of Neurophysiology*, 36(4):649–666, 1973.
- R. Maex and E. De Schutter. Oscillations in the cerebellar cortex: a prediction of their frequency bands. *Progress in Brain Research*, 148:181–188, 2005.
- L. Mandolesi, M. G. Leggio, A. Graziano, P. Neri, and L. Petrosini. Cerebellar contribution to spatial event processing: involvement in procedural and working memory components. *European Journal of Neuroscience*, 14(12):2011–2022, 2001.

- L. Mandolesi, M. G. Leggio, F. Spirito, and L. Petrosini. Cerebellar contribution to spatial event processing: do spatial procedures contribute to formation of spatial declarative knowledge? *European Journal of Neuroscience*, 18(9):2618–2626, 2003.
- L. Mandolesi, F. Foti, D. Cutuli, D. Laricchiuta, F. Gelfo, P. D. Bartolo, and L. Petrosini. Features of sequential learning in hemicerebellectomized rats. *J Neurosci Res*, 88(3):478–486, 2010.
- P. Mann-Metzer and Y. Yarom. Electrotonic coupling interacts with intrinsic properties to generate synchronized activity in cerebellar networks of inhibitory interneurons. *J. Neurosci.*, 19(9):3298–3306, 1999.
- Y. Manor, J. Rinzel, I. Segev, and Y. Yarom. Low-amplitude oscillations in the inferior olive: a model based on electrical coupling of neurons with heterogeneous channel densities. *Journal of Neurophysiology*, 77(5):2736–2752, 1997.
- M. Manto, E. Godaux, and J. Jacquy. Detection of silent cerebellar lesions by increasing the inertial load of the moving hand., 1995.
- M. Manto, E. Godaux, J. Jacquy, and J. Hildebrand. Cerebellar hypermetria associated with a selective decrease in the rate of rise of antagonist activity. *Annals of Neurology*, 39(2):271–274, 1996.
- P. Maquet, S. Laureys, P. Peigneux, S. Fuchs, C. Petiau, C. Phillips, J. Aerts, G. Del Fiore, C. Degueldre, T. Meulemans, A. Luxen, G. Franck, M. Van Der Linden, C. Smith, and a. Cleeremans. Experience-dependent changes in cerebral activation during human REM sleep. *Nat. Neurosci.*, 3(8):831–6, 2000.
- P. Maquet, S. Schwartz, R. Passingham, and C. D. Frith. Sleep-related consolidation of a visuomotor skill: brain mechanisms as assessed by functional magnetic resonance imaging. *The Journal of Neuroscience: The Official Journal of the Society for Neuroscience*, 23(4):1432–40, 2003.
- N. L. Marec, T. Stelz, N. Delhay-Bouchaud, J. Mariani, and J. Caston. Effect of cerebellar granule cell depletion on learning of the equilibrium behaviour: study in postnatally x-irradiated rats. *Eur J Neurosci*, 9(11):2472–2478, Nov 1997.
- J. Mariani and J. P. Changeux. Ontogenesis of olivocerebellar relationships. I. Studies by intracellular recordings of the multiple innervation of Purkinje cells by climbing fibers in the developing rat cerebellum. *J. Neurosci.*, 1(7):696–702, 1981.
- D. Marr. A theory of cerebellar cortex. *The Journal of Physiology*, 202(2):437–470, 1969.
- T. A. Martin, J. G. Keating, H. P. Goodkin, A. J. Bastian, and W. T. Thach. Throwing while looking through prisms. *Brain*, 119(4):1183–1198, 1996a.
- T. a. Martin, J. G. Keating, H. P. Goodkin, a. J. Bastian, and W. T. Thach. Throwing while looking through prisms. II. Specificity and storage of multiple gaze-throw calibrations. *Brain : a journal of neurology*, 119 (Pt 4):1199–211, 1996b.

- L.-E. Martinet, D. Sheynikhovich, K. Benchenane, and A. Arleo. Spatial learning and action planning in a prefrontal cortical network model. *PLoS Comput. Biol.*, 7 (5):in press, 2011.
- N. Masuda. Modeling Memory Transfer and Saving in Cerebellar Motor Learning. *Advances in Neural Information Processing Systems*, 2006.
- N. Masuda and S. ichi Amari. A computational study of synaptic mechanisms of partial memory transfer in cerebellar vestibulo-ocular-reflex learning. *Journal of Computational Neuroscience*, 24(2):137–156, 2008.
- A. Mathy, S. S. N. Ho, J. T. Davie, I. C. Duguid, B. a. Clark, and M. Häusser. Encoding of oscillations by axonal bursts in inferior olive neurons. *Neuron*, 62(3):388–99, 2009.
- D. Matthews, A. White, E. Brush, and P. Best. Construction of the spatial cognitive map does not require active exploration of the environment. Society for Neuroscience Abstracts 21: 2086. *Society for Neuroscience*, 21:2086, 1995.
- M. Mauk, J. Medina, W. Nores, and T. Ohyama. Cerebellar function: Coordination, learning or timing? *Curr. Biol.*, 10(14):R522–R525, 2000.
- M. D. Mauk and D. V. Buonomano. The neural basis of temporal processing. *Annu. Rev. Neurosci.*, 27(1):307–40, 2004.
- P. Mazzoni and J. W. Krakauer. An implicit plan overrides an explicit strategy during visuomotor adaptation. *J. Neurosci.*, 26(14):3642–3645, 2006.
- P. Mazzoni, A. Hristova, and J. W. Krakauer. Why don't we move faster? Parkinson's disease, movement vigor, and implicit motivation. *J. Neurosci.*, 27(27):7105–7116, 2007.
- D. A. McCormick and R. F. Thompson. Cerebellum: essential involvement in the classically conditioned eyelid response. *Science*, 223(4633):296–299, 1984.
- R. J. McDonald and N. M. White. A triple dissociation of memory systems: hippocampus, amygdala, and dorsal striatum. *Behavioral Neuroscience*, 107:3–22, 1993.
- R. J. McDonald and N. M. White. Parallel information processing in the water maze: evidence for independent memory systems involving dorsal striatum and hippocampus. *Behavioral and Neural Biology*, 61(3):260–270, 1994.
- B. E. McKay, J. D. T. Engbers, W. H. Mehaffey, G. R. J. Gordon, M. L. Molineux, J. S. Bains, and R. W. Turner. Climbing fiber discharge regulates cerebellar functions by controlling the intrinsic characteristics of purkinje cell output. *Journal of Neurophysiology*, 97 (4):2590–2604, 2007.
- J. L. McKinstry, G. M. Edelman, and J. L. Krichmar. A cerebellar model for predictive motor control tested in a brain-based device. *Proc Natl Acad Sci U S A*, 103(9):3387–3392, 2006.

- J. L. McKinstry, A. K. Seth, G. M. Edelman, and J. L. Krichmar. Embodied models of delayed neural responses: spatiotemporal categorization and predictive motor control in brain based devices. *Neural Netw*, 21:553–561, 2008.
- B. L. McNaughton, L. L. Chen, and E. J. Markus. Dead reckoning, landmark learning, and the sense of direction: A neurophysiological and computational hypothesis. *Journal of Cognitive Neuroscience*, 3(2):190–202, 1991.
- B. L. McNaughton, F. P. Battaglia, O. Jensen, E. I. Moser, and M.-B. Moser. Path integration and the neural basis of the ‘cognitive map’. *Nature reviews. Neuroscience*, 7(8):663–678, 2006.
- J. Medina and M. D. Mauk. Computer simulation of cerebellar information processing. *Nat. Neurosci.*, 3 Suppl(Box 1):1205–11, 2000.
- J. Medina, K. S. Garcia, W. L. Nores, N. M. Taylor, and M. D. Mauk. Timing mechanisms in the cerebellum: testing predictions of a large-scale computer simulation. *The Journal of Neuroscience: The Official Journal of the Society for Neuroscience*, 20(14):5516–25, 2000.
- J. Medina, K. S. Garcia, and M. D. Mauk. A mechanism for savings in the cerebellum. *The Journal of Neuroscience: The Official Journal of the Society for Neuroscience*, 21(11):4081–9, 2001.
- J. Medina, J. C. Repa, M. D. Mauk, and J. E. LeDoux. Parallels between cerebellum- and amygdala-dependent conditioning. *Nature reviews. Neuroscience*, 3(2):122–31, 2002.
- J. F. Medina and M. D. Mauk. Simulations of cerebellar motor learning: Computational analysis of plasticity at the mossy fiber to deep nucleus synapse. *J. Neurosci.*, 19(16):7140–7151, 1999.
- S. Mednick, K. Nakayama, and R. Stickgold. Sleep-dependent learning: a nap is as good as a night. *Nat. Neurosci.*, 6(7):697–698, 2003.
- R. C. Miall. The cerebellum, predictive control and motor coordination. *Novartis Foundation Symposium*, 218:272–284; discussion 284–290, 1998.
- R. C. Miall, D. J. Weir, D. M. Wolpert, and J. F. Stein. Is the cerebellum a smith predictor? *Journal of Motor Behavior*, 25(3):203–216, 1993.
- R. C. Miall, G. Z. Reckess, and H. Imamizu. The cerebellum coordinates eye and hand tracking movements. *Nat. Neurosci.*, 4(6):638–644, 2001.
- R. C. Miall, L. O. D. Christensen, O. Cain, and J. Stanley. Disruption of State Estimation in the Human Lateral Cerebellum. *PLoS Biol.*, 5(11):12, 2007.
- O. Michel. Webots: Professional Mobile Robot Simulation. *International Journal of Advanced Robotic System*, 1(1):39–42, 2004.
- F. A. Middleton and P. L. Strick. Cerebellar projections to the prefrontal cortex of the primate. *J. Neurosci.*, 21(2):700–712, 2001.

- S. J. Middleton, C. Racca, M. O. Cunningham, R. D. Traub, H. Monyer, T. Knöpfel, I. S. Schofield, A. Jenkins, and M. A. Whittington. High-frequency network oscillations in cerebellar cortex. *Neuron*, 58(5):763–774, 2008.
- F. A. Miles and S. G. Lisberger. Plasticity in the vestibulo-ocular reflex: a new hypothesis. *Annu. Rev. Neurosci.*, 4(1):273–299, 1981.
- H. Mittelstaedt and M. L. Mittelstaedt. Mechanismen der Orientierung ohne richtende Außenreize. *Fortschritte Der Zoologie*, 21:46–58, 1973.
- M. L. Mittelstaedt and H. Mittelstaedt. Homing by path integration in the mammal. *Naturewissenschaften*, 67:566–567, 1980.
- Y. Miyashita. Neuronal correlate of visual associative long-term memory in the primate temporal cortex. *Nature*, 335(6193):817–820, 1988.
- S. J. Y. Mizumori, C. B. Puryear, and A. K. Martig. Basal ganglia contributions to adaptive navigation. *Behavioural Brain Research*, 199(1):32–42, 2009.
- M. Molinari and M. G. Leggio. Cerebellar information processing and visuospatial functions. *Cerebellum (London, England)*, 6(3):214–220, 2007.
- J. W. Moore, J. E. Desmond, and N. E. Berthier. Adaptively timed conditioned responses and the cerebellum: a neural network approach. *Biological Cybernetics*, 62(1):17–28, 1989.
- W. Morishita and B. R. Sastry. Postsynaptic mechanisms underlying long-term depression of GABAergic transmission in neurons of the deep cerebellar nuclei. *Journal of Neurophysiology*, 76(1):59–68, 1996.
- R. Morris. Developments of a water-maze procedure for studying spatial learning in the rat. *Journal of Neuroscience Methods*, 11(1):47–60, 1984.
- R. G. Morris, P. Garrud, J. N. Rawlins, and J. O’Keefe. Place navigation impaired in rats with hippocampal lesions. *Nature*, 297(5868):681–683, 1982.
- R. G. M. Morris. Spatial localization does not require the presence of local cues. *Learning and Motivation*, 12(2):239–260, 1981.
- E. I. Moser, E. Kropff, and M. B. Moser. Place cells, grid cells, and the brain’s spatial representation system. *Annu. Rev. Neurosci.*, 31:69–89, 2008.
- E. Mugnaini. The relation between cytochrome and the formation of different types of synaptic contact. *Brain Res.*, 17(2):169–179, 1970.
- E. Mugnaini. The length of cerebellar parallel fibers in chicken and rhesus monkey. *Journal of Comparative Neurology*, 220(1):7–15, 1983.
- R. Muller, J. Kubie, and J. Ranck. Spatial firing patterns of hippocampal complex-spike cells in a fixed environment. *J. Neurosci.*, 7(7):1935–1950, 1987.

- R. Muller, J. Kubie, E. Bostock, J. Taube, and G. Quirk. Spatial firing correlates of neurons in the hippocampal formation of freely moving rats. In J. Paillard, editor, *Brain and Space*, page 296–333. Oxford University Press, New York, 1991.
- R. U. Muller, J. L. Kubie, and B. Ranck. Spatial Firing Patterns Fixed Environment of Hippocampal Complex-Spike Cells in a. *Cell*, 7(7):1935–50, 1987.
- R. U. Muller, B. Poucet, and B. Rivard. Sensory determinants of hippocampal place cell firing fields. In *The neural basis of navigation evidence from singlecell recording*, pages 1–22. Norwell, MA: Kluwer Academic, 2001.
- G. H. Mulliken, S. Musallam, and R. A. Andersen. Forward estimation of movement state in posterior parietal cortex. *Proc. Natl. Acad. Sci. U. S. A.*, 105(24):8170–8177, 2008.
- J. Na, S. Kakei, and Y. Shinoda. Cerebellar input to corticothalamic neurons in layers V and VI in the motor cortex. *Neuroscience Research*, 28(1):77–91, 1997.
- Z. Nadasdy, H. Hirase, A. Czurko, J. Csicsvari, and G. Buzsaki. Replay and time compression of recurring spike sequences in the hippocampus. *J. Neurosci.*, 19(21):9497–9507, 1999.
- S. Nagao. Effects of reversible shutdown of the monkey flocculus on the retention of adaptation of the horizontal vestibulo-ocular reflex. *Neuroscience*, 118(2):563–570, 2003.
- S. Nagao and M. Ito. Subdural application of hemoglobin to the cerebellum blocks vestibuloocular reflex adaptation. *NeuroReport*, 2(4):193–196, 1991.
- S. Nagao, M. Ito, and L. Karachot. Eye field in the cerebellar flocculus of pigmented rabbits determined with local electrical stimulation. *Neuroscience Research*, 3(1):39–51, 1985.
- E. Nakano, H. Imamizu, R. Osu, Y. Uno, H. Gomi, T. Yoshioka, and M. Kawato. Quantitative examinations of internal representations for arm trajectory planning: minimum commanded torque change model. *Journal of Neurophysiology*, 81(5):2140–2155, 1999.
- R. M. Napier, M. Macrae, and E. J. Kehoe. Rapid reacquisition in conditioning of the rabbit’s nictitating membrane response. *Journal of Experimental Psychology Animal Behavior Processes*, 18(2):182–192, 1992.
- R. M. Napper and R. J. Harvey. Number of parallel fiber synapses on an individual Purkinje cell in the cerebellum of the rat. *Journal of Comparative Neurology*, 274(2):168–177, 1988.
- W. L. Nelson. Physical principles for economies of skilled movements. *Biological Cybernetics*, 46(2):135–147, 1983.
- T. R. Nichols and J. C. Houk. Improvement in linearity and regulation of stiffness that results from actions of stretch reflex. *Journal of Neurophysiology*, 39(1):119–142, 1976.

- R. I. Nicolson and A. J. Fawcett. Developmental dyslexia, learning and the cerebellum. *Journal of neural transmission Supplementum*, (69):19–36, 2005.
- M. P. Nieto-Bona, L. M. Garcia-Segura, and I. Torres-Alemán. Transynaptic modulation by insulin-like growth factor I of dendritic spines in Purkinje cells. *International journal of developmental neuroscience the official journal of the International Society for Developmental Neuroscience*, 15(6):749–754, 1997.
- M. Nishida and M. P. Walker. Daytime Naps, Motor Memory Consolidation and Regionally Specific Sleep Spindles. *PLoS ONE*, 2(4):7, 2007.
- D. Nitz. Tracking route progression in the posterior parietal cortex. *Neuron*, 49(5):747–756, 2006.
- S. A. Norris, B. Greger, E. N. Hathaway, and W. T. Thach. Purkinje cell spike firing in the posterolateral cerebellum: correlation with visual stimulus, oculomotor response, and error feedback. *Journal of Neurophysiology*, 92(3):1867–1879, 2004.
- D. A. Nowak, D. Timmann, and J. Hermsdörfer. Dexterity in cerebellar agenesis., 2007.
- S. Obayashi. Possible mechanism for transfer of motor skill learning: implication of the cerebellum. *Cerebellum (London, England)*, 3(4):204–11, 2004.
- D. L. O’Donoghue and G. A. Bishop. A quantitative analysis of the distribution of Purkinje cell axonal collaterals in different zones of the cat’s cerebellum: an intracellular HRP study. *Experimental Brain Research*, 80(0014-4819 LA - eng):63–71, 1990.
- W. H. Oertel. Neurotransmitters in the cerebellum. Scientific aspects and clinical relevance. *Advances in Neurology*, 61:33–75, 1993.
- J. O’Keefe and N. Burgess. Geometric determinants of the place fields of hippocampal neurons. *Nature*, 381(6581):425–428, 1996.
- J. O’Keefe and D. H. Conway. Hippocampal place units in the freely moving rat: why they fire where they fire. *Experimental brain research. Experimentelle Hirnforschung. Expérimentation cérébrale*, 31(4):573–90, 1978.
- J. O’Keefe and J. Dostrovsky. The hippocampus as a spatial map. preliminary evidence from unit activity in the freely-moving rat. *Brain Res.*, 34(1):171–175, 1971.
- J. O’Keefe and L. Nadel. *The Hippocampus as a Cognitive Map*, volume 3. Oxford University Press, 1978.
- B. A. Olshausen and D. J. Field. Sparse coding of sensory inputs. *Curr. Opin. Neurobiol.*, 14(4):481–487, 2004.
- D. S. Olton and R. J. Samuelson. Remembrance of places passed: Spatial memory in rats. *Journal of Experimental Psychology Animal Behavior Processes*, 2(2):97–116, 1976.

- L. Optican. Sensorimotor Transformation for Visually Guided Saccades. *New York*, 148 (Clinical and Basic Oculomotor Research: In Honor of David S. Zee):132–148, 2005.
- O. Oscarsson. Spatial distribution of climbing and mossy fibre inputs into the cerebellar cortex. In *Afferent and Intrinsic Organization of Laminated Structures in the Brain.*, pages 34–42. Springer-Verlag, Berlin, creutzfeldt, o. edition, 1976.
- M. Ouardouz and B. R. Sastry. Mechanisms underlying LTP of inhibitory synaptic transmission in the deep cerebellar nuclei. *Journal of Neurophysiology*, 84(3):1414–1421, 2000.
- M. G. Packard and J. L. McGaugh. Double dissociation of fornix and caudate nucleus lesions on acquisition of two water maze tasks: further evidence for multiple memory systems. *Behavioral Neuroscience*, 106(3):439–446, 1992.
- G. D. Paige and S. H. Seidman. Characteristics of the VOR in response to linear acceleration. *Annals of the New York Academy of Sciences*, 871(OTOLITH FUNCTION IN SPATIAL ORIENTATION AND MOVEMENT):123–135, 1999.
- S. L. Palay. *Cerebellar cortex: cytology and organization*. Springer, (Berlin, Heidelberg, New York), 1974.
- M. Palkovits, E. Mezey, J. Hámori, and J. Szentágothai. Quantitative histological analysis of the cerebellar nuclei in the cat. I. Numerical data on cells and on synapses. *Experimental Brain Research*, 28(1-2):189–209, 1977.
- S. Panzeri and A. Treves. Analytical estimates of limited sampling biases in different information measures. *Network Computation in Neural Systems*, 7(1):87–107, 1996.
- J. Parvizi, S. W. Anderson, C. O. Martin, H. Damasio, and A. R. Damasio. Pathological laughter and crying: a link to the cerebellum., 2001.
- S. Pasalar, A. V. Roitman, W. K. Durfee, and T. J. Ebner. Force field effects on cerebellar purkinje cell discharge with implications for internal models. *Nat. Neurosci.*, 9(11): 1404–1411, 2006.
- J.-B. Passot, N. Luque, and A. Arleo. Internal models in the cerebellum: a coupling scheme for online and offline learning in procedural tasks. In *Proceedings of the 11th international conference on Simulation of adaptive behavior: from animals to animats SAB'10*, pages 435—446. Springer-Verlag, Berlin, 2010.
- J. P. Pellerin and Y. Lamarre. Local field potential oscillations in primate cerebellar cortex during voluntary movement. *Journal of Neurophysiology*, 78(6):3502–3507, 1997.
- A. Pellionisz and J. Szentágothai. Dynamic single unit simulation of a realistic cerebellar network model. *Brain Res.*, 49(1):83–99, 1973.
- S. P. Perrett, B. P. Ruiz, and M. D. Mauk. Cerebellar cortex lesions disrupt learning-dependent timing of conditioned eyelid responses. *J. Neurosci.*, 13(4):1708–1718, 1993.

- S. E. Petersen, P. T. Fox, M. I. Posner, M. Mintun, and M. E. Raichle. Positron emission tomographic studies of the processing of single words. *Journal of Cognitive Neuroscience*, 1(2):153–170, 1989.
- L. Petrosini, M. Molinari, and M. E. Dell’Anna. Cerebellar contribution to spatial event processing: Morris water maze and T-maze. *European Journal of Neuroscience*, 8(9): 1882–1896, 1996.
- L. Petrosini, M. G. Leggio, and M. Molinari. The cerebellum in the spatial problem solving: a co-star or a guest star? *Progress in Neurobiology*, 56(2):191–210, 1998.
- D. Philipona and O. J.-M. D. Coenen. Model of granular layer encoding in the cerebellum. *Neurocomputing*, 58:575–580, 2004.
- C. Pichitpornchai, J. A. Rawson, and S. Rees. Morphology of parallel fibres in the cerebellar cortex of the rat: an experimental light and electron microscopic study with biocytin. *Journal of Comparative Neurology*, 342(2):206–220, 1994.
- D. G. Placantonakis, A. A. Bukovsky, S. A. Aicher, H.-P. Kiem, and J. P. Welsh. Continuous electrical oscillations emerge from a coupled network: a study of the inferior olive using lentiviral knockdown of connexin36. *J. Neurosci.*, 26(19):5008–5016, 2006.
- W. Plihal and J. Born. Effects of Early and Late Nocturnal Sleep on Declarative and Procedural Memory. *Journal of Cognitive Neuroscience*, 9(4):534–547, 1997.
- S. Pockett. *The Neuroscience of Movement*, pages 9–24. MIT Press, 2006.
- B. Poucet, C. Thinus-Blanc, and R. Muller. Place cells in the ventral hippocampus of rats. *Neuroreport*, 5(16):2045–2048, 1994.
- J. R. Pugh and I. M. Raman. Potentiation of mossy fiber EPSCs in the cerebellar nuclei by NMDA receptor activation followed by postinhibitory rebound current. *Neuron*, 51(1): 113–123, 2006.
- J. R. Pugh and I. M. Raman. Nothing can be coincidence: synaptic inhibition and plasticity in the cerebellar nuclei. *Trends Neurosci.*, 32(3):170–7, 2009.
- G. Quirk, R. Muller, and J. Kubie. The firing of hippocampal place cells in the dark depends on the rat’s recent experience. *J. Neurosci.*, 10(6):2008–2017, 1990.
- R. J. Racine, D. A. Wilson, R. Gingell, and D. Sunderland. Long-term potentiation in the interpositus and vestibular nuclei in the rat. *Experimental Brain Research*, 63(1):158–162, 1986.
- I. M. Raman and B. P. Bean. Properties of sodium currents and action potential firing in isolated cerebellar purkinje neurons. *Annals of the New York Academy of Sciences*, 868: 93–96, 1999.

- A. Rancillac and F. Crépel. Synapses between parallel fibres and stellate cells express long-term changes in synaptic efficacy in rat cerebellum. *The Journal of Physiology*, 554 (Pt 3):707–720, 2004.
- J. Rasmussen, M. Damsgaard, and M. Voigt. Muscle recruitment by the min/max criterion – a comparative numerical study. *Journal of Biomechanics*, 34(3):409–415, 2001.
- J. L. Raymond and S. G. Lisberger. Behavioral analysis of signals that guide learned changes in the amplitude and dynamics of the vestibulo-ocular reflex. *J. Neurosci.*, 16 (23):7791–7802, 1996.
- J. L. Raymond and S. G. Lisberger. Neural learning rules for the vestibulo-ocular reflex. *The Journal of Neuroscience: The Official Journal of the Society for Neuroscience*, 18(21):9112–29, 1998.
- A. Rechtschaffen and A. Kales. *A manual of standardized terminology, techniques and scoring system for sleep stages of human subjects*. Washington DC, 1968.
- A. D. Redish. *Beyond the Cognitive Map, From Place Cells to Episodic Memory*. MIT Press-Bradford Books, 1999.
- D. Riva and C. Giorgi. The cerebellum contributes to higher functions during development: evidence from a series of children surgically treated for posterior fossa tumours. *Brain: A journal of neurology*, 123 (Pt 5(Pt 5):1051–1061, 2000.
- E. Rolls. A model of the operation of the hippocampus and entorhinal cortex in memory. *International Journal of Neural Systems*, 6:51–70, 1995.
- L. Rondi-Reig, N. L. Marec, J. Caston, and J. Mariani. The role of climbing and parallel fibers inputs to cerebellar cortex in navigation. *Behav Brain Res*, 132(1):11–18, Apr 2002.
- L. Rondi-Reig, G. Petit, C. TOBIN, and E. Burguière. The starmaze: a new paradigm to characterize multiple spatial navigation strategies. *Behavior Research Methods*, 2005.
- F. Rosenblatt. The perceptron, 1958.
- M. F. Rushworth, P. D. Nixon, and R. E. Passingham. Parietal cortex and movement. I. Movement selection and reaching. *Experimental brain research. Experimentelle Hirnforschung Expérimentation cérébrale*, 117(2):292–310, 1997.
- R. Saegusa, G. Metta, and G. Sandini. Active learning for sensorimotor coordinations of autonomous robots. In *2009 2nd Conference on Human System Interactions*, pages 701–706, Catania, Italy, 2009.
- P. Safo and W. G. Regehr. Timing dependence of the induction of cerebellar LTD. *Neuropharmacology*, 54(1):213–218, 2008.
- M. Sahin and S. Hockfield. Molecular identification of the Lugaro cell in the cat cerebellar cortex. *Journal of Comparative Neurology*, 301(4):575–84, 1990.

- J. A. Saint-Cyr and D. J. Woodward. Activation of mossy and climbing fiber pathways to the cerebellar cortex by stimulation of the fornix in the rat. *Experimental Brain Research*, 40(1):1–12, 1980.
- M. Sakurai. Synaptic modification of parallel fibre-Purkinje cell transmission in in vitro guinea-pig cerebellar slices. *The Journal of Physiology*, 394(0022-3751 (Print) LA - eng PT - Journal Article SB - IM):463–480, 1987.
- B. Scelfo and P. Strata. Correlation between multiple climbing fibre regression and parallel fibre response development in the postnatal mouse cerebellum. *European Journal of Neuroscience*, 21(4):971–978, 2005.
- M. E. Scheibel and A. B. Scheibel. Observations on the intracortical relations of the climbing fibers of the cerebellum; a Golgi study. *The Journal of comparative neurology*, 101(3):733–63, 1954.
- J. D. Schmahmann. From movement to thought: anatomic substrates of the cerebellar contribution to cognitive processing. *Human Brain Mapping*, 4(3):174–198, 1996.
- J. D. Schmahmann and D. N. Pandya. Projections to the basis pontis from the superior temporal sulcus and superior temporal region in the rhesus monkey. *Journal of Comparative Neurology*, 308(2):224–248, 1991.
- J. D. Schmahmann and J. C. Sherman. Cerebellar cognitive affective syndrome. Technical Report 4, Department of Neurology, Massachusetts General Hospital, Boston, USA., 1997.
- J. D. Schmahmann and J. C. Sherman. The cerebellar cognitive affective syndrome. *Brain*, 121(0006-8950 (Print) LA - eng PT - Journal Article SB - AIM SB - IM):561–579, 1998.
- M. Schonewille, a. Belmeguenai, S. K. Koekkoek, S. H. Houtman, H. J. Boele, B. J. van Beugen, Z. Gao, a. Badura, G. Ohtsuki, W. E. Amerika, E. Hosal, F. E. Hoebeek, Y. Elgersma, C. Hansel, and C. I. De Zeeuw. Purkinje Cell-Specific Knockout of the Protein Phosphatase PP2B Impairs Potentiation and Cerebellar Motor Learning. *Neuron*, 67(4):618–628, 2010a.
- M. Schonewille, A. Belmeguenai, S. K. Koekkoek, S. H. Houtman, H. J. Boele, B. J. van Beugen, Z. Gao, A. Badura, G. Ohtsuki, W. E. Amerika, E. Hosal, F. E. Hoebeek, Y. Elgersma, C. Hansel, and C. I. D. Zeeuw. Purkinje cell-specific knockout of the protein phosphatase pp2b impairs potentiation and cerebellar motor learning. *Neuron*, 67(4):618–628, 2010b.
- M. Schonewille, Z. Gao, H.-J. Boele, M. F. V. Veloz, W. E. Amerika, A. A. M. Simek, M. T. D. Jeu, J. P. Steinberg, K. Takamiya, F. E. Hoebeek, D. J. Linden, R. L. Huganir, and C. I. D. Zeeuw. Reevaluating the role of ltd in cerebellar motor learning. *Neuron*, 70(1):43–50, 2011.
- H. Schulz. Rethinking sleep analysis. *Journal of Clinical Sleep Medicine : JCSM : official publication of the American Academy of Sleep Medicine*, 4(2):99–103, 2008.

- N. Schweighofer, M. A. Arbib, and P. F. Dominey. A model of the cerebellum in adaptive control of saccadic gain II. Simulation results. *Biological Cybernetics*, 36:29–36, 1996.
- N. Schweighofer, J. Spoelstra, M. a Arbib, and M. Kawato. Role of the cerebellum in reaching movements in humans. II. A neural model of the intermediate cerebellum. *The European journal of neuroscience*, 10(1):95–105, 1998.
- N. Schweighofer, K. Doya, and M. Kawato. Electrophysiological properties of inferior olive neurons: A compartmental model. *Journal of Neurophysiology*, 82(2):804–817, 1999.
- N. Schweighofer, K. Doya, and F. Lay. Unsupervised learning of granule cell sparse codes enhances cerebellar adaptive control. *Neuroscience*, 103(1):35–50, 2001.
- N. Schweighofer, K. Doya, H. Fukai, J. V. Chiron, T. Furukawa, and M. Kawato. Chaos may enhance information transmission in the inferior olive. *Proc. Natl. Acad. Sci. U. S. A.*, 101(13):4655–4660, 2004.
- T. J. Sejnowski. Storing covariance with nonlinearly interacting neurons. *Journal of Mathematical Biology*, 4(4):303–321, 1977.
- R. Shadmehr and J. W. Krakauer. A computational neuroanatomy for motor control. *Experimental Brain Research*, 185(3):359–381, 2008.
- R. Shadmehr, M. a Smith, and J. W. Krakauer. Error Correction, Sensory Prediction, and Adaptation in Motor Control. *Annu. Rev. Neurosci.*, 33:89–108, 2010.
- A. G. Shaikh, H. Meng, and D. E. Angelaki. Multiple reference frames for motion in the primate cerebellum. *J Neurosci*, 24(19):4491–4497, May 2004.
- C. Shannon. A mathematical theory of communication. *Bell System Technical Journal*, 27:379–423, 1948.
- P. Sharp, J. Kubie, and R. Muller. Firing properties of hippocampal neurons in a visually symmetrical environment: contributions of multiple sensory cues and mnemonic processes. *J. Neurosci.*, 10(9):3093–3105, 1990.
- P. Sharp, H. Blair, D. Etkin, and D. Tzanetos. Influences of vestibular and visual motion information on the spatial firing patterns of hippocampal place cells. *J. Neurosci.*, 15(1 Pt 1):173–189, 1995.
- D. Sheynikhovich, R. Chavarriaga, T. Strösslin, A. Arleo, and W. Gerstner. Is there a geometric module for spatial orientation? Insights from a rodent navigation model. *Psychological Review*, 116(3):540–566, 2009.
- Y. P. Shimansky. Spinal motor control system incorporates an internal model of limb dynamics. *Biological Cybernetics*, 83(4):379–389, 2000.
- J. I. Simpson, D. R. Wylie, and C. I. De Zeeuw. On climbing fiber signals and their consequence(s). *Behavioral and Brain Sciences*, 19(3):1–48, 1996.

- W. E. Skaggs, B. L. McNaughton, K. M. Gothard, and E. J. Markus. An Information-Theoretic Approach to Deciphering the Hippocampal Code. In S. J. Hanson, J. D. Cowan, and L. C. Giles, editors, *Neural Information Processing Systems*, volume 1990 (5), pages 1030–1037. Morgan Kaufmann, 1993.
- J. B. Smeets and E. Brenner. A new view on grasping. *Motor Control*, 3(3):237–271, 1999.
- G. J. Soler-Llavina and B. L. Sabatini. Synapse-specific plasticity and compartmentalized signaling in cerebellar stellate cells. *Nat. Neurosci.*, 9(6):798–806, 2006.
- L. R. Squire and S. M. Zola. Structure and function of declarative and nondeclarative memory systems. *Proc. Natl. Acad. Sci. U. S. A.*, 93(24):13515–13522, 1996.
- L. R. Squire, B. Knowlton, and G. Musen. The structure and organization of memory. *Annual Review of Psychology*, 44:453–95, 1993.
- J. E. Steinmetz, D. J. Rosen, P. F. Chapman, D. G. Lavond, and R. F. Thompson. Classical conditioning of the rabbit eyelid response with a mossy-fiber stimulation CS: I. Pontine nuclei and middle cerebellar peduncle stimulation. *Behavioral Neuroscience*, 100(6):878–887, 1986.
- V. Steuber, D. Willshaw, and A. Van Ooyen. Generation of time delays: simplified models of intracellular signalling in cerebellar Purkinje cells. *Network*, 17(2):173–91, 2006.
- C. A. Stewart and R. G. M. Morris. The watermaze. *Behavioural neuroscience: a practical approach*, 1:107–122., 1993.
- R. Stickgold. Sleep-dependent memory consolidation. *Nature*, 437(7063):1272–1278, 2005.
- R. Stickgold, L. James, and J. A. Hobson. Visual discrimination learning requires sleep after training. *Nat. Neurosci.*, 3(12):1237–1238, 2000a.
- R. Stickgold, D. Whidbee, B. Schirmer, V. Patel, and J. A. Hobson. Visual discrimination task improvement: A multi-step process occurring during sleep. *Journal of Cognitive Neuroscience*, 12(2):246–254, 2000b.
- P. L. Strick, R. P. Dum, and J. A. Fiez. Cerebellum and nonmotor function. *Annu. Rev. Neurosci.*, 32:413–434, 2009.
- I. Sugihara, E. J. Lang, and R. Llinás. Uniform olivocerebellar conduction time underlies Purkinje cell complex spike synchronicity in the rat cerebellum. *The Journal of Physiology*, 470(1):243–271, 1993.
- I. Sugihara, E. J. Lang, and R. Llinás. Serotonin modulation of inferior olivary oscillations and synchronicity: a multiple-electrode study in the rat cerebellum. *European Journal of Neuroscience*, 7(4):521–534, 1995.
- G. R. Sutherland and B. McNaughton. Memory trace reactivation in hippocampal and neocortical neuronal ensembles. *Curr. Opin. Neurobiol.*, 10(2):180–186, 2000.

- R. J. Sutherland, G. L. Chew, J. C. Baker, and R. C. Linggard. Some limitations on the use of distal cues in place navigation by rats. *Psychobiology*, 15(1):48–57, 1987.
- H. Tabata, K. Yamamoto, and M. Kawato. Computational study on monkey VOR adaptation and smooth pursuit based on the parallel control-pathway theory. *Journal of neurophysiology*, 87(4):2176, 2002.
- J. Tan, A. H. Epema, and J. Voogd. Zonal organization of the flocculovestibular nucleus projection in the rabbit: a combined axonal tracing and acetylcholinesterase histochemical study. *Journal of Comparative Neurology*, 356(1):51–71, 1995a.
- J. Tan, N. M. Gerrits, R. Nanhoe, J. I. Simpson, and J. Voogd. Zonal organization of the climbing fiber projection to the flocculus and nodulus of the rabbit: a combined axonal tracing and acetylcholinesterase histochemical study. *Journal of Comparative Neurology*, 356(1):23–50, 1995b.
- W. T. Thach. What is the role of the cerebellum in motor learning and cognition? *Trends in Cognitive Sciences*, 2(9):331–337, 1998.
- W. T. Thach, H. P. Goodkin, and J. G. Keating. The cerebellum and the adaptive coordination of movement. *Annu. Rev. Neurosci.*, 15:403–42, 1992.
- L. Thompson and P. Best. Place cells and silent cells in the hippocampus of freely-behaving rats. *J. Neurosci.*, 9(7):2382–2390, 1989.
- M. A. Thomson, G. Piat, V. Cordonnier, L. Ellouze-Kallel, N. Delhay-Bouchaud, and J. Mariani. Representation of vibrissae inputs through the climbing fiber pathway in lobule VII of the adult rat cerebellar vermis. *Brain Res.*, 488(1-2):241–252, 1989.
- G. Tigyí, C. Matute, and R. Miledi. Monoclonal antibodies to cerebellar pinceau terminals obtained after immunization with brain mRNA-injected *Xenopus* oocytes. *Proc. Natl. Acad. Sci. U. S. A.*, 87(2):528–532, 1990.
- D. Timmann and I. Daum. Cerebellar contributions to cognitive functions: a progress report after two decades of research. *Cerebellum (London, England)*, 6(3):159–62, 2007.
- D. Timmann, J. Drepper, M. Frings, M. Maschke, S. Richter, M. Gerwig, and F. P. Kolb. The human cerebellum contributes to motor, emotional and cognitive associative learning. A review. *Cortex; a journal devoted to the study of the nervous system and behavior*, 46(7):845–857, 2009.
- E. Todorov. Cosine tuning minimizes motor errors. *Neural Computation*, 14(6):1233–1260, 2002.
- E. Todorov. Optimality principles in sensorimotor control. *Nat. Neurosci.*, 7(9):907–915, 2004.
- E. Todorov and M. I. Jordan. Smoothness maximization along a predefined path accurately predicts the speed profiles of complex arm movements. *Journal of Neurophysiology*, 80(2):696–714, 1998.

- E. Todorov and M. I. Jordan. Optimal feedback control as a theory of motor coordination. *Nat. Neurosci.*, 5(11):1226–35, 2002.
- E. C. Tolman. Cognitive maps in rats and men. *Psych Review*, 55:189–208, 1948.
- E. C. Tolman, B. F. Ritchie, and D. Kalish. Studies in spatial learning: II. Place learning versus response. *Journal of Experimental Psychology*, 36:221–229, 1946.
- O. Trullier, S. I. Wiener, A. Berthoz, and J. A. Meyer. Biologically based artificial navigation systems: review and prospects. *Progress in Neurobiology*, 51(5):483–544, 1997.
- Y. Uno, M. Kawato, and R. Suzuki. Formation and control of optimal trajectory in human multijoint arm movement. *Biological Cybernetics*, 61(2):89–101, 1989.
- C. Van Vreeswijk and H. Sompolinsky. Chaos in Neuronal Networks with Balanced Excitatory and Inhibitory Activity. *Science*, 274(5293):1724–1726, 1996.
- L. R. Vandervert, P. H. Schimpf, and H. Liu. How Working Memory and the Cerebellum Collaborate to Produce Creativity and Innovation. *Creativity Research Journal*, 19(1): 1–18, 2007.
- S. Vaziri, J. Diedrichsen, and R. Shadmehr. Why does the brain predict sensory consequences of oculomotor commands? Optimal integration of the predicted and the actual sensory feedback. *J. Neurosci.*, 26(16):4188–4197, 2009.
- W. E. Vinje and J. L. Gallant. Sparse coding and decorrelation in primary visual cortex during natural vision. *Science*, 287(5456):1273–1276, 2000.
- J. Voogd and M. Glickstein. The anatomy of the cerebellum. *Trends Neurosci.*, 21(9):370–5, 1998.
- B. P. Vos, R. Maex, A. Volny-Luraghi, and E. De Schutter. Parallel fibers synchronize spontaneous activity in cerebellar Golgi cells. *J. Neurosci.*, 19(11):RC6, 1999.
- U. Wagner, S. Gais, H. Haider, R. Verleger, and J. Born. Sleep inspires insight. *Nature*, 427 (6972):352–5, 2004.
- M. P. Walker and R. Stickgold. Sleep-dependent learning and memory consolidation. *Neuron*, 44(1):121–133, 2004.
- M. P. Walker, T. Brakefield, A. Morgan, J. A. Hobson, and R. Stickgold. Practice with sleep makes perfect: sleep-dependent motor skill learning. *Neuron*, 35(1):205–211, 2002.
- M. P. Walker, T. Brakefield, J. Seidman, A. Morgan, J. A. Hobson, and R. Stickgold. Sleep and the Time Course of Motor Skill Learning. *Learning Memory*, 10(4):275–284, 2003.
- S. S. H. Wang, L. Khiroug, and G. J. Augustine. Quantification of spread of cerebellar long-term depression with chemical two-photon uncaging of glutamate. *Proc. Natl. Acad. Sci. U. S. A.*, 97(15):8635–8640, 2000.

- Y. T. Wang and D. J. Linden. Expression of cerebellar long-term depression requires post-synaptic clathrin-mediated endocytosis. *Neuron*, 25(3):635–647, 2000.
- M. Wehr and A. M. Zador. Balanced inhibition underlies tuning and sharpens spike timing in auditory cortex. *Nature*, 426(6965):442–446, 2003.
- I. Q. Whishaw. Cholinergic receptor blockade in the rat impairs locale but not taxon strategies for place navigation in a swimming pool. *Behavioral Neuroscience*, 99(5):979–1005, 1985.
- I. Q. Whishaw. Latent learning in a swimming pool place task by rats: evidence for the use of associative and not cognitive mapping processes. *The Quarterly Journal of Experimental Psychology Section B: Comparative and Physiological Psychology*, 43(1):83–103, 1991.
- I. Q. Whishaw and G. Mittleman. Visits to starts, routes, and places by rats (*Rattus norvegicus*) in swimming pool navigation tasks. *Journal of comparative psychology*, 100(4):422–31, 1986.
- I. Q. Whishaw, J. E. McKenna, and H. Maaswinkel. Hippocampal lesions and path integration. *Curr. Opin. Neurobiol.*, 7(2):228–234, 1997.
- N. M. White and R. J. McDonald. Multiple parallel memory systems in the brain of the rat. *Neurobiology of Learning and Memory*, 77:125–184, 2002.
- J. M. Wiener, A. Berthoz, and T. Wolbers. Dissociable cognitive mechanisms underlying human path integration. *Experimental Brain Research*, 208:61–71, 2011.
- S. Wiener and J. Taube. *Head Direction Cells and the Neural Mechanisms of Spatial Orientation*. MIT Press, 2005.
- B. Willmore and D. J. Tolhurst. Characterizing the sparseness of neural codes. *Population English Edition*, 12:255–270, 2001.
- M. A. Wilson and B. L. McNaughton. Dynamics of the hippocampal ensemble code for space. *Science*, 261(5124):1055–1058, 1993.
- M. A. Wilson and B. L. McNaughton. Reactivation of hippocampal ensemble memories during sleep. *Science*, 265(5172):676–679, 1994.
- M. Witter. Organization of the entorhinal-hippocampal system: a review of current anatomical data. *Hippocampus*, 3 Spec No:33–44, 1993.
- D. M. Wolpert and Z. Ghahramani. Computational principles of movement neuroscience. *Nat. Neurosci.*, 3 Suppl:1212–1217, 2000.
- D. M. Wolpert and M. Kawato. Multiple paired forward and inverse models for motor control. *Neural Networks*, 11(7-8):1317–1329, 1998.

- D. M. Wolpert and R. C. Miall. Forward models for physiological motor control. *Neural Networks*, 9:1265–1279, 1996.
- D. M. Wolpert, R. C. Miall, and M. Kawato. Internal models in the cerebellum. *Trends in Cognitive Sciences*, 2(9):338–347, 1998.
- J. Xia, H. J. Chung, C. Wihler, R. L. Huganir, and D. J. Linden. Cerebellar long-term depression requires PKC-regulated interactions between GluR2/3 and PDZ domain-containing proteins. *Neuron*, 28(2):499–510, 2000.
- T. A. Yakusheva, A. G. Shaikh, A. M. Green, P. M. Blazquez, J. D. Dickman, and D. E. Angelaki. Purkinje cells in posterior cerebellar vermis encode motion in an inertial reference frame. *Neuron*, 54(6):973–985, 2007.
- S. B. Yakushin, T. Raphan, and B. Cohen. Context-specific adaptation of the vertical vestibuloocular reflex with regard to gravity. *Journal of Neurophysiology*, 84(6):3067–3071, 2000.
- J. Yamada and H. Noda. Afferent and efferent connections of the oculomotor cerebellar vermis in the macaque monkey. *Journal of Comparative Neurology*, 265(2):224–241, 1987.
- T. Yamazaki and S. Tanaka. Neural modeling of an internal clock. *Neural Computation*, 17(5):1032–1058, 2005.
- T. Yamazaki and S. Tanaka. The cerebellum as a liquid state machine. *Neural Networks*, 20(3):290–297, 2007.
- T. Yamazaki and S. Tanaka. Computational models of timing mechanisms in the cerebellar granular layer. *Cerebellum (London, England)*, 8(4):423–32, 2009.
- Y. Yarom and D. Cohen. The olivocerebellar system as a generator of temporal patterns. *Annals of the New York Academy of Sciences*, 978(978):122–134, 2002.
- H. Yu, D. Sternad, D. M. Corcos, and D. E. Vaillancourt. Role of hyperactive cerebellum and motor cortex in Parkinson’s disease. *NeuroImage*, 35(1):222–233, 2007.
- I. S. Zagon, P. J. McLaughlin, and S. Smith. Neural populations in the human cerebellum: estimations from isolated cell nuclei. *Brain Res.*, 127(2):279–282, 1977.
- W. Zhang and D. J. Linden. Long-term depression at the mossy fiber-deep cerebellar nucleus synapse. *The Journal of Neuroscience: The Official Journal of the Society for Neuroscience*, 26(26):6935–6944, 2006.